

The Role of Tensin in Cell Migration and Fibronectin Fibrillogenesis

**Thesis submitted for the degree of Doctor of
Philosophy at the University of Leicester**

by

**Jonathan David Howe BSc (Hons)
Department of Biochemistry
University of Leicester**

September 2009

For my Nan

Abstract

Title: The Role of Tensin in Cell Migration and Fibronectin Fibrillogenesis.

Author: Jonathan David Howe

The tensin family of cytoskeletal-associated proteins are implicated in fibronectin fibrillogenesis and integrin-mediated cell migration. There are four members of the human tensin family. Tensin1, 2 and 3 are large proteins (~150-200 kDa) with widespread expression in adult tissues that are thought to couple integrins to the actin cytoskeleton, whereas tensin4 (cten) is a smaller protein (77 kDa) with a restricted expression profile that is not thought to interact with actin.

To study the role of tensin in fibronectin fibrillogenesis, which is mediated by fibrillar adhesions, I first characterised the isoform specificities of several anti-tensin antibodies. These antibodies were then used to determine the tensin expression profile of human foreskin fibroblasts (HFFs), which were found to express tensin1, 2 and 3. Unfortunately, most of the antibodies did not work sufficiently well for immunofluorescence microscopy so the sub-cellular localisation of the tensins was largely investigated using GFP-tagged proteins. Tensin1, 2 and 3 localised to both focal and fibrillar adhesions, although relative distribution between these two adhesion types was isoform-specific. Since tensin3 preferentially localised to fibrillar adhesions, I used an siRNA approach to investigate its role in fibronectin fibrillogenesis, and found that tensin3 was required for this process.

Although tensins play an important role in cell migration, it is unclear whether they act as positive or negative regulators. Therefore, I used over-expression and siRNA-mediated knockdown to clarify the role of tensin1, 2 and 3 in both 2D and 3D migration. Interestingly, I found that modulating tensin expression did not affect the 2D migration of HFF, HEK293, or A2780 ovarian cancer cells. However, all three tensins were required for the 3D migration of A2780 cells in fibronectin-containing microenvironments.

Over-expressing Rab25, a small GTPase up-regulated in aggressive ovarian cancers, in A2780 cells promotes invasive migration in 3D microenvironments by recycling and retaining integrin at the cell front (Caswell *et al.*, 2007). Tensin was required for the invasive migration and morphology of Rab25-expressing A2780 cells. However, tensin depletion did not affect global $\alpha 5$ integrin recycling or the retention of photoactivated GFP- $\alpha 5$ integrin at the cell front. Interestingly, Rab25 over-expression was also found to promote tensin-dependent fibronectin fibrillogenesis in A2780 cells, suggesting that tensin promotes 3D migration by facilitating fibronectin fibril remodelling.

Acknowledgements

First and foremost I would like to thank my supervisor David Critchley for his guidance and wisdom both throughout my time in the lab and during the preparation of this thesis. I would also like to thank Kath Clark for her practical supervision, help with thesis writing, support and friendship - Team Tensin! I owe my gratitude to all members of lab 3/43, past and present, for creating a warm and productive working environment. In particular I would like to thank Bipin Patel for his humour and friendship - and of course for many enjoyable rounds of our interpretation of golf! I'm also especially grateful to Kees Straatman for his technical expertise on the microscopes, and his willingness to lend a helping hand despite the consistency with which I requested his assistance just as he was about to leave for home. I would also like to acknowledge Andrew Fry and Catrin Pritchard for their valuable input as my PhD committee members, and the Medical Research Council (MRC) for funding my PhD studies.

I would like to thank Jim Norman and Pat Caswell for their collaboration and enthusiasm, which was immensely helpful for the progression of my project. I'm especially grateful to Pat and his wife Elaine for allowing me to stay with them during my numerous extended visits to Glasgow to work at the Beatson Institute for Cancer Research, and for saving me dinner (or should I say breakfast) to eat when I came home from my marathon microscope sessions.

Special thanks must go to my girlfriend Cat for her love and support throughout my PhD, and for her seemingly limitless patience. I'm also immensely grateful for the encouragement and friendship of Ian, Stacey and Vaclav. Finally, I would like to acknowledge my Mum, Dad and Brother Adrian for their love and belief in me.

I dedicate this thesis to my Nan.

With love and gratitude,

Jonathan Howe

Table of Contents

Abstract	i
Acknowledgements	ii
Table of Contents	iii
List of Figures and Tables	vi
Abbreviations	viii
Chapter 1 Introduction	1
1.1 Cell Adhesion to the Extracellular Matrix	2
1.1.1 <i>The Role of Cell Adhesion</i>	2
1.1.2 <i>The ECM</i>	3
1.1.3 <i>Integrin-Mediated Cell Adhesion</i>	3
1.1.4 <i>Integrin Structure</i>	4
1.1.5 <i>Integrin Activation</i>	9
1.1.6 <i>Integrin Signalling</i>	10
1.1.7 <i>The Integrin-Cytoskeletal Connection</i>	12
1.2 Cellular Junctions with the ECM.....	13
1.2.1 <i>Different Types of Cell-ECM Adhesions</i>	13
1.2.2 <i>Focal Complexes</i>	15
1.2.3 <i>Focal Adhesions</i>	16
1.2.4 <i>Fibrillar Adhesions</i>	18
1.2.5 <i>3D-Matrix Adhesions</i>	22
1.2.6 <i>Podosomes and Invadopodia</i>	23
1.3 FN Fibrillogenesis	25
1.3.1 <i>Fibronectin</i>	25
1.3.2 <i>The Process of FN Fibrillogenesis</i>	27
1.4 Cell Migration	29
1.4.1 <i>The Role of Cell Migration</i>	29
1.4.2 <i>The Migration Cycle</i>	30
1.4.3 <i>Regulation by Rho-Family GTPases</i>	37
1.4.4 <i>Cell Migration in 3D Microenvironments</i>	42
1.5 Tensin	44
1.5.1 <i>Tensin Identification and Initial Characterisation</i>	44
1.5.2 <i>The Human Tensin Family</i>	45
1.5.3 <i>Genetic Studies on Tensin</i>	47
1.5.4 <i>Domain Homology between the Human Tensins</i>	49
1.5.5 <i>Tensin Binding Partners</i>	51
1.5.6 <i>Deleted in Liver Cancer-1 (DLC-1)</i>	55
1.5.7 <i>Tensin Expression in Cancer</i>	58
1.5.8 <i>Cellular Functions of Tensin</i>	59
1.6 Project Aims and Objectives	62
Chapter 2 Materials and Methods	64
2.1 Molecular Biology	65
2.1.1 <i>Materials</i>	65
2.1.1.1 <i>Host Strains and Media</i>	65
2.1.1.2 <i>Expression Plasmids</i>	66
2.1.1.3 <i>Small Interfering RNAs (siRNAs)</i>	66
2.1.2 <i>E. coli Transformation</i>	67
2.1.3 <i>Plasmid Amplification and Purification</i>	67
2.1.3.1 <i>Density Centrifugation Plasmid DNA Purification (Caesium Chloride)</i>	68

2.1.3.2	Column-Based Plasmid DNA Purification (Maxiprep).....	69
2.1.4	<i>Quantitative Real-Time Polymerase Chain Reaction (qPCR)</i>	70
2.1.4.1	RNA Isolation	70
2.1.4.2	DNase I Treatment	70
2.1.4.3	cDNA Synthesis (Reverse Transcription).....	71
2.1.4.4	qPCR Reaction.....	72
2.1.4.5	Primer Validation	73
2.1.4.6	Relative Abundance Quantification using Delta Delta C _T ($\Delta\Delta C_T$) Analysis.....	75
2.2	Biochemistry	75
2.2.1	<i>Protein Expression in E. coli</i>	75
2.2.2	<i>Affinity Purification of Anti-Tensin Polyclonal Antibodies</i>	76
2.2.2.1	Ammonium Sulphate Precipitation.....	76
2.2.2.2	Nickel Ion Affinity Chromatography.....	77
2.2.2.3	Antigen Affinity Chromatography	78
2.2.3	<i>Protein Analysis and Detection</i>	79
2.2.3.1	Preparation of Protein Lysates.....	79
2.2.3.2	SDS-Polyacrylamide Gel Electrophoresis (SDS-PAGE)	80
2.2.3.3	Western Blotting	80
2.3	Cell Biology	81
2.3.1	<i>Materials</i>	81
2.3.1.1	Cell Lines and Media	81
2.3.2	<i>Mammalian Cell Transfection</i>	83
2.3.2.1	Transfection of HEK293 Cells.....	83
2.3.2.2	Transfection of HFF Cells	85
2.3.2.3	Transfection of A2780 Cells.....	87
2.3.3	<i>Indirect Immunofluorescence Microscopy</i>	88
2.3.3.1	Conventional (Widefield) Fluorescence Microscopy.....	88
2.3.3.2	Confocal Fluorescence Microscopy	89
2.4	Other Cell-Based Assays	91
2.4.1	<i>Scratch-Wound Assays</i>	91
2.4.1.1	Scratch-Wound assay on HEK293 Cells.....	91
2.4.1.2	Scratch-Wound assay on A2780 Cells.....	91
2.4.2	<i>Matrigel-Plug Inverted Invasion Assay</i>	92
2.4.3	<i>Analysis of Cell Morphology and Migration on Cell-Derived Matrix (CDM)</i> .	94
2.4.3.1	Generation of CDM.....	94
2.4.3.2	Time-Lapse Imaging and Analysis	96
2.4.4	<i>Integrin Recycling Assay</i>	96
2.4.4.1	Recycling Protocol.....	96
2.4.4.2	Capture ELISA	97
2.4.5	<i>Photoactivation Assay (Integrin Diffusion/Retention)</i>	98
Chapter 3 Anti-Tensin Antibody Characterisation and Tensin Localisation ...		100
3.1	Introduction	101
3.2	Results.....	102
3.2.1	<i>Anti-Tensin Antibody Characterisation using GFP-Tensin Fusions</i>	102
3.2.2	<i>HFFs Express All Three Large Tensin Isoforms</i>	109
3.2.3	<i>Anti-Tensin Antibody Characterisation by siRNA-Directed Tensin Knockdown</i>	113
3.2.4	<i>Tensin Localisation in HFFs</i>	118
3.3	Discussion.....	131
3.3.1	<i>Anti-Tensin Antibody Characterisation</i>	131
3.3.2	<i>Differential Tensin Localisation in HFFs</i>	136

Chapter 4 The Role of Tensin in Fibronectin Fibrillogenesis and Cell Migration in 2-Dimensional (2D) Culture	142
4.1 Introduction	143
4.1.1 <i>Tensin and FN Fibrillogenesis</i>	143
4.1.2 <i>Tensin and 2D Cell Migration</i>	144
4.2 Results.....	148
4.2.1 <i>The Role of Tensin3 in FN Matrix Assembly in HFFs</i>	148
4.2.2 <i>The Role of Tensin in the 2D Cell Migration of the HEK293 Cell Line</i>	157
4.2.3 <i>The Role of Tensin in the 2D Cell Migration of the A2780 Human Ovarian Cancer Cell Line</i>	166
4.3 Discussion.....	172
4.3.1 <i>The Limited Requirement for Tensin3 during FN Fibrillogenesis in HFFs</i> .172	
4.3.2 <i>Tensin is Not Required for 2D Cell Migration</i>	176
Chapter 5 The Role of Tensin in Invasive Cell Migration in 3-Dimensional (3D) Microenvironments	182
5.1 Introduction	183
5.1.1 <i>Tensin and 3D Migration</i>	183
5.2 Results.....	184
5.2.1 <i>Tensin is Required for the 3D Invasive Migration of A2780 Cells</i>	184
5.2.2 <i>Tensin Localises to Cell-ECM Adhesions in Rab25 Cells Migrating in a 3D Matrix</i>	193
5.2.3 <i>Tensin is Required for Rab25-Driven Invasive Morphology and Directionally Persistent Migration in 3D Matrix</i>	195
5.2.4 <i>The Mechanism of Tensin-Dependent 3D Migration</i>	201
5.3 Discussion.....	207
5.3.1 <i>Tensin is Required for 3D Migration</i>	207
5.3.2 <i>Validation of siRNA Specificity</i>	212
5.3.3 <i>The Mechanism of Tensin-Dependent 3D Migration</i>	213
Chapter 6 Conclusions	216
References.....	220

List of Figures and Tables

Figure 1.1: Human integrin heterodimer combinations.	5
Figure 1.2: Domain structure of an integrin heterodimer.	8
Figure 1.3: Adaptor-binding sites in $\beta 3$ integrin cytoplasmic tail.	14
Figure 1.4: Fibrillar adhesion formation.	19
Figure 1.5: Fibronectin.	26
Figure 1.6: The Rho GTPase cycle.	38
Figure 1.7: The role of the classical Rho-family GTPases in cell migration.	40
Figure 1.8: Alignment of the human tensins indicating domain homology.	50
Figure 1.9: Tensin binding partners.	52
Figure 1.10: Potential mechanism for the effect of DLC-1 on proliferation through adhesion modulation.	57
Figure 2.1: Matrigel-plug inverted invasion assay.	93
Figure 3.1: Expression of GFP-tagged tensin proteins in HEK293 cells.	103
Figure 3.2: Characterisation of commercial anti-tensin monoclonal antibodies.	104
Figure 3.3: Characterisation of the Santa Cruz anti-tensin polyclonal antibody.	105
Figure 3.4: Characterisation of the anti-tensin2 polyclonal antibodies.	107
Figure 3.5: Characterisation of the anti-tensin3 polyclonal antibodies.	108
Figure 3.6: Detection of endogenous tensin protein isoforms in HFFs.	110
Figure 3.7: Validation of the amplification efficiency of the qPCR primers.	112
Figure 3.8: Detection of tensin mRNAs in HFFs.	114
Figure 3.9: Optimisation of siRNA transfection into HFFs.	115
Figure 3.10: Validation of anti-tensin antibody specificity by siRNA-mediated tensin knockdown in HFFs.	117
Figure 3.11: Confirmation of endogenous tensin1 localisation by immunofluorescent staining of untransfected HFFs with the Santa Cruz anti-tensin1 antibody.	119
Figure 3.12: GFP-tensin1 localisation in HFFs.	121
Figure 3.13: GFP-tensin1 localisation in HFFs.	122
Figure 3.14: GFP-tensin1 localisation in HFFs.	123
Figure 3.15: GFP-tensin2 localisation in HFFs.	124
Figure 3.16: GFP-tensin2 localisation in HFFs.	125
Figure 3.17: GFP-tensin2 localisation in HFFs assessed by conventional (widefield) fluorescence microscopy.	126
Figure 3.18: GFP-tensin3 localisation in HFFs.	127
Figure 3.19: GFP-tensin3 localisation in HFFs assessed by conventional (widefield) fluorescence microscopy.	128
Figure 3.20: GFP-tensin3 localisation in HFFs.	129
Figure 3.21: GFP-tensin3 localisation in HFFs.	130
Figure 3.22: GFP localisation in HFFs.	132
Figure 3.23: GFP localisation in HFFs.	133
Figure 4.1: Dominant negative effect of expression of GFP-AH2 region in HFFs.	149
Figure 4.2: siRNA-mediated knockdown of tensin3 in HFFs.	151
Figure 4.3: Linearity between FN abundance and band density.	153
Figure 4.4: Quantitation of FN fibrillogenesis in tensin3 knockdown HFFs.	154
Figure 4.5: Immunofluorescent analysis of FN fibrillogenesis in tensin3 knockdown HFFs.	156
Figure 4.6: Scratch-wound assay on HEK293 cells over-expressing GFP-tensins.	158
Figure 4.7: Detection of tensin mRNAs in HEK293 cells.	161
Figure 4.8: siRNA-mediated knockdown of tensin3 in HEK293 cells.	163
Figure 4.9: Scratch-wound assay on tensin3 knockdown HEK293 cells.	164
Figure 4.10: Detection of tensin mRNAs in A2780 cells.	168
Figure 4.11: Validation of tensin knockdown in A2780 cells.	169
Figure 4.12: Tensin is not required for the 2D migration of A2780 cells.	171

Figure 5.1: Invasive migration of DNA3 and Rab25 cells through 3D matrix.....	185
Figure 5.2: The effect of tensin knockdown on the invasive migration of DNA3 cells through 3D matrix.....	187
Figure 5.3: The effect of tensin knockdown on the invasive migration of Rab25 cells through 3D matrix in the presence or absence of supplemented FN.	189
Figure 5.4: Analysis of the integrin dependency of invasive migration in control and tensin knockdown Rab25 cells.	190
Figure 5.5: Analysis of the efficacy of individual siRNA oligos from the tensin1, 2 and 3 SMARTpools by qPCR.....	192
Figure 5.6: The effect of tensin knockdown using individual siRNA oligos on the invasive migration of Rab25 cells through 3D matrix.	194
Figure 5.7: GFP-tensin1 localisation in Rab25 cells on cell-derived matrix.	196
Figure 5.8: GFP-tensin2 localisation in Rab25 cells on cell-derived matrix.	197
Figure 5.9: GFP-tensin3 localisation in Rab25 cells on cell-derived matrix.	198
Figure 5.10: The effect of tensin knockdown on Rab25-driven invasive morphology on cell-derived matrix.	200
Figure 5.11: The effect of tensin knockdown using individual siRNA oligos on Rab25-driven invasive morphology on cell-derived matrix.	202
Figure 5.12: The effect of tensin knockdown on the migration of Rab25 cells on cell-derived matrix.....	203
Figure 5.13: Recycling of $\alpha 5$ integrin in control and tensin knockdown Rab25 cells...	205
Figure 5.14: Tensin knockdown does not compromise Rab25-driven integrin retention in pseudopodial tips.....	206
Figure 5.15: Tensin is required for FN fibril formation.	208
Figure 5.16: Tensin is required for the formation of $\alpha 5$ integrin-containing adhesions	209
Table 1.1: Human integrin ligand specificity.....	6
Table 1.2: Relative tissue expression levels of the four human tensin isoforms.....	46
Table 2.1: siRNA sequences.....	67
Table 2.2: qPCR primer sequences.....	73
Table 2.3: Antibodies for Western blotting.	82
Table 2.4: Antibodies for immunofluorescence microscopy.	90

Abbreviations

2D	Two-dimensional
3D	Three-dimensional
AEBSF	4-[2-aminoethyl] benzenesulfonyl fluoride hydrochloride
AH2	Actin homology 2
ARP2/3	Actin-related proteins 2/3
BSA	Bovine serum albumin
CDM	Cell-derived matrix
cDNA	Complementary deoxyribonucleic acid
cm	Centimetre
C _T	Threshold cycle
Cten	C-terminal tensin-like protein
DAPI	6-diamidino-2-phenylindole
DLC	Deleted in liver cancer
DNA	Deoxyribonucleic acid
DOC	Deoxycholate
DOCi	Deoxycholate insoluble fraction
DOCs	Deoxycholate soluble fraction
ECM	Extracellular matrix
EDTA	Ethylene diamine tetraacetic acid
EGF	Epidermal growth factor
EGTA	Ethylene glycol tetraacetic acid
ELISA	Enzyme-linked immunosorbent assay
EM	Electron microscopy
ERK	Extracellular signal-regulated kinase
FAB	Focal adhesion binding
FAK	Focal adhesion kinase

FCS	Foetal calf serum
FN	Fibronectin
FRAP	Fluorescence recovery after photobleaching
FRET	Förster resonance energy transfer
g	Gram
GAP	GTPase-activating protein
GAPDH	Glyceraldehyde-3-phosphate dehydrogenase
GDI	Guanine nucleotide dissociation inhibitor
GEF	Guanine nucleotide exchange factor
GFP	Green fluorescent protein
HA	Haemagglutinin
HCC	Hepatocellular carcinoma
HEK293	Human embryonic kidney 293
HFF	Human foreskin fibroblast
ILK	Integrin-linked kinase
kDa	Kilodalton
KO	Knockout
l	Litre
M	Molar
mg	Milligram
ml	Millilitre
MLC	Myosin light chain
MLCK	Myosin light chain kinase
mM	Millimolar
MMP	Matrix metalloproteinase
mRNA	Messenger ribonucleic acid
MTOC	Microtubule organising centre
nM	Nanomolar

p130Cas	p130 crk-associated substrate
PBS	Phosphate-buffered saline
PI3K	Phosphoinositide 3-kinase
PIP	Phosphatidylinositol 4-phosphate
PIP2	Phosphatidylinositol 4,5-bisphosphate
PINCH	Particularly interesting new cysteine-histidine-rich protein
PTB	Phosphotyrosine-binding domain
PTEN	Phosphatase and tensin homolog
qPCR	Real-time quantitative polymerase chain reaction
RGD	Arginine-glycine-aspartate
RNA	Ribonucleic acid
RNAi	Ribonucleic acid interference
ROCK	Rho-associated kinase
rpm	Revolutions per minute
Scar/WAVE	Suppressor of cAMP receptor/WASP family verprolin-homologous protein
SDS	Sodium dodecyl sulphate
SDS-PAGE	Sodium dodecyl sulphate polyacrylamide gel electrophoresis
SH2	Src homology 2 domain
siCON	Control siRNA
sihT	Tensin siRNA
siRNA	Small interfering ribonucleic acid
TIF	Telomerase-immortalized fibroblast
v/v	Volume/volume
VASP	Vasodilator-stimulated phosphoprotein
w/v	Weight/volume
(N)-WASP	(Neural)-Wiskott-Aldrich syndrome protein
µg	Microgram

μl	Microlitre
μM	Micromolar

Chapter 1 Introduction

1.1 Cell Adhesion to the Extracellular Matrix

1.1.1 The Role of Cell Adhesion

Complex multicellular organisms are composed of many distinct cell types organised into a variety of different tissues. In order to develop and then to maintain the architecture of such tissues, cell surface molecules have evolved which allow cells to interact both with each other and with the extracellular matrix (ECM). The expression and activity of these molecules is under tight spatiotemporal control to ensure that particular cell adhesion events only occur at the appropriate place and time. During embryogenesis, for example, gastrulation and organogenesis are driven by strictly regulated changes in cell adhesion, and accordingly the genetic disruption of adhesion-related genes in mice often results in developmental defects or embryonic lethality (Hynes, 1996; Bouvard *et al.*, 2001). In adult organisms, cell adhesion is necessary to preserve tissue organisation and to support cell migration events such as those that are required for wound healing. The dynamic regulation of cell adhesion is particularly important for the function of immune cells, and abnormalities in the receptors that mediate these adhesive interactions can impair the immune response, such is the case for the leukocyte adhesion deficiency (LAD) syndromes (Ley *et al.*, 2007; Abram and Lowell, 2009).

Cell culture studies have demonstrated the fundamental importance of cell-ECM interactions in a wide range of biological processes, including cell migration, proliferation, the suppression of apoptosis, and differentiation (Vicente-Manzanares *et al.*, 2009; Streuli, 2009). Both the composition and physical properties of the ECM are thought to influence cell behaviour, and changes in the recognition of, or response to, these properties can have pathological consequences such as the uncontrolled proliferation and metastatic migration of cancer cells.

1.1.2 The ECM

The ECM is composed of many different proteins such as collagens, laminins, and fibronectin (FN) as well as polysaccharides of the glycosaminoglycan (GAG) class, which are often covalently attached to proteins to form proteoglycans (Alberts, 2002). These molecules interact with each other to form a macromolecular complex that can be organised into specialised structures such as the basement membrane that separates epithelial cells from the underlying tissue. The polysaccharides of the ECM form a highly hydrated gel, which resists compressive forces and permits the diffusion of smaller molecules through tissues. The fibrous proteins are embedded within this gel and help to determine the structural and adhesive properties of the ECM. Variation in the relative amounts and organisation of these different matrix macromolecules determine the chemical and physical properties of the ECM, and this must be tailored to suit the functional requirements of the particular tissue in which they are secreted and assembled (Alberts, 2002).

The correct assembly of the ECM is necessary for directing morphogenesis during development and in the maintenance of tissue integrity and patterning in the adult. However, it is becoming clear that in addition to its structural role, the ECM also plays an active part in regulating many aspects of cell behaviour by initiating signalling events inside the cell.

1.1.3 Integrin-Mediated Cell Adhesion

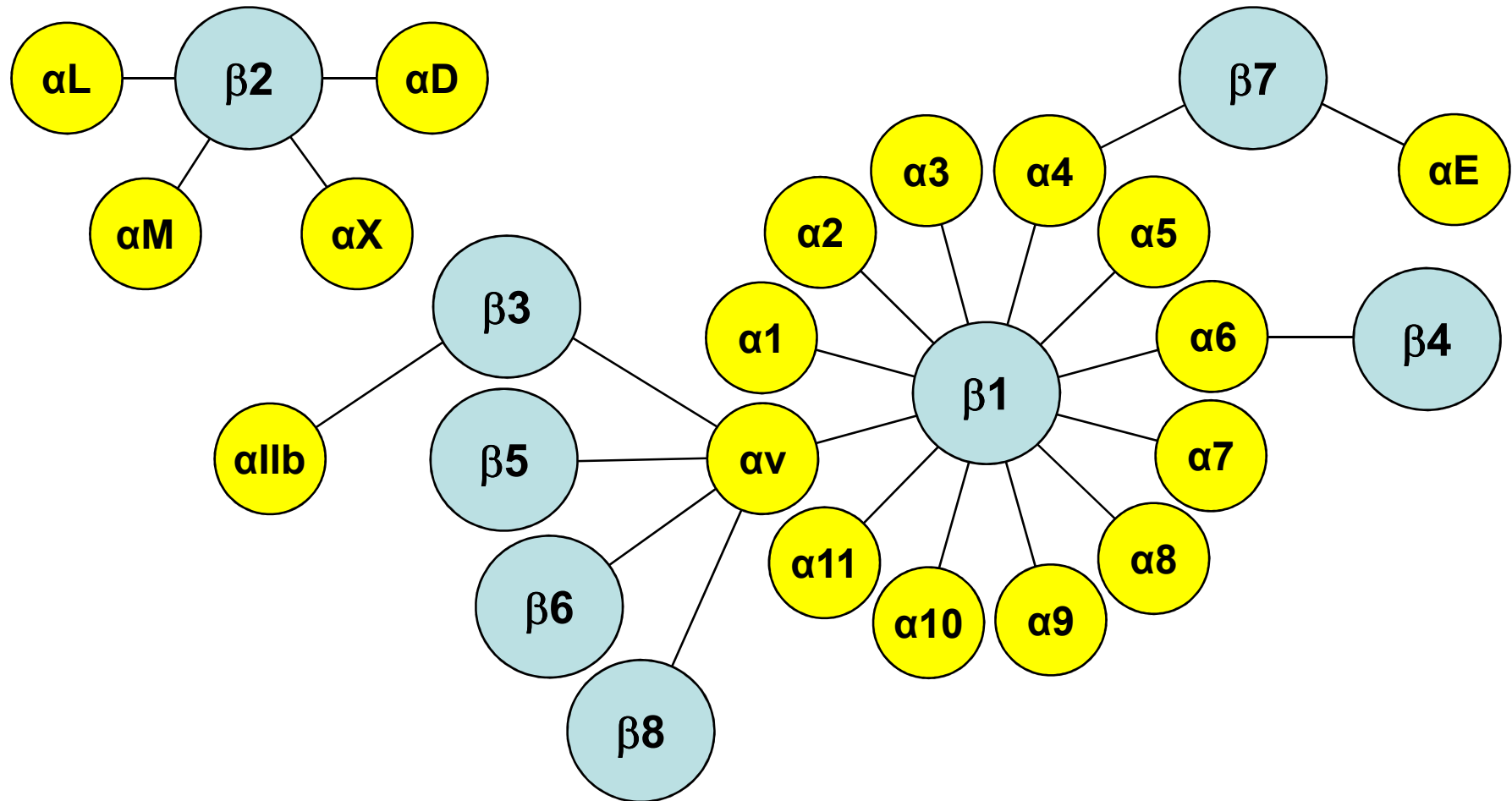
Cell adhesion to the ECM is mediated predominantly by the integrin family of heterodimeric transmembrane glycoproteins. Each integrin dimer consists of an α and a β subunit, which are non-covalently linked. The complete set of mammalian integrins is thought to comprise of 18 α and 8 β subunits, which can assemble into 24 distinct

integrin heterodimers (Hynes, 2002) (Figure 1.1). The combination of α and β subunit in an integrin heterodimer determines the specificity of the integrin receptor for a particular set of ligands (Humphries *et al.*, 2006) (Table 1.1). For example, the $\alpha_5\beta_1$ integrin shows specificity towards FN, whereas the preferred ligands of the $\alpha_2\beta_1$ integrin are collagen and laminin. It is noteworthy that some integrin heterodimers can also bind to counter receptors on the surface of other cells, and this form of integrin-mediated cell-cell adhesion is particularly important for the immune response. In leukocytes, for example, integrins facilitate rolling and firm adhesion to the blood vessel wall at sites of inflammation by interacting with intercellular adhesion molecules (ICAMs) and vascular cell adhesion molecules (VCAMs) expressed on the surface of endothelial cells (Evans *et al.*, 2009).

The importance of integrin-mediated adhesion during development and in the adult organism is exemplified by genetic ablation studies in mice and diseases in humans that result from the disruption of integrin function (Bouvard *et al.*, 2001; Hillis and MacLeod, 1996). For example, mutant mice lacking β_1 integrin die at implantation and fail to gastrulate (Stephens *et al.*, 1995; Fassler and Meyer, 1995), which is not surprising given that this integrin is known to pair with at least 12 different α subunits to mediate interactions with a diverse array of ligands. The human bleeding disorder Glanzmann Thrombasthenia is caused by abnormalities in the fibrinogen receptor $\alpha_{IIb}\beta_3$, which results in the failure of platelet aggregation and thus defective thrombus formation at sites of blood vessel injury (Nurden, 2006). Finally, integrin expression is often deregulated in cancer cells (Mizejewski, 1999; Thomas *et al.*, 2006).

1.1.4 Integrin Structure

Both α and β integrin subunits are type I transmembrane proteins with large (>700 residue) N-terminal extracellular domains and generally short (13-70 residue) C-



5

Figure 1.1: Human integrin heterodimer combinations. Integrins are heterodimeric glycoproteins, consisting of one α and one β subunit. The human genome is thought to encode 18 α and 8 β subunits, which can assemble into 24 distinct $\alpha\beta$ heterodimers.

Integrin Heterodimer	Major Ligands
$\alpha 1$ ————— $\beta 1$	Laminin, Collagen
$\alpha 2$ ————— $\beta 1$	Laminin, Collagen, Thrombospondin
$\alpha 3$ ————— $\beta 1$	Laminin
$\alpha 4$ ————— $\beta 1$	FN, VCAM-1
$\alpha 5$ ————— $\beta 1$	FN
$\alpha 6$ ————— $\beta 1$	Laminin
$\alpha 7$ ————— $\beta 1$	Laminin
$\alpha 8$ ————— $\beta 1$	Nephronectin, FN, Tenascin
$\alpha 9$ ————— $\beta 1$	Tenascin, VCAM-1
$\alpha 10$ ————— $\beta 1$	Collagen, Laminin
$\alpha 11$ ————— $\beta 1$	Collagen
αV ————— $\beta 1$	FN, Osteopontin
αL ————— $\beta 2$	ICAM-1, -2, -3
αM ————— $\beta 2$	ICAM-1, Fibrinogen, iC3b, Factor X
αX ————— $\beta 2$	ICAM-1, Fibrinogen, iC3b, Factor X
αD ————— $\beta 2$	VCAM-1, ICAM, Fibrinogen
αIIb ————— $\beta 3$	Fibrinogen
αV ————— $\beta 3$	FN, Vitronectin
$\alpha 6$ ————— $\beta 4$	Laminin
αV ————— $\beta 5$	Vitronectin
αV ————— $\beta 6$	Vitronectin, FN, Latent TGF- β
$\alpha 4$ ————— $\beta 7$	MAdCAM-1, FN, VCAM
αE ————— $\beta 7$	E-Cadherin
αV ————— $\beta 8$	Vitronectin, Laminin, TGF- β -LAP

Table 1.1: Human integrin ligand specificity. Listed above are the major ligands for the 24 known integrin heterodimers. VCAM (vascular cell adhesion molecule), ICAM (intercellular adhesion molecule), iC3b (inactivated complement component 3b), Latent TGF- β (latent transforming growth factor β), MAdCAM-1 (mucosal addressin cell adhesion molecule 1), TGF- β -LAP (transforming growth factor β latency associated peptide).

terminal cytoplasmic domains. Of the 18 mammalian α subunits, nine contain an additional ~200 amino acid insert (the α A-domain) that is homologous to the A-domain of von Willebrand factor (Humphries, 2000). As a result, integrin heterodimers can be divided into two subfamilies according to the presence or absence of an A-domain in the α subunit. The inclusion or exclusion of this domain has a profound effect on the mechanism of ligand binding exhibited by the integrin heterodimer, which will be discussed later.

In the 1980s electron microscopy (EM) studies on purified integrin receptors revealed that an integrin heterodimer consists of a large headpiece with two protruding rod-like legs (Carrell *et al.*, 1985; Nermut *et al.*, 1988). More than a decade later the X-ray crystal structure of the extracellular segment of $\alpha_v\beta_3$ integrin was published (Xiong *et al.*, 2001), and this was closely followed by the structure of this integrin in complex with its ligand by soaking an arginine-glycine-aspartate (RGD)-containing peptide into pre-existing $\alpha_v\beta_3$ crystals (Xiong *et al.*, 2002). These high resolution studies revealed that the extracellular portion of each integrin subunit adopts a modular conformation (schematically represented in Figure 1.2). The membrane-distal head consists of a seven-bladed β -propeller domain from the α subunit and an A-domain from the β subunit (termed the β A-domain), which together form the functional unit required for ligand binding. The remainder of the α subunit is composed of an Ig-like 'thigh' domain and two β -sandwich domains known as 'calf1' and 'calf2', which form a leg-like structure with a highly flexible 'knee' (or 'genu') between the thigh and calf1 domains. The β subunit leg is comprised of an Ig-like hybrid domain, a plexin-semaphorin-integrin (PSI) domain, four epidermal growth factor (EGF)-like repeats and a membrane proximal β -tail domain (containing a cystatin-like fold). The β subunit leg is thought to bend through the flexibility of several domain linkers, although a knee region may be located between the EGF-1 and EGF-2 domains, which were poorly resolved in the crystal structure. Surprisingly, in the crystal structures the integrin legs were shown

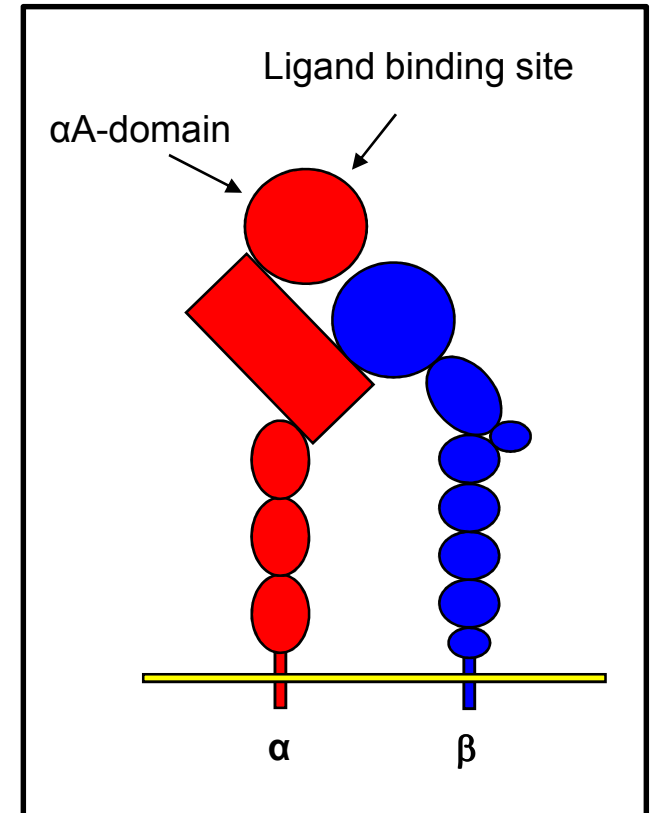
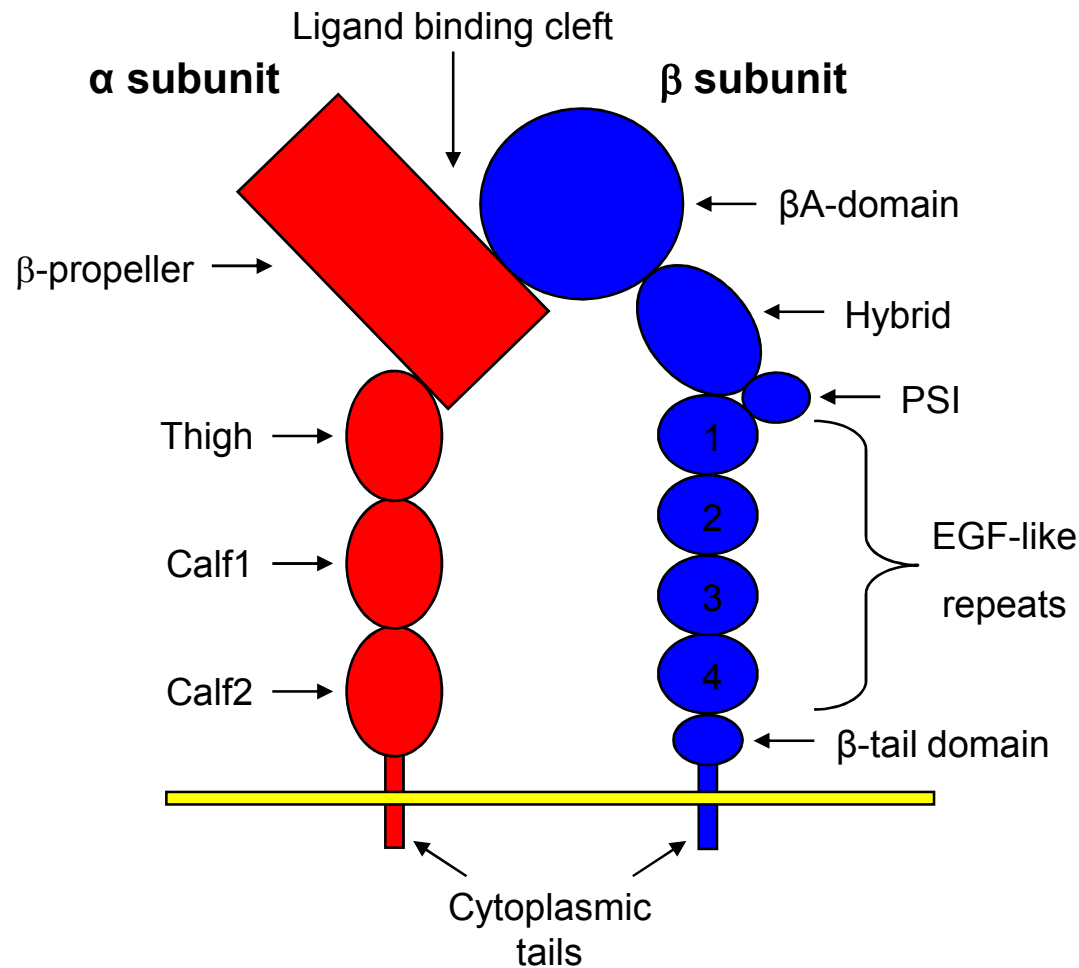


Figure 1.2: Domain structure of an integrin heterodimer. The ectodomains of α and β integrin subunits adopt a modular conformation. This is a schematic representation of the proposed modular structure of an integrin heterodimer, based on the crystal structures obtained by Xiong and co-workers. Inset: hypothesised structure of an α A-domain-containing integrin heterodimer. PSI (plexin-semaphorin-integrin), EGF (epidermal growth factor).

to be bent through 135°, which would position the ligand-binding headpiece towards the cell surface. This unexpected finding raises a number of questions regarding the relationship between integrin conformation and function, which will be discussed later (Arnaout *et al.*, 2007; Askari *et al.*, 2009).

The crystal structure of the $\alpha_v\beta_3$ -RGD complex revealed that the peptide ligand lies at the interface between the upper surfaces of the α subunit β -propeller domain and β subunit β A-domain (Xiong *et al.*, 2002). The arginine residue fits into a cleft in the β -propeller whilst the carboxyl group of the aspartate residue coordinates a Mn^{2+} ion bound to a metal ion-dependent adhesion site (MIDAS) in the β A-domain. This ligand-cation-receptor interaction was also seen in the crystal structure of the α_2 A-domain in complex with a triple helical collagen peptide (Emsley *et al.*, 2000). Hence, for α A-domain-containing integrin receptors it is thought that this additional domain, which is inserted into the α subunit β -propeller on the same face that interacts with the β A-domain, represents the major or exclusive ligand binding site (Figure 1.2).

1.1.5 Integrin Activation

Integrins are known to adopt three major functional states; inactive (low affinity), primed/active (high affinity), and ligand occupied. However, there is uncertainty surrounding the nature of the conformation adopted by the integrin ectodomain in each of these functional states, which has led to the proposal of several different models to explain the relationship between integrin structure and function. The most widely accepted theory is the 'switchblade' model in which the three functional states correspond to bent, extended, and extended with open head piece conformations, respectively (Askari *et al.*, 2009). In support of this model, several EM studies have reported that the bent and extended conformations represent inactive and active integrin receptors, respectively (Takagi *et al.*, 2002; Nishida *et al.*, 2006). However, it

was recently suggested that leg extension does not itself cause increased affinity for ligand, but rather increases ligand capture efficiency (Chigaev *et al.*, 2007), and one EM study has shown that the $\alpha_v\beta_3$ integrin remains in a bent conformation whilst in complex with a fragment of FN (Adair *et al.*, 2005). These studies, together with the crystallographic data of the bent $\alpha_v\beta_3$ -RGD complex, favour an alternative theory of integrin activation that negates the requirement for gross conformational changes in the integrin before ligand-binding. This is known as the 'deadbolt' model (Xiong *et al.*, 2003; Arnaout *et al.*, 2007).

Despite the ongoing debate over the relationship between leg extension and ligand binding, it is generally accepted that ligand binding is accompanied by structural rearrangements in the β A-domain, which are thought to be linked to the outward movement of the β subunit hybrid domain (Xiao *et al.*, 2004). For α A-domain containing integrin heterodimers, it has been shown that an interaction between the β A-domain and a C-terminal linker connecting the α A-domain to the β -propeller may facilitate inter-subunit signal transmission (Yang *et al.*, 2004).

1.1.6 Integrin Signalling

In addition to their structural role as transmembrane adhesion molecules, integrins also serve to transmit signals in a bidirectional manner across the plasma membrane via so-called outside-in and inside-out signalling (Harburger and Calderwood, 2009). Outside-in signalling involves activation of the integrin through ligand binding, which in turn triggers intracellular signal transduction pathways through molecules associated with the integrin cytoplasmic tails (Hynes, 2002; Miranti and Brugge, 2002). Conversely, inside-out signalling describes the alteration of integrin activation state by signalling events occurring within the cell that impinge on the integrin cytoplasmic tails (Calderwood, 2004a). Integrin signalling can modulate many aspects of cell behaviour

including proliferation, survival/apoptosis, shape, polarity, motility, matrix remodelling, gene expression and differentiation (Harburger and Calderwood, 2009).

In the 1960s it was shown that normal adherent cells are unable to proliferate in suspension, and they are said to be 'anchorage-dependent' for growth (Stoker *et al.*, 1968). Thirty years later it was found that integrins were the adhesion molecules responsible for this anchorage dependence, and in the absence of integrin-mediated adhesion cells undergo apoptosis, a phenomenon that was subsequently named anoikis (a term derived from the Greek word for homelessness) (Meredith *et al.*, 1993; Frisch and Francis, 1994). These studies demonstrated that integrin engagement could somehow signal to the cell interior to promote proliferation and prevent apoptosis i.e. outside-in signalling. However, integrins lack intrinsic enzymatic activity. Therefore, to mediate outside-in signalling, ligated integrins cluster and recruit a number of structural and signalling proteins via their cytoplasmic tails, which leads to the assembly of a signalling adhesion plaque at the cell surface. The plethora of recruited signalling molecules includes protein and lipid kinases, protein and lipid phosphatases, and GTPases (Zaidel-Bar *et al.*, 2007a). Arguably the best studied integrin-activated signalling proteins are the non-receptor tyrosine kinases, focal adhesion kinase (FAK) and Src, which form a dual kinase complex (Mitra and Schlaepfer, 2006). Integrin-induced FAK-Src activation triggers multiple signalling cascades that function to promote cell proliferation, survival and motility, and aberrant FAK-Src activation is thought to be responsible for tumour growth and metastasis in many cancers (Mitra and Schlaepfer, 2006). It is now becoming clear that integrins can co-operate, both directly (through complex formation) and indirectly (through signalling), with other receptor systems to regulate biochemical responses in multiple cell types (Streuli and Akhtar, 2009). For example, integrins can promote growth factor signalling both through ECM-induced integrin clustering, which can activate integrin-bound receptor

tyrosine kinases in the absence of growth factor (Miyamoto *et al.*, 1996), and via shared downstream signalling molecules (Alam *et al.*, 2007).

Integrins are not constantly maintained in a ligand-competent state awaiting contact with their cognate binding partners as this would result in inappropriate adhesion events at the wrong time and place in the body. Instead, integrin-independent signals, such as the ligation of selectins on neutrophils (Green *et al.*, 2004) or the binding of thrombin to receptors on platelets (Stouffer and Smyth, 2003), initiate intracellular signalling cascades that activate integrins from within the cell i.e. inside-out signalling. In low affinity (inactive) integrins, it is proposed that the cytoplasmic integrin tails are held together (possibly through a membrane-proximal inter-subunit salt bridge) and disrupting this interaction was shown to activate integrins (Hughes *et al.*, 1996; Vinogradova *et al.*, 2000). Disruption of this salt bridge along with the separation of the integrin transmembrane domains, which are held together through hydrophobic interactions (Lau *et al.*, 2009), appears to drive the conformational rearrangements of the extracellular domains required for integrin activation. It is widely accepted that the cytoskeletal protein talin activates integrins by binding to the β integrin cytoplasmic tail and inducing tail separation (Wegener *et al.*, 2007; Vinogradova *et al.*, 2002; Kim *et al.*, 2003; Tadokoro *et al.*, 2003). However, recent studies have also implicated the kindlin family of integrin-binding proteins as regulators of integrin activation (Ussar *et al.*, 2008; Montanez *et al.*, 2008; Moser *et al.*, 2008).

1.1.7 The Integrin-Cytoskeletal Connection

The generally short integrin cytoplasmic tails are frequently linked to the actin cytoskeleton. The exception to this rule is the $\alpha_6\beta_4$ integrin, which binds to intermediate filaments by virtue of the abnormally long cytoplasmic domain of the β_4 integrin, and is localised to hemi-desmosomes (Wilhelmsen *et al.*, 2006). Coupling to F-actin allows

integrins to act as tension-bearing mechanical links between the ECM and the actomyosin contractile apparatus, which is particularly important for the ability of integrins to facilitate cell migration and matrix remodelling. Integrins are unable to associate directly with the actin cytoskeleton; instead a series of proteins have emerged throughout the course of evolution that bridge the gap between integrins and the cytoskeleton, either directly or indirectly. These proteins often contain multiple protein-binding modules, which enable them to recruit other structural and signalling molecules to the site of integrin clustering, ready to participate in integrin signalling events.

Many of these linker molecules can bind directly to the short integrin tails, which contains hotspots, such as the NPXY motif in the β integrin tail, which are capable of binding several adaptor proteins (Figure 1.3). Indeed, a recent study identified 42 β integrin tail-binding adaptor proteins, which compete for relatively few binding sites (Legate and Fassler, 2009). Therefore, the cell has developed regulatory mechanisms, such as phosphorylation of the β integrin tail, to regulate the spatial and temporal binding of these adaptor proteins, which in turn modulates the composition and signalling capacity of the adhesion. Finally, some adaptor molecules can directly couple integrins to actin, including talin, α -actinin, filamin, and tensin, the focus of this study.

1.2 Cellular Junctions with the ECM

1.2.1 Different Types of Cell-ECM Adhesions

As alluded to previously, ligand-bound integrins are not spread randomly over the cell surface. Instead, they cluster at sites of cell-ECM attachment due to the multivalent nature of their ligands. Integrin clustering induces the formation of multiprotein

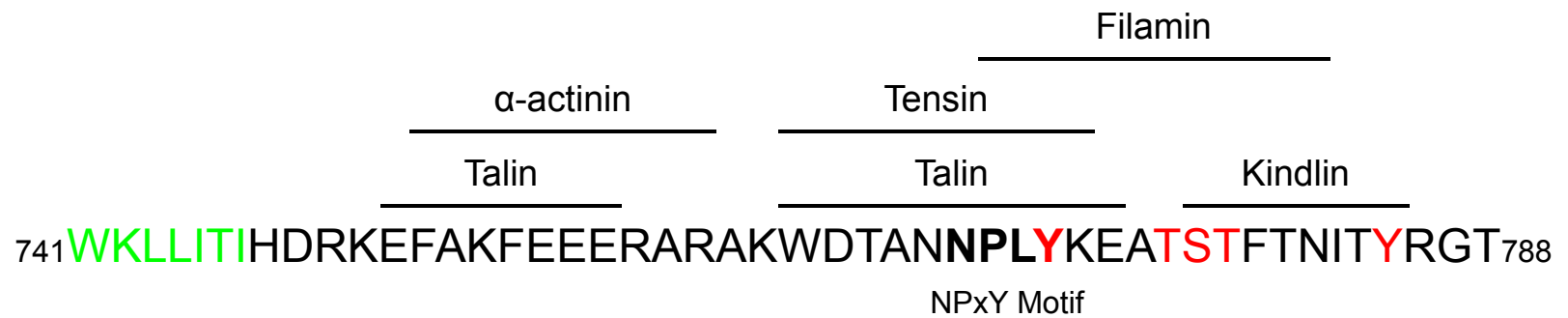


Figure 1.3: Adaptor-binding sites in β 3 integrin cytoplasmic tail. Shown by black lines are the mapped binding sites for selected adaptor proteins. Residues in green are buried in the membrane and residues in red can be phosphorylated by various kinases.

adhesion plaques on the cytoplasmic side of the plasma membrane, which physically link integrin tails to the actin cytoskeleton, and also concentrates the proteins necessary for integrin-mediated signalling. Database mining combined with an extensive literature search has recently identified 156 different components that localise to integrin-mediated adhesions, which together with the interactions they make with each other are referred to as the 'integrin adhesome' (Zaidel-Bar *et al.*, 2007a). This diverse array of components includes adhesion proteins, transmembrane receptors, adaptor proteins, cytoskeletal proteins, actin-binding proteins, kinases, phosphatases, GTPases and their regulatory proteins.

There are several different types of integrin-mediated adhesion structures, namely focal complexes, focal adhesions, fibrillar adhesions, 3-dimensional (3D)-matrix adhesions, podosomes and invadopodia, which share varying degrees of molecular similarity with one another (Zaidel-Bar *et al.*, 2004; Cukierman *et al.*, 2002; Block *et al.*, 2008). Collectively, these adhesive contacts enable cells to sense the chemical and physical properties of their environment and respond accordingly by facilitating cell adhesion and migration, as well as ECM assembly, remodelling and degradation.

1.2.2 Focal Complexes

The formation of focal complexes, focal adhesions and fibrillar adhesions is thought to occur in a sequential manner through a series of maturation events (Zaidel-Bar *et al.*, 2004). However, prior to the formation of these integrin-mediated adhesions it has been shown that cells first attach to external surfaces through a several micrometer-thick hyaluronan-based pericellular coat (Zimmerman *et al.*, 2002). This hyaluronan-mediated early adhesion is then followed about 2-10 minutes later by the formation of paxillin-rich focal complexes (Cohen *et al.*, 2006).

Focal complexes are small dot-like structures, which emerge from highly dynamic nascent adhesions at the edges of lamellipodia in spreading and migrating cells (Bershadsky *et al.*, 1985; Nobes and Hall, 1995; Choi *et al.*, 2008). The formation of focal complexes is induced by activation of Rac, a member of the Rho-family of small GTP binding proteins (Nobes and Hall, 1995; Rottner *et al.*, 1999), which is active at the leading edge of motile cells (Kraynov *et al.*, 2000). Focal complexes are enriched with $\alpha_v\beta_3$ integrin and phosphotyrosine, but their precise molecular composition is highly dependent on their age, with proteins such as talin and paxillin incorporated soon after formation, followed later by vinculin and FAK, and then VASP (vasodilator-stimulated phosphoprotein) and α -actinin (Zaidel-Bar *et al.*, 2003). It is noteworthy that other adhesion-related proteins such as tensin and zyxin are essentially absent from focal complexes (Zaidel-Bar *et al.*, 2003).

Focal complexes are essential for cell spreading and migration, but they are thought to exist only transiently. In advancing lamellipodia, focal complexes are disassembled and replaced by new adhesions formed in front of them (Rottner *et al.*, 1999); however, if the lamella stops protruding or retracts then a subset of focal complexes will persist and mature into larger structures called focal adhesions (Zaidel-Bar *et al.*, 2003).

1.2.3 Focal Adhesions

Focal adhesions were first discovered in the 1970s using EM and interference-reflection microscopy on cells grown in culture (Abercrombie and Dunn, 1975; Abercrombie *et al.*, 1971). These studies demonstrated that cells do not attach uniformly to the ECM, but instead contain specialised regions (around a few microns in length) along the ventral plasma membrane that are closely apposed to the substratum. By definition, focal adhesions are formed by cultured cells growing on rigid surfaces, which led many to speculate that they were artifactual structures that did not

assemble *in vivo*. However, it has since been demonstrated that structures with similar molecular properties to focal adhesions are formed in a number of physiological situations, such as by skeletal muscle cells at myotendinous junctions (Turner *et al.*, 1991) and in blood vessels at points of high fluid shear stress (Romer *et al.*, 2006).

Focal complex maturation into focal adhesions occurs at the lamellipodium-lamella interface and requires the activation of Rho, which promotes actomyosin contraction and thereby triggers integrin clustering in the plane of the membrane i.e. adhesion growth (Clark *et al.*, 1998; Rottner *et al.*, 1999). In addition to an increase in size, maturation is also accompanied by an increase in adhesion complexity through the recruitment of several further proteins, including zyxin (Zaidel-Bar *et al.*, 2003), tensin, and $\alpha_5\beta_1$ integrin (Cukierman *et al.*, 2001). Furthermore, Rho-stimulated actomyosin contractility also induces the assembly of an actin stress fibre that terminates at the focal adhesion (Chrzanowska-Wodnicka and Burridge, 1996). Stress fibres consist of a bundle of antiparallel actin filaments and a number of accessory proteins, including actin filament cross-linkers such as α -actinin and myosin II (Pellegrin and Mellor, 2007). By anchoring actin stress fibres, focal adhesions form a strong, tension-bearing link between the cytoskeleton and the ECM.

Despite their robust appearance, focal adhesions are highly dynamic in nature. Early fluorescence recovery after photobleaching (FRAP) studies revealed that many components of focal adhesions, including actin, vinculin and α -actinin, are in rapid exchange between adhesion-associated and cytoplasmic pools (Kreis *et al.*, 1982; Birchmeier *et al.*, 1982). Moreover, some focal adhesion proteins, including zyxin (Nix and Beckerle, 1997) and paxillin (Woods *et al.*, 2002), have been found to shuttle between the cytoplasm and the nucleus, where they may influence gene transcription or facilitate the nuclear export of mRNAs (Hervy *et al.*, 2006). Furthermore, focal adhesions can also completely disassemble which is particularly important for cell

migration, and is thought to be regulated at least in part by microtubule targeting (Kaverina *et al.*, 1999) and FAK-Src signalling (Webb *et al.*, 2004).

The application of contractile force to adhesions appears to induce one of two responses, depending on the physical properties of the matrix. When the matrix is rigid, endogenous tension results in adhesion growth, as described above. However, if the matrix is flexible, then pulling can lead to translocation of the receptor, along with the ECM, which results in the formation of an elongated fibrillar adhesion in some cell types, most notably fibroblasts (Katz *et al.*, 2000a).

1.2.4 Fibrillar Adhesions

Fibrillar adhesions, previously known as ECM contacts (Chen and Singer, 1982), are elongated structures, located on the ventral and dorsal side of cells cultured on 2-dimensional (2D) surfaces (Zamir *et al.*, 1999). Fibrillar adhesions are molecularly distinct from focal adhesions, and are enriched in $\alpha_5\beta_1$ integrin and tensin, whilst they are deficient in other focal adhesion markers such as $\alpha_v\beta_3$ integrin, talin, α -actinin, vinculin, FAK and phosphotyrosine (Zamir *et al.*, 1999; Katz *et al.*, 2000a). Fibrillar adhesion formation is characterised by the translocation of FN, $\alpha_5\beta_1$ integrin and tensin along actin filaments from peripherally located focal adhesions towards the centre of the cell (Pankov *et al.*, 2000; Zamir *et al.*, 2000). This process, which requires both an intact actin cytoskeleton and actomyosin contraction, is thought to exert force on surface-associated FN, exposing cryptic self-association sites within the FN molecules, thereby promoting FN fibrillogenesis (Pankov *et al.*, 2000; Zamir *et al.*, 2000; Ohashi *et al.*, 2002) (Figure 1.4). Actomyosin contraction is thought to be required for fibrillar adhesion formation, although it is not required for their maintenance, unlike in the case of focal adhesions (Chrzanowska-Wodnicka and Burridge, 1996; Zamir *et al.*, 1999; Zamir *et al.*, 2000). FN itself is also a key regulator of the segregation of fibrillar

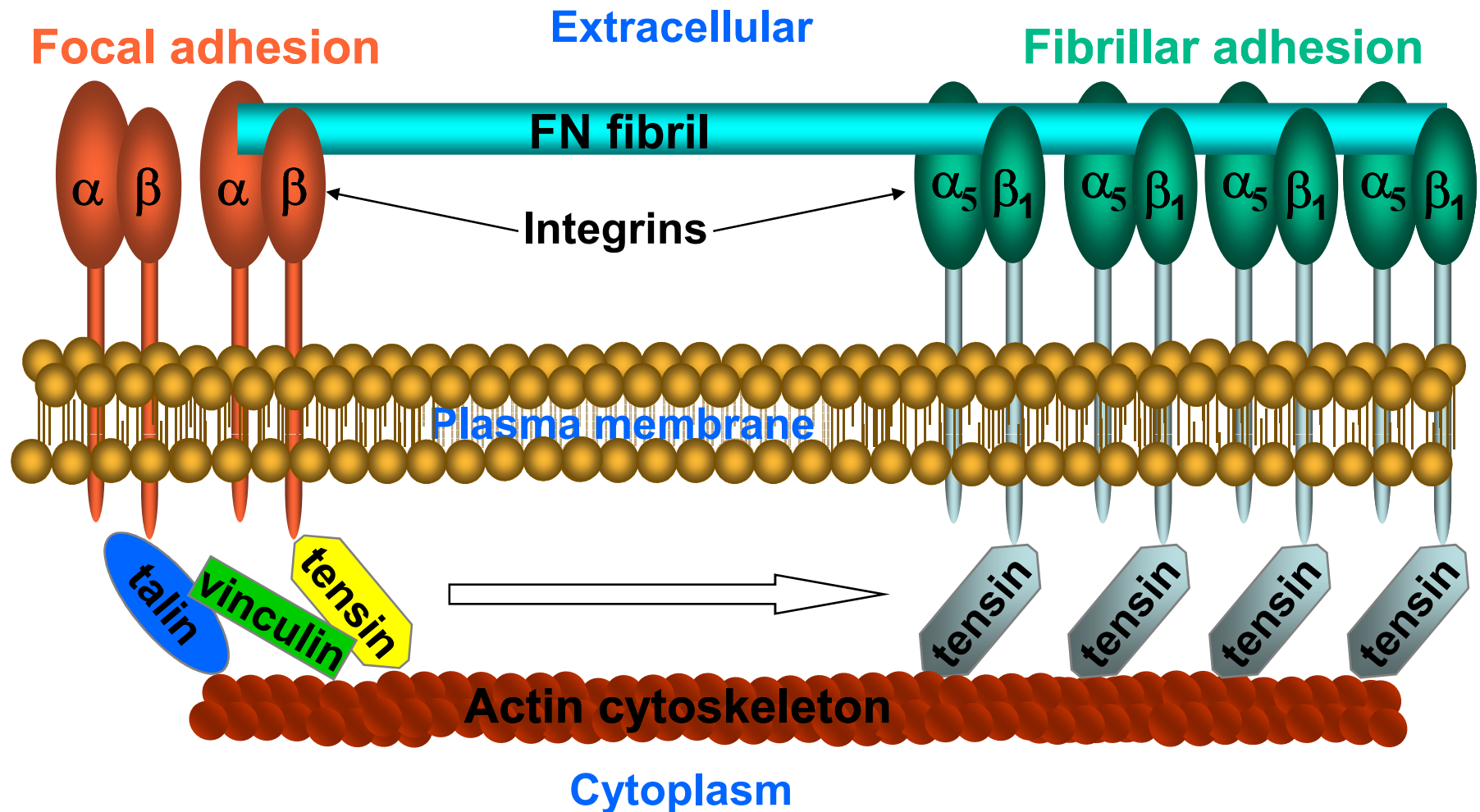


Figure 1.4: Fibrillar adhesion formation. Fibrillar adhesion formation is characterised by the centripetal translocation of tensin in association with $\alpha_5\beta_1$ integrin and FN from peripherally located focal adhesions towards the centre of the cell. Integrin translocation into fibrillar adhesions is thought to facilitate FN matrix assembly through the unfolding of FN molecules using force transduced from the actomyosin contractile apparatus.

adhesions from focal adhesions, as FN-null cells are unable to form fibrillar adhesions, instead displaying only focal adhesions containing both vinculin and tensin (Sottile and Hocking, 2002).

The initiation of fibrillar adhesion formation is thought to require the activity of two adhesion-associated tyrosine kinases, namely Src and FAK (Volberg *et al.*, 2001; Ilic *et al.*, 2004). Src-null cells display reduced tyrosine phosphorylation of several adhesion plaque proteins, including FAK, paxillin and tensin, and are also incapable of segregating tensin into fibrillar adhesions, which results in the formation of large phosphotyrosine-poor, tensin-rich focal adhesions (Volberg *et al.*, 2001). Similarly, FAK-null cells also lack fibrillar adhesions and exhibit impaired FN fibrillogenesis, and only the re-expression of wild-type FAK, and not a kinase-dead mutant, is able to rescue this phenotype (Ilic *et al.*, 2004). The mechanism by which FAK and Src promote fibrillar adhesion formation is incompletely understood, although tensin seems to play a key role. Tensin is a known substrate and binding partner for both FAK (Zhu *et al.*, 1998b) and Src (Qian *et al.*, 2009). Therefore, it was hypothesised that tensin phosphorylation may induce an intramolecular interaction between the phosphorylation site and one of the two phosphotyrosine-binding modules within the C-terminus of the molecule, thereby perturbing interactions with other focal adhesion proteins and permitting its translocation. This type of conformational rearrangement is thought to regulate the binding activity of several other adhesion-related proteins, most notably vinculin (Ziegler *et al.*, 2006). However, recent studies have identified another mechanism through which kinase activity could regulate fibrillar adhesion formation, whereby tyrosine phosphorylation of the integrin tail, by Src for example (Tapley *et al.*, 1989), could promote tensin recruitment to focal adhesions and consequently induce their maturation (Calderwood *et al.*, 2003; McCleverty *et al.*, 2007; Legate and Fassler, 2009). This model will be discussed in more detail later.

More recently integrin-linked kinase (ILK) has been identified as a key player in fibrillar adhesion formation (Vouret-Craviari *et al.*, 2004). ILK was found to co-localise with $\alpha_5\beta_1$ integrin in fibrillar adhesions, and the siRNA-mediated depletion of ILK expression prevented fibrillar adhesion formation and FN fibrillogenesis (Vouret-Craviari *et al.*, 2004). Despite its name, ILK is thought to function more as an adaptor molecule than a kinase, through its numerous protein-binding modules (Zervas and Brown, 2002; Boulter and Van Obberghen-Schilling, 2006). ILK forms a trimeric complex with the proteins PINCH (particularly interesting new cysteine-histidine-rich protein) and parvin, known as the IPP-complex (Legate *et al.*, 2006). ILK is the central component of the IPP-complex, which is thought to assemble in the cytoplasm prior to its recruitment to adhesion sites through a direct interaction between ILK the β integrin tail (Zhang *et al.*, 2002; Hannigan *et al.*, 1996). Formation of the IPP-complex is thought to be essential for the stability of each of its components as depletion of one leads to extensive proteasome-mediated degradation of the other two (Fukuda *et al.*, 2003). A recent study reported that disruption of the IPP-complex through deletion of the genes encoding ILK or PINCH1 blocks the maturation of focal adhesions into fibrillar adhesions (Stanchi *et al.*, 2009). Moreover, in ILK- and PINCH1-null cells, tensin1 and zyxin protein levels were also down-regulated through an unknown mechanism. Furthermore, fusing ILK, PINCH1 or α -parvin to the cytoplasmic tail of β_3 integrin led to the tight association of the IPP complex with this focal adhesion integrin, and also drove its localisation to tensin-rich, phosphotyrosine-poor fibrillar adhesions in wild-type cells (Stanchi *et al.*, 2009).

Changes in the expression, post-translational modification, and structural conformation of several other proteins have been implicated in fibrillar adhesion formation, including calreticulin, paxillin and the $\alpha_5\beta_1$ integrin itself (Papp *et al.*, 2007; Zaidel-Bar *et al.*, 2007b; Clark *et al.*, 2005). Expression of the Ca^{2+} -binding protein calreticulin, which acts as a chaperone in the ER, positively correlates with the formation of fibrillar

adhesion and the extent FN fibrillogenesis (Papp *et al.*, 2007). Calreticulin also induces vinculin expression and focal adhesion formation (Opas *et al.*, 1996). Vinculin is thought to stabilise focal adhesions (Ziegler *et al.*, 2006) and this could provide a firm anchorage point for the tension-dependent assembly of fibrillar adhesions and the stretching of FN that is required for FN fibrillogenesis. The focal adhesion protein paxillin was initially viewed as a relatively minor component of fibrillar adhesions (Zamir *et al.*, 1999; Katz *et al.*, 2000a). However, a more recent study has revealed that fibrillar adhesions are rich in the non-phosphorylated form of this protein, and dephosphorylation of paxillin is required for fibrillar adhesion formation and enhances FN fibrillogenesis (Zaidel-Bar *et al.*, 2007b). Finally, the $\alpha_5\beta_1$ integrin is thought to adopt a unique conformation in fibrillar adhesions, and an antibody which preferentially recognised $\alpha_5\beta_1$ integrin in this conformation was shown to convert this integrin into a ligand-competent form and therefore stimulate fibrillar adhesion formation and FN fibrillogenesis (Clark *et al.*, 2005).

1.2.5 3D-Matrix Adhesions

The adhesion types described thus far are all formed by fibroblasts cultured on 2D surfaces. However, given time, fibroblastic cells will synthesise and assemble an elaborate cell-associated matrix, and detach from the rigid 2D substratum in favour of this more *in vivo*-like environment, which leads to the assembly of a new class of adhesion structure, known as the 3D-matrix adhesion (Cukierman *et al.*, 2001; Cukierman *et al.*, 2002).

3D-matrix adhesions, which have also been detected in tissues, are very long structures that possess a distinct molecular composition and phosphorylation pattern from the previously mentioned adhesion structures (Cukierman *et al.*, 2001). Like fibrillar adhesions, 3D-matrix adhesions align with FN fibrils and are highly dependent

on the FN receptor $\alpha_5\beta_1$ integrin and tensin; however, they are also enriched in several focal adhesion proteins, such as vinculin and FAK, and contain high levels of phosphotyrosine (Cukierman *et al.*, 2001). Interestingly, levels of FAK Y397 phosphorylation (an indicator of FAK activity) are low in 3D-matrix adhesions compared to focal adhesions, which would suggest that integrin signalling can differ substantially in 3D versus 2D environments (Green and Yamada, 2007; Yamada *et al.*, 2003).

Culturing fibroblastic cells within 3D cell-derived matrix (CDM), which is rich in fibrillar FN and collagen, has also been shown to increase attachment rate, induce the rapid acquisition of a more *in vivo*-like morphology that is slender and elongated, promote cell migration, and even increase cell proliferation rates, compared to 2D substrates of purified FN or collagen (Cukierman *et al.*, 2001). Moreover, sandwiching cells between two 2D surfaces, which partially mimics a 3D environment, can also induce the acquisition of an *in vivo*-like morphology (Beningo *et al.*, 2004). However, converting 3D CDMs into 2D substrates, either by mechanical compression or solubilisation and coating onto planar surfaces, abolished the enhancing effects of 3D matrix on attachment, spreading, and proliferation (Cukierman *et al.*, 2001). These studies indicate that dimensionality plays an important role in the response of cells to cell-ECM adhesion.

1.2.6 Podosomes and Invadopodia

Podosomes and invadopodia, collectively known as podosome-type adhesions (PTAs), are matrix-degrading adhesions that are predominantly formed by migratory and invasive cells that have to cross tissue boundaries (Linder, 2007). For example, podosomes are common in cells of the monocytic lineage, such as macrophages (Lehto *et al.*, 1982), osteoclasts (Marchisio *et al.*, 1984), and dendritic cells (Burns *et*

al., 2001), whereas invadopodia are mostly found in cancer cells (Buccione *et al.*, 2009).

PTAs are integrin-dependent dot-like protruding adhesions that differ structurally and functionally from the cell-matrix adhesions described previously. Their architecture is defined by a core of F-actin and actin regulators, such as WASP (Wiskott-Aldrich syndrome protein), the actin-related proteins2/3 (arp2/3)-complex and cortactin, which is not seen in other cell-matrix adhesions (Block *et al.*, 2008). In podosomes, this actin-rich core is surrounded by a ring of adhesion plaque proteins, including paxillin, vinculin and talin, whereas invadopodia appear to lack this two-part architecture, although they may still recruit a similar set of components (Block *et al.*, 2008). Podosomes and invadopodia also differ in their respective size, numbers and stability (Linder, 2007). Podosomes are generally smaller, with a diameter of $\sim 1 \mu\text{m}$ and a matrix-penetrating depth of $\sim 0.4 \mu\text{m}$, compared to $\sim 8 \mu\text{m} \times \sim 5 \mu\text{m}$ for invadopodia. However, cells will typically assemble a large number of small podosomes (20-100/cell), compared to only a few large invadopodia (1-10/cell). Finally, podosomes have a relatively short life span of 2-12 minutes (Destaing *et al.*, 2003), whereas invadopodia can persist for several hours (Yamaguchi *et al.*, 2005). Similar to the relationship between small dynamic focal complexes and large stable focal adhesions, it has been proposed that invadopodia might develop from podosomal precursors.

The regulation of PTA assembly and disassembly involves a combination of integrin and cytokine signalling, which together augment the activity of intracellular kinases such as PI3K (phosphoinositide 3-kinase), PKC (protein kinase C) and Src, GTPases such as RhoA, Rac and Cdc42, and also modify cytoskeletal dynamics (Linder and Kopp, 2005; Buccione *et al.*, 2009). Functionally, the ability of PTAs to locally concentrate matrix-degrading enzymes, such as matrix metalloproteinases (MMPs), clearly distinguishes them from the before-mentioned adhesions, and strongly

implicates them in both physiological migration events, such as monocyte extravasation, and in pathological processes, such as cancer cell invasion and metastasis (Linder, 2007).

1.3 FN Fibrillogenesis

1.3.1 Fibronectin

FN is a vital ECM protein that plays important roles in cell adhesion, migration, growth and differentiation (Hynes, 1990; Danen and Yamada, 2001). FN is expressed by a wide variety of cell types, most notably fibroblasts, and is essential during development, as demonstrated by the early embryonic lethality seen in the FN knockout (KO) mouse (George *et al.*, 1993). FN usually exists as a dimer of two similar or identical 220-250 kDa subunits linked by a pair of C-terminal disulphide bonds. Around 90% of each FN monomer is composed of homologous repeating units, of which there are three different types, known as type I, type II and type III repeats. Type I, II, and III repeats are about 40, 60, and 90 amino acid residues in length, respectively, and type I and II repeats both contain two intra-domain disulphide bonds. Each FN monomer contains 12 type I repeats, 2 type II repeats, and 15-17 type III repeats, which collectively enable FN to interact with a number of molecules, including the ECM components collagen, fibrin, and heparin, as well as FN itself (Figure 1.5) (Pankov and Yamada, 2002). FN can also interact with at least 11 members of the integrin receptor family (Leiss *et al.*, 2008). For example, the tripeptide RGD sequence contained within the 10th type III repeat is the primary recognition sequence of the $\alpha_5\beta_1$ integrin (Pytela *et al.*, 1985; Ruoslahti, 2003), with the so-called 'synergy sequence' (PHSRN) that enhances integrin binding being present in the neighbouring 9th type III repeat (Aota *et al.*, 1994). Furthermore, a non-homologous segment connecting the 14th and 15th type III repeats of FN, known as the V (variable in length) region, contains

interaction motifs for two non-RGD binding integrins, namely $\alpha_4\beta_1$ and $\alpha_4\beta_7$ (Wayner *et al.*, 1989; Guan and Hynes, 1990; Rugg *et al.*, 1992).

There is a single human FN gene, located just 2.5 megabases from the *tensin1* gene on chromosome 2, whose primary mRNA transcript is alternatively spliced to generate at least 20 different isoforms (White *et al.*, 2008). Broadly, there are two major forms of FN; plasma FN and cellular FN. Plasma FN, which lacks two alternatively spliced type III domains (known as extra domains A and B; EDA and EDB), is synthesised and secreted by hepatocytes and circulates in the blood as a soluble dimer in a closed/inactive conformation awaiting vessel damage. Cellular FN, which contains variable proportions of the EDA and EDB domains, is secreted into the ECM by fibroblasts and other cell types and is incorporated into a multimeric insoluble meshwork of fibrils on the cell surface through the process of FN fibrillogenesis (Mao and Schwarzbauer, 2005a).

1.3.2 The Process of FN Fibrillogenesis

FN fibrillogenesis is required for a number of physiological processes during development and in the adult. During embryogenesis, for example, fibrillar FN is a major component of the pathways that guide gastrulation (Boucaut *et al.*, 1990) and neural crest cell migration (Duband *et al.*, 1986), and the assembly of FN fibrils is required for branching morphogenesis during lung, kidney and salivary gland formation (Sakai *et al.*, 2003; Larsen *et al.*, 2006). Endothelial cells also assemble a fibrillar FN matrix during neovessel formation, implicating FN fibrillogenesis in both vasculogenesis and angiogenesis (Zhou *et al.*, 2008). Finally, during skin wound repair the fibrin clot is degraded and replaced by a provisional FN-containing matrix, thereby providing a surface for migrating epidermal cells to re-populate the wound (Clark, 1990). FN fibrillogenesis also regulates the deposition of other ECM molecules, including fibulin

(Roman and McDonald, 1993), fibrinogen (Pereira *et al.*, 2002), collagen and thrombospondin-1 (McDonald *et al.*, 1982; Sottile and Hocking, 2002). FN fibrillogenesis has been extensively studied *in vitro* using 2D monolayer culture, which has led to the identification of fibrillar adhesions as the cellular machinery that drives matrix assembly (Pankov *et al.*, 2000; Ohashi *et al.*, 2002). FN fibrillogenesis can be monitored *in vitro* by immunofluorescent staining (Pankov and Momchilova, 2009) or by following the conversion of FN fibrils from a soluble form to an insoluble fibrillar network (McKeown-Longo and Mosher, 1983). Using this methodology it was shown that plating cells within pre-assembled 3D cell-derived matrices, which more closely resemble the *in vivo* environment, promoted FN fibrillogenesis (Mao and Schwarzbauer, 2005b).

FN fibrillogenesis is a cell-dependent process that is mediated predominantly by the $\alpha_5\beta_1$ integrin (Fogerty *et al.*, 1990), although other integrins can perform this function under certain conditions, including $\alpha_{11b}\beta_3$ (Wu *et al.*, 1995), $\alpha_V\beta_3$ (Wennerberg *et al.*, 1996; Wu *et al.*, 1996), and $\alpha_4\beta_1$ (Sechler *et al.*, 2000). The interaction between FN and integrins promotes FN-FN association through the cell-driven exposure of cryptic self-association sites in FN. This process is thought to occur through the mechanical stretching of FN, which is likely to be driven by actomyosin contraction as treatments that enhance contractility stimulate fibrillogenesis whereas pharmacological inhibition of Rho or myosin light chain kinase (MLCK) reduces fibrillogenesis (Zhang *et al.*, 1994; Zhang *et al.*, 1997; Zhong *et al.*, 1998). In support of this mechanism, almost all of the cryptic self-association sites of FN are contained within the disulphide bond-lacking type III repeats, which are known to unfold reversibly in response to applied force (Erickson, 1994). Furthermore, a Förster resonance energy transfer (FRET) study using FN that was randomly labelled on amine residues with donor fluorophores and site-specifically labelled on cysteine residues in type III repeats with acceptor fluorophores demonstrated a decrease in intra-molecular FRET during fibril assembly (Baneyx *et al.*, 2002). Moreover, treatment with cytochalasin D was shown to increase

FRET (Baneyx *et al.*, 2002), which compliments the findings of others who showed that disruption of the actin cytoskeleton with this inhibitor results in a substantial contraction of FN fibrils (Ohashi *et al.*, 2002).

FN fibrillogenesis is dependent on several signal transducers downstream of integrins, including ILK (Vouret-Craviari *et al.*, 2004), FAK (Ilic *et al.*, 2004), Src and PI3K (Wierzbicka-Patynowski and Schwarzbauer, 2002). Importantly, all of these signalling molecules are known to modulate various Rho-family members and affect cytoskeletal remodelling. However, in a recent study it was shown that the individual depletion of RhoA, RhoB, RhoC, Rac1 or Cdc42 using siRNA did not significantly decrease the amount of FN deposition, but instead altered the arrangement of FN fibres (Fernandez-Sauze *et al.*, 2009). Hence, the previous finding that pharmacological inhibition of Rho reduces FN fibrillogenesis was probably due to the cumulative effect of simultaneous targeting of several Rho-family members.

1.4 Cell Migration

1.4.1 The Role of Cell Migration

Cell migration is a complex process that is essential to a diverse range of organisms, from unicellular amoeba to humans. Whereas the primary role of cell migration in amoeba is to facilitate mating and the search for food (Manahan *et al.*, 2004), in humans it is required for a number of physiological events that occur during embryogenesis and in the adult organism, including gastrulation (Keller, 2005), wound healing (Li *et al.*, 2007) and the immune response (Luster *et al.*, 2005). Moreover, cell migration also contributes towards several pathological conditions, including vascular disease, osteoporosis, rheumatoid arthritis, and cancer (Ridley *et al.*, 2003). In cancer, for example, it is the aberrant invasive migration of cells away from the primary tumour

that ultimately leads to the formation of distant metastases, which is the most life-threatening aspect of the disease (Sahai, 2005; Nguyen *et al.*, 2009). It is also noteworthy that some cell migration events, particularly those that occur during morphogenesis, regeneration, and cancer, can involve the collective movement of groups of cells that maintain cell-cell contact throughout the process (Friedl and Gilmour, 2009).

1.4.2 The Migration Cycle

In general, cell migration can be usefully conceptualized as a cyclic process (Lauffenburger and Horwitz, 1996; Ridley *et al.*, 2003; Vicente-Manzanares *et al.*, 2005). Initially the cell undergoes polarisation in response to an environmental cue, such as a chemoattractant gradient. This polarisation is followed by the extension of protrusions, such as sheet-like lamellipodia or spike-like filopodia, in the direction of migration. These protrusions, which are usually driven by actin polymerisation, are then stabilised by the formation of integrin-mediated cell-ECM adhesions that link to the actin cytoskeleton and serve as traction points for migration. Finally, as the cell moves forward the cell rear retracts through actomyosin contraction and adhesion disassembly. It is now becoming clear that the actin cytoskeleton plays an active role in all aspects of the migration cycle by dictating where and how protrusions and adhesions form, develop and disassemble (Vicente-Manzanares *et al.*, 2009). Moreover, the Rho-family of small GTPases have emerged as important regulators of actin cytoarchitecture and dynamics, and therefore controllers of cell migration (Charest and Firtel, 2007; Ridley, 2001)

Polarisation, the first step in the migration cycle, is the establishment of molecular asymmetry within the cell in response to extracellular stimuli. Establishing and maintaining cell polarity leads to polarised actin polymerisation at the leading edge and

actomyosin-driven retraction of the trailing edge, which ultimately promotes directional cell migration (Petrie *et al.*, 2009). In addition to these effects on the actin cytoskeleton, polarisation is also characterised by positioning of the nucleus toward the trailing edge, and reorientation of the Golgi apparatus and microtubule organising centre (MTOC) towards the leading edge. Golgi/MTOC reorientation is thought to facilitate the polarized delivery of vesicles along microtubules towards the leading edge, thereby providing the membrane and proteins required to sustain protrusion (Bergmann *et al.*, 1983; Yadav *et al.*, 2009). Polarisation appears to be mediated by a series of positive feedback loops involving Rho-family GTPases, PI3Ks, integrins, microtubules, and vesicular transport (Petrie *et al.*, 2009; Ridley *et al.*, 2003).

Protrusion is controlled by actin polymerisation in the current paradigm for cell migration (Pollard and Borisy, 2003). In this model, protrusive force at the cell front is generated by a 'treadmilling' process in which depolymerisation of actin filaments at their pointed ends, which are directed towards the cell body, feeds the fast elongation of actin filaments at their barbed ends, which are directed towards the leading edge (Wang, 1985). The rate of actin treadmilling is modulated by the activity of several actin-binding proteins (Le Clainche and Carlier, 2008). For example, cofilin, or ADF (actin-depolymerising factor), induces pointed end depolymerisation and therefore promotes barbed end polymerisation by increasing the concentration of monomeric (free) actin (Carlier *et al.*, 1999). Cofilin is also thought to sever actin filaments, thereby generating new barbed ends ready for elongation (Maciver *et al.*, 1991; Van Troys *et al.*, 2008). Profilin, another actin-binding protein, is thought to target monomeric actin to barbed ends, and the combined activity of cofilin and profilin enhances the rate of actin treadmilling by 125-fold *in vitro* (Didry *et al.*, 1998). Other actin-binding proteins have been shown to decrease polymerisation, including capping proteins such as gelsolin and the actin-integrin linker tensin, which bind to barbed ends and block monomer addition (Le Clainche and Carlier, 2008; Chuang *et al.*, 1995). Paradoxically, some

capping proteins have been shown to increase the rate of cell migration (Hug *et al.*, 1995; Chen *et al.*, 2002), possibly through the ‘funneling’ of increased amounts of monomeric actin to rare uncapped barbed ends (Carlier and Pantaloni, 1997). Actin adopts different organizations in lamellipodia and filopodia, the two main types of protrusive structures. In lamellipodia, actin nucleation is driven by the arp2/3-complex, which binds to the sides or tips of a pre-existing actin filaments and induces the formation of a new daughter filament at a 70° angle to the mother filament, leading to the assembly of a branched dendritic-like actin network (Mullins *et al.*, 1998; Le Clainche and Carlier, 2008). Interestingly, a recent study showed that arp2/3-based nucleation and branching was increased by barbed end capping, which has led to an alternate model to explain the positive effects of some capping proteins on cell migration (Akin and Mullins, 2008; Bear, 2008). In filopodia, protrusion is driven by linear actin polymerisation via the actin-nucleating activity of formins and the barbed end anti-capping activity of VASP, whilst the actin-bundling protein fascin organises polymerised actin filaments into elongated parallel bundles (Mattila and Lappalainen, 2008). It is now becoming apparent that actin polymerisation at the leading edge actually drives adhesion formation (Galbraith *et al.*, 2007).

Adhesion acts as a ‘molecular clutch’ that controls the mechanical coupling between actin dynamics and the substratum, and thereby regulates cell migration by modulating the rate of leading edge protrusion, traction of the cell body, and retraction of the tail (Vicente-Manzanares *et al.*, 2009; Le Clainche and Carlier, 2008). For example, actin polymerisation at the cell front is not sufficient to drive protrusion in the absence of an engaged actin-integrin ‘clutch’. This is because the force generated by directional actin polymerisation is counteracted by membrane tension at the leading edge and myosin II contraction in the region behind the protrusion known as the lamella, which leads to the continual ‘retrograde flow’ of actin (Wang, 1987; Lin *et al.*, 1996). However, the assembly of adhesions at the leading edge engages the integrin-actin clutch, which

prevents retrograde flow by anchoring actin filaments to the fixed substratum, thereby converting the force generated by actin assembly into protrusion (Lin and Forscher, 1995; Alexandrova *et al.*, 2008). In support of this model, inhibiting the activity of myosin IIA decreases the retrograde flow of actin and enhances protrusion rate (Cai *et al.*, 2006; Even-Ram *et al.*, 2007), whereas inactivating the actin-integrin linker talin increases retrograde flow and reduces protrusion rate (Zhang *et al.*, 2008; Sydor *et al.*, 1996). Interestingly, recent studies comparing the velocity of several adhesion-associated molecules with that of actin retrograde flow have revealed the efficiency of the actin-integrin linkage, and identified points of slippage (Brown *et al.*, 2006; Hu *et al.*, 2007). In short, α -actinin displays a high level of coupling with actin, whereas the motion of talin and vinculin are only partially coupled, and integrins remain uncoupled and stationary. These data suggest that talin and vinculin form transient linkages that enable the partial transmission of force to the substrate. Indeed, as well as supporting the formation of protrusions, newly formed adhesions at the cell front also exert actomyosin-driven tractional forces on the substratum that pull the cell body forward (Beningo *et al.*, 2001). Many cell types exhibit a biphasic relationship between cell migration speed and adhesiveness (Huttenlocher *et al.*, 1996; Palecek *et al.*, 1997), with optimum speed occurring at intermediate adhesiveness (DiMilla *et al.*, 1993). If cell-matrix adhesion is insufficient then the cell cannot form the stable adhesions required for traction; conversely, when adhesion is excessive the cell cannot release adhesions to move forward. Hence, cell-matrix adhesions are vital for the transmission of intracellular tension to the substratum that is required for cell migration; however, adhesions both at the front and rear of the cell must also turnover to allow progression of the leading edge and retraction of the trailing edge (Broussard *et al.*, 2008).

Tail retraction, the final step in the migration cycle, can often be the rate-limiting step of cell migration (Chen, 1981; Palecek *et al.*, 1998). Myosin II-driven contraction is thought to be vital for tail retraction (Jay *et al.*, 1995; Chung *et al.*, 2001), and recent

studies have specifically implicated the myosin IIA isoform in this process (Vicente-Manzanares *et al.*, 2007; Even-Ram *et al.*, 2007). Actomyosin-driven tail retraction is accompanied by the release of adhesive contacts at the rear of the cell, which permits cell body translocation (Kirfel *et al.*, 2004). Adhesion disassembly is regulated primarily by the proteolytic cleavage and phosphorylation/dephosphorylation of adhesion components. Calpain, a Ca^{2+} -dependent cysteine protease that localises to focal adhesions (Beckerle *et al.*, 1987), is known to cleave a number of adhesion-relevant targets, including talin (Carragher *et al.*, 1999), tensin (Chen *et al.*, 2000; Kook *et al.*, 2003), and integrins (Pfaff *et al.*, 1999; Flevaris *et al.*, 2007), and inhibition of calpain activity stabilises adhesions and reduces the rate of rear end detachment (Huttenlocher *et al.*, 1997; Palecek *et al.*, 1998; Franco and Huttenlocher, 2005). The non-receptor tyrosine kinases FAK and Src are important regulators of cell migration (Carragher and Frame, 2004; Mitra and Schlaepfer, 2006). Cells isolated from FAK-null mice display impaired cell migration and increased numbers of focal adhesions (Ilic *et al.*, 1995). Similarly, Src-null cells also exhibit impaired migration (Klinghoffer *et al.*, 1999) and increased adhesion size (Volberg *et al.*, 2001), and expression of kinase-defective mutants of Src in normal cells promotes the formation of abnormally large focal adhesions (Fincham and Frame, 1998). Collectively, these studies suggest a role for FAK-Src activity in the regulation of adhesion assembly, maturation and/or disassembly. Indeed, FAK- and Src-null cells display impaired adhesion turnover at the cell front and defective adhesion disassembly at the trailing edge (Webb *et al.*, 2004). Webb *et al.* (2004) also showed that the adhesion-related adaptor molecules paxillin and p130Cas (p130 crk-associated substrate), and the kinases ERK (extracellular signal-regulated kinase) and MLCK are critical for adhesion turnover (Webb *et al.*, 2004). FAK-Src signalling could promote adhesion disassembly at the cell rear in a number of ways. Firstly, FAK-Src signalling is known to activate ERK (Schlaepfer *et al.*, 1999), which in turn can phosphorylate and activate MLCK (Klemke *et al.*, 1997), resulting in increased actomyosin-driven contractility that could drive tail retraction and

provide the force required for adhesion disassembly (Crowley and Horwitz, 1995). Secondly, by acting as an adaptor molecule FAK is known to recruit ERK and calpain to adhesion sites, where the activation of calpain by ERK is thought promote adhesion disassembly (Carragher *et al.*, 2003; Glading *et al.*, 2000). Finally, FAK-Src-mediated phosphorylation of various adhesion-related molecules, including paxillin (Bellis *et al.*, 1995; Schaller and Parsons, 1995) and p130Cas (Cary *et al.*, 1998), may regulate their interactions with other molecules and thereby favour adhesion disassembly. Phosphatase activity is also required throughout the migration cycle, including rear retraction (Larsen *et al.*, 2003; Zheng *et al.*, 2009). For example, an unknown type 1 and/or type 2A serine/threonine phosphatase seems to regulate the dephosphorylation of the plasma membrane-actin filament cross-linker moesin, resulting in tail retraction (Yoshinaga-Ohara *et al.*, 2002). The Ca^{2+} -calmodulin-dependent phosphatase calcineurin has also been implicated in the detachment of integrin-mediated adhesions (Hendey *et al.*, 1992) and, along with calpain, could be activated by local rises in Ca^{2+} concentration caused by the opening of stretch-activated Ca^{2+} channels in response to actomyosin-driven tension (Lee *et al.*, 1999). The microtubule network is also thought to play an important role in adhesion turnover/disassembly (Broussard *et al.*, 2008). The repetitive targeting of microtubule ends to adhesions was shown to induce adhesion disassembly and precede cell edge retraction (Kaverina *et al.*, 1999). Microtubule targeting has been proposed to induce adhesion disassembly through a number of mechanisms, including calpain-driven proteolysis of adhesion proteins (Bhatt *et al.*, 2002), FAK-dependent, dynamin-driven endocytosis (Ezratty *et al.*, 2005), and the modulation of actomyosin contractility (Broussard *et al.*, 2008).

Under certain conditions, focal adhesions at the rear of the cell can themselves translocate centripetally in the direction of the attached actin stress fibre, which is thought to signify the gradual release of the integrin-substratum linkage (Smilenov *et al.*, 1999). This process was termed adhesion 'sliding'; however, it is thought to be

caused by the polarised renewal of focal adhesions i.e. loss of integrins from the distal edge of the adhesion and addition at the proximal edge (Ballestrem *et al.*, 2001). Sometimes, a combination of tail retraction and adhesion disassembly is sufficient to physically break the linkage between integrins and the cytoskeleton even though the integrins are still engaged with the substratum, which is particularly common in slow-moving cells such as fibroblasts, and results in the integrin being left behind in 'footprints' or 'streaks' on the substratum as the cell moves forward (Regen and Horwitz, 1992; Palecek *et al.*, 1996). Moreover, the amount of integrin released appears to be an increasing function of cell-substratum adhesiveness (Palecek *et al.*, 1998). This integrin 'ripping' from the cell rear has also been observed in highly aggressive cancer cells migrating through 3D collagen gels (Friedl *et al.*, 1997). Initially it was suggested that fast-moving cells did not exhibit this traumatic form of detachment and instead relied heavily on biochemical mechanisms to detach their trailing edge; however, it has since been shown that keratinocytes leave behind similar migration tracks (Kirfel *et al.*, 2003).

The migration cycle is a useful model for describing cell movement on 2D surfaces, although it is by no means universal. The steps described above are observed most distinctly in individual slow-moving cells such as fibroblasts, which contain thick actin stress fibres anchored to large focal adhesions. For other cell types, such as fast-moving fish keratocytes, which appear to glide over the substratum using only small focal complexes, these separate steps are less obvious. As alluded to previously, some cell types retain cell-cell contact during migration (Friedl and Gilmour, 2009), such as epithelial monolayers, which move collectively whilst maintaining polarization across the sheet. Interestingly, certain cell types, including leukocytes and tumour cells under some conditions, can actually migrate in an integrin-independent manner (Lammermann *et al.*, 2008; Wolf *et al.*, 2003; Fackler and Grosse, 2008). Finally, the morphology and motility mechanisms adopted by cells migrating within 3D

environments is significantly different to those migrating on rigid planar substrates (Cukierman *et al.*, 2001; Even-Ram and Yamada, 2005), which will be discussed later.

1.4.3 Regulation by Rho-Family GTPases

The Rho-family GTPases belong to the Ras superfamily of small GTPases and are highly conserved throughout eukaryotes (Wennerberg *et al.*, 2005). There are 22 human Rho-family genes encoding at least 25 proteins, although the majority of research has focused on just three 'classical' members; RhoA, Rac1 and Cdc42 (Wennerberg and Der, 2004; Vega and Ridley, 2007). Rho-family GTPases control multiple cellular processes, including cell polarity, actin and microtubule dynamics, cell adhesion, membrane transport, gene expression and the cell cycle, through interactions with numerous downstream effectors (Schwartz, 2004). Most Rho-family members contain lipid anchors at their C-termini, enhancing their interaction with membranes and often defining their localisation to specific subcellular compartments (Wennerberg and Der, 2004). Like Ras, most Rho-family GTPases act as molecular switches that control signal transduction pathways by cycling between inactive (GDP-bound) and active (GTP-bound) conformations (Figure 1.6). Three classes of regulatory proteins control the activation state of Rho GTPases (Buchsbbaum, 2007); guanine nucleotide exchange factors (GEFs) promote the exchange of GDP for GTP to cause activation (Rossman *et al.*, 2005), GTPase-activating proteins (GAPs) enhance the intrinsic GTP-hydrolysis activity of the GTPases to cause inactivation (Moon and Zheng, 2003), and guanine nucleotide dissociation inhibitors (GDIs) inhibit GTPase signalling by blocking GDP/GTP exchange (antagonising GEF activity), inhibiting GTP hydrolysis (both intrinsic and GAP-catalyzed), and sequestering the GTPase away from cellular membranes, which are their place of action, by masking their lipid-anchors (DerMardirossian and Bokoch, 2005) (Figure 1.6). The migration-related targets of the 'classical' Rho-family GTPases are largely limited to regulators of actin polymerisation

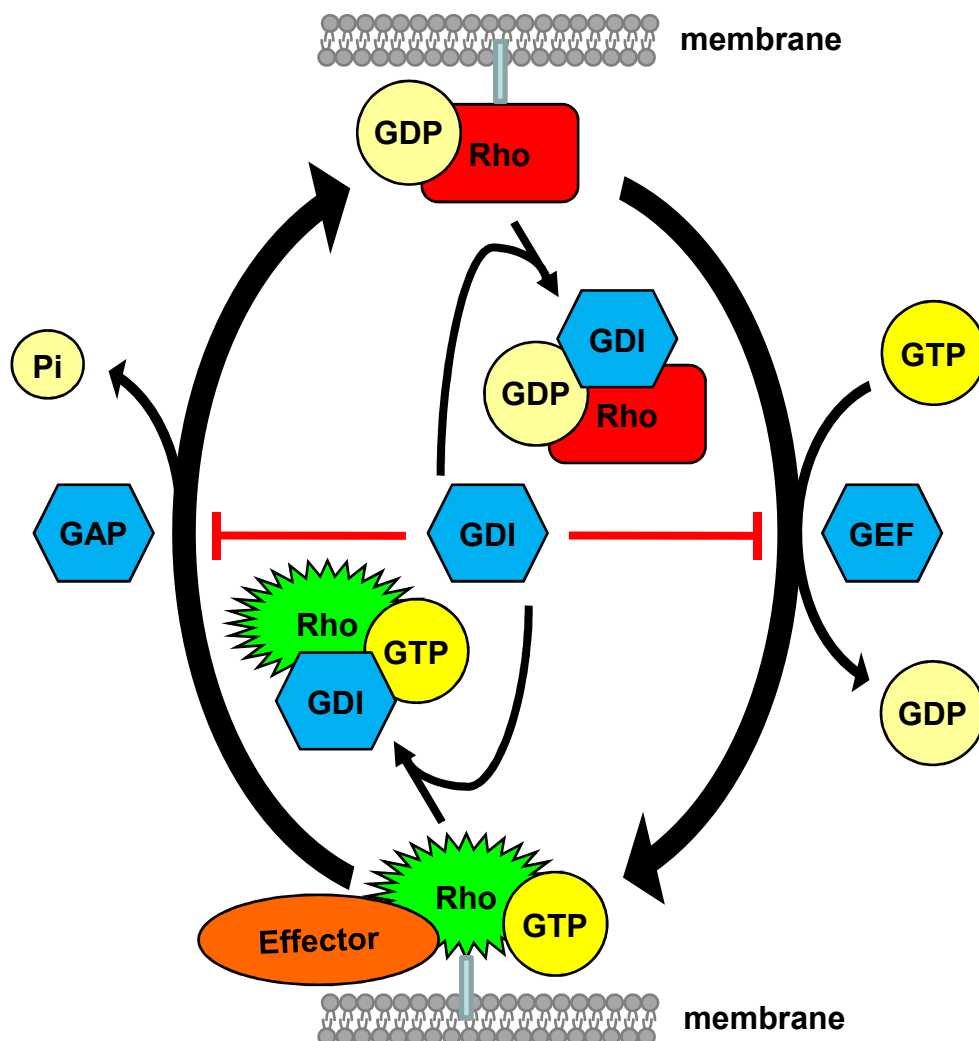


Figure 1.6: The Rho GTPase cycle. Rho-family GTPases cycle between an inactive (GDP-bound) form and an active (GTP-bound) form. This cycle is regulated by guanine nucleotide exchange factors (GEFs) that promote the exchange of GDP for GTP to activate the GTPase, GTPase-activating proteins (GAPs) that enhance the intrinsic GTP-hydrolysis activity of the GTPases to cause inactivation, and guanine nucleotide dissociation inhibitors (GDIs) that inhibit GTPase signalling by blocking GDP/GTP exchange (antagonising GEF activity), inhibiting GTP hydrolysis (both intrinsic and GAP-catalyzed), and sequestering the GTPase away from cellular membranes, which are their place of action, by masking their lipid-anchors.

(the arp2/3-complex and formins) (Pollard, 2007), myosin II activation or inactivation (Clark *et al.*, 2007), and microtubule dynamics (Watanabe *et al.*, 2005) (Figure 1.7).

The Cdc42 GTPase is regarded as a key regulator of the first step of the migration cycle i.e. polarisation (Etienne-Manneville, 2004). Cells injected with a dominant negative form of Cdc42 are able to migrate but cannot chemotax due to their inability to polarize in the direction of a chemoattractant gradient (Allen *et al.*, 1998). Cdc42 is active towards the front of migrating cells and in the trans-Golgi apparatus (Itoh *et al.*, 2002; Nalbant *et al.*, 2004), and Cdc42 inhibition leads to protrusive lamellipodial activity all around the cell periphery and also prevents Golgi apparatus reorientation (Nobes and Hall, 1999). Cdc42 is thought to regulate many of the characteristic changes that occur within the cell during polarisation. Starting at the back of the migrating cell, nuclear positioning occurs through myosin-dependent actin retrograde flow and is catalyzed by Cdc42 acting through its effector myotonic dystrophy kinase-related Cdc42 binding kinase (MRCK) (Gomes *et al.*, 2005), which is capable of activating myosin II by phosphorylating MLC (Leung *et al.*, 1998). Secondly, reorientation of the Golgi apparatus and MTOC between the nucleus and the leading edge is thought to be driven by Cdc42 acting through a Par6-PKC ζ (partitioning-defective 6-protein kinase C zeta) complex (Etienne-Manneville and Hall, 2001; Tzima *et al.*, 2003). Cdc42 is thought to recruit and activate this complex at the leading edge, which leads to the localised inactivation of glycogen synthase kinase 3 β (GSK3 β) via PKC ζ -induced phosphorylation (Etienne-Manneville and Hall, 2001; Etienne-Manneville and Hall, 2003). GSK3 β inactivation leads to the association of APC (adenomatous polyposis coli) with microtubule plus ends, which is required for MTOC reorientation, perhaps by regulating microtubule dynamics and/or plus end capture at the leading edge (Etienne-Manneville and Hall, 2003). Finally, Cdc42 is thought to influence polarity by restricting where the leading edge can form (Srinivasan *et al.*, 2003).

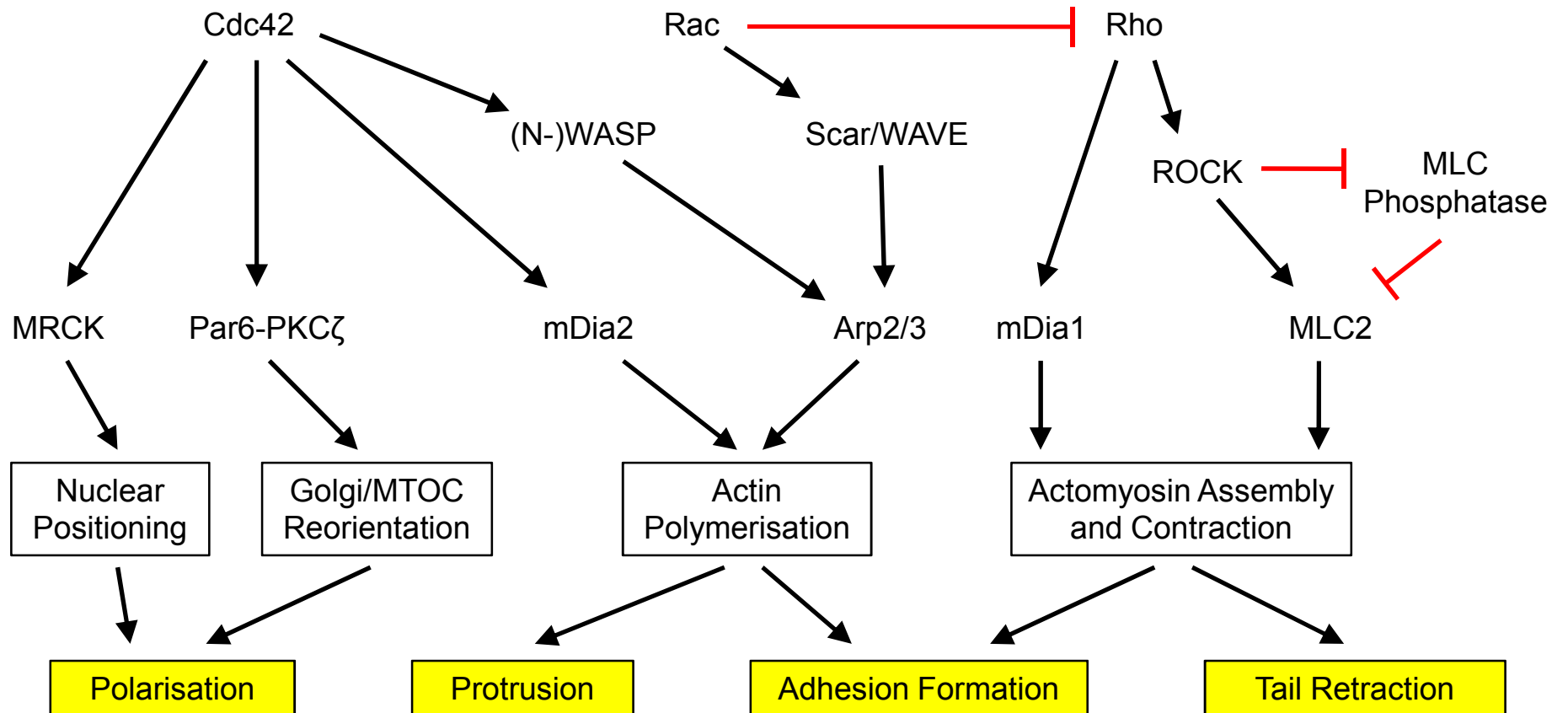


Figure 1.7: The role of the classical Rho-family GTPases in cell migration. Some of the pathways through which the classical Rho-family GTPases influence the steps of the migration cycle are listed above. See text for detailed description. (N-)WASP ([neural]-Wiskott-Aldrich syndrome protein), Scar/WAVE (suppressor of cAMP receptor/WASP family verprolin-homologous protein), ROCK (Rho-associated kinase), MLC (myosin light chain), MRCK (myotonic dystrophy kinase-related Cdc42 binding kinase), Par6-PKC ζ (partitioning-defective 6-protein kinase C zeta complex), mDia (mammalian Diaphanous [-related formin]), Arp2/3 (actin-related proteins2/3-complex), MTOC (microtubule organising centre).

Protrusion, the second step of the migration cycle, is regulated by Rac and Cdc42, which induce the formation of lamellipodia and filopodia, respectively (Ridley *et al.*, 1992; Nobes and Hall, 1995; Ladwein and Rottner, 2008). Rac, which is active at the leading edge of motile cells (Kraynov *et al.*, 2000), indirectly activates members of the Scar/WAVE (suppressor of cAMP receptor/WASP family verprolin-homologous protein) family of scaffold proteins that stimulate the arp2/3-complex, leading to the assembly of the dendritic-like actin network of lamellipodia (Miki *et al.*, 1998b). The mechanism by which Cdc42 promotes filopodia formation is still unclear (Mellor, 2009). The discovery that Cdc42 could directly interact with the arp2/3-complex activators WASP and N (neural)-WASP, and the finding that N-WASP potentiates the ability of Cdc42 to induce filopodia suggested that the arp2/3-complex is involved in the formation of this type of protrusion (Aspenstrom *et al.*, 1996; Miki *et al.*, 1998a). However, the branched actin network formed by the arp2/3-complex is clearly incompatible with the tightly bundled unbranched actin filaments found in filopodia. The 'convergent elongation' model of filopodia formation was proposed to explain this inconsistency (Svitkina *et al.*, 2003). In this model, the dendritic-like actin network of the lamellipodium is reorganised to form filopodia. This process begins with the clustering of uncapped barbed filament ends to form a fishtail-shaped structure termed the Λ -precursor, which points outward towards the plasma membrane. The actin-binding proteins fascin and VASP are recruited to the tip of this structure to promote bundling and prevent barbed-end capping, thereby favouring the collective elongation of a filament bundle, leading to the formation of a filopodium (Svitkina *et al.*, 2003). However, the discovery that active Cdc42 can directly interact with the linear actin nucleator formin mDia2 (Alberts *et al.*, 1998), which is also localised at the tips of Cdc42-induced filopodia (Peng *et al.*, 2003), has led to the proposal of an alternate model of filopodia formation, known as the 'tip nucleation' model. In this model, rather than reorganising the highly-branched lamellipodial actin network into a linear filopodial bundle, mDia2 stimulates the nucleation and elongation of long, parallel actin filaments at the leading edge, which are bundled by actin cross-

linkers. In addition to Cdc42, other Rho-family members have also been implicated in filopodia formation (Aspenstrom *et al.*, 2004), including Rif, which was also shown to act through mDia2 (Pellegrin and Mellor, 2005). It is likely that the true mechanism of filopodia formation is a combination of these two models, with the contribution made by the arp2/3-complex versus mDia2 depending on cell type and filopodial length.

Rho, the last of the 'classical' Rho-family GTPases, is especially important for the latter stages of the cell migration cycle. The best studied effector of Rho is the serine/threonine kinase ROCK (Rho-associated kinase) (Ishizaki *et al.*, 1996; Leung *et al.*, 1996), which activates myosin II both directly by phosphorylating myosin light chain (MLC)-2 (Amano *et al.*, 1996), and indirectly by phosphorylating and inactivating MLC phosphatase (Kimura *et al.*, 1996). Rho-stimulated myosin II activation is associated with the actomyosin-driven contractility that induces focal adhesion and actin stress fibre formation (Chrzanowska-Wodnicka and Burridge, 1996), cell body translocation and tail retraction (Worthylake *et al.*, 2001). Another important effector of Rho is the formin mDia1 (Watanabe *et al.*, 1997), which cooperates with ROCK in the assembly of actin stress fibres (Watanabe *et al.*, 1999; Hotulainen and Lappalainen, 2006). The finding that Rac signalling is able to antagonise Rho activity could provide a mechanism to inhibit Rho-mediated contractility at the leading edge, which would otherwise interfere with protrusion (Sander *et al.*, 1999).

1.4.4 Cell Migration in 3D Microenvironments

In multicellular organisms, migration across flat ECM substrates occurs only in a few situations, including epidermal wound healing (Kirfel and Herzog, 2004) and the lateral movement of the gut epithelium along the basement membrane following injury (Lotz *et al.*, 2000). More commonly, cell migration *in vivo* occurs through a 3D fibrillar ECM, such as interstitial connective tissue. In this environment, migrating cells adopt

spherical shapes of varying lengths, ranging from a short ellipsoid morphology to an elongated and spindle-shaped morphology (Friedl and Brocker, 2000). Moreover, cells in 3D also lack prominent actin stress fibres and instead form a cortical actin cytoskeleton, which reflects the increased pliability of the ECM compared to rigid 2D culture surfaces. Different cell types use different mechanisms to migrate within 3D microenvironments (Even-Ram and Yamada, 2005; Sahai, 2005), and broadly speaking there are three main modes of 3D migration; mesenchymal (Friedl and Wolf, 2009), amoeboid (Fackler and Grosse, 2008) and collective (Friedl and Gilmour, 2009). Mesenchymal migration is characterised by an elongated morphology with a leading edge protrusion that consists of one or few cylindrical pseudopodia with terminal filopodia (Friedl and Wolf, 2009). Protrusion formation is driven by Rac/WAVE-induced actin polymerisation (Sanz-Moreno *et al.*, 2008) and forward movement is facilitated by the pericellular proteolysis of ECM components by proteases such as secreted and membrane-type MMPs (Murphy and Gavrilovic, 1999; Friedl and Wolf, 2009). This slow form of migration (0.1-1 $\mu\text{m}/\text{min}$) is typical of tissue fibroblasts and highly dependent on integrins and the intracellular protease calpain (Cukierman *et al.*, 2001; Carragher *et al.*, 2006). Conversely, amoeboid migration is characterised by a rounded morphology with forward movement driven by bleb-like protrusions produced by Rho/ROCK-induced actomyosin contraction (Fackler and Grosse, 2008; Sahai and Marshall, 2003). This rapid form of migration (up to 4 $\mu\text{m}/\text{min}$) is typical of leukocytes and does not require ECM degradation as the cell instead forces its way through gaps in the matrix (Schor *et al.*, 1983; Wolf *et al.*, 2003). Compared to mesenchymal migration, amoeboid migration is also less dependent on integrins and calpain activity (Lammermann *et al.*, 2008; Carragher *et al.*, 2006). These two modes of migration have been observed in invading tumour cells *in vivo* (Wyckoff *et al.*, 2006), and there is considerable evidence to suggest that some tumour cells are capable of switching between mesenchymal and amoeboid modes of migration (Wolf *et al.*, 2003; Sahai and Marshall, 2003; Croft and Olson, 2008). For example, Wolf *et al.* (2003) demonstrated that inhibition of matrix-

degrading proteases led to the conversion of both fibrosarcoma (HT-1080) and breast cancer (MDA-MB-231) cells from a mesenchymal to an amoeboid mode of motility without significantly affecting migration rate; a process they referred to as mesenchymal-amoeboid transition (MAT) (Wolf *et al.*, 2003). This plasticity in migration mode may explain the relatively poor performance of MMP inhibitors as anti-metastatic drugs in clinical trials (Coussens *et al.*, 2002). A recent study identified a reciprocal inhibitory relationship between Rac and Rho signalling during 3D migration, which is thought to form a bistable switch that reinforces the selection of mesenchymal or amoeboid migration (Sanz-Moreno *et al.*, 2008; Symons and Segall, 2009). Finally, cells can also collectively migrate through 3D environments as sheets, strands, clusters or ducts, which is vital for the tissue remodelling events that occur during embryonic morphogenesis, wound repair and cancer invasion (Friedl and Gilmour, 2009). Three hallmarks characterise collective migration; 1) the maintenance of cell-cell junctions, 2) multicellular polarity and supracellular organisation of the actin cytoskeleton, and 3) ECM modification along the migration path e.g. proteolysis. Therefore, in many ways, collective migration resembles a cooperative form of mesenchymal migration.

1.5 Tensin

1.5.1 Tensin Identification and Initial Characterisation

Originally identified in the mid-1980s as an actin-binding contaminant of a vinculin preparation (Wilkins and Lin, 1986; Wilkins *et al.*, 1986), tensin is a cytoskeletal phosphoprotein, that serves to link β integrin cytoplasmic tails to the actin cytoskeleton (Lo, 2004; Lo, 2006). Initial characterisation of the chicken tensin protein using SDS-PAGE, dynamic light scattering, and gel filtration, suggested that tensin is a large molecule (~200 kDa) that can form a dimer (Lo *et al.*, 1994a). Moreover, chicken tensin was shown to contain three actin binding sites; two at its N-terminus that bind to the

sides of actin filaments, and one in the centre of the molecule that is thought to cap actin filament barbed ends (Lo *et al.*, 1994b; Chuang *et al.*, 1995). Consistent with its actin capping activity, several groups reported that chicken tensin was localised to the ends of actin stress fibres at focal adhesions (Wilkins *et al.*, 1986; Davis *et al.*, 1991; Bockholt and Burridge, 1993; Lo *et al.*, 1994a). Tensin is phosphorylated on tyrosine, serine and threonine residues, and tyrosine phosphorylation of tensin is induced by ECM attachment, treatment with platelet-derived growth factor (PDGF), thrombin or angiotensin, and upon transformation by oncogenes such as v-Src and Bcr/Abl (breakpoint cluster region/abelson) (Bockholt and Burridge, 1993; Jiang *et al.*, 1996; Ishida *et al.*, 1999; Sabe *et al.*, 1997; Davis *et al.*, 1991; Salgia *et al.*, 1995). Moreover, the Src-family of non-receptor tyrosine kinases are thought to be directly responsible for the tyrosine phosphorylation of tensin (Volberg *et al.*, 2001; Cui *et al.*, 2004; Qian *et al.*, 2009).

1.5.2 The Human Tensin Family

The human tensin gene family is comprised of four members; tensin1 (Chen *et al.*, 2000), tensin2 (Chen *et al.*, 2002), tensin3 (Cui *et al.*, 2004) and cten (C-terminal tensin-like protein; tensin4) (Lo and Lo, 2002), which are located on chromosomes 2, 12, 7 and 17, respectively. Northern blot analysis on human tissue samples has been used to analyse the expression patterns of the four human tensin genes (Chen *et al.*, 2000; Chen *et al.*, 2002; Cui *et al.*, 2004; Lo and Lo, 2002). The findings of these studies are summarised in Table 1.2. In short, human tensin1, 2 and 3 are expressed in most tissues. Tensin1 and 2 have very similar expression profiles, with higher expression in the heart, skeletal muscle and kidney, and lower expression in the brain, thymus, and peripheral blood leukocytes (Chen *et al.*, 2000; Chen *et al.*, 2002). Tensin1 and 2 are also highly expressed in the lung and liver, respectively. Tensin3 expression is very high in the kidney and placenta, and like tensin1 and 2, tensin3

	Brain	Heart	Skeletal Muscle	Colon	Thymus	Spleen	Kidney	Liver	Small Intestine	Placenta	Lung	PBL	Prostate	Testis	Ovary
Tensin1	Nil	***	***	**	*	**	***	**	**	**	***	Nil	NT	NT	NT
Tensin2	*	***	**	*	Nil	*	**	**	*	*	*	Nil	NT	NT	NT
Tensin3	Nil	**	**	*	*	**	***	**	*	***	**	Nil	NT	NT	NT
Cten	Nil	Nil	Nil	Nil	Nil	Nil	Nil	Nil	Nil	***	Nil	Nil	***	Nil	Nil

Table 1.2: Relative tissue expression levels of the four human tensin isoforms. *** - high expression, ** - moderate expression, * - low expression, Nil - no detected expression, NT - not tested, PBL - peripheral blood leukocytes. Derived from published Northern blot data (Chen *et al.*, 2000; Chen *et al.*, 2002; Cui *et al.*, 2004; Lo and Lo, 2002).

expression is very low in the brain, thymus, and peripheral blood leukocytes (Cui *et al.*, 2004). In contrast to other tensin isoforms, cten displays a much more restricted expression profile, with high expression in the prostate and placenta, and essentially no expression in all other tissues tested (Lo and Lo, 2002).

1.5.3 Genetic Studies on Tensin

A gene targeting approach using mouse embryonic stem cells has been used to develop tensin1 and tensin3 KO mice (Lo *et al.*, 1997; Chiang *et al.*, 2005). Tensin1 KO mice develop normally despite the widespread expression of the tensin1 gene during embryogenesis (Lo *et al.*, 1997), and these mice display a normal phenotype for several months after birth. However, with time the tensin1-null mice begin to display signs of weakness as a result of extensive kidney damage. Multiple large cysts develop in the proximal kidney tubules of these mice, leading to renal failure, and subsequent death. Immunoelectron microscopy revealed that cell-ECM junctions in these abnormal regions were disrupted, which suggests that tensin1 is required for the maintenance of focal adhesion integrity in the kidney. Tensin1 KO mice also exhibit delayed muscle regeneration following wounding (Ishii and Lo, 2001), a result consistent with the observation that tensin1-null fibroblasts display reduced migration speeds (Chen *et al.*, 2002).

The tensin3 KO phenotype is more severe than that of the tensin1 KO with one third of tensin3 KO mice exhibiting growth retardation and postnatal lethality (Chiang *et al.*, 2005). Histological analysis revealed incomplete lung, small intestine, and bone development in these mutant mice (Chiang *et al.*, 2005). The lungs of tensin3 KO mutant mice contained a relatively un-branched alveolar architecture and enlarged air spaces, which indicates a defect in terminal airway branching, a process that is thought to require FN fibrillogenesis (Sakai *et al.*, 2003). The digestive tract of tensin3 KO

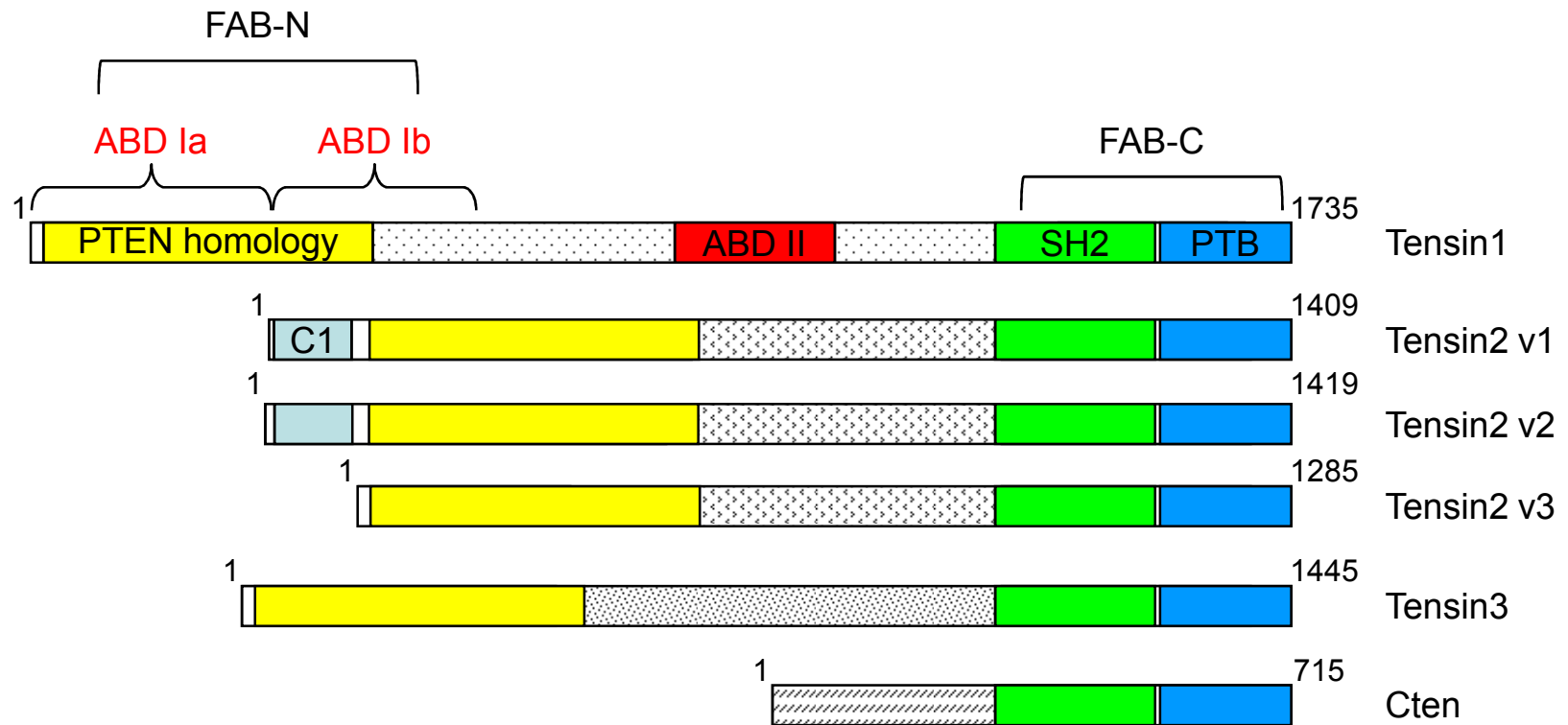
mutant mice was approximately half the length of its wild-type littermate's gut, and the small intestine of these mice also displayed a number of abnormalities, including defective differentiation of enterocytes (absorptive cells) and reduced migration of intestinal epithelial cells from the base of the crypt up the villi (Chiang *et al.*, 2005). Finally, the long bone growth plates of tensin3 KO mutant mice contained enlarged resting regions and much fewer proliferating chondrocytes, which together with malnutrition as a result of reduced nutrient absorption was proposed to be largely responsible for the runt phenotype of tensin3 KO mutant mice (Chiang *et al.*, 2005). The runt phenotype is comparable with the clinical presentation of human Silver-Russell syndrome (SRS), which is characterised by intrauterine growth restriction and low birth weight (Silver *et al.*, 1953; Russell, 1954). Interestingly, a significant proportion of SRS sufferers exhibit abnormalities in chromosome 7, particularly in the region 7p11.2-p13, which is the location of the human tensin3 gene (Abu-Amero *et al.*, 2008). Gene KO's can give some indication of the requirement for particular genes in specific tissues, but functional redundancy can compensate for the loss of a gene, thereby masking its true function. Since mice also have four tensin genes it is highly likely that such a situation may be occurring in the tensin KO mice.

Unlike humans and mice, *Drosophila* only has one tensin ortholog, which is encoded by the *blistery* gene and is important for wing development (Lee *et al.*, 2003; Torgler *et al.*, 2004). Tensin loss-of-function mutations in *Drosophila* lead to a blistered wing phenotype (Lee *et al.*, 2003), indicative of disruption of the integrin-mediated basal junctions that hold the two wing surfaces together (Prout *et al.*, 1997; Walsh and Brown, 1998). In another study, the blistered wing phenotype of tensin-null *Drosophila* was rescued by gluing the legs of mutant flies to a glass slide (Torgler *et al.*, 2004), which suggests that it is caused by a combination of tensin loss and the mechanical shear stress resulting from normal motion of the back legs against the wings that is thought to aid wing expansion and flattening (Johnson and Milner, 1987). Using other

mutants it was demonstrated that the localisation of tensin to adhesion sites *in vivo* requires integrins, talin, and ILK, but not PINCH (Torgler *et al.*, 2004). It is noteworthy that *Drosophila* tensin is a shortened protein (~80 kDa) with homology to the C-terminus of human tensin.

1.5.4 Domain Homology between the Human Tensins

The four members of the human tensin family display high sequence homology at the protein level (Figure 1.8). Tensins 1, 2 and 3 are large (~150-200 kDa) multi-domain proteins whereas cten is a shortened protein, which is approximately half the length of the larger tensins (MW ~77 kDa). All four tensins display significant homology at their C-termini, which contains a Src homology 2 (SH2) domain (Davis *et al.*, 1991) and a phosphotyrosine-binding (PTB) domain (Schultz *et al.*, 1998). The three larger tensin isoforms also display homology at their N-termini, where two actin-binding domains (Lo *et al.*, 1994b) and a region with homology to the protein and lipid phosphatase PTEN (phosphatase and tensin homolog) (Haynie and Ponting, 1996) can be found. There are 3 splice variants of the tensin2 isoform that vary only in their extreme N-termini, which leads to the inclusion or omission of a lipid-interacting C1 domain before the PTEN homology region (Chen *et al.*, 2002; Hafizi *et al.*, 2002). The N- and C-terminal regions of chicken tensin were shown to contain focal adhesion binding (FAB) sites necessary for its biological activity and cellular localisation (Chen and Lo, 2003), which are presumed to be conserved throughout the human tensin family. Tensin1 may also contain a centrally-located actin capping domain due to its high level of homology with chicken tensin (Chen *et al.*, 2000). The central regions of the larger tensins, and the N-terminus of cten, exhibit a low level of homology. This region may therefore convey functional divergence upon the different tensin proteins.



50

Figure 1.8: Alignment of the human tensins indicating domain homology. The human tensins display significant sequence homology at their C-termini, which contains a Src homology 2 (SH2) and phosphotyrosine-binding (PTB) domain in addition to focal adhesion binding (FAB) activity. The larger tensin isoforms also display homology at their N-termini where a region homologous to phosphatase and tensin homolog (PTEN) and another FAB site are located. The highly conserved N-terminus also contains actin-binding domain (ABD) Ia and Ib, which are thought to bind to the side of F-actin. Due to its high level of homology with chicken tensin, tensin1 is likely to contain a central actin-binding domain (ABD II), which is thought to cap the barbed end of F-actin. There are three tensin2 splice variants that differ only in their extreme N-termini as a result of different spliced first coding exons, which leads to the inclusion or omission of a lipid-interacting C1 domain. The central region of the three large tensin isoforms, and the N-terminus of cten, display high amino acid sequence divergence.

1.5.5 Tensin Binding Partners

Through its numerous binding modules tensin is able to interact with a variety of structural and signalling molecules, both proteins and lipids (Figure 1.9). First and foremost, the presence of PTB and actin-binding domains indicate that tensin has the potential to link integrin β subunits to the actin cytoskeleton. Several regions within tensin can bind actin with different binding characteristics and this gives tensin the capacity to both cross-link (bundle) and cap the barbed ends of actin filaments (Lo *et al.*, 1994b). The PTB domain of tensin binds to the NPxY motif in the cytoplasmic tail of integrins β 1, 3, 5 and 7 (Calderwood *et al.*, 2003). Moreover, this interaction is unaffected by the phosphorylation state of the NPxY tyrosine (McCleverty *et al.*, 2007). Consistent with this finding, the crystal structure of the chicken tensin PTB domain reveals a flexible loop containing two basic residues located next to the proposed tyrosine binding pocket that could contribute to the ability of this domain to accommodate either phosphorylated or unphosphorylated tyrosine (McCleverty *et al.*, 2007). This lack of preference is not shared by the PTB-like domain of talin, which dissociates from the integrin tail upon Src-mediated phosphorylation of the NPxY tyrosine (Tapley *et al.*, 1989). Fittingly, the analogous loop in talin is acidic (Garcia-Alvarez *et al.*, 2003). Tyrosine phosphorylation of the integrin tail, which occurs during the maturation of focal adhesions, could therefore act as a switch to promote the exchange of talin for tensin, thereby inducing fibrillar adhesion formation (McCleverty *et al.*, 2007; Legate and Fassler, 2009). This model is supported by the failure of tensin to segregate into fibrillar adhesions in Src-null cells (Volberg *et al.*, 2001). The NMR solution structure of the chicken tensin PTB domain has also been solved (Leone *et al.*, 2008). Leone *et al.* (2008) showed that the tensin PTB domain is able to interact with the phosphoinositides PIP (phosphatidylinositol 4-phosphate) and PIP2 (phosphatidylinositol 4,5-bisphosphate) through a pocket that is distinct from the integrin binding site. Moreover, PIP2 binding was shown to affect regions that may be

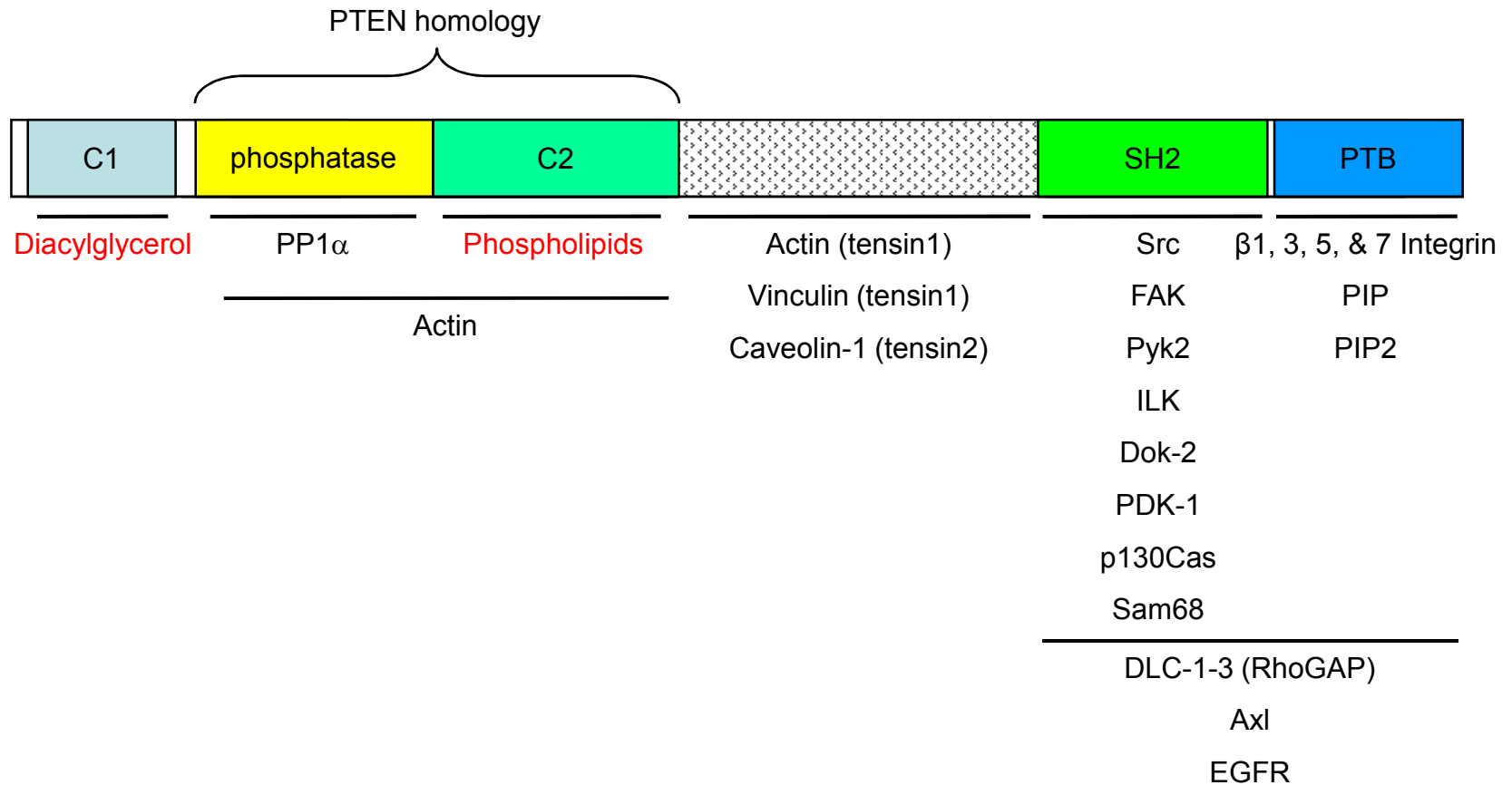


Figure 1.9: Tensin binding partners. Through its numerous binding modules tensin is able to interact with a variety of structural and signalling molecules, both proteins and lipids. Where it is known, the binding sites for these molecules are indicated. Molecules in red are hypothesized binding partners. PP1 α (protein phosphatase-1 α), FAK (focal adhesion kinase), Pyk2 (proline-rich tyrosine kinase 2), ILK (integrin-linked kinase), Dok-2 (downstream of protein kinase 2), PDK-1 (3-phosphoinositide-dependent protein kinase-1), p130Cas (p130 crk-associated substrate), Sam68 (68-kDa Src-associated protein in mitosis), DLC-1-3 (deleted in liver cancer-1-3), PIP (phosphatidylinositol 4-phosphate), PIP2 (phosphatidylinositol 4,5-bisphosphate), Axl (a receptor tyrosine kinase), EGFR (epidermal growth factor receptor).

involved in phosphotyrosine binding, which suggests that lipid binding to the PTB domain of tensin may modulate its affinity for peptide ligands such as the integrin cytoplasmic tail (Leone *et al.*, 2008).

Through its SH2 domain tensin has been shown to bind to the signalling molecules Src, FAK, Pyk2 (proline-rich tyrosine kinase 2; FAK2), ILK, Dok-2 (downstream of protein kinase 2) and PDK-1 (3-phosphoinositide-dependent protein kinase-1), the docking protein p130Cas, and the RNA-binding protein Sam68 (68-kDa Src-associated protein in mitosis) (Qian *et al.*, 2009; Zhu *et al.*, 1998b; Yamashita *et al.*, 2004; Benzing *et al.*, 2001; Wavreille and Pei, 2007; Salgia *et al.*, 1996). It was also reported that the tensin SH2 domain interacts with PI3K (Auger *et al.*, 1996); however, PI3K does not contain a sequence that matches the binding requirements of the tensin SH2 domain, which would suggest that this association is likely to be indirect (possibly via PDK1) (Wavreille and Pei, 2007). In a very recent study it was shown that the SH2 domain of tensin3 is directly tyrosine phosphorylated by the cytoplasmic kinase Src (Qian *et al.*, 2009). Moreover, tyrosine phosphorylation of the tensin3 SH2 domain was shown to enhance the binding of some ligands, including FAK, p130Cas, Sam68 and Src itself (Qian *et al.*, 2009). This represents a novel mechanism of regulation that has not previously been reported for an SH2 domain. Tensin has also been shown to interact with the adaptor protein crkII (Zhu *et al.*, 1998a); however, the tensin domain responsible for this interaction was not characterised, and it is probable that this interaction is also indirect, via the crkII-binding partner p130Cas (Salgia *et al.*, 1996; Chodniewicz and Klemke, 2004). The Axl receptor tyrosine kinase was also shown to interact directly with the SH2 and PTB domains of tensin, both individually and in combination (Hafizi *et al.*, 2002). Similarly, a tensin SH2-PTB domain fusion was shown to interact with the EGF receptor upon EGF treatment (Cui *et al.*, 2004).

Using both a blot-overlay technique and a solid-state binding assay it was shown that chicken tensin binds to vinculin through its central domain (Wilkins, 1987; Lin, 1996). This interaction was first suggested following the co-purification of tensin and vinculin from chicken gizzards (Wilkins and Lin, 1986). Given the high level of homology between chicken tensin and human tensin1 it is likely that tensin1 also interacts with vinculin in a similar manner. Indeed, vinculin was shown to co-immunoprecipitate with tensin from human mesangial cells using a tensin antibody that is now known to be tensin1-specific (Yamashita *et al.*, 2004) (Chapter 3 – this thesis). However, these studies do not preclude the possibility that the other human tensins may also bind to vinculin since the precise vinculin-binding motif has not been identified. Interestingly, neither chicken tensin, nor the human tensins, contain a sequence that corresponds to the consensus LXXAAXXVAXXVXXLIXXA that is found in the vinculin binding sites of talin (Gingras *et al.*, 2005) (Dr K Clark – personal communication), which suggests that tensin and talin bind to vinculin through different mechanisms. Tensin2 is thought to bind caveolin-1, the principle coat protein of caveolae, through a putative caveolin-1 binding motif in its central region (Yam *et al.*, 2006a). Tensin1 may also harbour such a binding motif in its N-terminus. This interaction may facilitate integrin internalisation, a process that is required for cell migration (Caswell and Norman, 2006).

The N-terminal PTEN homology region of tensin is known to interact with PP1 α , and this interaction is thought to recruit PP1 α to focal adhesions (Eto *et al.*, 2007). The PTEN homology region can be subdivided into a phosphatase domain and a phospholipid-binding C2 domain, which are likely to adopt the same folded structure as the equivalent domains in PTEN (Dr K Clark – personal communication). Moreover, splice variants 1 and 2 of tensin2 also contain a DAG (diacylglycerol)-binding C1 domain at their extreme N-termini. The activity of the C1 and C2 domains of tensin have yet to be investigated; however, these domains may serve to target tensin to the plasma membrane (Hurley, 2006).

It is becoming evident that tensin acts as a scaffold for a variety of structural and signalling proteins. Recently, much attention has been given to an interaction between tensin and the Rho GTPase activating protein (RhoGAP) deleted in liver cancer-1 (DLC-1; see below).

1.5.6 Deleted in Liver Cancer-1 (DLC-1)

DLC-1 is a candidate tumour suppressor gene mapped to chromosome 8p21, a region frequently deleted in hepatocellular carcinoma (HCC) and other solid tumours (Yuan *et al.*, 1998). DLC-1 is expressed in a wide variety of normal tissues, including brain, heart, kidney, liver, lung, skin, spleen and testis (Durkin *et al.*, 2002). In accordance with its proposed role as a tumour suppressor, several studies have shown a loss or reduction of human DLC-1 expression in liver, breast, lung, brain, stomach, colon and prostate cancer, as a result of genomic deletion or promoter hypermethylation (Liao and Lo, 2008). Re-expression of DLC-1 in liver, breast, and lung cancer cell lines has been shown to restore growth suppression (Zhou *et al.*, 2004; Wong *et al.*, 2005; Yuan *et al.*, 2003; Goodison *et al.*, 2005; Yuan *et al.*, 2004). The role of DLC-1 as a *bona fide* tumour suppressor in HCC was recently confirmed using a mouse model with liver-specific, shRNA-mediated DLC-1 knockdown (Xue *et al.*, 2008).

Mouse KO studies have revealed a vital role for DLC-1 during embryonic development. DLC-1 null mice die before 10.5 days post-coitum (dpc) with defects in the neural tube, brain, heart, and placenta (Durkin *et al.*, 2005). Interestingly, both DLC-1 and its rat homologue, p122RhoGAP, have been shown to localise to focal adhesions (Yam *et al.*, 2006a; Liao *et al.*, 2007; Qian *et al.*, 2007; Chan *et al.*, 2009; Kawai *et al.*, 2004). Cultured fibroblasts isolated from DLC-1-deficient embryos display disrupted actin filaments and have fewer focal adhesions, which is somewhat unexpected since one might have predicted that the cells would have more focal adhesions as a result of

increased RhoA activity. Several studies have shown that DLC-1 interacts directly with the C-terminus of tensin and that this interaction is required for the focal adhesion targeting of DLC-1 (Yam *et al.*, 2006a; Liao *et al.*, 2007; Qian *et al.*, 2007; Chan *et al.*, 2009; Qian *et al.*, 2009). DLC-1 is proposed to bind to both the SH2 and PTB domains of tensin; furthermore, the interaction with the SH2 domain is independent of the tyrosine phosphorylation of DLC-1, a highly unusual feature for SH2 binding (Liao *et al.*, 2007; Qian *et al.*, 2007). Two closely related molecules, known as DLC-2 (Ching *et al.*, 2003) and DLC-3 (Durkin *et al.*, 2007), which are also down-regulated in human tumours, have been shown to bind to various tensin isoforms (Kawai *et al.*, 2009; Chan *et al.*, 2009; Qian *et al.*, 2007).

DLC-1 is a RhoGAP and the rat homologue of DLC-1, p122RhoGAP, also binds to, and activates, phospholipase C δ_1 (PLC δ_1) (Homma and Emori, 1995; Sekimata *et al.*, 1999). Rho and PLC have opposing effects on focal adhesion formation (Figure 1.10). By inversely modulating the activity of these molecules, DLC-1 may serve to regulate focal adhesion dynamics and thereby cell proliferation. In agreement with this hypothesis, the growth suppressive activity of DLC-1 was found to be dependent on its proper focal adhesion targeting through tensin (Liao *et al.*, 2007; Qian *et al.*, 2007). DLC-1 also displays caveolae localisation in some cell lines (Yamaga *et al.*, 2004). Most proteins that are targeted to caveolae interact with caveolin-1, which is the major coat protein of caveolae (Williams and Lisanti, 2005). Intriguingly, DLC-1, like tensin2, also contains a putative caveolin-1 binding motif and has been shown to co-immunoprecipitate with caveolin-1 (Yam *et al.*, 2006a). The function of this interaction is currently unclear.

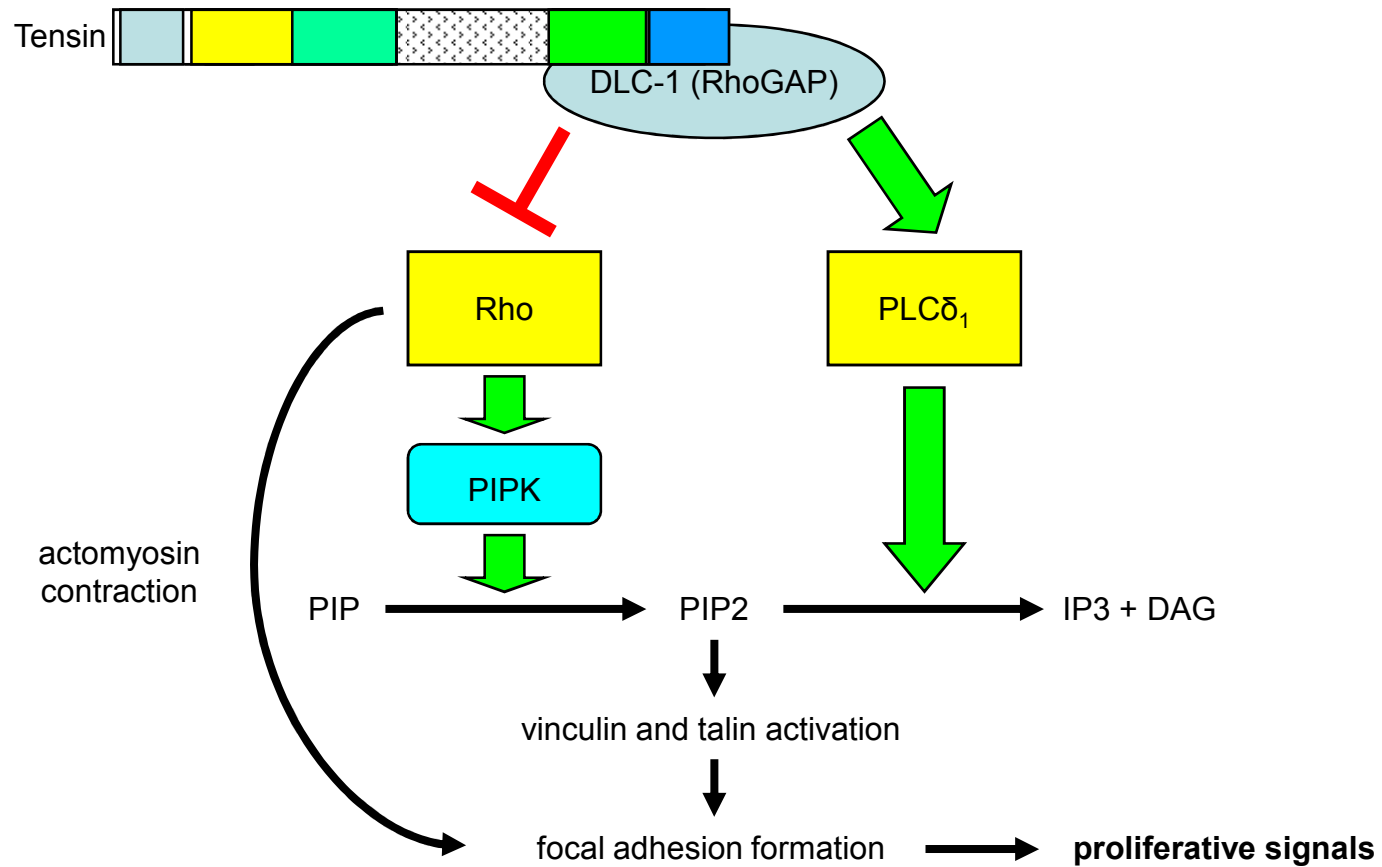


Figure 1.10: Potential mechanism for the effect of DLC-1 on proliferation through adhesion modulation. DLC-1 is a candidate tumour suppressor and one mechanism through which it may elicit its anti-proliferative activity is through the modulation of focal adhesion assembly, which in turn would affect adhesion-dependent signalling. DLC-1 (deleted in liver cancer-1), PLC δ_1 (phospholipase C δ_1), PIP (phosphatidylinositol 4-phosphate), PIP2 (phosphatidylinositol 4,5-bisphosphate), PIPK (PIP kinase), IP3 (inositol 1,4,5-trisphosphate), DAG (diacylglycerol).

1.5.7 Tensin Expression in Cancer

Several studies have highlighted alterations in the expression of the human tensins in cancer. Expression of tensin1 was shown to be down-regulated in prostate and breast cancer cell lines (Chen *et al.*, 2000). Correspondingly, tensin1 expression was induced in response to resveratrol treatment in tensin negative or deficient erythroleukemic and breast cancer cell lines, which was proposed to contribute towards the chemopreventative and anti-invasive activity of this natural dietary compound (Rodrigue *et al.*, 2005). Tensin2 expression was shown to be elevated in HCC tissues when compared to tissues isolated from non-tumourous livers (Yam *et al.*, 2006b). Conversely, the expression of tensin2 and tensin3 at the mRNA and protein level was largely absent in a diverse panel of human cancer cell lines, although this panel did not include any liver cancer cell lines (Martuszezwska *et al.*, 2009). Similarly, tensin3 expression was found to be down-regulated in thyroid tumour tissues compared to normal thyroid tissues (Maeda *et al.*, 2006). In normal tissues cten expression is largely restricted to the prostate and placenta, and analysis of cten expression in both normal and prostate cancer cell lines would suggest that cten expression is down-regulated upon prostatic cell transformation (Lo and Lo, 2002). In a very recent study, cten expression was found to be down-regulated by 10-fold in PC-3 prostate cancer cells with experimentally-induced resistance to the chemotherapy drug paclitaxel when compared to paclitaxel-sensitive PC-3 cells (Li *et al.*, 2010). Li and co-workers also showed that the over-expression of cten in paclitaxel-resistant cells restored paclitaxel sensitivity, suggesting that cten loss is a key event during the development of chemotherapy drug resistance in advanced prostate cancer (Li *et al.*, 2010). In support of this hypothesis, immunohistochemical analysis of normal and cancerous prostate tissues revealed that cten expression was inversely correlated with prostate tumour grade (Li *et al.*, 2010). Conversely, cten is frequently over-expressed in gastric cancer, and tumours with higher cten expression displayed more aggressive behaviour

(Sakashita *et al.*, 2008). Similarly, cten expression was correlated with evidence of tumour progression in lung cancer and thymoma (Sasaki *et al.*, 2003a; Sasaki *et al.*, 2003b), and with metastasis to lymph nodes in invasive breast cancer (Katz *et al.*, 2007). Furthermore, two recent studies have reported that cten expression is up-regulated in colorectal cancer cell lines and tumour samples (Albasri *et al.*, 2009; Liao *et al.*, 2009). Interestingly, Liao *et al.* (2009) also identified cten as a novel nuclear partner for β -catenin, which suggests that the oncogenic activity of cten may result from the modulation of wnt signalling. Finally, the expression of all four human tensins were found to be down-regulated in kidney tumours versus normal kidney tissue, and tensin expression mostly correlated negatively with tumour grade (Martuszezwska *et al.*, 2009). In summary, it would appear that the larger tensin isoforms are generally down-regulated in cancer, whereas cten is mostly up-regulated, with the exceptions of tensin2 in liver cancer and cten in prostate and kidney cancer.

1.5.8 Cellular Functions of Tensin

The tensin proteins have been implicated in a number of cellular processes. Like chicken tensin, all four human tensins are known to localise to focal adhesions (Chen *et al.*, 2000; Chen *et al.*, 2002; Cui *et al.*, 2004; Lo and Lo, 2002), which have led many groups to investigate the role of tensin in cell migration. Multiple studies have identified members of the tensin family as regulators of cell migration with most studies identifying tensin1, 2 and cten as positive regulators and tensin3 as a negative regulator (Chen *et al.*, 2002; Yam *et al.*, 2006b; Martuszezwska *et al.*, 2009; Albasri *et al.*, 2009). Indeed, it has been reported that a transcriptional switch in expression from tensin3 to cten promotes cell migration in response to EGF-signalling (Katz *et al.*, 2007). However, in a very recent study it was reported that tensin3 can also act as a positive regulator of cell migration (Qian *et al.*, 2009). These studies on the role of tensin in cell migration will be discussed in more detail in Chapters 4 and 5. The Rho-

family of small GTPases, particularly RhoA, Rac1, and Cdc42, play key regulatory roles in all phases of the migration cycle; from polarisation and adhesion formation to cell retraction and adhesion disassembly (Raftopoulou and Hall, 2004). Given the interaction between tensin and DLC-1, a RhoGAP, it is not surprising that tensin has been implicated in the control of cell migration.

Tensin is also thought to be required for FN matrix assembly. The idea that tensin plays a role in FN matrix assembly initially stemmed from the observation that tensin is highly abundant in fibrillar adhesions (Zamir *et al.*, 1999), which are the cellular machinery of FN fibrillogenesis (Pankov *et al.*, 2000; Mao and Schwarzbauer, 2005a). Fibrillar adhesion formation is characterised by the translocation of tensin, $\alpha_5\beta_1$ integrin and FN along actin filaments from peripherally located focal adhesions towards the centre of the cell (Pankov *et al.*, 2000; Zamir *et al.*, 2000). Pankov and co-workers showed that the actin homology 2 (AH2) region of chicken tensin acted as a dominant negative inhibitor, blocking fibrillar adhesion formation and FN fibrillogenesis when expressed in human fibroblasts (Pankov *et al.*, 2000). However, the AH2 region is not conserved in the human tensins, and no further data has been published supporting a functional role for tensin in fibrillar adhesion formation and/or FN fibrillogenesis.

A potential role for tensin3 in EGF signalling has been identified. EGF induces the Src-mediated tyrosine phosphorylation of tensin3 in a time- and dose-dependent manner, and the association of tensin3 with the EGF receptor (Cui *et al.*, 2004). Moreover, both tensin3- and EGFR-null mice display abnormalities in the development of the intestine, lung and bone, further implicating this tensin isoform in EGF signalling (Chiang *et al.*, 2005; Threadgill *et al.*, 1995). Interestingly, over-expression of chicken tensin was also shown to activate the JNK (c-Jun N-terminal kinase) and p38 MAPK (mitogen-activated protein kinase) pathways, which suggests a role for tensin in the response to cellular stress (Katz *et al.*, 2000b). Indeed, cten has been found to play a role in apoptosis.

Cten is cleaved by caspase-3 during staurosporin-induced apoptosis in normal prostate epithelial cells, and the resultant fragments of cten may also be able to induce further apoptosis (Lo and Lo, 2005). Tensin cleavage, and concomitant actin cytoskeleton disruption, was also observed during apoptosis in chicken, rat and mouse cell lines (Kook *et al.*, 2003; Korsnes *et al.*, 2007).

1.6 Project Aims and Objectives

The tensin family of proteins have been implicated in a variety of cellular processes, most notably FN fibrillogenesis and cell migration. However, little is known about the relative contributions that the different tensin isoforms make towards these processes, and thus the overall aim of this project is to determine the roles of the three large tensin isoforms.

Initially, the goal will be to generate reagents to detect and differentiate between human tensin1, 2 and 3. This will involve characterisation of the isoform specificities of several anti-tensin antibodies and the validation of qPCR primers designed to determine the levels of tensin mRNA. These reagents will then be used to investigate the tensin expression profile of HFFs, which are the classical cell line used for the study of fibrillar adhesion formation and FN fibrillogenesis. It will also be important to investigate the subcellular localisation of tensin1, 2 and 3 in HFFs either by immunocytochemistry or by expressing these proteins as GFP-fusions. An RNAi approach will then be used to investigate the requirement for the three large tensin isoforms in FN fibrillogenesis, initially focusing on the isoform(s) that localise to fibrillar adhesions.

The role of human tensin1, 2 and 3 in 2D cell migration in a number of cell types will then be investigated. This will be achieved through the modulation of tensin expression both by over-expression and RNAi-mediated knockdown followed by the examination of 2D migration using a scratch-wound assay. It is already known that tensin1 and 2 can promote 2D cell migration, however, very little is known about the role of tensin3 and therefore particular attention will be paid to this isoform.

2D migration assays do not accurately model the type of migration exhibited by cells *in vivo*. Therefore, the final goal will be to investigate the requirement for all three large human tensins in 3D migration through fibrillar protein matrices, which more closely resemble the type of environment encountered by cells in the body.

Chapter 2 Materials and Methods

Unless otherwise stated, chemical reagents were supplied by Sigma-Aldrich Company and cell culture solutions were supplied by Gibco Invitrogen Cell Culture. Cell culture plastics were manufactured by Nalge Nunc International.

2.1 Molecular Biology

2.1.1 Materials

2.1.1.1 Host Strains and Media

E. coli strains:

- DH5 α was used for the amplification of plasmid expression vectors for transfection of mammalian cells or transformation of bacterial cells.
- BL21(DE3) was used for the expression of recombinant polypeptides for the affinity purification of anti-tensin polyclonal antibodies.

Media:

- 2YT media (1% [w/v] yeast extract, 86 mM NaCl, 1.6% [w/v] Tryptone; Oxoid) containing the appropriate antibiotic (50 μ g/ml ampicillin or 25 μ g/ml kanamycin).
- 2YT agar (1% [w/v] yeast extract, 86 mM NaCl, 1.6% [w/v] Tryptone; Oxoid, 1.5% [w/v] agar) containing the appropriate antibiotic (100 μ g/ml ampicillin or 75 μ g/ml kanamycin).
- SOC media (0.5% [w/v] yeast extract, 8.6 mM NaCl, 2% [w/v] Tryptone; Oxoid, 20 mM glucose).

2.1.1.2 Expression Plasmids

cDNAs encoding the three large human tensin isoforms were each cloned into the pEGFP-C1 expression vector (Clontech) by Dr Katherine Clark. NCBI reference sequences; tensin1 - NM_022648.4, tensin2 (variant 3) - NM_198316.1, tensin3 - NM_022748.10. The GFP-chicken tensin AH2 region recombinant expression plasmid was a generous gift from Dr Kenneth Yamada (NIDCR, NIH, Bethesda, MD, USA) (Pankov *et al.*, 2000). The mCherry-Rab25 and photoactivatable(pa)EGFP- α 5 integrin recombinant expression plasmids were kindly provided by Dr Patrick Caswell (Beatson Institute for Cancer Research, Glasgow, UK) (Caswell *et al.*, 2007). All of the above expression constructs encoded fusion proteins with N-terminal fluorescent moieties. cDNAs encoding ~150 amino acid fragments of human tensin2 (residues 737-887) and human tensin3 (residues 374-522) were cloned into the pET151/D-TOPO expression vector (Invitrogen) by Dr Katherine Clark. The IPTG-induced expression of these recombinant plasmids in BL21(DE3) *E. coli* was used to produce fusion proteins with N-terminal polyhistidine (His₆) tags.

2.1.1.3 Small Interfering RNAs (siRNAs)

All siRNA oligos were purchased from Thermo Scientific Dharmacon. Where available, siRNA sequences are given in Table 2.1.

siRNA	Sequence 5'-3' (Sense Strand)
siGLO RISC-Free siRNA	Proprietary Sequence (Catalogue No. D-001600-01)
ON-TARGET _{plus} siCONTROL Non-Targeting Pool (siCON)	UGGUUUACAUGUCGACUAA UGGUUUACAUGUUGUGUGA UGGUUUACAUGUUUUCUGA UGGUUUACAUGUUUCCUA
TNS1 (human tensin1) siGENOME SMARTpool (sihT1)	GAAGGUACGUGCAUUACUU (sihT1.1) GCAACUACCUGCUGUUCUAA (sihT1.2) GCAAUGUGCUCUUCUUCUAA (sihT1.3) GAAGCUCCAUGCCAAGGUA (sihT1.4)
TENC1 (human tensin2) siGENOME SMARTpool (sihT2)	CAAAGGCGAUGUCAUGGUA (sihT2.1) GAGGAGCAGUUCUCCAGUUA (sihT2.2) GAAUGUGUGUCACCUCUUU (sihT2.3) GAACAGCAGCCCUCUCUUC (sihT2.4)
TENS1 (human tensin3) siGENOME SMARTpool (sihT3)	CCACGAAGCUGCCCUGAGA (sihT3.1) GAAGGAGGAUCUGGACAAU (sihT3.2) GUACAAGGCGGAUAAUUUCA (sihT3.3) GCACAAAGGAGGACGUGAA (sihT3.4)

Table 2.1: siRNA sequences.

2.1.2 *E. coli* Transformation

Competent DH5 α or BL21(DE3) *E. coli* (50 μ l) were prepared for transformation by defrosting on ice, mixing with approximately 10 ng vector DNA, and incubating on ice for 30 minutes. The bacteria were then subjected to a 45 second heat shock at 42°C before incubating on ice for 2-3 minutes. 300 μ l of SOC media was then added to the culture before incubating at 37°C for 1 hour with shaking (225 rpm) to allow expression of the relevant antibiotic resistance gene. Finally, the transformed culture was spread onto 2YT agar plates containing the appropriate antibiotic, which were inverted and incubated overnight at 37°C to allow the growth of resistant colonies.

2.1.3 Plasmid Amplification and Purification

A single colony of transformed DH5 α *E. coli* was used to inoculate 5 ml 2YT media containing the appropriate antibiotic and incubated at 37°C for at least 4 hours with

shaking (225 rpm). This starter culture was then diluted 1:100 into 500 ml 2YT media containing the appropriate antibiotic, and incubated overnight at 37°C with shaking (225 rpm).

Two different plasmid DNA purification methods were used to isolate recombinant plasmids from overnight cultures of transformed DH5 α *E. coli*. These methods are outlined below.

2.1.3.1 Density Centrifugation Plasmid DNA Purification (Caesium Chloride)

A 500 ml overnight culture of transformed DH5 α *E. coli* was centrifuged at 4,000 rpm (2,500 x g) for 10 minutes (Sorvall Evolution RC centrifuge, SLA-1 1500 rotor). Pelleted cells were resuspended in 10 ml P1 buffer (50 mM Tris-HCl; pH 8.0, 10 mM EDTA, 100 μ g/ml RNase A; Qiagen), and incubated on ice for 5 minutes. 20 ml of P2 buffer (200 mM NaOH, 1% [w/v] sodium dodecyl sulphate; SDS) was added to lyse the bacteria, followed by incubation on ice for 5 minutes. 15 ml of P3 buffer (3 M potassium acetate; pH 5.5) was added to precipitate protein and chromosomal DNA, which were then pelleted by centrifugation at 9,000 rpm (12,500 x g) for 15 minutes (Sorvall Evolution RC centrifuge, SLA-1 1500 rotor). The DNA within the supernatant was precipitated with the addition of 50 ml ice-cold isopropanol, and pelleted by centrifugation at 9,000 rpm (9,500 x g) for 15 minutes (Sorvall Evolution RC centrifuge, SS-34 rotor). The pellet was air-dried and resuspended in 5.5 ml Tris-EDTA (10 mM Tris-HCl; pH 8.0, 1 mM EDTA). 6 g caesium chloride (CsCl) and 225 μ l ethidium bromide (10 mg/ml) was added to the DNA solution. This solution was centrifuged at 4,000 rpm (3,000 x g) for 5 minutes (Eppendorf Centrifuge 5810 R, A-4-62 rotor), and the supernatant transferred into 2 Quickseal ultracentrifuge tubes (Beckman). These tubes were sealed and centrifuged at 100,000 rpm (540,000 x g) for 12-16 hours (Beckman Ultima Ultracentrifuge, TLA 100.3 rotor). The plasmid DNA band was removed with a 19 G

needle (Becton Dickinson) and the ethidium bromide was extracted from the aqueous sample by mixing 5-10 times with an equal volume of water-saturated butanol. The plasmid DNA was precipitated with ethanol and pelleted by centrifugation at 11,000 rpm (14,500 x g) for 15 minutes (Sorvall Evolution RC centrifuge, SS-34 rotor). The DNA was washed with 70% (v/v) ethanol and re-pelleted by centrifugation at 11,000 rpm (14,500 x g) for 15 minutes (Sorvall Evolution RC centrifuge, SS-34 rotor). The supernatant was discarded and the DNA pellet air-dried before resuspension in 500 μ l of ultrapure water.

DNA concentration was measured by spectrophotometry using a BioPhotometer (Eppendorf), assuming that an absorbance of 1.0 at 260 nm corresponds to a DNA concentration of 50 μ g/ml. DNA purity was also estimated from 260/280 ratios.

2.1.3.2 Column-Based Plasmid DNA Purification (Maxiprep)

Plasmid DNA was purified from a 500 ml overnight culture of transformed DH5 α *E. coli* using PureLink HighPure plasmid purification columns (Invitrogen); manufacturer's guidelines were followed. This method is based on a modified alkaline lysis procedure, followed by passage of the lysate through a pre-packed anion exchange column. Under moderate salt conditions, plasmid DNA remains bound to the resin while RNA, proteins, carbohydrates and other impurities are washed away with wash buffer. The plasmid DNA is finally eluted under high salt conditions with an elution buffer, desalted and concentrated by alcohol precipitation, and resuspended in 500 μ l of ultrapure water. DNA concentration was determined by spectrophotometry as described previously.

2.1.4 Quantitative Real-Time Polymerase Chain Reaction (qPCR)

2.1.4.1 RNA Isolation

RNA was isolated from mammalian cells using an Rneasy mini kit (Qiagen); manufacturer's guidelines were followed. Cells were washed twice with phosphate buffered saline (PBS; 160 mM NaCl, 3 mM KCl, 8 mM Na₂HPO₄, 1 mM KH₂PO₄; pH 7.3) and lysed through the addition of a highly denaturing guanidine isothiocyanate-containing buffer. This buffer, which immediately inactivates RNases, was added directly to the cell monolayer, and cell lysates were harvested using a cell scraper. Lysates were homogenized by passage through a spin column, termed the QIAshredder, at 13,400 rpm (12,100 x g) for 2 minutes (Eppendorf MiniSpin centrifuge, F-45-12-11 rotor). Following homogenisation, 75% (v/v) ethanol was added to the lysate, which was then applied onto an RNeasy spin column. Centrifugation of this spin column at 13,400 rpm (12,100 x g) for 15 seconds (Eppendorf MiniSpin centrifuge, F-45-12-11 rotor) led to the absorption of RNA onto a silica-gel membrane. Further contaminants were removed through washing of the silica-gel membrane with a series of different buffers. Finally, the RNA was eluted from the spin column with RNase-free water (2 x 30 µl) by centrifugation at 13,400 rpm (12,100 x g) for 1 minute (Eppendorf MiniSpin centrifuge, F-45-12-11 rotor). RNA concentration was measured by spectrophotometry using a BioPhotometer (Eppendorf), assuming that an absorbance of 1.0 at 260 nm corresponds to an RNA concentration of 40 µg/ml.

2.1.4.2 DNase I Treatment

RNA was treated with DNase I to remove any potential genomic DNA (gDNA) contamination prior to cDNA synthesis and the qPCR reaction using the DNA-free kit (Ambion; Applied Biosystems); manufacturer's guidelines were followed and the so-

called “rigorous protocol” was carried out to ensure complete gDNA removal. 5 µl 10x DNase I buffer and 0.5 µl (1 unit) DNase I were added to 44 µl (up to 8.8 µg) RNA (up to 0.2 µg/µl), mixed and incubated at 37°C for 30 minutes. After 30 minutes, another 0.5 µl DNase I was added to the solution and incubated at 37°C for a further 30 minutes. To remove the DNase 5 µl of resuspended DNase Inactivation Reagent was added to the samples, which were mixed, incubated at room temperature for 2 minutes (mixing occasionally), and centrifuged at 10,000 x g for 1.5 minutes (Eppendorf MiniSpin centrifuge, F-45-12-11 rotor). The supernatant, which contains the RNA, was carefully transferred to a fresh tube and either reverse transcribed or snap frozen on dry ice and stored at -20°C. RNA concentration was re-calculated after DNase I treatment so that the appropriate amount of RNA was included in the subsequent cDNA synthesis reaction.

2.1.4.3 cDNA Synthesis (Reverse Transcription)

DNase I-treated RNA was reverse transcribed with the Superscript II reverse transcriptase kit (Invitrogen). 1 µg RNA was incubated with a 3.3 mM dNTP mixture and 0.5 µg oligo(dT)₁₂₋₁₈ primer in a total volume of 12 µl, for 5 minutes at 65°C. Once the RNA had been denatured, the solution was chilled on ice for 5 minutes to allow primer annealing. Following this, 2 µl of 0.1 M dithiothreitol (DTT), 1 µl (40 units) of RNase Out (RNase inhibitor), and 4 µl of 5x first strand buffer were added, and incubated at 42°C for 2 minutes. 1 µl (200 units) of Superscript II reverse transcriptase enzyme was then added and incubated at 42°C for 50 minutes to allow primer extension. Finally, the reverse transcriptase enzyme was inactivated at 70°C for 15 minutes. cDNA was snap frozen on dry ice and stored at -20°C.

2.1.4.4 qPCR Reaction

qPCR reactions were carried out in a MiniOpticon Real-Time PCR Detection System (Bio-Rad Laboratories) in the presence of the SYBR Green dsDNA-specific fluorescent dye. Reactions were performed in triplicate or quadruplicate using a 25 μ l reaction volume. Reaction conditions were optimised with the use of the 2x iQ SYBR Green Supermix (Bio-Rad Laboratories). 0.625 ng to 20 ng of cDNA was amplified using one of four primer pairs (Invitrogen; Table 2.2) with each primer (forward and reverse) at 0.8 μ M concentration. No template controls (NTCs) were prepared for each primer pair to monitor for contamination; however, amplification from the NTC reactions was always insignificantly small or completely absent. The qPCR thermal profile consisted of a 3 minute 95°C denaturation step, followed by 40 cycles of; (i) a 15 second 95°C denaturation step, (ii) a 20 second 58°C annealing step, and (iii) a 15 second 72°C extension step. After the final amplification cycle was complete, a dissociation curve analysis was performed. During this procedure the temperature was raised from 58°C to 95°C using 1°C increments. Fluorescence intensity was measured once every cycle during the amplification phase, and once every 1°C incremental increase during the dissociation curve analysis. Visual inspection of the dissociation curves confirmed the presence of a single PCR product and the absence of primer dimer formation for each primer pair.

Primer	Sequence 5'-3'
GAPDH Forward	GAGTCAACGGATTTGGTCGT
GAPDH Reverse	GACAAGCTTCCCGTTCTCAG
Tensin1 Forward	GGCTTAGAGCGAGAGAAGCA
Tensin1 Reverse	CCCGTCCAGAGAAGAGAGTG
Tensin2 Forward	GAATGAACAGCAGCCCTCTC
Tensin2 Reverse	TACCATGACATCGCCTTTGA
Tensin3 Forward	GGACGCATAGGAGTGGTCAT
Tensin3 Reverse	GGGAGAGGCATTCATTTTCA

Table 2.2: qPCR primer sequences.

2.1.4.5 Primer Validation

Primer validation is a prerequisite for the success of any qPCR experiment, and the delta delta C_T ($\Delta\Delta C_T$) method of relative quantification requires that all primer pairs have an efficiency of approximately 100%, thereby ensuring that the amount of PCR product doubles every cycle. In essence, primer validation determines the ability of a primer pair to amplify linearly over a wide range of template concentrations, thereby confirming that the amount of fluorescence signal measured is proportional to the amount of starting material.

The efficiency of all four primer pairs was assessed using the standard curve method in which each primer pair was used to amplify cDNA samples of known relative concentrations (i.e. serial dilutions). Fluorescence intensity, which corresponds directly to the production of dsDNA products, was plotted against cycle number to give rise to an amplification plot for each reaction. A threshold line was placed on this graph to signify the point at which fluorescence intensity increased to above background levels and amplification was in the log-linear phase, when none of the reaction components are limiting. The cycle at which a particular amplification plot crosses this threshold line

is termed the threshold cycle (or C_T). C_T is inversely proportional to the log of the initial input amount, i.e. the higher the abundance of the template DNA, the fewer cycles are required for the fluorescence signal to become significantly higher than the background noise. Primer pair amplification efficiencies were determined by constructing standard curves in which C_T was plotted against the log of the initial input quantity. The gradient of each standard curve corresponds to the amplification efficiency of the primer pair in question (see below).

Theoretically, the amount of PCR product doubles every cycle. Therefore, in theory, the course of a PCR reaction can be represented using the following equation: -

$$N = N_0 2^n$$

Where N is the number of amplified molecules (amplicons), N_0 is the initial number of template molecules, and n is the number of cycles.

Many factors can influence the efficiency of a PCR reaction, and therefore, amplification efficiency (E) is very often less than perfect, ranging from zero to 1 (or 0 to 100%). Hence, the equation above must be modified: -

$$N = N_0(1+E)^n$$

OR

$$N = N_0(1+E)^{C_T}, \text{ which can also be written as, } \log N = \log N_0 + C_T \log(1+E).$$

Therefore, a graph in which the threshold cycle (C_T) is plotted against the log of the initial target copy number will have a gradient of $-[1/\log(1+E)]$ which can be rearranged to calculate the amplification efficiency: -

$$E = 10^{(-1/\text{gradient})} - 1$$

2.1.4.6 Relative Abundance Quantification using Delta Delta C_T ($\Delta\Delta C_T$) Analysis

The $\Delta\Delta C_T$ method (Livak and Schmittgen, 2001; Schmittgen and Livak, 2008) was used to calculate changes in the relative abundance of tensin mRNAs upon siRNA treatment through comparison back to the GAPDH internal control, using the following equations: -

$$\text{Fold change} = 2^{-\Delta\Delta C_T}$$

$$\text{Where, } \Delta\Delta C_T = (C_{T,\text{tensin}} - C_{T,\text{GAPDH}})_{\text{tensin siRNA}} - (C_{T,\text{tensin}} - C_{T,\text{GAPDH}})_{\text{control siRNA}}$$

2.2 Biochemistry

2.2.1 Protein Expression in *E. coli*

A single colony of transformed BL21(DE3) *E. coli* was used to inoculate 5 ml 2YT media containing the appropriate antibiotic and incubated overnight at 37°C with shaking (225 rpm). This starter culture was then diluted 1:100 into 500 ml 2YT media containing the appropriate antibiotic and returned to the 37°C shaking incubator until an $OD_{600\text{nm}}$ of 0.4 was reached. At this density the bacteria were induced to express the recombinant protein with 250 μM IPTG and cultured for a further 4 hours at 37°C with shaking (225 rpm). The bacteria were then pelleted by centrifugation at 6,000 rpm

(5,500 x g) for 10 minutes (Sorvall Evolution RC centrifuge, SLA-1 1500 rotor), and the pelleted cells were lysed in 20 ml of 0.1% (v/v) Triton X-100 (in PBS) on ice before adding 200 µl of 2% (w/v) PMSF to prevent proteolysis. Lysates were stored at -20°C.

2.2.2 Affinity Purification of Anti-Tensin Polyclonal Antibodies

Rabbit polyclonal antibodies were raised against human tensin2 (Rb31 and Rb32) and tensin3 (Rb33 and Rb34) (Biosource; Invitrogen) using short peptide immunogens based on the central divergent regions of the tensin proteins; tensin2 (residues 802-822) and tensin3 (residues 439-457). The purification of these antibodies is described below.

2.2.2.1 Ammonium Sulphate Precipitation

Rather than affinity purifying the anti-tensin polyclonal antibodies directly from serum, which contains additional proteins that may interfere with antibody binding to the antigen affinity column, a preparation enriched in IgG was produced from the serum by ammonium sulphate precipitation. An equal volume of PBS was added to the serum before incubation on ice. Once ice-cold, 2 volumes of saturated ammonium sulphate (in PBS) were slowly added to the serum whilst stirring, and the solution was left stirring for a further 1 hour on ice to allow protein precipitation. Precipitated protein was pelleted by centrifugation at 9,000 rpm (10,000 x g) for 20 minutes at 4°C (Sorvall Evolution RC centrifuge, SS-34 rotor). The pellet was resuspended in 6 ml PBS, and dialysed at 4°C overnight against 2 litres of PBS with one buffer change.

2.2.2.2 Nickel Ion Affinity Chromatography

His₆-tagged polypeptides corresponding to human tensin2 (residues 737-887) and tensin3 (residues 374-522) were purified from BL21(DE3) *E. coli* protein lysates by nickel ion affinity chromatography. These recombinant polypeptides contained the sequence of the immunogens used to generate the anti-tensin2 and 3 polyclonal antibodies, respectively.

BL21(DE3) *E. coli* lysate was sonicated on ice by 3 x 30 second pulses (~12 μ m oscillation magnitude) with 15 second breaks between each pulse, clarified by centrifugation at 11,000 rpm (14,500 x g) for 10 minutes (Sorvall Evolution RC centrifuge, SS-34 rotor), and passed through a 0.45 μ m filter. The nickel affinity column (Amersham Pharmacia Biotech; GE Healthcare) was washed with water, charged with charge buffer (50 mM NiSO₄) and prepared for the sample with binding buffer (0.5 mM imadazole, 0.5 M NaCl, 20 mM Tris; pH 7.9). The protein sample was then applied to the column and non-binding proteins were eluted with wash buffer (60 mM imadazole, 0.5 M NaCl, 20 mM Tris; pH 7.9). Bound protein was eluted with elution buffer (1 M imadazole, 0.5 M NaCl, 20 mM Tris; pH 7.9), collecting 1 ml fractions. The column was then washed with strip buffer (0.5 M NaCl, 100 mM EDTA, 20 mM Tris; pH 7.9), then with water, and stored in 20% (v/v) ethanol ready for reuse. Protein concentration in the eluate was assessed using the Coomassie Plus (Bradford) Protein Assay (Thermo Scientific Pierce). 5 μ l of each fraction was added to 1 ml Bradford reagent and mixed before measuring absorbance at 595 nm by spectrophotometry using a BioPhotometer (Eppendorf). Protein concentration was determined by comparison to absorbance readings for BSA samples of known concentration plotted on a standard curve. Protein-containing fractions were pooled and dialysed against PBS.

2.2.2.3 *Antigen Affinity Chromatography*

Purified tensin polypeptides were used to affinity purify anti-tensin antibodies by coupling them to CNBr-activated Sepharose 4 Fast Flow beads (Amersham Biosciences; GE Healthcare) following the manufacturer's guidelines. The beads were hydrated in 1 mM HCl for 30 minutes on a rotator, and washed twice by centrifugation at 300 x g for 1 minute (Eppendorf Centrifuge 5702, A-4-38 rotor) and resuspension in 1 mM HCl. CNBr groups were activated by washing with PBS and coupled to the relevant tensin polypeptides (in PBS) by incubation for 3 hours at room temperature on a rotator. The derivatised gel was washed in PBS before blocking unused active groups by incubation in 1 M ethanolamine for 2 hours at room temperature on a rotator. Non-covalently bound proteins were removed by 5 alternate washes in high and low pH buffers before washing the coupled beads with PBS. Once the coupling procedure was complete the beads were packed into a 10 ml filter column and washed with PBS before applying the IgG serum fraction. Non-binding proteins were eluted with PBS. Bound proteins (i.e. the anti-tensin antibodies) were eluted with 0.1 M glycine-HCl (pH 2.7), collecting 1 ml fractions, which were immediately neutralised with 1 M Tris (pH 9.0) and stored on ice. Antibody-containing fractions identified using the Bradford assay were pooled and dialysed against PBS. Antibody concentration was determined by spectrophotometry using a BioPhotometer (Eppendorf), assuming that an absorbance of 1.4 at 280 nm corresponds to an antibody concentration of 1 mg/ml (based on IgG; MW = 145,000 g/mol, extinction coefficient = 203,000 M⁻¹cm⁻¹).

2.2.3 Protein Analysis and Detection

2.2.3.1 Preparation of Protein Lysates

Whole cell lysates prepared in RIPA buffer:

Culture media was removed and cells washed with ice-cold PBS before the addition of RIPA lysis buffer (50 mM HEPES; pH 7.5, 150 mM NaCl, 10% [v/v] glycerol, 1 mM EGTA, 1 mM sodium vanadate, 1 mM NaF, 2 mM 4-[2-aminoethyl] benzenesulfonyl fluoride hydrochloride [AEBSF], 1% [v/v] Triton X-100, 1% [w/v] sodium deoxycholate, 0.1% [w/v] SDS, 1x Complete protease inhibitor; Roche). Cells were removed from the tissue culture plastic with a cell scraper and disrupted by passing 5 times through a 23 G needle (Becton Dickinson). Lysates were clarified by centrifugation at 13,000 rpm for 10 minutes at 4°C (Sanyo Hawk 15/05 centrifuge). The supernatant was collected, mixed with 5x SDS sample buffer (final concentration; 2% [w/v] SDS, 5% [v/v] glycerol, 25 mM Tris-HCl; pH 6.8, 0.002% [w/v] bromophenol blue, 2% [v/v] β -mercaptoethanol), and boiled for 3 minutes. Protein lysates were stored at -20°C.

Soluble and insoluble FN fractions prepared using deoxycholate (DOC)-containing lysis buffer:

Culture media was removed and cells were washed with ice-cold PBS before the addition of DOC lysis buffer (20 mM Tris-HCl; pH 8.5, 1% [w/v] DOC, 2 mM N-ethylmaleimide, 2 mM iodoacetic acid, 2 mM EDTA, 2 mM AEBSF). Cells were removed from the tissue culture plastic with a cell scraper and disrupted by passing 5 times through a 23 G needle (Becton Dickinson). Lysates were clarified by centrifugation at 13,000 rpm for 20 minutes at 4°C (Sanyo Hawk 15/05 centrifuge). The supernatant (DOC soluble fraction) was collected, mixed with 5x SDS sample buffer,

boiled for 3 minutes, and frozen. 200 µl DOC lysis buffer was gently added to the pellet before centrifugation at 13,000 rpm for 5 minutes at 4°C (Sanyo Hawk 15/05 centrifuge). The supernatant was removed and the pellet (DOC insoluble fraction) was resuspended in 2x SDS sample buffer (final concentration; 2% [w/v] SDS, 5% [v/v] glycerol, 25 mM Tris-HCl; pH 6.8, 0.002% [w/v] bromophenol blue, 2% [v/v] β-mercaptoethanol), boiled for 3 minutes, and frozen.

2.2.3.2 SDS-Polyacrylamide Gel Electrophoresis (SDS-PAGE)

7.5% or 12% (v/v) Bis-acrylamide (37.5:1, Flowgen Bioscience) resolving gels were used for protein molecular weight separation by electrophoresis (125 mM Tris-HCl; pH 8.9, 0.1% [w/v] SDS, 2 mM EDTA). The resolving gel was overlaid with a 4% (v/v) acrylamide stacking gel (125 mM Tris-HCl; pH 6.7, 0.1% [w/v] SDS, 2 mM EDTA). Gels were run in SDS-running buffer (25 mM Tris-Base, 0.1% [w/v] SDS, 192 mM glycine). Reduced protein lysate samples were electrophoresed at 100 V for 20 minutes to clear the stacking gel, and then at 150 V for 40-60 minutes to achieve the required protein separation. Molecular weight markers were run alongside protein samples for comparison; SDS-PAGE Standards or Precision Plus Protein Standards (Bio-Rad Laboratories).

2.2.3.3 Western Blotting

Proteins were electro-transferred from the SDS gel onto Hybond-C Extra nitrocellulose membrane (Amersham Biosciences; GE Healthcare) using the Xcell II blotting module (Invitrogen) at 30 V for 1 hour in transfer buffer (25 mM Tris-Base; pH8.3, 192 mM glycine, 10% [v/v] methanol, 0.05% [w/v] SDS). The transferred protein was identified by Ponceau red staining (0.2% [w/v] Ponceau S, 3% [v/v] acetic acid). Non-specific protein-binding sites were blocked by incubation for 30 minutes in 5% (w/v) Marvel

non-fat powdered milk (Premier Foods) in Tris-buffered saline-Tween (TBST; 25 mM Tris-HCl; pH8, 150 mM NaCl, 0.05% [v/v] Tween 20) at room temperature with gentle shaking. Nitrocellulose was incubated in the appropriate dilutions of primary antibody (in 5% Marvel/TBST) overnight at 4°C with gentle shaking (see Table 2.3 for antibodies). To remove any unbound primary antibody the nitrocellulose was washed in TBST (3 x 15 minutes). Nitrocellulose was then incubated in the appropriate HRP-conjugated secondary antibody (in 5% Marvel/TBST) for 1 hour at room temperature with gentle shaking. To remove any unbound secondary antibody the nitrocellulose was again washed in TBST (3 x 15 minutes). The SuperSignal chemiluminescent reagent (Thermo Scientific Pierce) was added to the membrane before exposure to Super RX photographic films (Fuji Photo Film [UK]) for varying lengths of time. Where necessary, densitometry was performed on scanned images of films where exposure was non-saturating using the measure function in ImageJ (NIH, Bethesda, MD, USA).

2.3 Cell Biology

2.3.1 Materials

2.3.1.1 Cell Lines and Media

Four human cell lines were maintained for use in the experiments described in this thesis; HEK (human embryonic kidney) 293 cells, primary human foreskin fibroblasts (HFFs), telomerase-immortalised fibroblasts (TIFs), and A2780 human ovarian epithelial cancer cells (stably transfected with HA-Rab25 or the empty pcDNA3 vector i.e. A2780-Rab25 and A2780-DNA3). Stable clones of A2780-DNA3 and A2780-Rab25 cells were generated as described previously (Cheng *et al.*, 2004). All cell types were cultured at 37°C in an atmosphere of 10% (v/v) CO₂. HEK293 cells and HFFs were grown in Dulbecco's modified Eagles medium (DMEM; 1000 mg/l glucose, 4 mM L-

Antibody	Description	Source	Working Dilution/Concentration
GFP	Poyclonal rabbit anti-green fluorescent protein (GFP)	Molecular Probes	1 in 1000
Tensin	Monoclonal mouse anti-chicken tensin	BD Transduction Laboratories	1 µg/ml
Tensin	Monoclonal mouse anti-chicken tensin	Chemicon International	1 µg/ml
Tensin	Monoclonal mouse anti-chicken tensin	Upstate Biotechnology	1 µg/ml
Tensin	Polyclonal rabbit anti-human tensin1	Santa Cruz Biotechnology	1 in 200
Rb31	Polyclonal rabbit anti-human tensin2	Biosource (Invitrogen)	1 µg/ml
Rb32	Polyclonal rabbit anti-human tensin2	Biosource (Invitrogen)	1 µg/ml
Rb33	Polyclonal rabbit anti-human tensin3	Biosource (Invitrogen)	1 µg/ml
Rb34	Polyclonal rabbit anti-human tensin3	Biosource (Invitrogen)	1 µg/ml
FN	Polyconal rabbit anti-human FN	D R Critchley (University of Leicester, UK)	1 in 20000 (RIPA), 1 in 10000 (DOCi), 1 in 5000 (DOCs)
Human FN	Monoclonal mouse anti-human FN (does not react with bovine FN)	Abcam	1 µg/ml
GAPDH	Monoclonal mouse anti-rabbit glyceraldehyde-3-phosphate dehydrogenase	Chemicon International	0.1 µg/ml
Vimentin	Monoclonal mouse anti-human vimentin	Sigma	1 in 100 (DOCi), 1 in 2000 (DOCs)
Pan-Cytokeratin	Monoclonal mouse anti-human cytokeratin	Sigma	1 in 4000
HA	Polyclonal rabbit anti-haemagglutinin	Santa Cruz Biotechnology	1 in 500
Anti-Mouse-HRP	Polyclonal sheep anti-mouse IgG (horseradish peroxidase-conjugated)	Amersham	1 in 5000
Anti-Rabbit-HRP	Polyclonal goat anti-rabbit IgG (horseradish peroxidase-conjugated)	Sigma	1 in 3500

Table 2.3: Antibodies for Western blotting. DOCi and DOCs refer to insoluble and soluble fractions prepared using deoxycholate (DOC)-containing lysis buffer, respectively.

glutamine, 110 mg/l sodium pyruvate) supplemented with 10% (v/v) foetal calf serum (FCS; Sigma), 2 mM L-glutamine, 100 U/ml penicillin and 100 µg/ml streptomycin. TIFs were cultured in the same medium with an additional 10% (v/v) FCS (20% in total), 10 mM HEPES (4-(2-hydroxyethyl)-1-piperazineethanesulfonic acid) and 0.25 µg/ml Amphotericin B (Fungizone). A2780 cells were grown in Roswell Park Memorial Institute 1640 medium (RPMI; 2 mM GlutaMAX) supplemented with 10% (v/v) FCS, 2 mM L-glutamine, 100 U/ml penicillin, 100 µg/ml streptomycin and 0.25 µg/ml Amphotericin B (Fungizone).

2.3.2 Mammalian Cell Transfection

Several different methods of transfection were used depending on cell type and the nature of the nucleic acid to be delivered into the cell (i.e. expression construct DNA or siRNA duplex): -

HEK293: Lipofection (DNA - Fugene 6, siRNA - Lipofectamine 2000)
HFF: Electroporation (DNA)
Lipofection (DNA - Lipofectamine LTX, siRNA - Lipofectamine 2000, Oligofectamine)
A2780: Nucleofection (DNA and siRNA)

2.3.2.1 Transfection of HEK293 Cells

i) Lipofection of HEK293 cells with expression construct DNA using Fugene6:

One day prior to transfection, a confluent 10 cm plate of HEK293 cells was divided 1 in 5 into 10 cm plates in antibiotic-free media and cultured overnight at 37°C. After 24 hours, a single 10 cm plate of cells (50-80% confluent) was used for each transfection.

100 μ l DMEM was mixed with 3 μ l of the Fugene6 transfection reagent (Roche) and incubated for 5 minutes at room temperature. Transfection complexes were formed through the addition of 1 μ g vector DNA, mixing and incubation for 40 minutes at room temperature. Cell culture media was replaced with 10 ml fresh antibiotic-free media. Transfection complexes were applied dropwise to the cells, which were then cultured at 37°C until required. Note: For scratch-wound assay, transfection conditions were proportionally scaled down to a 6-well plate format.

ii) Lipofection of HEK293 cells with siRNA duplexes using Lipofectamine 2000:

One day prior to transfection, HEK293 cells were seeded into 6-well culture plates at a density of 3×10^5 cells/well in antibiotic-free culture medium such that 90% confluence would be achieved 24 hours later. siRNA solutions at 100x working concentration were made up in siRNA buffer (20 mM KCl, 0.2 mM $MgCl_2$, 6 mM HEPES; pH7.5, in RNase-free water). 25 μ l of 100x siRNA was diluted in 225 μ l Opti-MEM medium and mixed by pipetting. Separately, 5 μ l Lipofectamine 2000 transfection reagent (Invitrogen) was mixed with 245 μ l Opti-MEM medium and incubated for 15 minutes at room temperature. The two solutions were mixed together and incubated for 15 minutes at room temperature to allow the formation of transfection complexes. During this incubation, medium was aspirated from the cells and replaced with 2 ml of antibiotic-free medium. Transfection complexes were added dropwise to the cells to give a total volume of 2.5 ml, mixed by gentle rocking, and cultured at 37°C until required.

2.3.2.2 *Transfection of HFF Cells*

i) Electroporation of HFFs with expression construct DNA:

One day prior to transfection, confluent HFFs were seeded into 10 cm plates at a density of 1.5×10^6 cells/plate. Thymidine (final concentration - 2.72 mM) was added to the culture medium to arrest the cell cycle, and the cells were incubated overnight at 37°C. After approximately 16 hours, the thymidine block was removed by washing the cells three times with Hanks Balanced Salt Solution (HBSS), and the synchronised cells were incubated for 7-8 hours in regular culture medium at 37°C. Cells were washed twice with PBS and detached from the culture surface (trypsinised) through incubation in trypsin-EDTA (0.05% [w/v] trypsin, 0.02% [w/v] EDTA) for 3-5 minutes at 37°C. The trypsin was neutralised using complete culture medium and the cells were pelleted by centrifugation at 300 x g for 3 minutes (Eppendorf Centrifuge 5702, A-4-38 rotor). The cell pellet was resuspended in electroporation buffer (20 mM HEPES; pH 7.05, 137 mM NaCl, 5 mM KCl, 0.7 mM Na₂HPO₄, 6 mM dextrose) at a density of 1.5×10^6 cells/550 µl. For each transfection, 30 µg of expression construct DNA was mixed with 550 µl of cell suspension in a 0.4 cm electroporation cuvette (Bio-Rad Laboratories). Cells were transfected using a Gene Pulser Electroporation System (Bio-Rad Laboratories) with the parameters of 170 kV and 960 mFd, which resulted in a time constant of 18-24 ms. Electroporated cells were immediately transferred to a culture plate containing 10 ml pre-warmed regular culture medium (supplemented with 5 mM sodium butyrate), and incubated overnight at 37°C. After overnight incubation the cells were washed once with HBSS to remove the sodium butyrate, and the culture media replaced. Cells were incubated at 37°C until required. For fluorescence microscopy, 24 hours post-transfection the cells were seeded onto ethanol-flamed 12 mm coverslips (Hecht-Assistent) in 24-well plates at a density of 5000 cells/well in regular culture medium and cultured for 24 hours at 37°C prior to fixation.

ii) Lipofection of HFFs with expression construct DNA using Lipofectamine LTX:

This method was used for transfection of HFFs with expression construct DNA prior to fluorescence microscopy, replacing electroporation, which gave very low transfection efficiencies. One day prior to transfection, HFFs were seeded directly onto ethanol-flamed 19 mm coverslips (Menzel Glaser) in 12-well plates at a density of 6×10^4 cells/well in antibiotic-free medium and cultured overnight at 37°C. For each transfection, 1 µg of expression construct DNA was diluted in 100 µl Opti-MEM medium before adding 0.5 µl Plus reagent (Invitrogen), mixing and incubating for 15 minutes at room temperature. After incubation, 1.75 µl of Lipofectamine LTX (Invitrogen) was added, and the solution was mixed and incubated for a further 25 minutes at room temperature to allow the formation of transfection complexes. During this incubation, medium was aspirated from the cells and replaced with 500 µl of antibiotic-free medium. Transfection complexes were added dropwise to the cells, followed by incubation for 24 hours at 37°C prior to fixation.

iii) Lipofection of HFFs with siRNA duplexes using Lipofectamine 2000 or Oligofectamine:

One day prior to transfection, HFFs were seeded into 6-well culture plates at a density of 2×10^5 cells/well in antibiotic-free culture medium, such that they would reach 60-80% confluence 24 hours later. Next day, approximately 4 hours prior to transfection, the culture media was replaced to remove any dead cells. siRNA solutions at 200x working concentration were made up in siRNA buffer.

Transfection of HFFs using Lipofectamine 2000: 5 µl of 200x siRNA was diluted in 245 µl Opti-MEM medium and mixed by pipetting. Separately, 5 µl of Lipofectamine 2000 (Invitrogen) was mixed with 245 µl Opti-MEM medium and incubated for 5 minutes at

room temperature. The two solutions were mixed together and incubated for 30 minutes at room temperature to allow the formation of transfection complexes. During this incubation, medium was aspirated from the cells and replaced with 500 μ l of antibiotic-free medium. Transfection complexes were added dropwise to the cells to give a final volume of 1 ml, mixed by gentle rocking, and cultured for 4 hours at 37°C. Four hours post-transfection an additional 1 ml of antibiotic-free medium was added to each well and the cells were cultured at 37°C until required.

Transfection of HFFs using Oligofectamine: 5 μ l of 200x siRNA was diluted in 175 μ l Opti-MEM medium and mixed by pipetting. Separately, 2 μ l of Oligofectamine (Invitrogen) was mixed with 18 μ l Opti-MEM medium and incubated for 5 minutes at room temperature. The two solutions were mixed together and incubated for 20 minutes at room temperature to allow the formation of transfection complexes. During this incubation, medium was aspirated from the cells and replaced with 800 μ l of Opti-MEM medium. Transfection complexes were added dropwise to the cells to give a total volume of 1 ml, mixed by gentle rocking, and cultured for 4 hours at 37°C. Four hours post-transfection an additional 500 μ l of culture medium containing 30% (v/v) FCS was added to each well and the cells were cultured at 37°C until required.

2.3.2.3 Transfection of A2780 Cells

A2780 cells were transfected with expression construct DNA or siRNA duplexes by an electroporation-based method using a nucleofector system (Lonza Group, formally Amaxa Biosystems). One day prior to transfection, a single confluent 10 cm plate of cells was seeded into a single 15 cm plate in regular culture medium and incubated overnight at 37°C. Next day, the cells were washed twice with PBS and trypsinised for 3-5 minutes at 37°C. The trypsin was neutralised using complete culture medium and

the cells were pelleted by centrifugation at 300 x g for 3 minutes (Eppendorf Centrifuge 5702, A-4-38 rotor). The cell pellet was resuspended in PBS and centrifuged again to remove any residual culture medium before resuspension in 100 µl nucleofection solution T (Lonza Group, formally Amaxa Biosystems). 3-6 µg expression construct DNA, or 0.1/0.3 nmoles siRNA duplexes (for 1 and 3 µM final concentration, respectively), was added to the cell suspension and mixed by pipetting before being transferred to an electroporation cuvette and nucleofected using the A-23 programme. Immediately following nucleofection, the cells were transferred to a 10 cm plate containing pre-warmed culture medium and incubated at 37°C until required.

2.3.3 Indirect Immunofluorescence Microscopy

Initially, conventional (widefield) fluorescence microscopy was used for the imaging of fixed samples; however, the fact that fibrillar adhesions often form on the dorsal surface of the cell in a different plane of focus to focal adhesions, which always form on the ventral surface, led to difficulties in obtaining images in which both adhesion types were in focus. Therefore, laser scanning confocal fluorescence microscopy with optical sectioning was used to overcome this problem. However, the method of sample preparation had to be modified and optimised due to a number of technical difficulties encountered upon switching from conventional to confocal fluorescence microscopy. The two different methods of sample preparation and imaging are outlined below.

2.3.3.1 Conventional (Widefield) Fluorescence Microscopy

Culture media was aspirated, and the cells were washed with PBS and fixed in 4% (w/v) paraformaldehyde/5% (w/v) sucrose (in PBS) for 20 minutes at room temperature or in ice-cold methanol for 5 minutes. The fixative was removed and replaced with PBS prior to antibody staining. Cells were incubated in primary antibody mixtures (in PBS)

for 1 hour at room temperature (see Table 2.4 for antibodies). Unbound primary antibody was removed by washing with PBS (4 x 5 minutes) before incubation with the appropriate fluorescently-conjugated secondary antibodies (in PBS) for 1 hour at room temperature. Unbound secondary antibody was removed by PBS washes (4 x 5 minutes). Where nuclear DNA staining was required, cells were incubated in 1 µg/ml 6-diamidino-2-phenylindole (DAPI; in PBS) for 1 hour at room temperature, followed by PBS washes (4 x 5 minutes). Coverslips were mounted onto glass slides in Gel Mount and imaged by fluorescence microscopy with a Nikon Eclipse TE300 inverted microscope using a DAPI/FITC/TRITC filter set. Images were captured with a Hamamatsu ORCA-ER (C4742-95) digital camera using the Openlab software package (Improvision).

2.3.3.2 Confocal Fluorescence Microscopy

Fixation was performed as described above before blocking non-specific binding sites with 1% (w/v) BSA (in PBS) for 30 minutes at room temperature. Cells were incubated in primary antibody mixtures (in 0.1% [w/v] BSA, in PBS) for 1 hour at room temperature (see Table 2.4 for antibodies). Unbound primary antibody was removed by washing with 0.1% (w/v) BSA (in PBS) (4 x 5 minutes) before incubation with the appropriate fluorescently-conjugated secondary antibodies (in 0.1% [w/v] BSA, in PBS) for 1 hour at room temperature. Where necessary, 1 µg/ml DAPI was included with the secondary antibodies. Unbound secondary antibody/DAPI was removed by washing once in 0.1% (w/v) BSA (in PBS) and a further 3 times in PBS alone, before mounting the coverslips onto glass slides in Prolong Gold antifade reagent (Invitrogen). Cells were imaged with a Leica TCS SP5 laser scanning confocal microscope (built around a Leica DMI600B inverted microscope) using the LAS AF software package (Leica Microsystems) and the 488, 561 and 633 nm laser lines. The collected data was deconvolved using Huygens Essential 3.3.0p3 (Scientific Volume Imaging B.V.).

Antibody	Description	Source	Working Dilution/Concentration
L230	Monocloal mouse anti-human α V integrin	American Type Culture Collection (ATCC)	10 μ g/ml
SNAKA51	Monoclonal mouse anti-human α 5 integrin; fibrillar adhesion-specific	M J Humphries (University of Mancester, UK)	20 μ g/ml
Rb745	Polyclonal rabbit anti-human FN	K M Yamada (NIDCR, NIH, Bethesda, MD, USA)	1 in 400
FN	Polyconal rabbit anti-human FN	D R Critchley (University of Leicester, UK)	1 in 200
α 5 integrin	Monoclonal mouse anti-human α 5 integrin	BD Pharmingen	5 μ g/ml
Anti-Mouse-RedX	Polyclonal donkey F(ab') ₂ anti-mouse IgG (Rhodamine Red -conjugated)	Jackson ImmunoResearch Laboratories	1 in 250
Anti-Rabbit-AMCA	Polyclonal donkey F(ab') ₂ anti-rabbit IgG (AMCA-conjugated) - non-confocal	Jackson ImmunoResearch Laboratories	1 in 50
Anti-Rabbit-CY5	Polyclonal donkey F(ab') ₂ anti-rabbit IgG (CY5-conjugated) – confocal-specific	Jackson ImmunoResearch Laboratories	1 in 200
Anti-Mouse-CY2	Polyclonal donkey IgG (H+L) anti-mouse IgG (CY2-conjugated) - Fig 5.16 only	Jackson ImmunoResearch Laboratories	1 in 100

Table 2.4: Antibodies for immunofluorescence microscopy.

2.4 Other Cell-Based Assays

2.4.1 Scratch-Wound Assays

Two different protocols were used for scratch-wound assays on HEK293 and A2780 cells. These methods are outlined below.

2.4.1.1 Scratch-Wound assay on HEK293 Cells

Twenty-four hours post-transfection the monolayer of HEK293 cells were scratched with a small (10 μ l) pipette tip and the culture medium aspirated and replaced with 2 ml antibiotic-free medium to remove detached cells, followed by incubation at 37°C for 10 minutes. A single area of interest was marked per well using an object marker attached to a Nikon TMS-F light microscope. Images were manually captured at 0, 2, 6, 16 and 24 hour time points with a Nikon DXM1200 digital camera attached to a Leica MZ16F microscope using the ACT-1 software package (Nikon Instruments). Cell lysates were harvested after the 24 hour time point i.e. 48 hours post-transfection. Wound width was measured from images in Microsoft PowerPoint (Microsoft Corporation).

2.4.1.2 Scratch-Wound assay on A2780 Cells

Twenty-four hours post-transfection, A2780 cells were washed twice with PBS and trypsinised for 3-5 minutes at 37°C. The trypsin was neutralised using complete culture medium, and the cells were counted, seeded into a 6-well plate at a density of 5.5×10^5 cells/well and grown to confluence overnight at 37°C. Next morning the cell monolayers were fed with fresh culture medium, incubated at 37°C for ~4 hours and then scratched with a small (10 μ l) pipette tip. Detached cells were removed by washing twice with media. Wound closure was monitored at 5 regions of interest per well by automated

time-lapse microscopy with a 10x objective on a Nikon Eclipse TE300 inverted microscope using a Ludl motorized stage (Ludl Electronic Products) in an atmosphere of 5% (v/v) CO₂ at 37°C. Images were captured with a Hamamatsu ORCA-ER (C4742-95) digital camera using the Openlab software package (Improvision) every 10 minutes over a period of 16 hours and movies were generated. The positions of cell nuclei were evaluated at each time point using the manual tracking plugin in ImageJ (NIH, Bethesda, MD, USA), and track plots following the path of individual cells were created using the chemotaxis tool plugin in ImageJ (NIH, Bethesda, MD, USA). Average migration speed and persistence (net displacement/overall path length) were calculated from the raw output data of the manual tracking plugin using Microsoft Excel (Microsoft Corporation).

2.4.2 Matrigel-Plug Inverted Invasion Assay

Inverted invasion assays were performed as described previously (Hennigan *et al.*, 1994). Matrigel (BD Biosciences) was defrosted on ice and mixed 1:1 with ice-cold PBS (supplemented with 50 µg/ml FN). 100 µl aliquots of this protein mixture were applied into transwell inserts (8 µm pore size; Corning) in a 24-well plate and allowed to polymerise for 30 minutes to 1 hour at 37°C (Figure 2.1). A2780 cells were washed twice with PBS and trypsinised for 3-5 minutes at 37°C. The trypsin was neutralised using complete culture medium, and the cells were counted and diluted to a density of 5x10⁵ cells/ml. Transwell inserts were inverted onto the lid of the 24-well plate and 100 µl aliquots of cell suspension (5x10⁴ cells) were applied directly onto the underside of the filter (Figure 2.1). Transwells were covered with the inverted base of the 24-well plate such that the bottom of the wells contacted the droplets, and incubated for 3-4 hours at 37°C to allow the cells to firmly adhere. Transwells were then inverted again and dipped sequentially into 2x1 ml serum-free medium (to wash away serum) before placing them into 1 ml serum-free medium in a new 24-well plate. 100 µl aliquots of

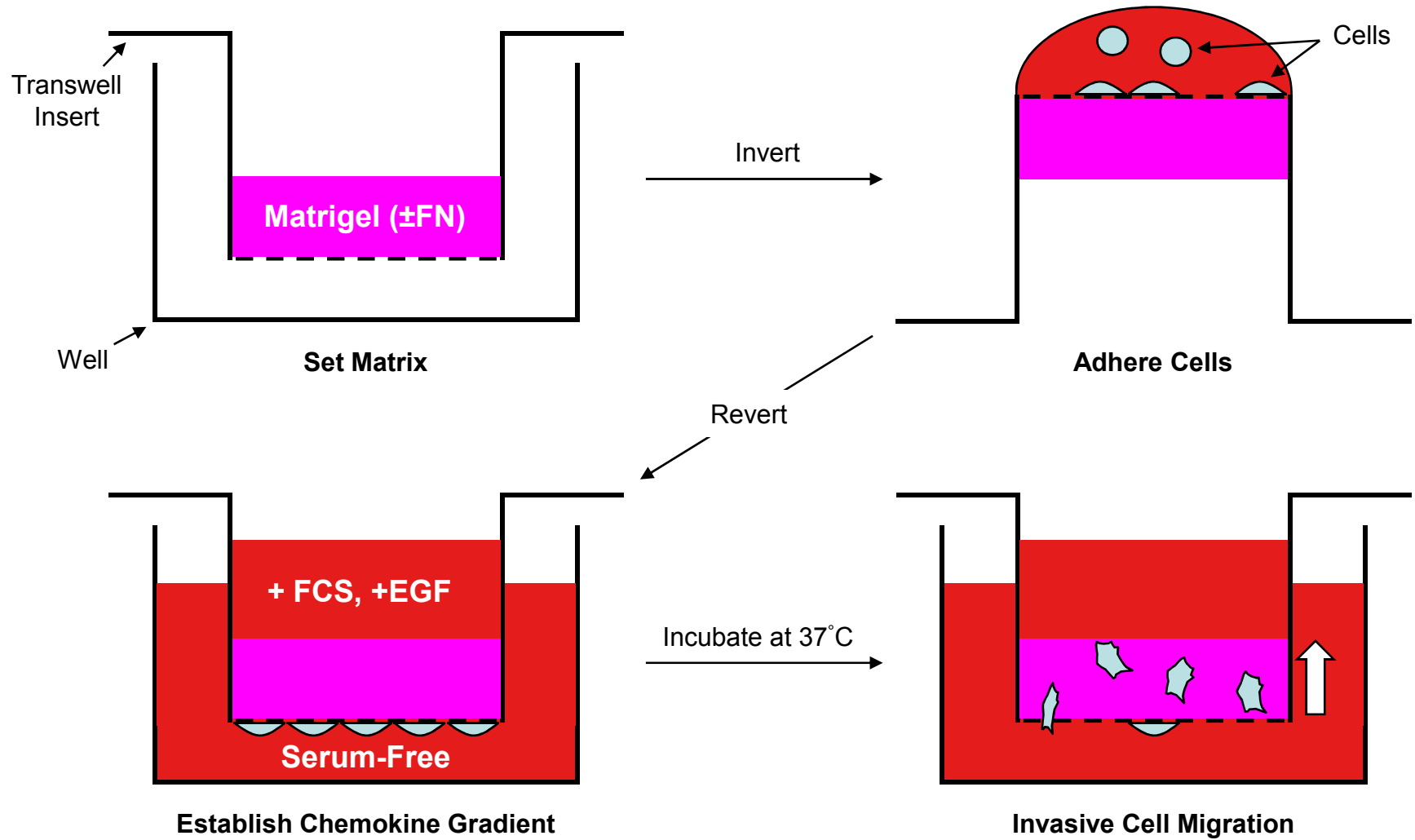


Figure 2.1: Matrigel-plug inverted invasion assay. See methods section 2.4.2 for detailed description. FCS (foetal calf serum), EGF (epidermal growth factor).

complete culture medium (supplemented with 30 ng/ml EGF) were applied on top of the matrix in the transwells, providing a chemotactic gradient (Figure 2.1). Assays were incubated for 48 hours at 37°C to allow invasion to occur (Figure 2.1). Where appropriate, inhibitory antibodies (1 µg/ml) directed against β1 integrin (mAb13; M J Humphries, University of Manchester, UK) or α_vβ₅ integrin (P1F6; Chemicon) were added to the top and bottom media reservoirs, and to the Matrigel plugs prior to polymerisation. Forty-eight hours after establishing the chemotactic gradient, the transwells were transferred into a clean 24-well plate, overlaid with 1 ml of serum-free medium supplemented with 4 µM Calcein-AM (Molecular Probes; Invitrogen), and incubated at 37°C for 1 hour 15 minutes to allow staining of the invading cells.

Invasion assays were imaged using a Leica TCS SP2 laser scanning confocal microscope with the LCS software package (Leica Microsystems) by placing the transwells onto large coverslips over a 20x objective lens and capturing optical sections every 15 µm from the bottom of the plug upwards (3 regions of interest per transwell). Invasion data was quantified using the area calculator plugin in ImageJ (NIH, Bethesda, MD, USA).

2.4.3 Analysis of Cell Morphology and Migration on Cell-Derived Matrix (CDM)

2.4.3.1 Generation of CDM

Cell-derived matrix was generated as described previously (Beacham *et al.*, 2007; Bass *et al.*, 2007). Culture-ware (6-well plates) were washed with PBS and coated with 0.2% (w/v) sterile gelatin (in PBS) for 1 hour at 37°C. Excess gelatin was removed by washing twice with PBS before cross-linking the coated gelatin with 1% (v/v) sterile glutaraldehyde (in PBS) for 30 minutes at room temperature. Excess glutaraldehyde was removed by washing twice with PBS and the cross-linking reaction was quenched

with 1 M sterile glycine (in PBS) for 20 minutes at room temperature. Excess glycine was removed by washing twice with PBS and the prepared culture-ware was equilibrated in complete culture medium for 30 minutes at 37°C in preparation for the addition of cells. TIFs were washed twice with PBS and trypsinised for 3-5 minutes at 37°C. The trypsin was neutralised using complete culture medium, and the cells were counted, seeded onto prepared culture-ware at a density of 2×10^5 cells/well in complete culture medium and cultured overnight at 37°C. Twenty-four hours later the cells were confluent and the medium was changed for fresh complete culture medium (supplemented with 50 µg/ml ascorbic acid to increase collagen production). The cells were grown for 8-9 days in ascorbic acid-containing medium to allow them to become over-confluent and surround themselves within a fibrillar 3D matrix (visible by phase contrast microscopy). Ascorbic acid degrades over time in culture, so the media on the cells was replaced every other day with media containing fresh ascorbic acid. After 8-9 days the matrices were washed with PBS and denuded of living cells by gently adding pre-warmed extraction buffer (20 mM NH_4OH , 0.5% [v/v] Triton X-100; in PBS) and incubating for 2 minutes at room temperature. Extraction buffer was removed and the matrix was washed twice with PBS containing calcium and magnesium (Sigma; Catalogue No. D8662). DNA released during lysis was digested with 10 µg/ml DNase I (Roche; in PBS plus Ca^{2+} and Mg^{2+}) for 30 minutes at 37°C. DNase I was removed by washing the matrix twice with PBS (plus Ca^{2+} and Mg^{2+}). Cell-derived matrix was then either stored at 4°C in PBS (plus Ca^{2+} and Mg^{2+}) supplemented with 100 U/ml penicillin, 100 µg/ml streptomycin and 0.25 µg/ml Amphotericin B (Fungizone), or prepared for the plating of cells. Matrix was prepared by blocking with 10 mg/ml heat-denatured BSA (First Link [UK]; in PBS) for 1 hour at 37°C. Note: Heat-denatured BSA was produced by heating to 85°C for 13 minutes, and then cooling and sterilising by passage through a 0.45 µm filter. Heat-denatured BSA was removed and the matrix washed three times with PBS (plus Ca^{2+} and Mg^{2+}) prior to plating cells in complete culture medium.

2.4.3.2 Time-Lapse Imaging and Analysis

Twenty-four hours post-transfection, A2780 cells were washed twice with PBS and trypsinised for 3-5 minutes at 37°C. The trypsin was neutralised using complete culture medium, and the cells were counted, seeded onto CDM-coated 6-well plates at a density of 5×10^4 cells/well and incubated at 37°C for 4 hours to allow the cells to adhere and begin migrating. Five regions of interest per well were imaged by automated time-lapse microscopy with a 10x objective on a Nikon Eclipse TE2000 inverted microscope in an atmosphere of 5% (v/v) CO₂ at 37°C. Images were captured every 10 minutes over a period of 12 hours using the Metamorph software package (Molecular Devices) and movies were generated. Average cell length was determined 4 hours into the movie (~8 hours after plating) using the measure function in ImageJ (NIH, Bethesda, MD, USA). Cell migration was analysed using ImageJ (NIH, Bethesda, MD, USA) and Microsoft Excel (Microsoft Corporation), as described earlier for the A2780 scratch-wound assays.

2.4.4 Integrin Recycling Assay

2.4.4.1 Recycling Protocol

Forty-eight hours after siRNA transfection, control and triple tensin knockdown A2780-Rab25 cells were washed twice with PBS and serum-starved by incubating in serum-free media for 30 minutes to 1 hour at 37°C. Serum-starved cells were transferred onto ice, washed three times with ice-cold PBS and surface-labelled with 0.15 mg/ml *N*-hydroxysuccinimide-S-S-biotin (in PBS) for 30 minutes at 4°C on a slow rocker. Cells were washed twice with ice-cold PBS to remove excess biotin before applying serum-free media pre-adjusted to 12°C, and the cells incubated for 30 minutes at 37°C to allow receptor internalization. Control plates for total surface labeling (total), and “cold”

internalization occurring at 4°C (blank), were left on ice in PBS. Following internalization, plates were transferred onto ice, washed once with ice-cold PBS, and then equilibrated for disulphide bond reduction by washing once with ice-cold pH 8.6 buffer (50 mM Tris; pH 8.6, 100 mM NaCl). Biotin remaining at the cell surface was removed by reduction with the membrane impermeable reducing agent sodium 2-mercaptoethanesulfonate (MESNa). Cells were incubated in 20 mM MESNa (in pH 8.6 buffer) for 20 minutes at 4°C on a slow rocker (note: blank plate was included in reduction step, but total plate was left on ice in PBS). Excess reducing agent was removed by washing twice with ice-cold PBS before adding serum-containing media pre-adjusted to 37°C and incubating at 37°C to allow recycling (note: total, blank, and zero minute time point [zero] plates were left on ice in PBS). At the indicated recycling times (6, 12 and 18 minutes), media was aspirated and the plates were returned to ice and washed once in ice-cold PBS. All plates (except totals) were then washed in pH 8.6 buffer before removing biotin from proteins that had been recycled to the surface by a second reduction with MESNa. Unreacted MESNa was quenched with 20 mM iodoacetamide (in PBS) for 10 minutes at 4°C. All cells were washed twice in ice-cold PBS and lysed in 100 µl of non-denaturing lysis buffer (200 mM NaCl, 75 mM Tris, 15 mM NaF, 1.5 mM Na₃VO₄, 7.5 mM EDTA, 7.5 mM EGTA, 1.5% [v/v] Triton X-100, 0.75% [v/v] NP-40, 50 µg/ml leupeptin; Fluka, 50 µg/ml aprotinin; Fluka, 1 mM AEBSF; Melford). Cell lysates were harvested from the dish with a cell scraper, disrupted by passage through a 21 G needle (Becton Dickinson), and clarified by centrifugation at 13,000 rpm for 10 minutes at 4°C (Sanyo Hawk 15/05 centrifuge). Biotinylated integrin was determined by capture enzyme-linked immunosorbent assay (ELISA).

2.4.4.2 *Capture ELISA*

MaxiSorp ELISA plates (Nunc) were coated with 5 µg/ml anti-α5 integrin mouse monoclonal antibody (clone VC5; BD Pharmingen, diluted in 0.05 M sodium carbonate;

pH 9.6) overnight at 4°C. Any unbound protein was removed by washing the plate once with PBS-Tween (PBST; PBS supplemented with 0.1% [v/v] Tween 20). Blocking was performed in 5% (w/v) BSA (First Link [UK]; in PBST) at room temperature for the duration of recycling assay (approximately 6 hours). Excess blocking solution was removed by washing the ELISA plate three times with PBST before applying clarified cell lysates (in duplicate) and incubating overnight at 4°C. After approximately 16 hours, the plate was washed four times with PBST before applying 1:700 streptavidin-HRP (Amersham; GE Healthcare; in PBST, 0.1% [w/v] BSA) and incubating for 1 hour at room temperature. The plate was then washed four times with PBST before developing with a solution containing 2,2'-azino-bis (3-ethylbenzthiazoline 6-sulphonic acid) (ABTS) (2 mM ABTS, 0.03% [v/v] H₂O₂, 50 mM Na₂HPO₄, 0.1 M sodium acetate; pH 5.0). The reaction was stopped with 1% (w/v) SDS before measuring absorbance at 405 nm by spectrophotometry (Tecan GENios). Absorbance levels were corrected by subtracting the averaged reading from cells that were surface-labelled and then reduced without being warmed to 37°C during the internalisation period (blank); this corrected for cold internalisation, the efficiency of reduction, and background absorbance. Approximately equal levels of internalisation between the control and triple tensin knockdown cells were confirmed by comparing the averaged readings from cells that had not been warmed to 37°C during the recycling period (zero) to cells that were left on ice following labelling and exempt from the reduction steps (total). Levels of recycled biotinylated integrin were expressed relative to the levels found in the zero plates, which represents the internal pool of integrins from which recycling occurs.

2.4.5 Photoactivation Assay (*Integrin Diffusion/Retention*)

CDMs were prepared on glass-bottomed 3 cm plates using an identical method to that described earlier. Twenty-four hours post-siRNA transfection, A2780-Rab25 cells were co-transfected with 1.2 µg mCherry-Rab25 and 4.8 µg photoactivatable(pa)EGFP-α5

integrin recombinant expression plasmids, and cultured overnight at 37°C to allow expression of these fusion proteins. Twenty-four hours post-transfection, cells were washed twice with PBS and trypsinised for 3-5 minutes at 37°C. The trypsin was neutralised using complete culture medium and the cells were counted, seeded onto CDM-coated glass-bottomed 3 cm plates at a density of 5×10^4 cells/well in complete culture medium, and incubated at 37°C for 4 hours to allow the cells to adhere and begin migrating. Cells were imaged with a 60x objective on an Olympus Fluoview FV1000 laser scanning confocal microscope in an atmosphere of 5% (v/v) CO₂ at 37°C using the Olympus Fluoview software package (Olympus Corporation). Transfected cells were identified by the expression of mCherry-Rab25, and photoactivation of paGFP in these cells was achieved with a 405 nm laser aimed at a region at the front of the migrating cell with an Olympus SIM scanner. Images were captured every second over a period of 4 minutes and movies were generated. Photoactivation was also performed on whole cells, in addition to regions at the cell front, to generate data for the correction of fluorescence loss through photobleaching. The average pixel intensity of the photoactivated region was quantified for each frame using the series analysis tool in the Olympus Fluoview software package (Olympus Corporation). This data was exported to Microsoft Excel (Microsoft Corporation), calculated relative to the intensity of the frame immediately after photoactivation, corrected for photobleaching, and plotted against time.

**Chapter 3 Anti-Tensin Antibody
Characterisation and Tensin
Localisation**

3.1 Introduction

Isoform-specific antibodies are required to differentiate between the different human tensin proteins. Such antibodies are essential to determine the expression patterns of the various tensin isoforms by Western blotting and their subcellular localisation by immunofluorescence microscopy. There are a number of commercially available anti-tensin antibodies including those from BD Transduction Laboratories, Chemicon International, Upstate Biotechnology and Santa Cruz Biotechnology, but the isoform specificity of these antibodies has not been determined. We have also raised rabbit polyclonal antibodies against short (~20 amino acid) peptide immunogens from the central divergent regions of human tensin2 (known as Rb31 and Rb32) and tensin3 (known as Rb33 and Rb34) using a commercial provider (Biosource; Invitrogen), and purified these antibodies by antigen affinity column chromatography. The isoform-specificity of all these antibodies was investigated by testing their reactivity against GFP-tensins expressed in HEK (human embryonic kidney) 293 cells using Western blotting. These antibodies were then used alongside quantitative real-time PCR (qPCR) to establish which tensin isoforms are expressed in human foreskin fibroblasts (HFFs), a cell type in which tensin has previously been shown to localise to both focal and fibrillar adhesions (Zamir *et al.*, 2000). Finally, siRNA-directed knockdown of endogenous tensins in HFFs was used to confirm the specificities of these antibodies by Western blotting.

HFFs are the best studied cell line known to assemble fibrillar adhesions *in vitro*; therefore, this model cell line was used to characterise the localisation of human tensin1, 2 and 3. GFP-fusions of each tensin were exogenously expressed in HFFs and their localisation relative to various cell-matrix adhesion markers was assessed by indirect immunofluorescence microscopy. It was found that each tensin isoform was

capable of localising to both focal and fibrillar adhesions. However, each isoform displayed a slightly different pattern of localisation.

3.2 Results

3.2.1 Anti-Tensin Antibody Characterisation using GFP-Tensin Fusions

GFP-tensin expression constructs encoding human tensin1, 2 or 3 were transfected into HEK293 cells by lipofection. Proteins in cell lysates harvested 48 hours post-transfection were separated by SDS-PAGE (7.5% acrylamide) and probed with an antibody directed against GFP by Western blotting. The resulting blot indicated that the GFP-tensin1, 2 and 3 fusion proteins were efficiently expressed in HEK293 cells (Figure 3.1). Moreover, the migration of each GFP-tensin isoform corresponded to the expected molecular weight (GFP-tensin1, 2 and 3 have predicted molecular weights of 211 kDa, 167 kDa and 183 kDa, respectively). Furthermore, this antibody did not react with any proteins in untransfected cell lysate, nor did it detect any degradation products in transfected cell lysates confirming that the expressed proteins were stable.

To characterise the isoform specificities of the various tensin antibodies, the above-mentioned cell lysates were probed with each antibody by Western blotting. Using this methodology it was shown that the Transduction, Chemicon, Upstate and Santa Cruz anti-tensin antibodies all reacted with a single protein band, which was only present in the lysate of GFP-tensin1-transfected cells, and had the expected molecular weight of GFP-tensin1 (Figures 3.2, 3.3). Before characterising their specificity, the rabbit polyclonal antibodies were first purified from serum. Initially, a preparation enriched in IgG was produced from the serum by ammonium sulphate precipitation. Anti-tensin antibodies were then purified from this preparation by antigen affinity chromatography using ~150 amino acid His₆-tagged tensin polypeptides encompassing the relevant

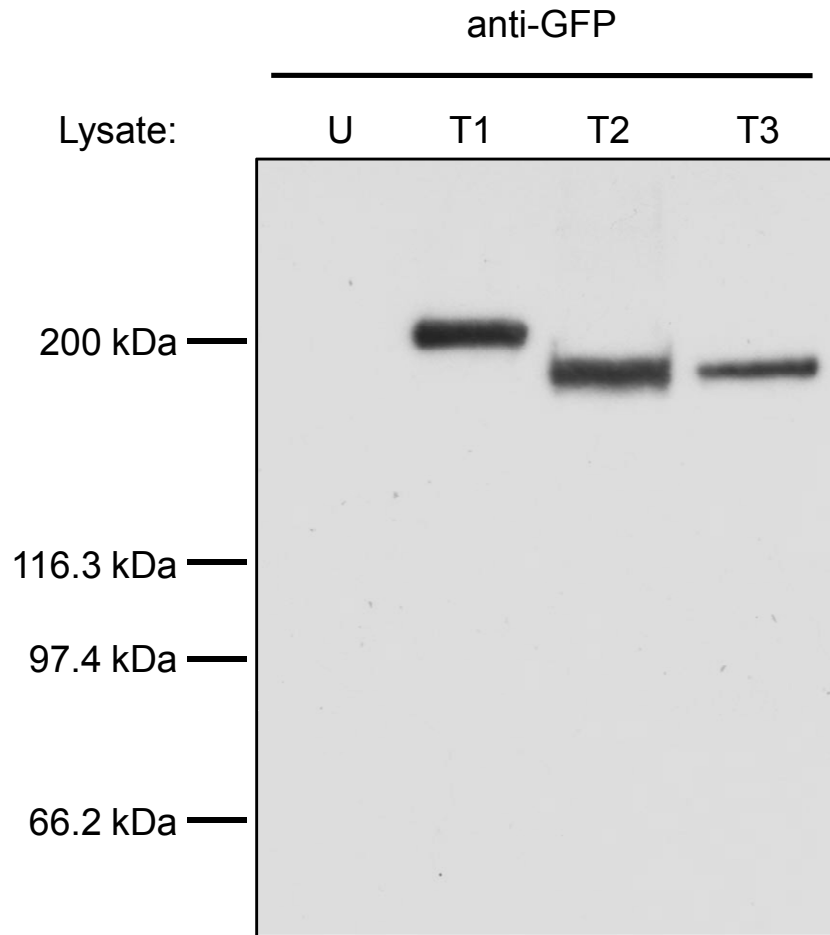


Figure 3.1: Expression of GFP-tagged tensin proteins in HEK293 cells. HEK293 cells were transfected with expression constructs encoding GFP-tensin1, 2 or 3. Proteins in cell lysates harvested 48 hours post-transfection were separated by SDS-PAGE (7.5% acrylamide) and probed for the presence of the GFP-fusion proteins by Western blotting with an anti-GFP antibody. U - Untransfected control, T1 - GFP-tensin1-, T2 - GFP-tensin2-, T3 - GFP-tensin3-transfected cell lysates. Note: GFP-tensin1, 2 and 3 fusion proteins were efficiently expressed at their expected molecular weights of 211 kDa, 167 kDa and 183 kDa, respectively.

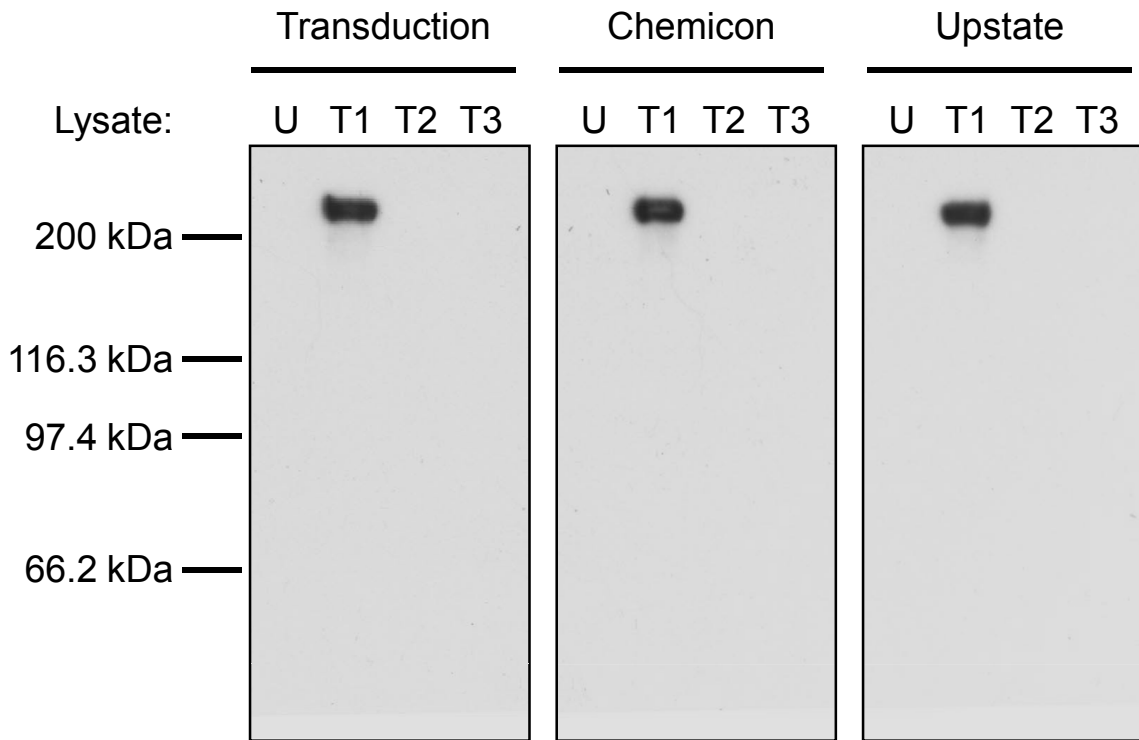


Figure 3.2: Characterisation of commercial anti-tensin monoclonal antibodies. HEK293 cells were transfected with expression constructs encoding GFP-tensin1, 2 or 3. Proteins in cell lysates harvested 48 hours post-transfection were separated by SDS-PAGE (7.5% acrylamide) and probed with three commercial anti-tensin mouse monoclonal antibodies by Western blotting. Anti-tensin antibodies were from Transduction Laboratories (Transduction), Chemicon International (Chemicon) and Upstate Biotechnology (Upstate). U - Untransfected control, T1 - GFP-tensin1-, T2 - GFP-tensin2-, T3 - GFP-tensin3-transfected cell lysates. Note: The three anti-tensin monoclonal antibodies reacted with a protein that was only present in the lysate of GFP-tensin1-transfected cells, indicating that these antibodies are all tensin1-specific.

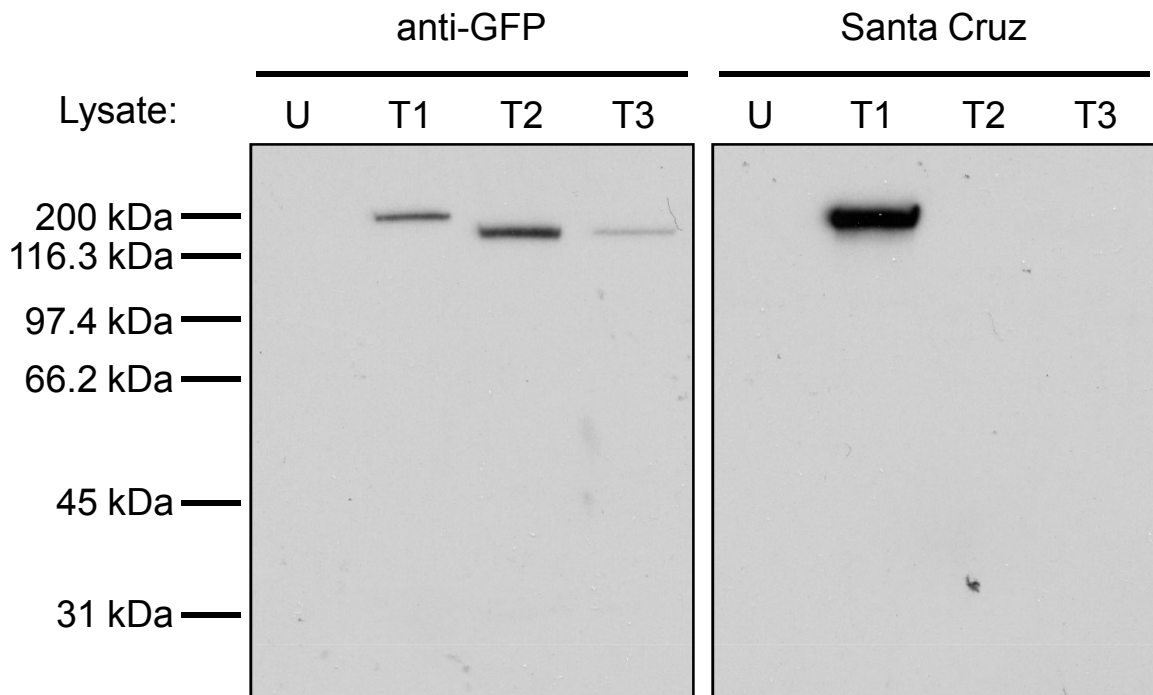


Figure 3.3: Characterisation of the Santa Cruz anti-tensin polyclonal antibody.

HEK293 cells were transfected with expression constructs encoding GFP-tensin1, 2 or 3. Proteins in cell lysates harvested 48 hours post-transfection were separated by SDS-PAGE (7.5% acrylamide) and probed with an antibody directed against GFP or with the Santa Cruz anti-tensin rabbit polyclonal antibody by Western blotting. U - Untransfected control, T1 - GFP-tensin1-, T2 - GFP-tensin2-, T3 - GFP-tensin3-transfected cell lysates. Note: The Santa Cruz anti-tensin antibody reacted with a protein that was only present in the lysate of GFP-tensin1-transfected cells, indicating that this antibody is tensin1-specific.

immunogens, which were expressed in BL21(DE3) *E. coli* and purified by Nickel ion affinity chromatography. The affinity purified Rb31 antibody reacted with a single protein band, which was only present in the lysate of GFP-tensin2-transfected cells and ran at the expected molecular weight of GFP-tensin2 (Figure 3.4). The affinity purified Rb32 antibody also recognised this band, but it also detected two smaller proteins which were present in all lysates. One was of an appropriate size for endogenous tensin2, and the other had an apparent molecular weight of ~60 kDa (Figure 3.4). The affinity purified Rb33 antibody reacted with a number of protein bands (Figure 3.5). Primarily, this antibody reacted with a protein that was only present in the lysate of GFP-tensin3-transfected cells and ran at the expected molecular weight of GFP-tensin3 (Figure 3.5). Moreover, this antibody also detected a number of smaller proteins exclusively in this lysate, which may correspond to GFP-tensin3 degradation products (Figure 3.5). Rb33 also detected a protein in all lysates of an appropriate size for endogenous tensin3 (Figure 3.5; arrow). However, it also detected two smaller proteins in all lysates from transfected but not untransfected cells with apparent molecular weights of ~60 kDa and ~70 kDa, and of unknown identity (Figure 3.5). The affinity purified Rb34 antibody primarily reacted with a single major protein species that was only present in the lysate of GFP-tensin3-transfected cells and ran at the expected molecular weight of GFP-tensin3 (Figure 3.5). Rb34 also reacted with a protein of ~70 kDa present in all cell lysates, although the reactivity towards this protein was very much less than that seen with Rb33 (Figure 3.5).

In summary, the four commercial anti-tensin antibodies were all specific for the tensin1 isoform. The rabbit polyclonal antibody Rb31 showed specificity for GFP-tensin2 and Rb34 for GFP-tensin3. Rb32 and Rb33 also showed the appropriate isoform specificity, but recognised additional proteins of uncertain origin. The Rb32 (anti-tensin2) and Rb33 (anti-tensin3) antibodies also recognised protein bands that probably correspond to endogenously expressed tensin2 and 3, respectively. Interestingly, the commercial

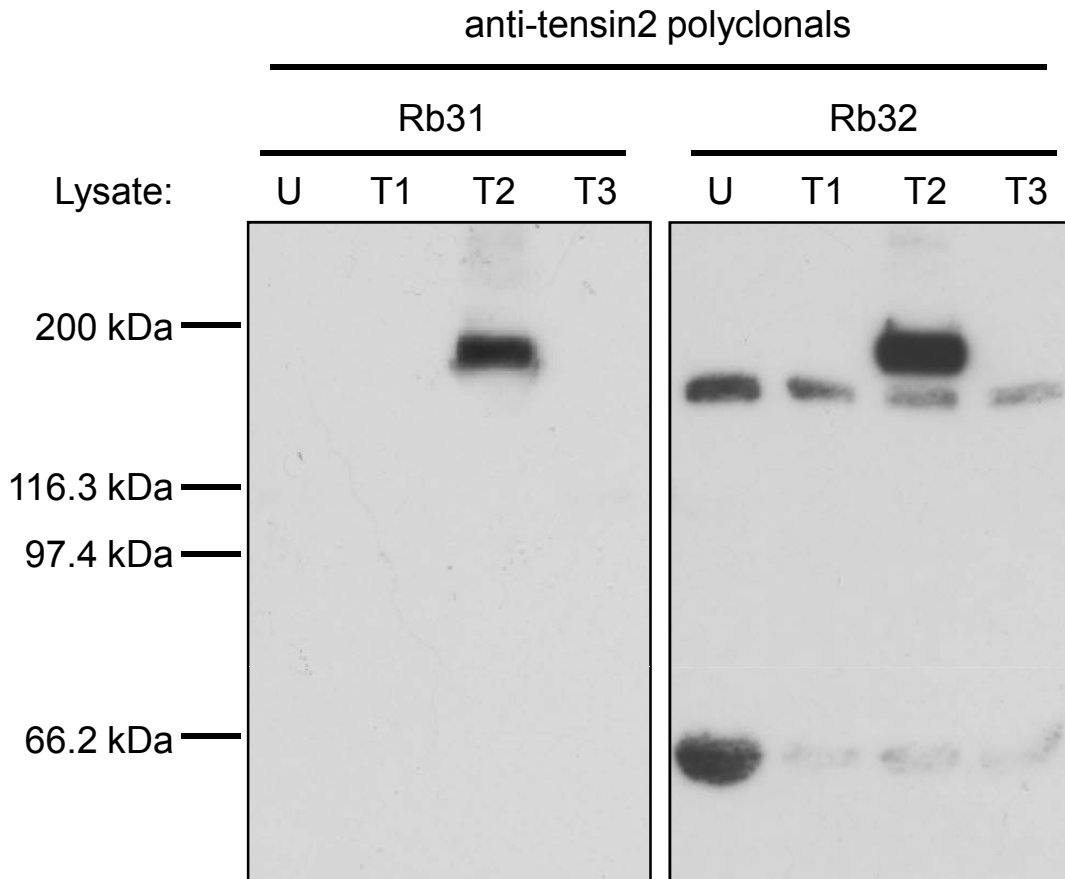


Figure 3.4: Characterisation of the anti-tensin2 polyclonal antibodies. HEK293 cells were transfected with expression constructs encoding GFP-tensin1, 2 or 3. Proteins in cell lysates harvested 48 hours post-transfection were separated by SDS-PAGE (7.5% acrylamide) and probed with two affinity purified anti-tensin2 polyclonal antibodies by Western blotting. U - Untransfected control, T1 - GFP-tensin1-, T2 - GFP-tensin2-, T3 - GFP-tensin3-transfected cell lysates. Note: Rb31 and Rb32 recognised GFP-tensin2. Furthermore, Rb32 may have also detected endogenous tensin2. Neither antibody showed cross-reactivity with the other tensin isoforms.

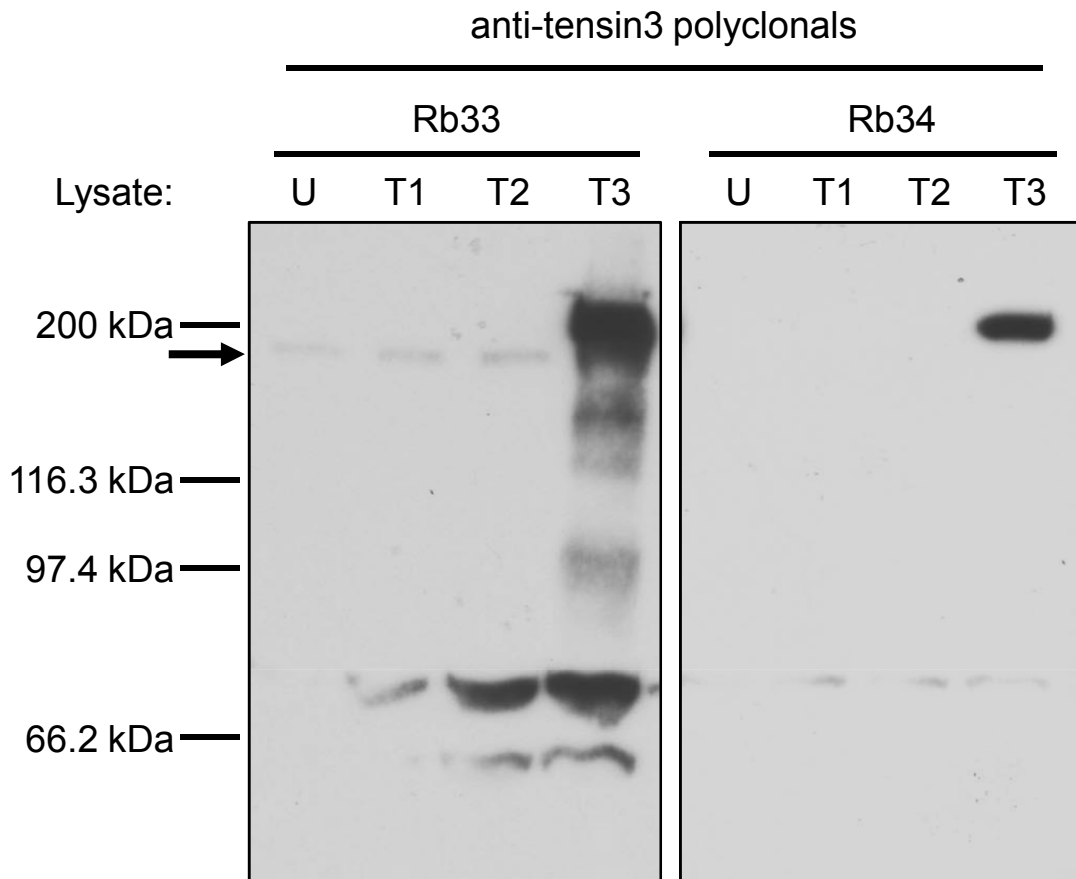


Figure 3.5: Characterisation of the anti-tensin3 polyclonal antibodies. HEK293 cells were transfected with expression constructs encoding GFP-tensin1, 2 or 3. Proteins in cell lysates harvested 48 hours post-transfection were separated by SDS-PAGE (7.5% acrylamide) and probed with two affinity purified anti-tensin3 polyclonal antibodies by Western blotting. U - Untransfected control, T1 - GFP-tensin1-, T2 - GFP-tensin2-, T3 - GFP-tensin3-transfected cell lysates. Note: Rb33 and Rb34 recognised GFP-tensin3. Furthermore, Rb33 may have also detected endogenous tensin3 (arrow). Neither antibody showed cross-reactivity with the other tensin isoforms.

tensin1-specific antibodies did not detect a band corresponding to endogenous tensin1 in HEK293 cell lysates. Importantly, none of the antibodies showed cross-reactivity with the other GFP-tensin isoforms.

3.2.2 HFFs Express All Three Large Tensin Isoforms

To further characterise the specificity of these antibodies and to identify the cellular localisation of the human tensins it was necessary to find an appropriate model cell line. The HFF cell line was selected as it had previously been shown to express tensin by immunofluorescence microscopy using the Transduction anti-tensin antibody (Zamir *et al.*, 2000). Furthermore, in addition to the more common focal adhesions made by many adherent cell types on 2D substrates, HFFs are also known to assemble extensive fibrillar adhesions, which are enriched in tensin (Zamir *et al.*, 2000). To establish which tensins are expressed by HFFs, Western blotting with isoform-specific antibodies and qPCR with isoform-specific primers was performed.

Proteins in untransfected HFF cell lysate were separated by SDS-PAGE (7.5% acrylamide) and probed with the previously characterised anti-tensin1 monoclonal antibodies (Transduction, Chemicon, and Upstate) and the affinity purified anti-tensin2 (Rb31/32) and anti-tensin3 (Rb33/34) polyclonal antibodies by Western blotting. All of the commercial anti-tensin1 monoclonal antibodies detected a protein of the same size - its molecular weight was consistent with the protein being endogenous tensin1 (Figure 3.6). Interestingly, the Upstate antibody, which gave the strongest signal, also detected a higher molecular weight protein. The Rb31 anti-tensin2 antibody did not recognise a protein of an appropriate size for endogenous tensin2, but instead reacted with two ~110 kDa proteins which ran as a doublet (Figure 3.6). In contrast, the Rb32 anti-tensin2 antibody recognised a protein of the appropriate size for endogenous tensin2 and a second ~60 kDa protein (Figure 3.6). Both of the anti-tensin3 antibodies

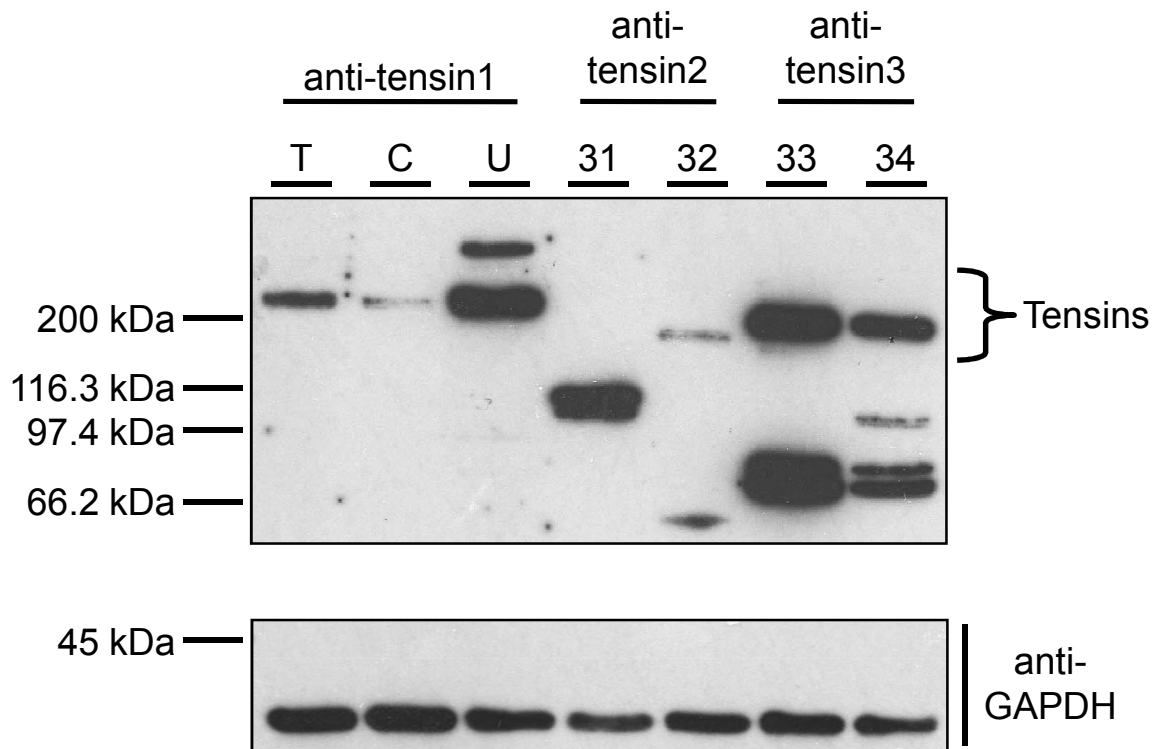


Figure 3.6: Detection of endogenous tensin protein isoforms in HFFs. Proteins in HFF cell lysate were separated by SDS-PAGE (7.5% acrylamide) and probed for the presence of tensin1, 2 and 3 by Western blotting using the previously characterised anti-tensin antibodies. The membrane was re-probed with an antibody directed against GAPDH as a loading control. T – Transduction Laboratories, C – Chemicon International, U – Upstate Biotechnology. 31-34 represent the in-house rabbit polyclonal antibodies. Note: The three commercial tensin1-specific monoclonal antibodies recognised a protein of the appropriate molecular weight for tensin1, the Rb32 anti-tensin2 antibody recognised a protein of the appropriate molecular weight for tensin2, and both the Rb33 and Rb34 anti-tensin3 antibodies recognised proteins of the appropriate molecular weight for tensin3. Therefore, all three of the large tensin isoforms are expressed in HFFs.

(Rb33 and Rb34) reacted strongly with a protein of the size expected of endogenous tensin3 as well as a ~70 kDa doublet (Figure 3.6). The Rb34 antibody also recognised an additional ~100 kDa doublet (Figure 3.6). These results suggest that HFFs express all three of the large tensin isoforms. Furthermore, it shows that most of the anti-tensin antibodies are capable of specifically detecting their respective endogenously expressed tensin isoforms.

Unfortunately, after this initial characterisation the Rb32 (anti-tensin2) antibody failed to recognise a protein of the correct molecular weight in cell extracts despite repeated attempts at affinity purification (data not shown). This inconsistency may be explained by the fact that the initial affinity purified antibody was from a test bleed whereas subsequent purifications were from the final bleed. This would imply that the immune reaction initially mounted by rabbit Rb32 against the tensin2 peptide was not maintained until it was sacrificed.

The relative expression levels of the three large tensin isoforms cannot be deduced from the data in Figure 3.6 as the various tensin antibodies are likely to have different affinities. However, some indication of relative expression may be inferred from the cellular levels of tensin1, 2 and 3 mRNA. Therefore, RNA was isolated from HFF cell lysate using an RNAeasy miniprep kit. This RNA was treated with DNase I to remove any DNA contamination before reverse transcribing the mRNA into cDNA using oligo d(T) primers. This cDNA was then amplified in a qPCR reaction with primer pairs specific to each of the tensin isoforms (Table 2.2 – Materials and Methods) in the presence of the SYBR Green dsDNA-specific fluorescent dye using a MiniOpticon qPCR machine. These three sets of primers give rise to amplicons of approximately equal size with similar amplification efficiencies (Figure 3.7) and therefore relative abundance information can be extracted from the raw fluorescence data. Fluorescence intensity, which corresponds directly to the production of dsDNA products, was plotted

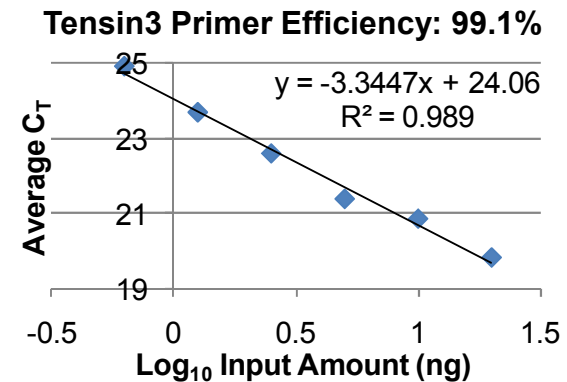
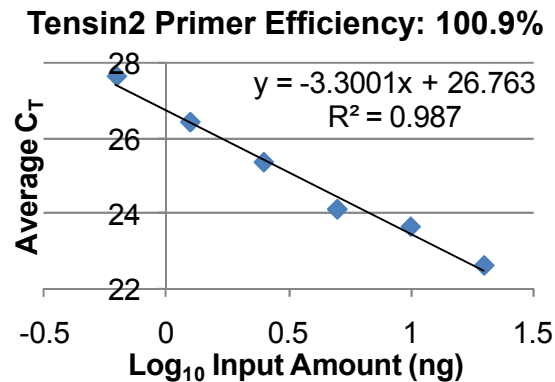
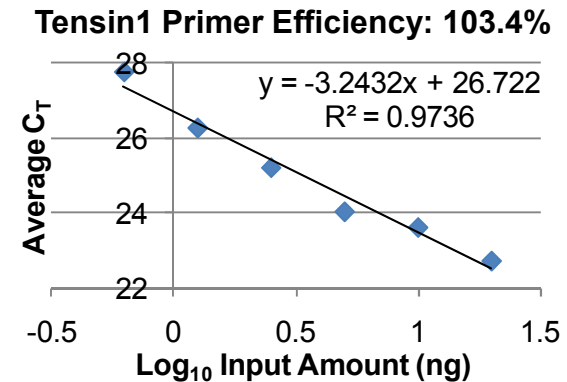
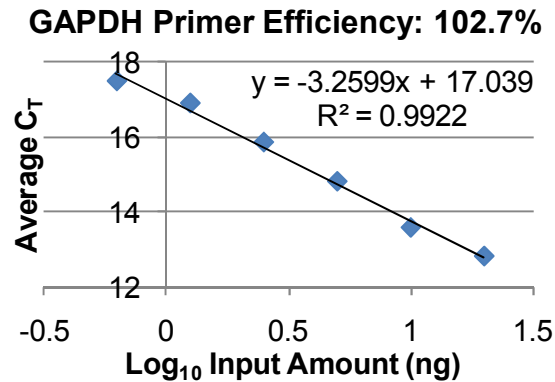


Figure 3.7: Validation of the amplification efficiency of the qPCR primers. RNA isolated from HFFs was DNase I treated and reverse transcribed into cDNA using oligo d(T) primers. Two-fold serial dilutions of this cDNA (20 ng-0.625 ng) were amplified in a qPCR assay with GAPDH, tensin1, tensin2 or tensin3 primer pairs in the presence of the SYBR Green dsDNA-specific fluorescent dye. Threshold cycles (C_T) were calculated from fluorescence amplification plots for each input amount with each primer pair. Shown are plots of average C_T vs. Log₁₀ input amount for each primer pair complete with calculated efficiencies derived from the gradient of the line-of-best-fit; amplification efficiency (%) = $(10^{(-1/\text{gradient})} - 1) \times 100$. Experiment was performed in triplicate. Note: All primer pairs amplified with similar efficiencies of approximately 100% over the range of template concentrations tested.

against cycle number to give rise to an amplification plot for the mRNA encoding each tensin isoform (Figure 3.8). The threshold line on this graph signifies the point at which fluorescence intensity increased to above background levels and amplification was in the log-linear phase. The cycle at which a particular amplification plot crosses this threshold line is termed the threshold cycle (or C_T). The tensin1 and tensin2 primers both gave C_T values of 21 whereas the tensin3 primers gave a C_T value of 19.7. Since C_T is inversely proportional to the amount of target DNA at the start of the PCR reaction, and as the amplification efficiencies of all the primer pairs were ~100%, a difference in C_T (ΔC_T) corresponds to a $2^{\Delta C_T}$ -fold difference in abundance. Based on this logic, the abundance of the tensin3 mRNA in HFFs is approximately 2.5-fold greater than tensin1 or tensin2, which are approximately equal (Figure 3.8). As the tensin isoforms were measured on the same cDNA sample no internal comparison control is required.

3.2.3 Anti-Tensin Antibody Characterisation by siRNA-Directed Tensin Knockdown

After establishing that HFFs express all three large tensin isoforms at the mRNA and protein level, these cells were used to further validate the isoform specificities of the anti-tensin antibodies by monitoring the effect of siRNA-directed tensin knockdown on their reactivity. In order to knockdown the expression of the different tensin isoforms it was necessary to identify an appropriate siRNA delivery method. Two lipofection-based transfection reagents, Oligofectamine and Lipofectamine 2000, were compared for their ability to efficiently deliver a fluorescently-tagged, non-functional, non-targeting siRNA (siGLO RISC-Free) into HFFs. Cells were transfected with 10 or 100 nM concentrations of this siRNA using either Oligofectamine or Lipofectamine 2000 (Figure 3.9). Twenty-four hours post-transfection the cells were fixed, stained with DAPI (DNA-binding nuclear dye), and mounted prior to analysis by fluorescence microscopy. siGLO siRNA

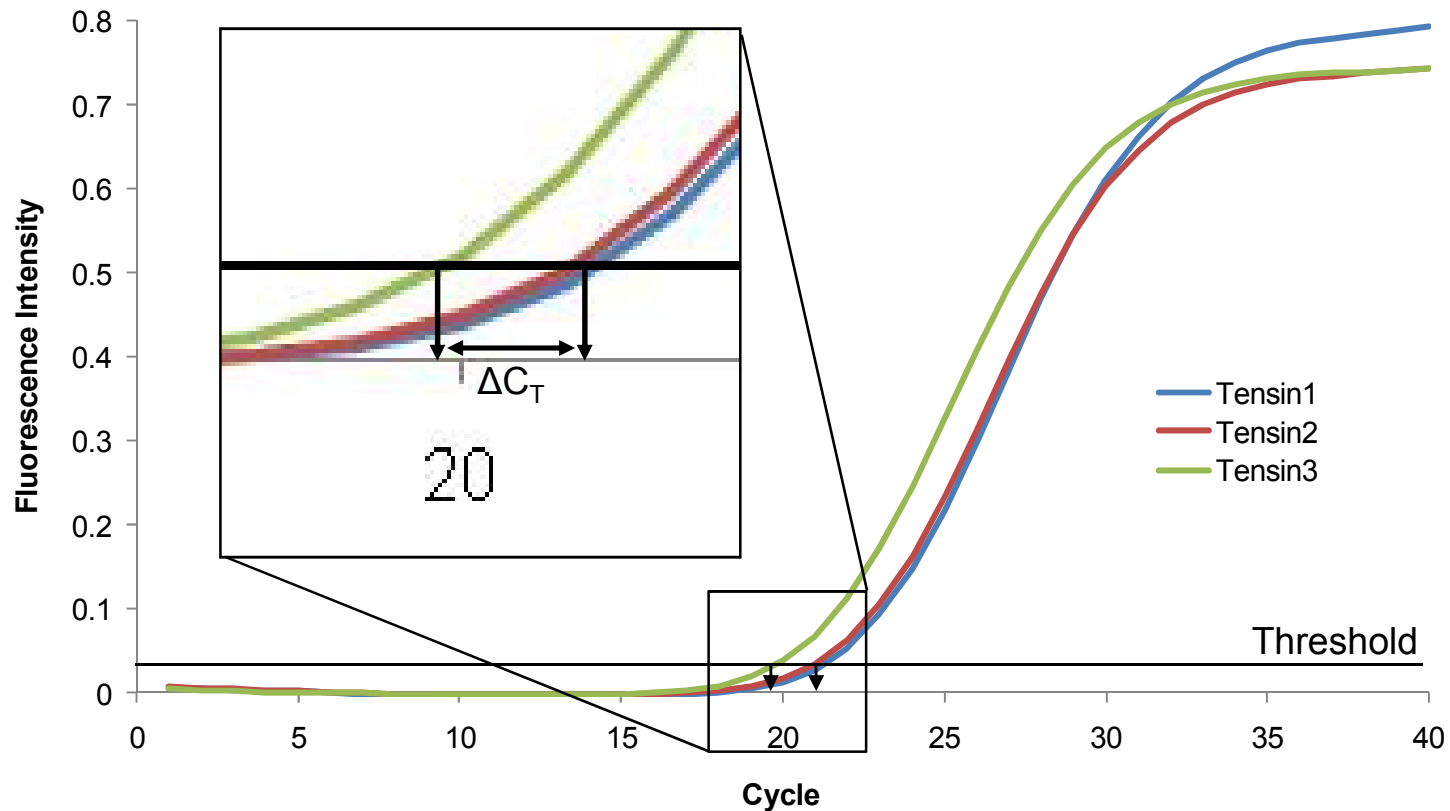


Figure 3.8: Detection of tensin mRNAs in HFFs. RNA isolated from HFFs was DNase I treated, reverse transcribed into cDNA using oligo d(T) primers, and amplified in a qPCR assay with tensin1, 2 and 3 primer pairs in the presence of the SYBR Green dsDNA-specific fluorescent dye. Shown are amplification plots of average fluorescence intensity vs. cycle number for each primer pair. Threshold cycles (C_T) for tensin3 and tensin1/2 amplifications are indicated with downward arrows. Note: Tensin3 amplification resulted in a lower C_T value than the amplification of both tensin1 and tensin2, which gave approximately equal C_T values. The C_T differential (ΔC_T) equates to an approximate 2.5-fold difference in expression i.e. tensin3 mRNA is approximately 2.5-fold more abundant than tensin1 or 2 mRNA. Experiment was performed in quadruplicate.

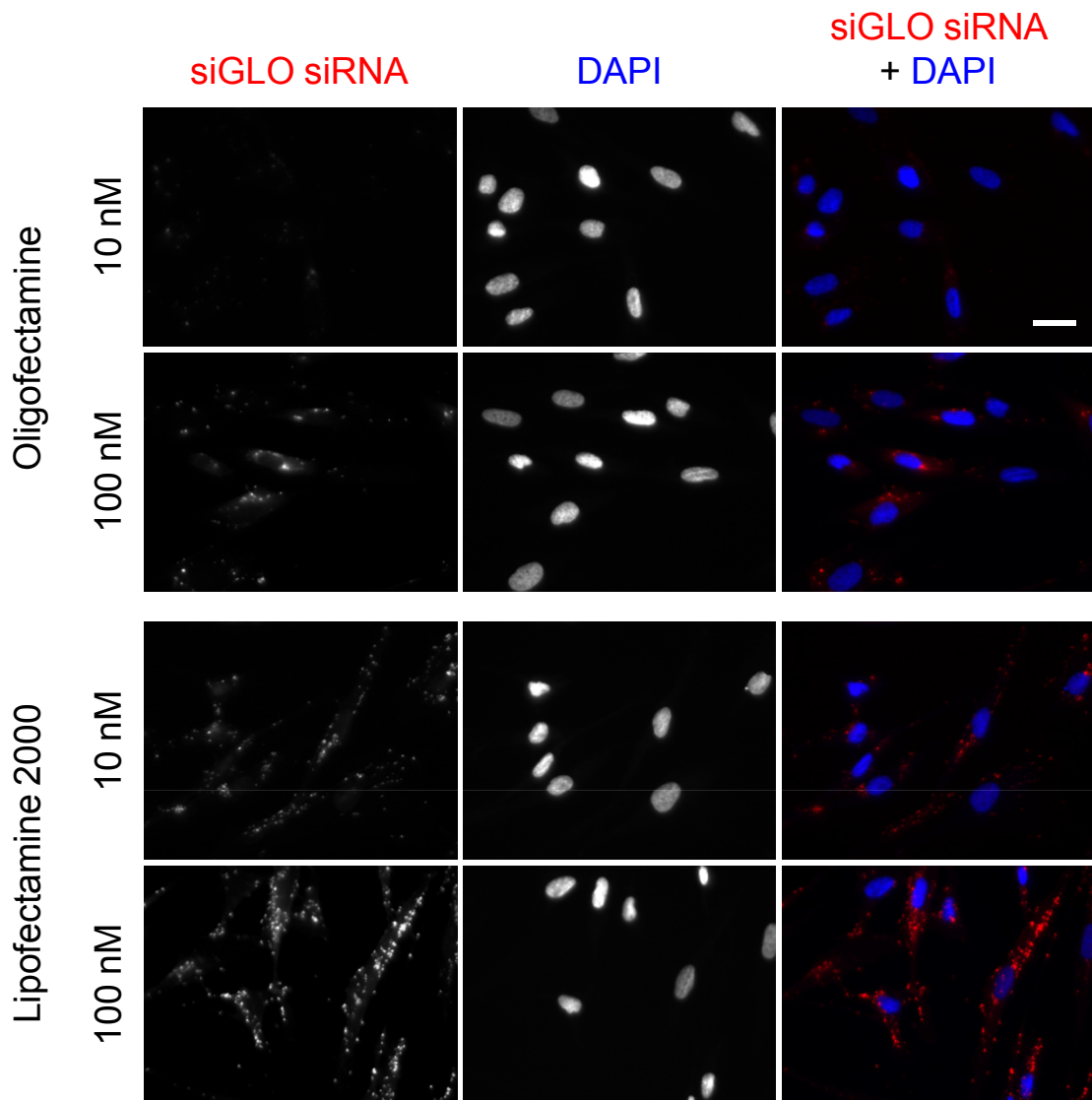


Figure 3.9: Optimisation of siRNA transfection into HFFs. The siGLO RISC-Free siRNA was transfected into HFFs at 10 or 100 nM concentration using the Oligofectamine or Lipofectamine 2000 transfection reagents. Cells were fixed 24 hours post-transfection, stained with the DAPI nuclear stain and imaged by fluorescence microscopy. Note: Both reagents gave transfection efficiencies of approximately 100%. However, the Lipofectamine 2000 reagent introduced more siRNA per cell than the Oligofectamine reagent. Scale bar – 30 μ m.

was not detectable at concentrations of 1 nM or less using this imaging system (data not shown). The siGLO siRNA was clearly visible in a granular pattern throughout the cytoplasm in ~100% of cells when using both transfection reagents. However, Lipofectamine 2000 introduced more siRNA per cell than Oligofectamine, and so was selected as the delivery system for all subsequent siRNA work in HFFs.

The isoform specificities of the Santa Cruz, Chemicon and Transduction anti-tensin1 antibodies, and the Rb33 anti-tensin3 antibody were further investigated by testing their reactivity against HFF cell lysates in which each tensin isoform was knocked down singly and in combination using siRNAs (Figure 3.10). The Santa Cruz, Chemicon and Transduction antibodies all reacted with a single protein band of the expected molecular weight for endogenous tensin1 (Figure 3.10). The house-keeping gene GAPDH was used as a loading control. The abundance of the tensin isoform detected by these antibodies was markedly reduced in lysates from cells pre-treated with a SMARTpool of four siRNA duplexes directed against the tensin1 isoform (Figure 3.10). In contrast, the tensin2 and tensin3 siRNA SMARTpools had no effect on the tensin1 levels detected with the commercial anti-tensin1 antibodies confirming the tensin1-specificity of these antibodies. However, the extent of the reduction detected with the Santa Cruz antibody was somewhat less than with the other antibodies.

The Rb33 antibody reacted with a protein band of the expected molecular weight for endogenous tensin3 (Figure 3.10). The abundance of this protein was substantially reduced in lysates harvested from cells that had been pre-treated with a SMARTpool of four siRNA duplexes directed against the tensin3 isoform, whereas the tensin1 and tensin2 siRNA SMARTpools had no effect, thereby confirming the tensin3-specificity of the Rb33 antibody (Figure 3.10). In summary, using this methodology further proof was obtained for the specificity of the tensin1 and tensin3 antibodies.

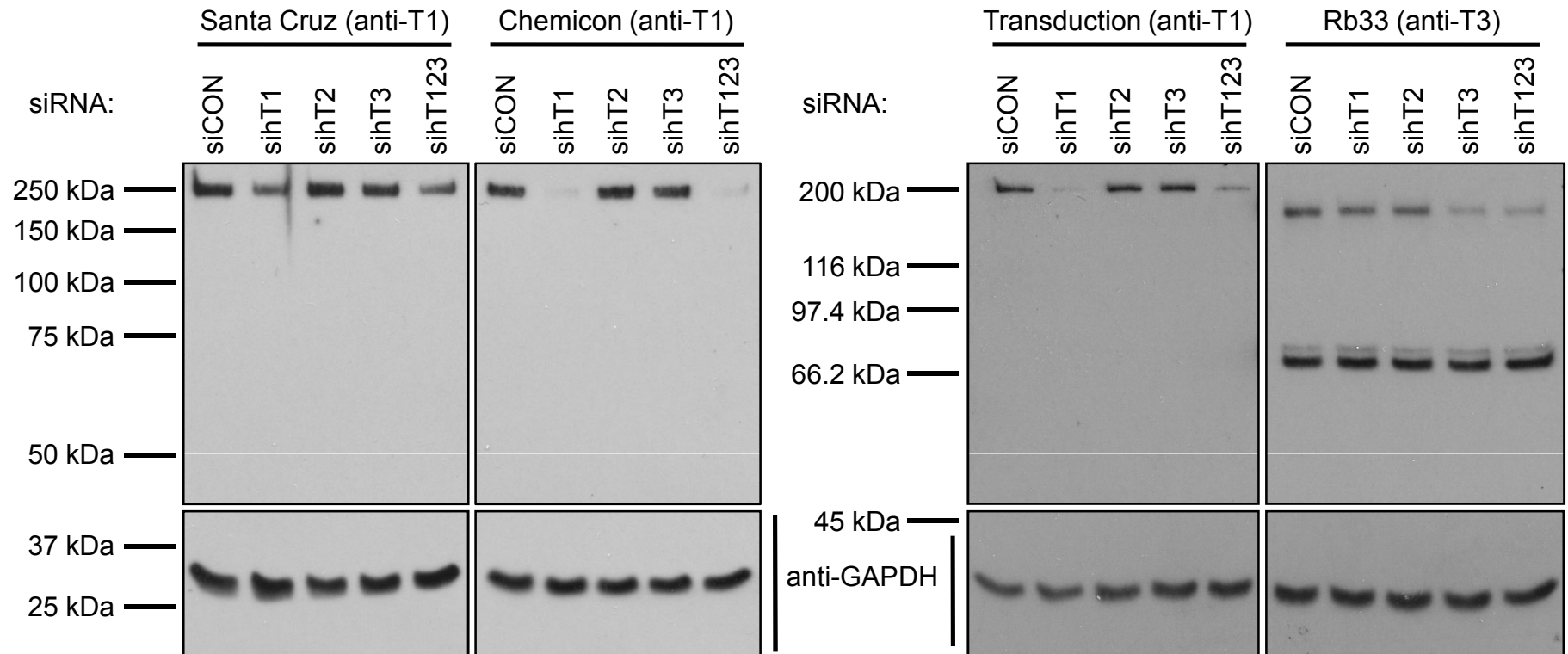


Figure 3.10: Validation of anti-tensin antibody specificity by siRNA-mediated tensin knockdown in HFFs. HFFs were transfected with SMARTpool siRNAs directed against human tensin1, 2 and 3 individually (sihT1, sihT2, sihT3) or in combination (sihT123), or with a control non-targeting siRNA pool (siCON); 10nM each. Proteins in cell lysates harvested 48 hours post-transfection were separated by SDS-PAGE (7.5% acrylamide) and probed with the anti-tensin1 antibodies from Santa Cruz Biotechnology (Santa Cruz), Chemicon International (Chemicon) and Transduction Laboratories (Transduction), and with the Rb33 anti-tensin3 antibody by Western blotting. GAPDH was used as a loading control. Note: The anti-tensin1 and anti-tensin3 antibodies recognised proteins of the appropriate molecular weights for tensin1 and tensin3, respectively. The abundance of the tensin isoforms recognised by the anti-tensin1 and anti-tensin3 antibodies were substantially reduced in the lysate of cells pre-treated with siRNAs directed against tensin1 and tensin3, respectively, thereby confirming the previously characterised isoform specificities of these antibodies.

3.2.4 Tensin Localisation in HFFs

To investigate the subcellular localisation of the three large tensin isoforms, HFFs were fixed with paraformaldehyde, permeabilised with Triton X-100, and stained with the commercial tensin1-specific antibodies and the in-house affinity purified rabbit polyclonal tensin2- and tensin3-specific antibodies, followed by the appropriate fluorescently-conjugated secondary antibodies and imaged by fluorescence microscopy. Unfortunately, most of the antibodies did not work sufficiently well to allow the localisation of these tensin isoforms to be determined, showing an unexpectedly diffuse cytoplasmic staining pattern (data not shown). However, limited success was achieved with the Santa Cruz antibody following fixation with ice-cold methanol (Figure 3.11; green staining). The cell shown in Figure 3.11 was co-stained with an antibody directed against $\alpha 5$ integrin (SNAKA51; red), which recognises a conformation-specific epitope that is revealed when this integrin is in fibrillar adhesions (Clark *et al.*, 2005). Endogenous tensin1 co-localised with $\alpha 5$ integrin in elongated fibrillar adhesions, and also located to focal adhesion-like structures at the cell periphery (Figures 3.11; arrows and arrow heads, respectively).

To further investigate the localisation of the various tensin isoforms, HFFs were transfected by lipofection or electroporation with mammalian expression constructs encoding GFP-tagged tensin isoforms. Twenty-four or 48 hours post-transfection the cells were fixed with paraformaldehyde and co-stained with antibodies directed against markers of focal and fibrillar adhesions. Focal adhesions were identified with an antibody directed against αV integrin (L230; red) and fibrillar adhesions were identified with antibodies directed against $\alpha 5$ integrin (SNAKA51; red) and FN (Rb745; blue). Following incubation with the appropriate fluorescently-conjugated secondary antibodies the localisation of these markers and the GFP-tagged protein were visualised by conventional (widefield) or confocal fluorescence microscopy.

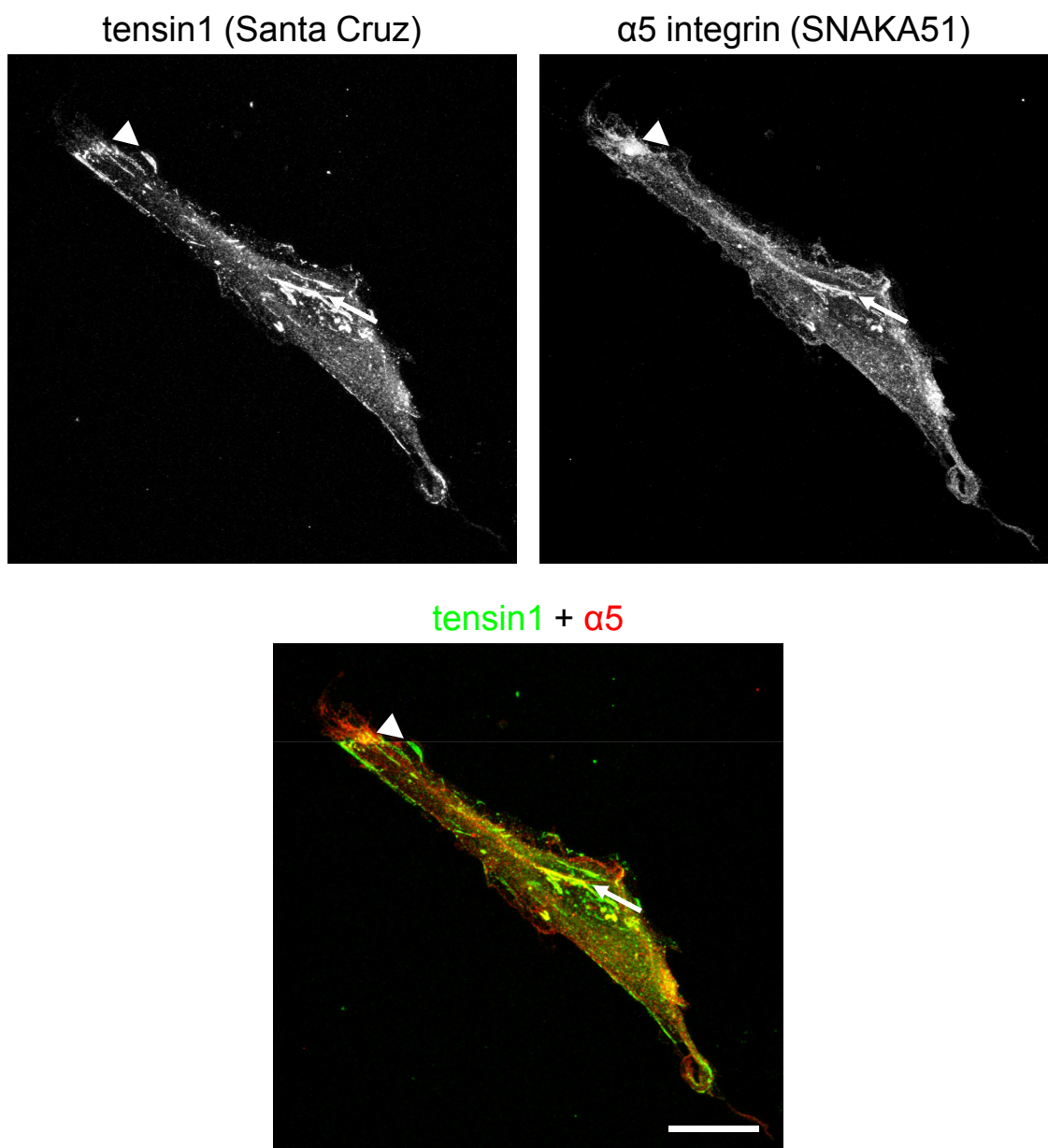


Figure 3.11: Confirmation of endogenous tensin1 localisation by immunofluorescent staining of untransfected HFFs with the Santa Cruz anti-tensin1 antibody. Untransfected cells were fixed with ice-cold methanol and immunostained with antibodies directed against tensin1 (Santa Cruz) and $\alpha 5$ integrin (SNAKA51). Note: endogenous tensin1 co-localised with $\alpha 5$ integrin at fibrillar adhesions (arrows) and also localised to focal adhesion-like structures at the cell periphery (arrow heads). Scale bar – 20 μ m.

GFP-tensin1 located to focal adhesion-like structures around the cell periphery and to elongated structures towards the centre of the cell (Figures 3.12-3.14; arrow heads and arrows, respectively). The peripheral structures were confirmed to be focal adhesions by co-staining with an antibody directed against α V integrin (Figure 3.12; arrow heads). The elongated central structures showed co-localisation with α 5 integrin and FN, suggesting that they were fibrillar adhesions (Figures 3.13, 3.14; arrows). Hence, in agreement with the staining of endogenous tensin1 with the Santa Cruz antibody (Figure 3.11), GFP-tensin1 localises to both focal and fibrillar adhesions.

GFP-tensin2 localised to focal adhesion-like structures at the cell periphery (Figures 3.15-3.17; arrow heads). These structures, which are deficient in α 5 integrin and fibrillar FN, are most likely focal adhesions. On careful inspection it was apparent that GFP-tensin2 also co-localised with FN and α 5 integrin in short fibrillar adhesions in some cells (Figure 3.15; arrows). GFP-tensin2 also showed diffuse cytoplasmic staining, possibly due to the saturation of tensin2 binding sites within the focal adhesions. Obtaining good quality images of GFP-tensin2-expressing HFFs proved to be very difficult. The main problem was that tensin2 over-expression resulted in the formation of large spherical accumulations of the fusion protein, which made imaging the true localisation of this protein difficult (Figure 3.17; asterisks). Consequently, only a very small percentage of lower expressing cells were appropriate for imaging. In summary, GFP-tensin2 predominantly locates to focal adhesions, and to a lesser extent to fibrillar adhesions.

GFP-tensin3 located to focal adhesion-like structures around the cell periphery and also more strongly to elongated structures towards the centre of the cell (Figures 3.18-3.21; arrow heads and arrows, respectively). The peripheral structures were confirmed to be focal adhesions by co-staining with an antibody directed against α V integrin (Figures 3.18, 3.19; arrow heads). The elongated central structures showed co-

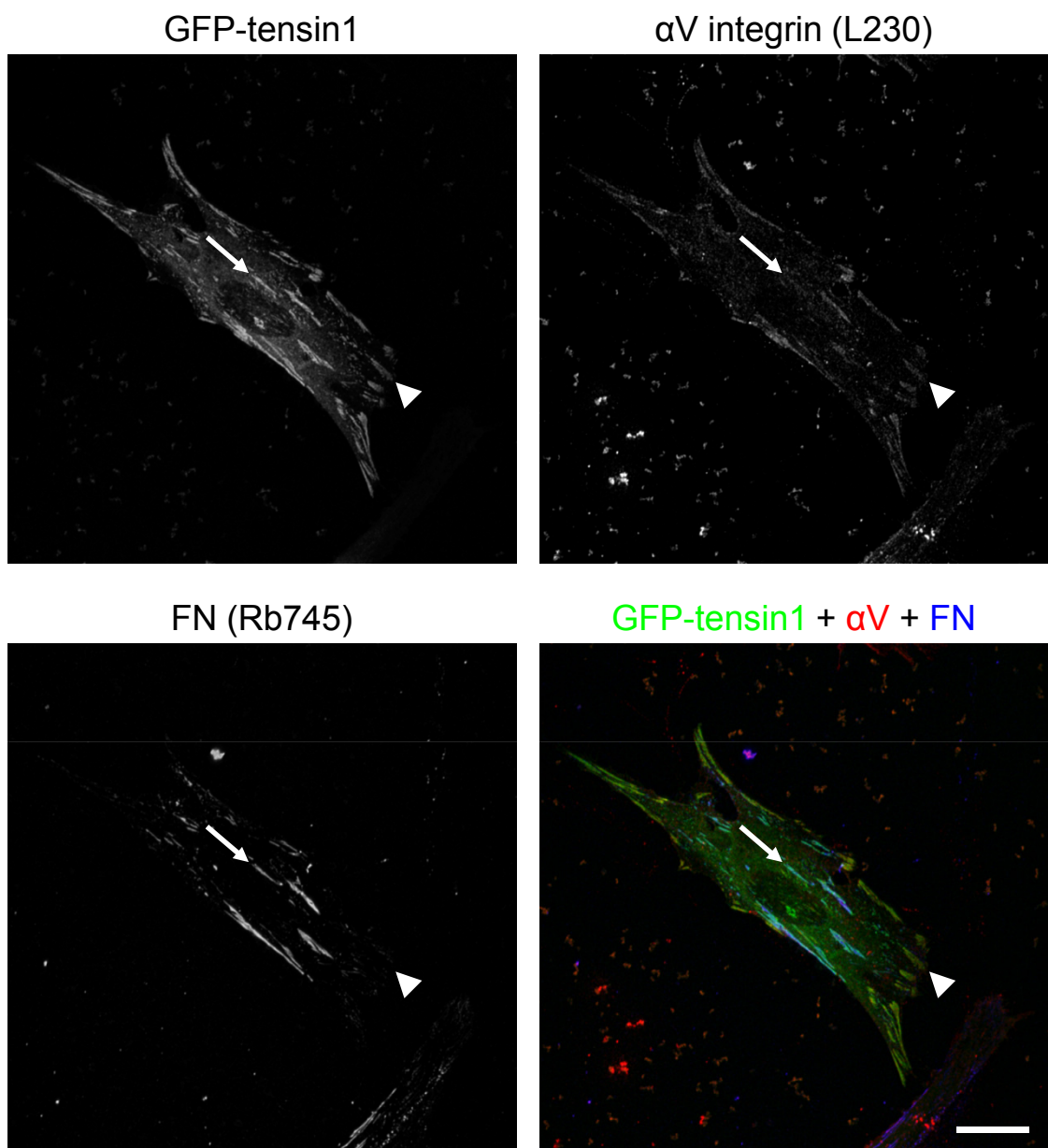


Figure 3.12: GFP-tensin1 localisation in HFFs. Cells were transfected with an expression construct encoding GFP-tensin1. Immunostaining was performed with antibodies directed against αV integrin (L230) and FN (Rb745). Note: GFP-tensin1 co-localised with αV integrin at focal adhesions (arrow heads) and with FN-positive fibrillar structures (arrows). Scale bar – 20 μm.

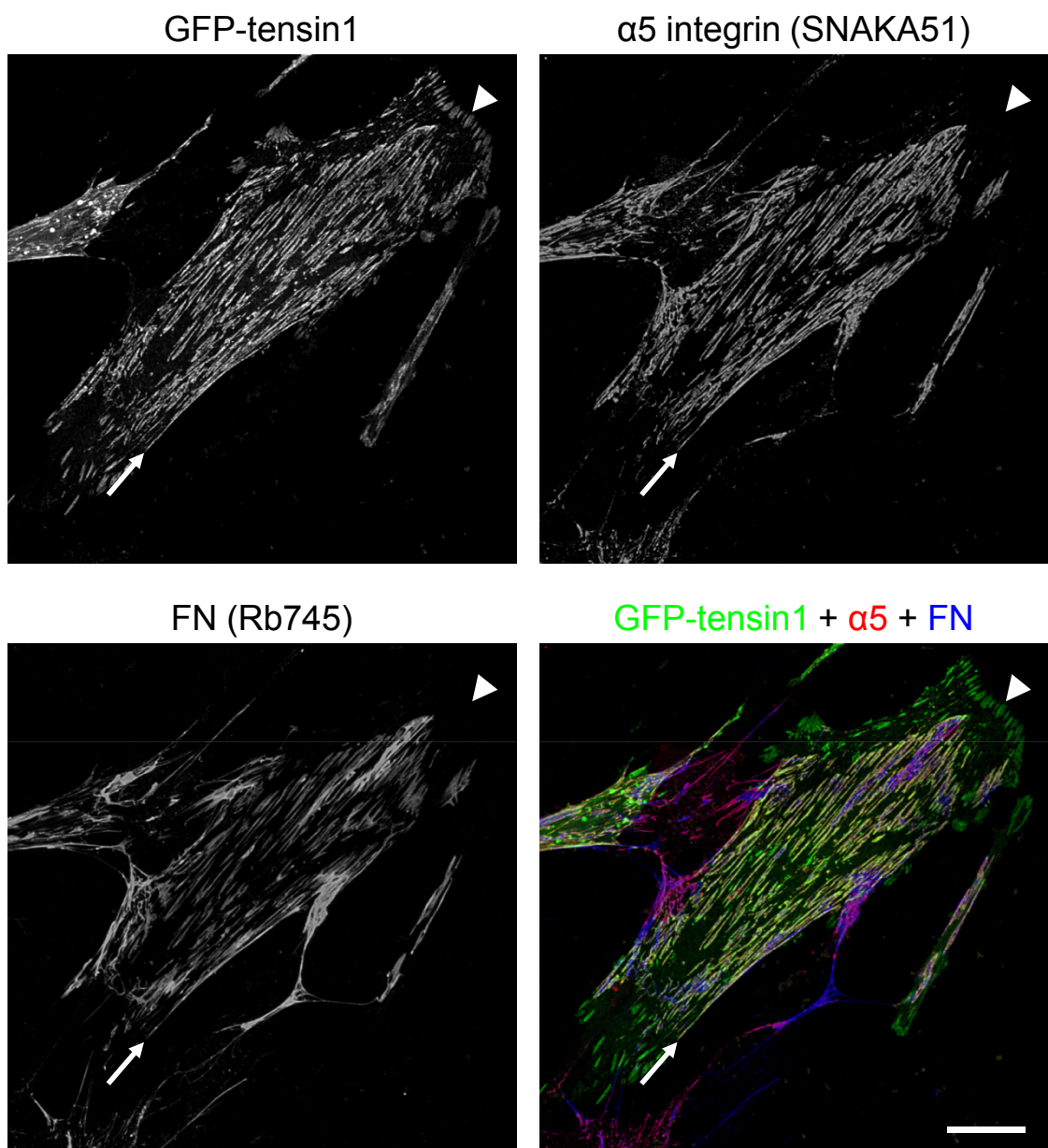


Figure 3.13: GFP-tensin1 localisation in HFFs. Cells were transfected with an expression construct encoding GFP-tensin1. Immunostaining was performed with antibodies directed against $\alpha 5$ integrin (SNAKA51) and FN (Rb745). Note: GFP-tensin1 co-localised with $\alpha 5$ integrin and FN at fibrillar adhesions (arrows) and also localised to focal adhesion-like structures at the cell periphery (arrow heads). Scale bar – 20 μm .

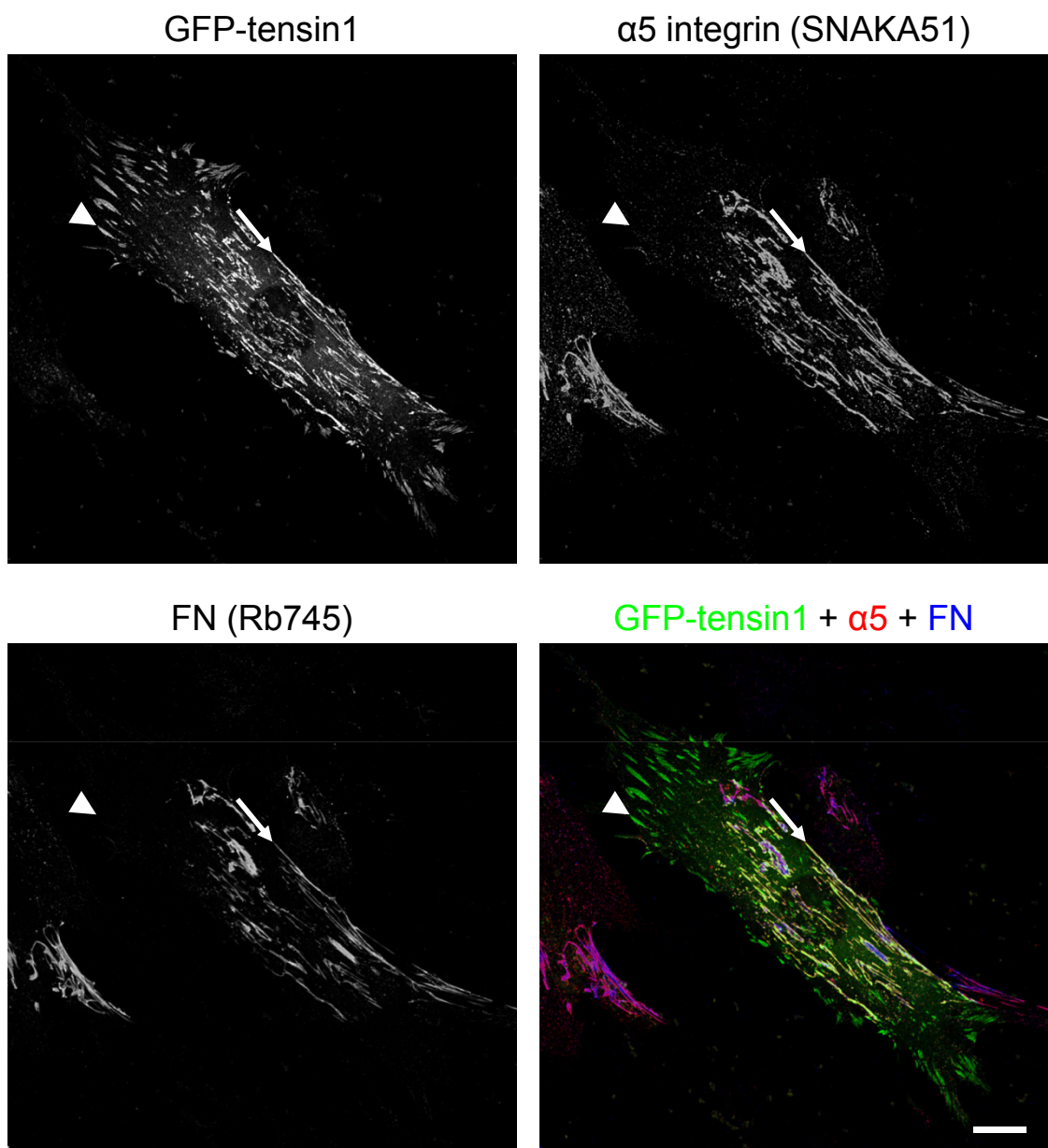


Figure 3.14: GFP-tensin1 localisation in HFFs. Cells were transfected with an expression construct encoding GFP-tensin1. Immunostaining was performed with antibodies directed against $\alpha 5$ integrin (SNAKA51) and FN (Rb745). Note: GFP-tensin1 co-localised with $\alpha 5$ integrin and FN at fibrillar adhesions (arrows) and also localised to focal adhesion-like structures at the cell periphery (arrow heads). Scale bar – 20 μm .

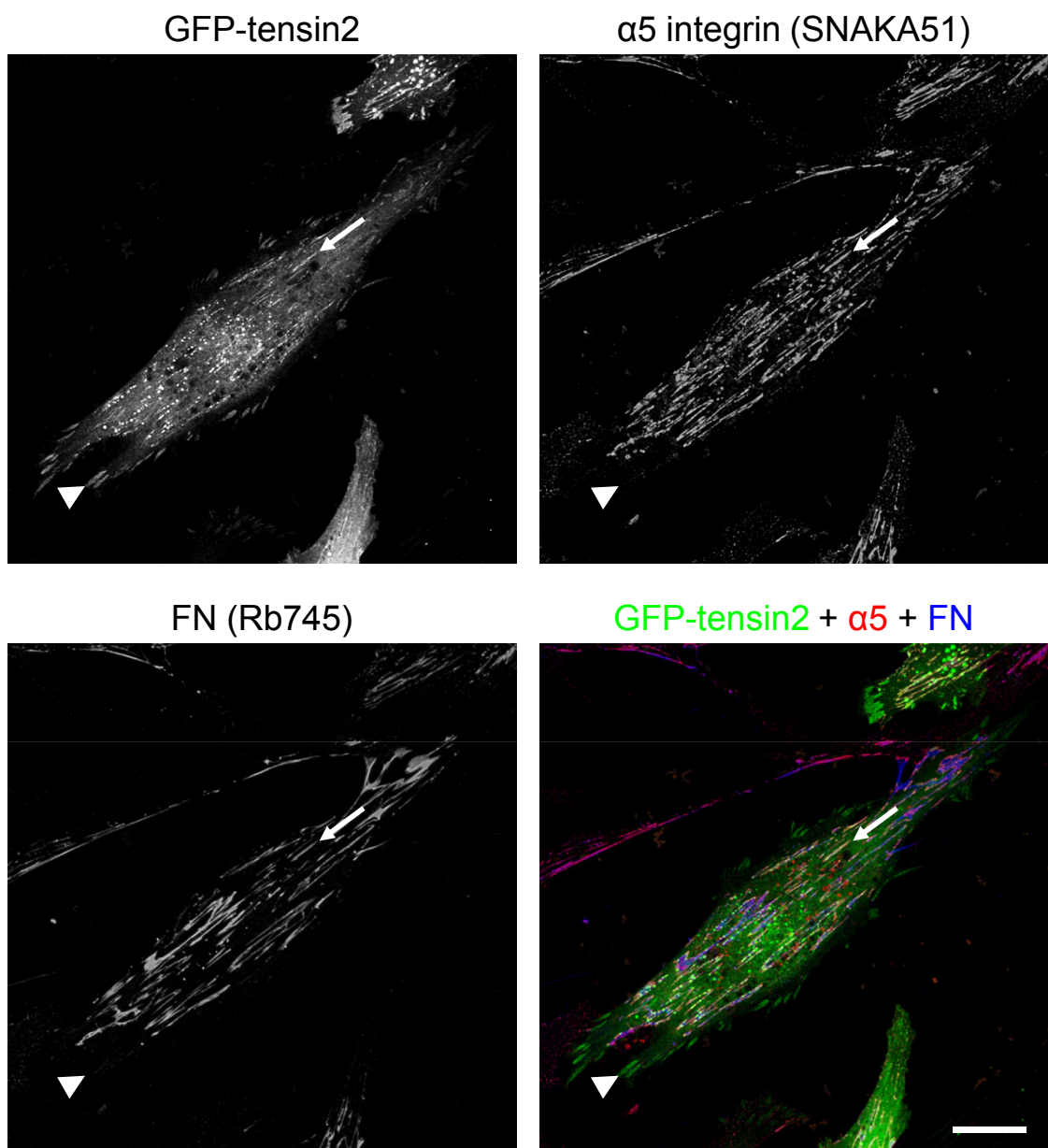


Figure 3.15: GFP-tensin2 localisation in HFFs. Cells were transfected with an expression construct encoding GFP-tensin2. Immunostaining was performed with antibodies directed against $\alpha 5$ integrin (SNAKA51) and FN (Rb745). Note: GFP-tensin2 showed diffuse cytoplasmic staining along with localisation to focal adhesion-like structures at the cell periphery (arrow heads), and to a lesser extent, co-localisation with $\alpha 5$ integrin and FN at fibrillar adhesions (arrows). Scale bar – 20 μm .

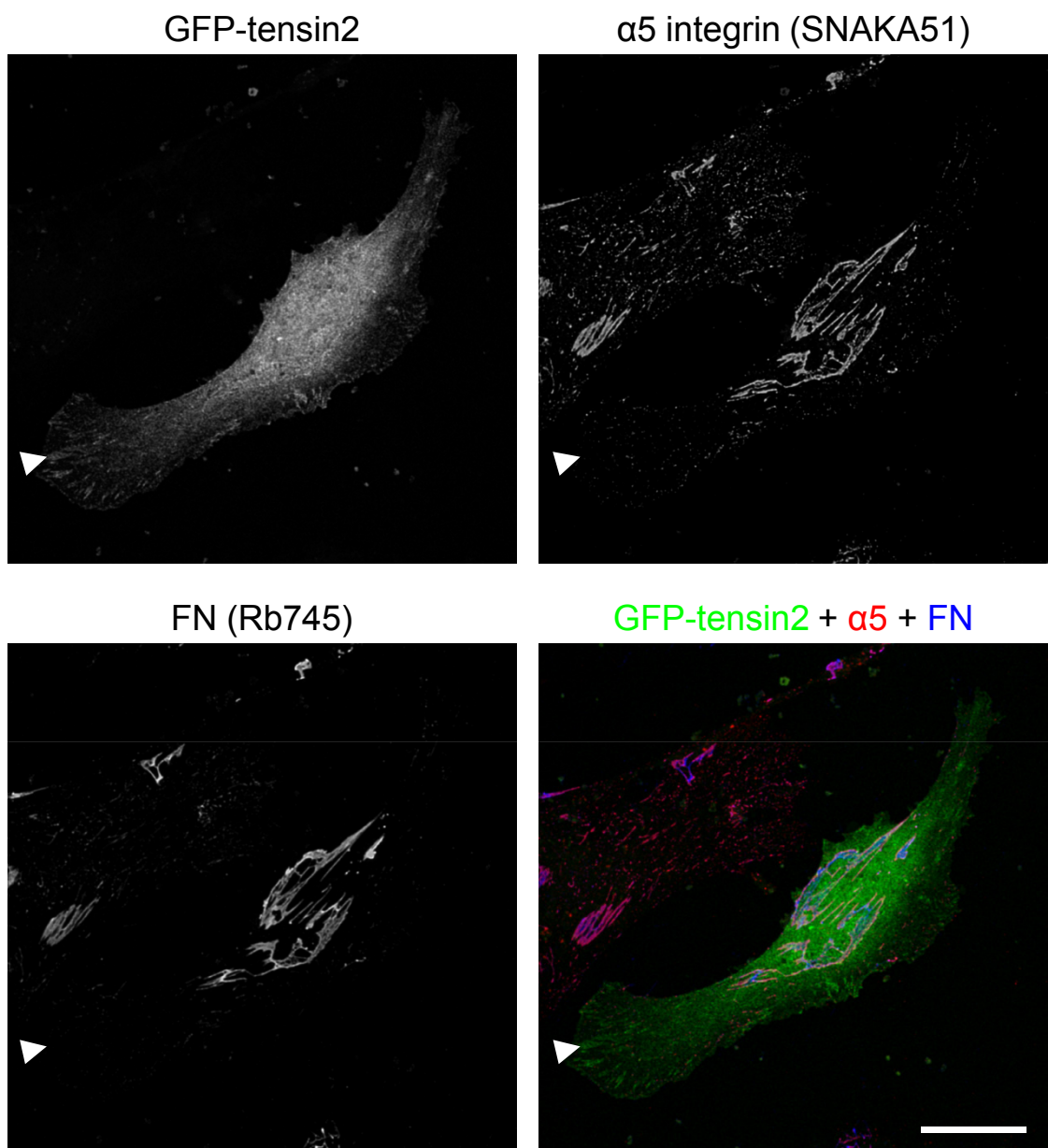


Figure 3.16: GFP-tensin2 localisation in HFFs. Cells were transfected with an expression construct encoding GFP-tensin2. Immunostaining was performed with antibodies directed against $\alpha 5$ integrin (SNAKA51) and FN (Rb745). Note: GFP-tensin2 showed diffuse cytoplasmic staining along with localisation to focal adhesion-like structures at the cell periphery (arrow heads). Scale bar – 20 μ m.

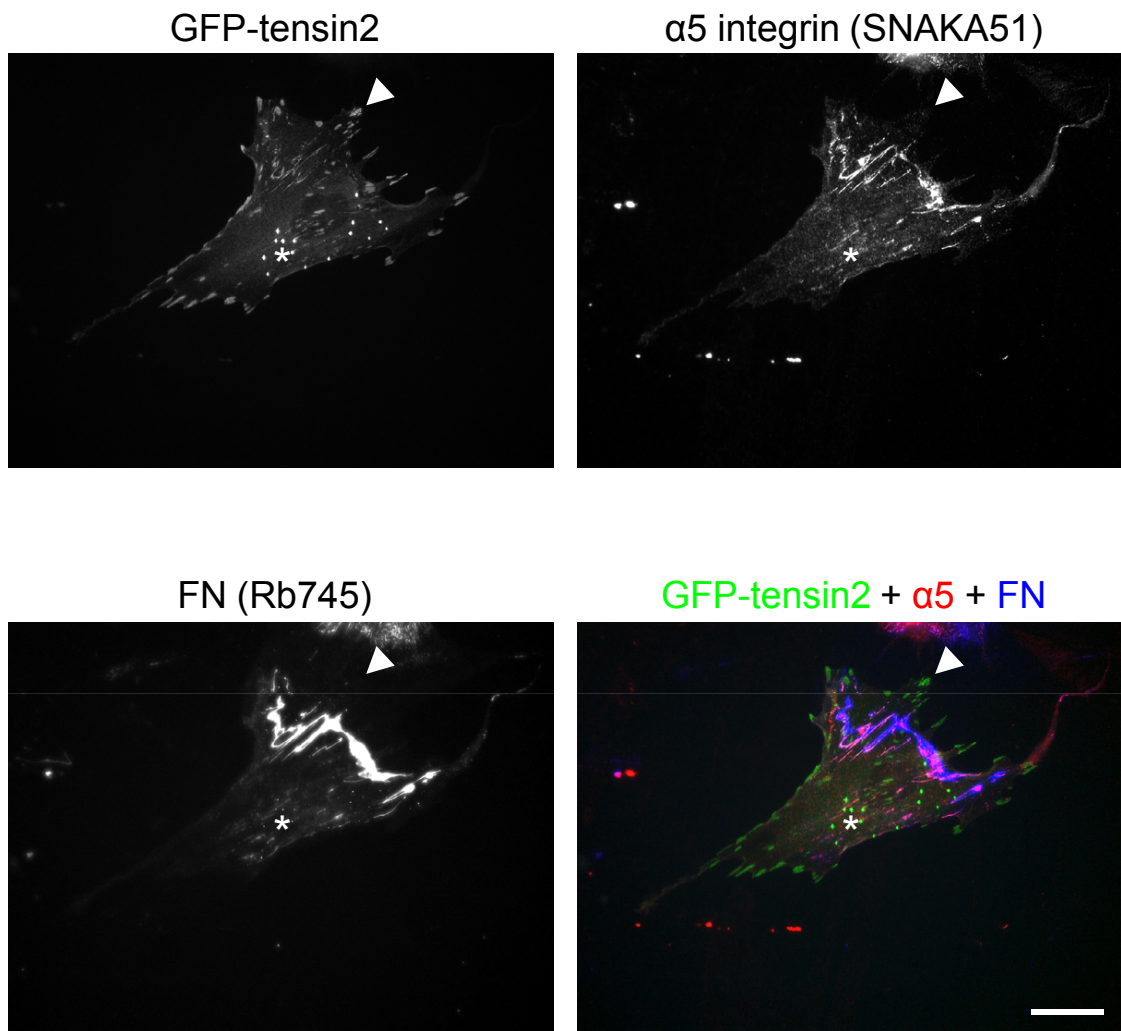


Figure 3.17: GFP-tensin2 localisation in HFFs assessed by conventional (widefield) fluorescence microscopy. Cells were transfected with an expression construct encoding GFP-tensin2. Immunostaining was performed with antibodies directed against $\alpha 5$ integrin (SNAKA51) and FN (Rb745). Note: GFP-tensin2 localised to focal adhesion-like structures at the cell periphery (arrow heads). Over-expression induced spherical accumulation of GFP-tensin2 (asterisks). Scale bar – 20 μm .

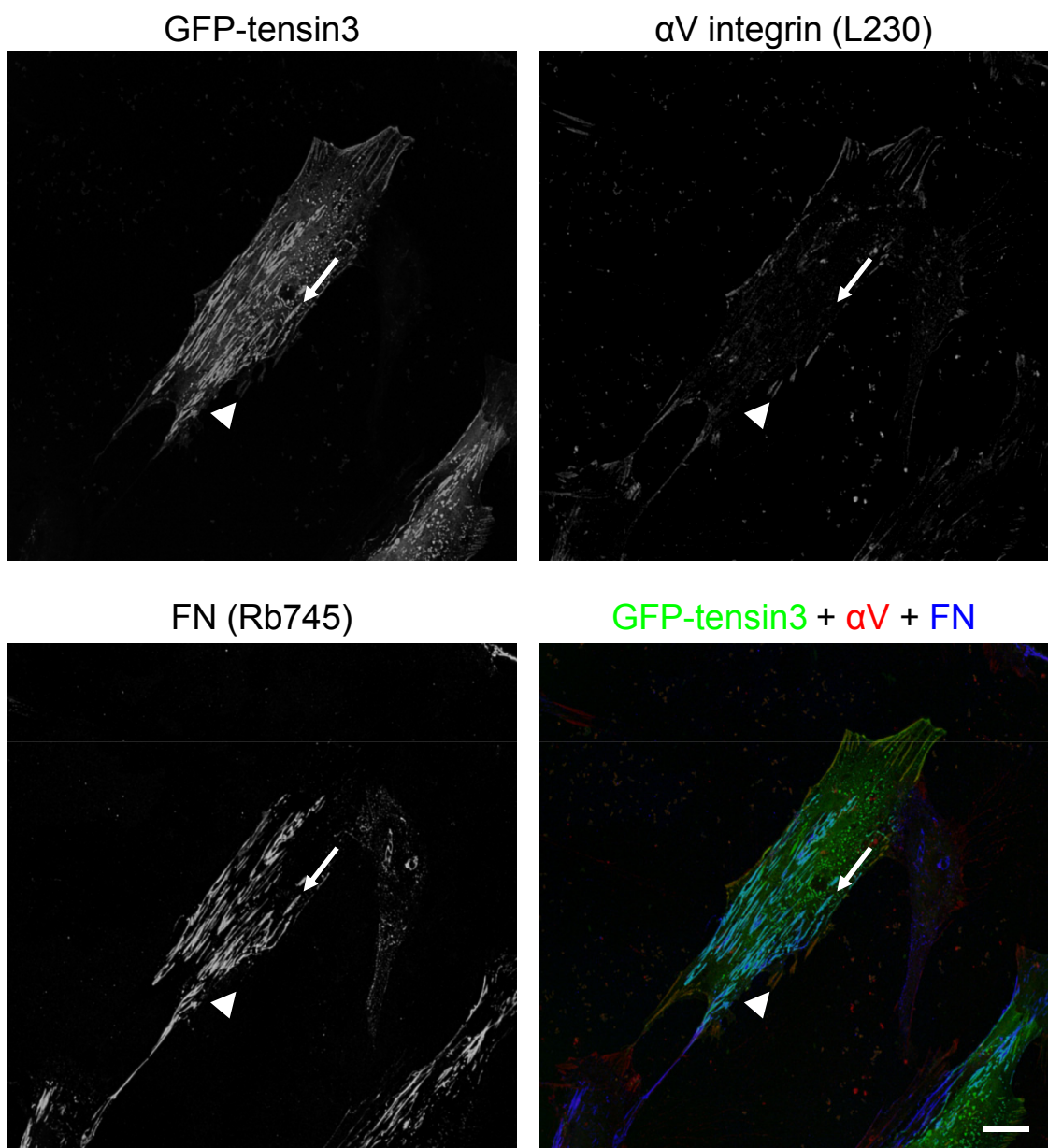


Figure 3.18: GFP-tensin3 localisation in HFFs. Cells were transfected with an expression construct encoding GFP-tensin3. Immunostaining was performed with antibodies directed against α V integrin (L230) and FN (Rb745). Note: GFP-tensin3 co-localised with α V integrin at focal adhesions (arrow heads) and with FN at fibrillar structures (arrows). Scale bar – 20 μ m.

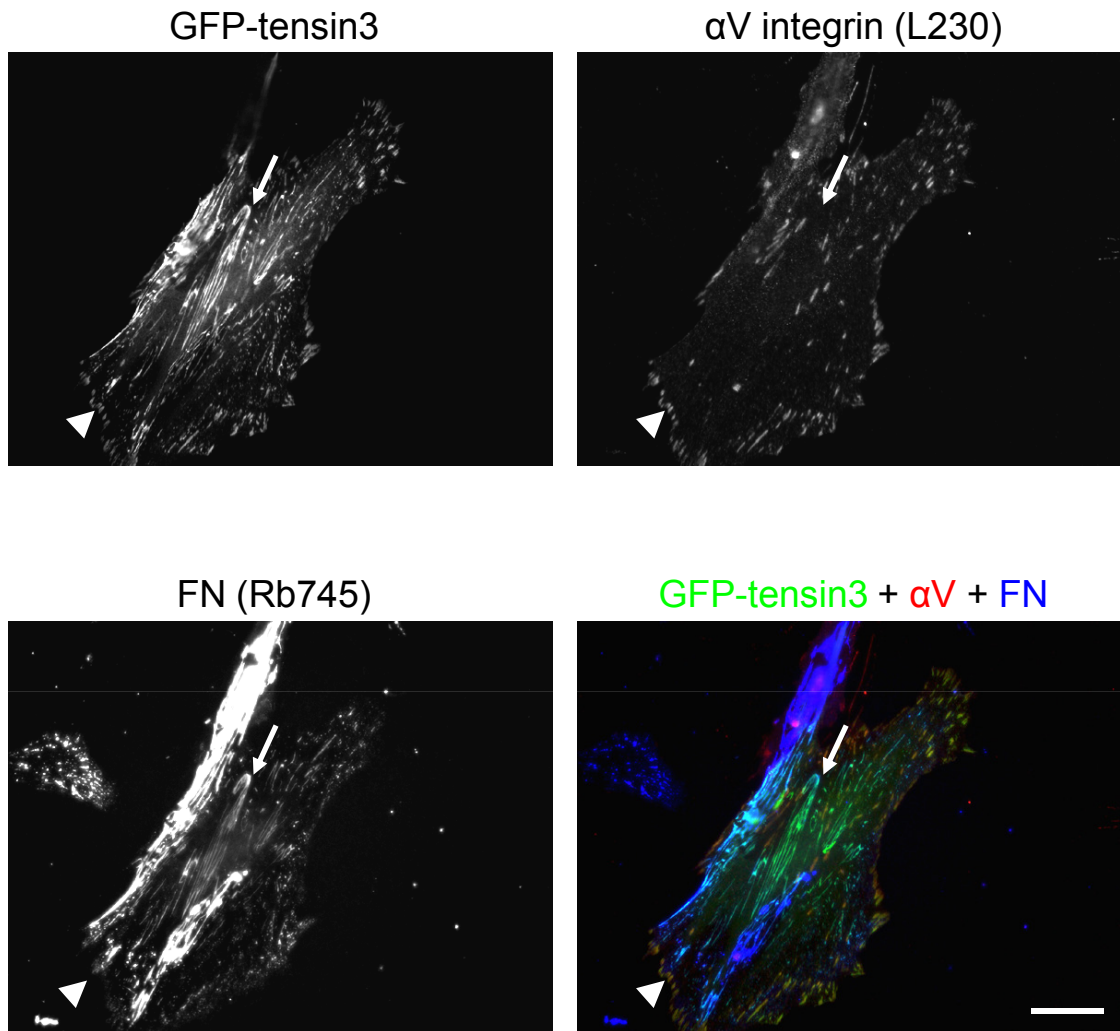


Figure 3.19: GFP-tensin3 localisation in HFFs assessed by conventional (widefield) fluorescence microscopy. Cells were transfected with an expression construct encoding GFP-tensin3. Immunostaining was performed with antibodies directed against α V integrin (L230) and FN (Rb745). Note: GFP-tensin3 co-localised with α V integrin at focal adhesions (arrow heads) and with FN at fibrillar structures (arrows). Scale bar – 20 μ m.

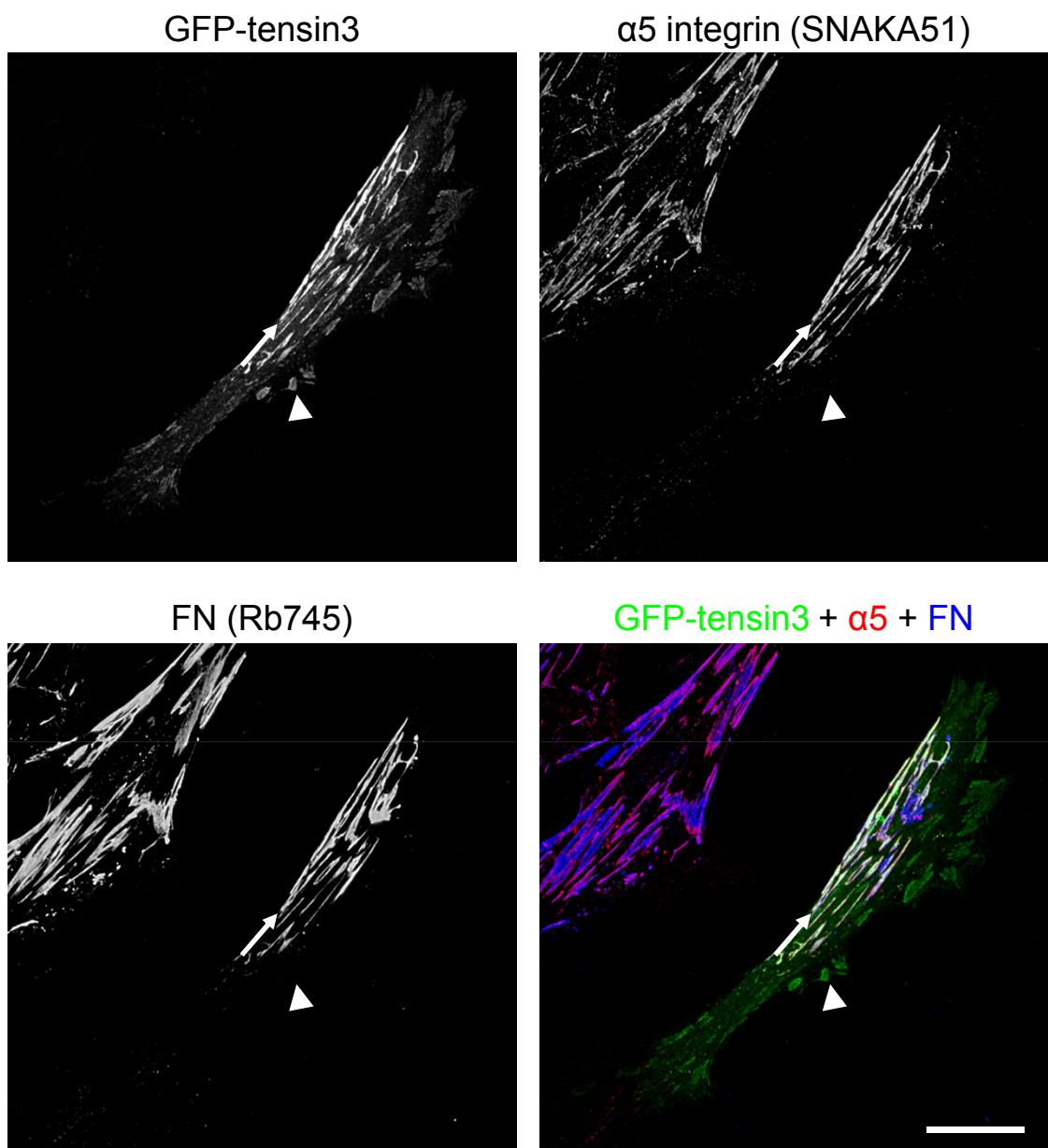


Figure 3.20: GFP-tensin3 localisation in HFFs. Cells were transfected with an expression construct encoding GFP-tensin3. Immunostaining was performed with antibodies directed against $\alpha 5$ integrin (SNAKA51) and FN (Rb745). Note: GFP-tensin3 co-localised with $\alpha 5$ integrin and FN at fibrillar adhesions (arrows) and also localised to focal adhesion-like structures at the cell periphery (arrow heads). Scale bar – 20 μm .

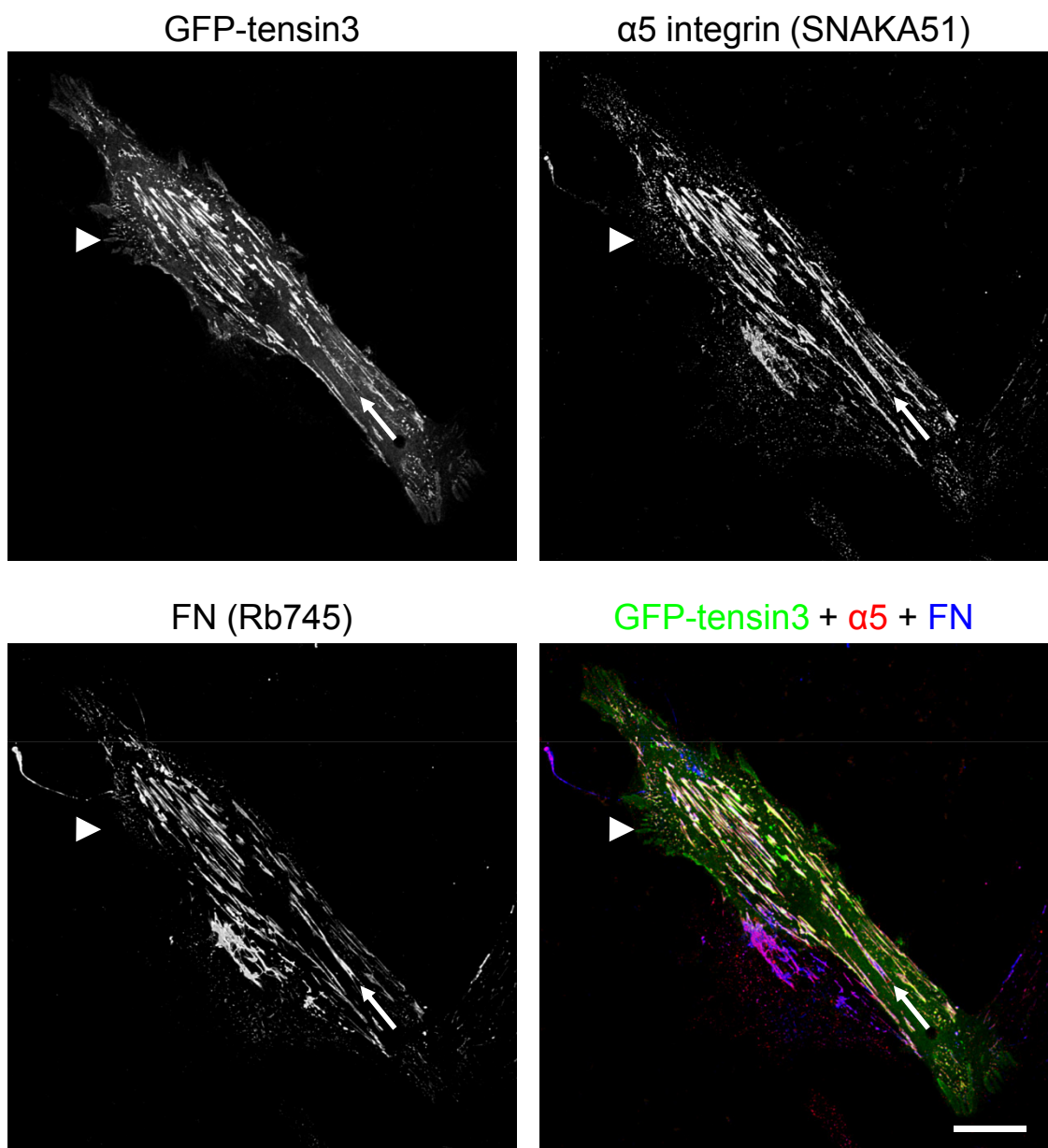


Figure 3.21: GFP-tensin3 localisation in HFFs. Cells were transfected with an expression construct encoding GFP-tensin3. Immunostaining was performed with antibodies directed against $\alpha 5$ integrin (SNAKA51) and FN (Rb745). Note: GFP-tensin3 co-localised with $\alpha 5$ integrin and FN at fibrillar adhesions (arrows) and also localised to focal adhesion-like structures at the cell periphery (arrow heads). Scale bar – 20 μm .

localisation with $\alpha 5$ integrin and FN, suggesting that they were fibrillar adhesions (Figures 3.20, 3.21; arrows). Therefore, GFP-tensin3 located to fibrillar adhesions more strongly than it did to focal adhesions, the reverse of that displayed by GFP-tensin2.

As a negative control, the empty GFP expression vector was transfected into HFFs, followed by immunofluorescence staining to identify focal and fibrillar adhesions. The GFP molecule showed a diffuse distribution and did not preferentially co-localise with αV integrin at focal adhesions (Figure 3.22; arrow heads) or with $\alpha 5$ integrin and FN at fibrillar adhesions (Figure 3.23; arrows).

In conclusion, all three of the large human tensin isoforms localise to both focal and fibrillar adhesions in HFFs. Tensin1 localises equally well to both types of adhesion. However, tensin2 preferentially localises to focal adhesions, whereas tensin3 shows preference for fibrillar adhesions.

3.3 Discussion

3.3.1 *Anti-Tensin Antibody Characterisation*

The large human tensin proteins display widespread expression in adult tissues and a high level of amino acid sequence homology at their N- and C-termini (Lo, 2004). In order to delineate the cellular functions of these proteins it is essential that the molecular tools are available to differentiate between each isoform. Therefore, the isoform specificities of a series of anti-tensin antibodies have been characterised.

The four commercially available anti-tensin antibodies were shown to be specific for the tensin1 isoform through their ability to detect GFP-tagged tensin1 and not GFP-tagged versions of the other tensins in HEK293 cell lysates. These antibodies also identified a

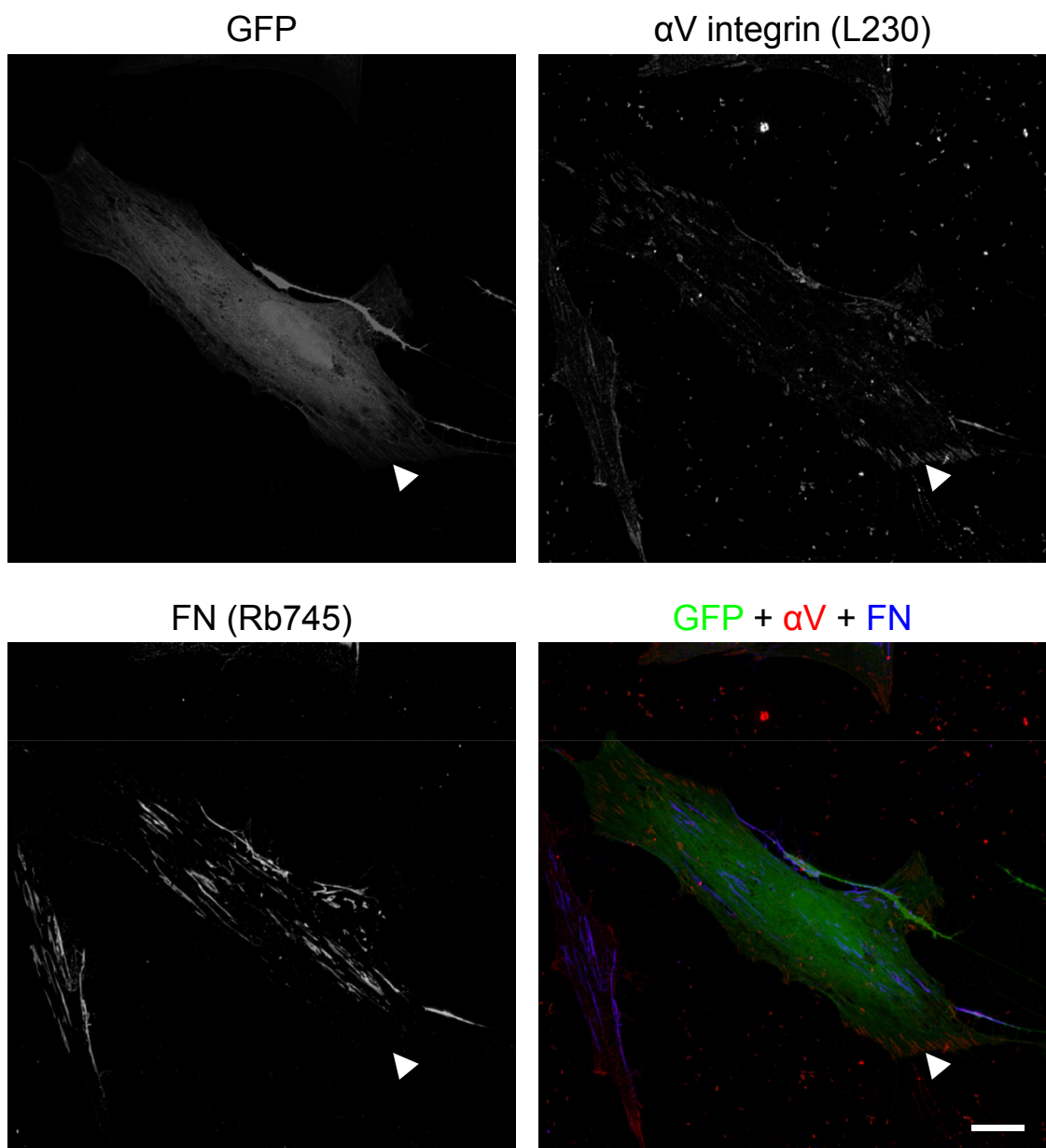


Figure 3.22: GFP localisation in HFFs. Cells were transfected with an expression construct encoding GFP. Immunostaining was performed with antibodies directed against αV integrin (L230) and FN (Rb745). Note: GFP showed diffuse cytoplasmic staining, and did not specifically localise to focal adhesions (arrow heads). Scale bar – 20 μm.

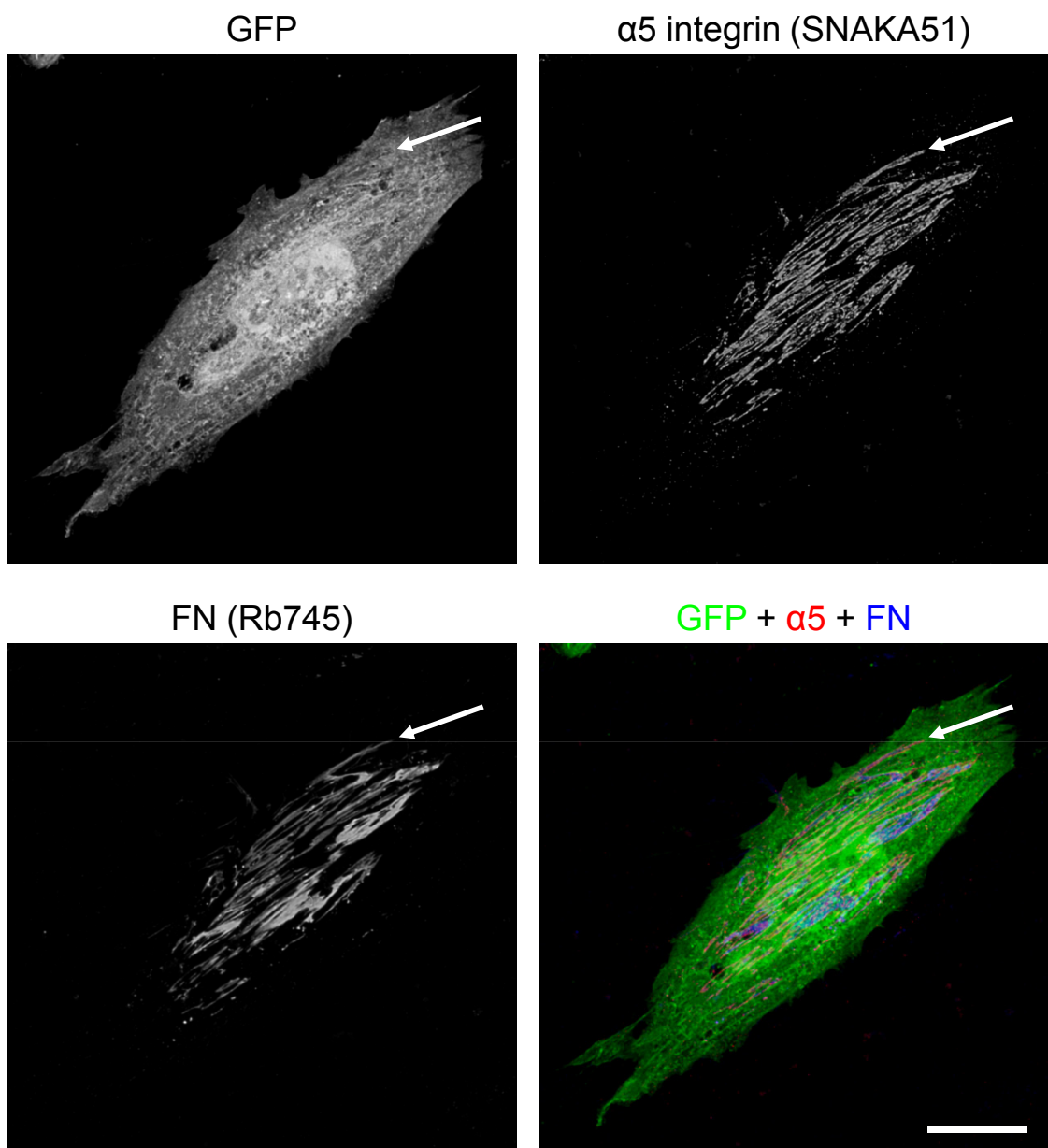


Figure 3.23: GFP localisation in HFFs. Cells were transfected with an expression construct encoding GFP. Immunostaining was performed with antibodies directed against $\alpha 5$ integrin (SNAKA51) and FN (Rb745). Note: GFP showed diffuse cytoplasmic staining, and did not specifically localise to fibrillar adhesions (arrows). Scale bar – 20 μm .

protein of the expected molecular weight for endogenous tensin1 in HFF cell lysate, and where examined their reactivity towards this band was specifically reduced upon the siRNA-directed knockdown of tensin1 expression. This isoform specificity was expected for the Santa Cruz polyclonal antibody since it was raised in rabbits using an immunogen corresponding to residues 661-960 from the divergent central region of human tensin1. The Transduction mouse monoclonal antibody was raised against full-length chicken tensin, which shares a high level of sequence similarity with human tensin1 throughout the length of the protein, particularly at the N- and C- termini (Chen *et al.*, 2000). Therefore, the finding that this antibody did not cross react with human tensin2 or 3 would suggest that its epitope is contained within the central region of the tensin1 protein, which is largely conserved across species but not conserved between the human tensin isoforms. The Chemicon and Upstate mouse monoclonal antibodies were raised against preparations of phosphotyrosine-containing proteins isolated from Rous sarcoma virus (RSV)-transformed chick embryo fibroblasts (CEFs). Database searching has revealed that the chicken genome is also likely to encode proteins homologous to human tensin2 and 3. Therefore, it was surprising that these antibodies were also specific for the human tensin1 isoform and failed to cross react with human tensin2 and 3, suggesting that their epitopes were again contained within the internal region of tensin1.

None of the commercial anti-tensin antibodies detected a protein of the appropriate size for endogenous tensin1 in HEK293 cell lysate (Figures 3.2, 3.3). This finding was not unexpected since others have previously shown that this cell line does not express detectable levels of tensin1 protein by Western blotting (Chen and Lo, 2003). In HFF cell lysate, the Upstate antibody detected a band of a higher molecular weight which may be an unrelated protein, or may represent a tensin1 homo- or heterodimer. The latter proposal is consistent with the findings of Lo *et al.* (1994) who presented evidence from dynamic light scattering and gel filtration experiments that chicken tensin

forms a dimer (Lo *et al.*, 1994). Perhaps under the conditions used in the present study, tensin was not fully reduced. However, the Chemicon and Transduction anti-tensin1 antibodies did not recognise this band. One possibility is that the epitopes for these antibodies are close to a tensin-tensin interaction region and become masked upon dimerisation.

The in-house polyclonal antibodies (Rb31-34) displayed isoform specificities that correlated with the antigens used to immunise the rabbits in which they were produced. Hence, the Rb31 and Rb32 antibodies, which were generated in rabbits injected with a synthetic peptide corresponding to residues 802-822 from the divergent central region of tensin2, were specific for tensin2. Similarly, the Rb33 and Rb34 antibodies, which were raised against a peptide corresponding to residues 439-457 from the internal region of tensin3, were tensin3-specific. The Rb31 anti-tensin2 antibody did not detect a band of the appropriate molecular weight for endogenous tensin2 in either HEK293 or HFF cell lysates despite recognising GFP-tensin2 (Figures 3.4, 3.6). This result could simply be a matter of sensitivity, i.e. the over-expressed GFP-tensin2 was detected whereas endogenous tensin2, which may be expressed at lower levels, was not. The Rb32 antibody recognised a protein band of the appropriate molecular weight for endogenous tensin2 in HEK293 and HFF cell lysates in addition to GFP-tensin2 (Figures 3.4, 3.6). However, this antibody also reacted with a ~60 kDa protein that was substantially more abundant in untransfected than GFP-tensin over-expressing HEK293 cells, which would suggest that the expression of this protein is down-regulated in response to elevated tensin expression. The identity of this protein is unknown. The Rb33 antibody recognised endogenous and GFP-tagged tensin3 (Figures 3.5, 3.6). This antibody also identified two unknown proteins (~60 kDa and ~70 kDa) in all lysates from transfected but not untransfected HEK293 cells, which would suggest that these proteins are expressed in response to increased tensin expression. These proteins are unlikely to be tensin3 degradation products or splice

variants as their abundance is unchanged upon siRNA-mediated tensin3 knockdown (Figure 3.10). Finally, the Rb34 antibody detected exogenously expressed GFP-tensin3 in HEK293 cell lysate and a protein of the expected molecular weight for endogenous tensin3 in HFF cell lysate (Figures 3.5, 3.6). However, this antibody did not detect a protein of the appropriate molecular weight for endogenous tensin3 in HEK293 cell lysate. It is difficult to explain this inconsistency, although it is conceivable that HEK293 cells may express endogenous tensin3 at insufficient levels to be detected by this antibody. Alternatively, it is possible, albeit unlikely, that HEK293 cells express a novel splice variant of tensin3, which does not contain the epitope for this antibody.

3.3.2 Differential Tensin Localisation in HFFs

The human tensin family of cytoskeletal-associated proteins are known to localise to focal adhesions (Chen *et al.*, 2000; Chen *et al.*, 2002; Cui *et al.*, 2004; Lo and Lo, 2002) and are thought to be required for FN fibrillogenesis (Pankov *et al.*, 2000). However, very few studies have investigated the capacity of the human tensin proteins to localise to fibrillar adhesions, the cellular machinery of FN fibrillogenesis. To address this issue, the localisation of the large tensins was assessed in the HFF cell line, which is the best characterised cell line for the study of fibrillar adhesions, and was also shown to express all three tensins at the protein and mRNA level (Figures 3.6, 3.8). Initially, the isoform-specific anti-tensin antibodies were used for immunocytochemistry experiments. Unfortunately, most of the antibodies worked insufficiently well to determine the subcellular localisation of the various tensin isoforms following paraformaldehyde fixation and permeabilisation with Triton X-100 (data not shown). However, previous studies have detected tensin1 in both focal and fibrillar adhesions in HFFs (Zamir *et al.*, 2000; Katz *et al.*, 2000a) and human skin fibroblasts (Borsani *et al.*, 2008) with the Transduction antibody, and in the human fibroblast cell line 1634 with the Santa Cruz antibody (Qian *et al.*, 2007). Indeed, limited success was achieved in

this study with the Santa Cruz antibody, which was able to detect tensin1 by immunofluorescence microscopy in both focal and fibrillar adhesions following methanol fixation (Figure 3.11). The reasons behind the poor performance of the Transduction antibody are unclear, particularly given the similarities between the fixation and staining conditions used in the present study and those used in the published studies (Zamir *et al.*, 2000; Katz *et al.*, 2000a; Borsani *et al.*, 2008). With the exception of the Santa Cruz antibody, the anti-tensin antibodies were only tested on HFFs fixed by paraformaldehyde cross-linking and permeabilised with Triton X-100. Therefore, it is conceivable that these antibodies might have performed better following fixation with a precipitating (or denaturing) fixative such as methanol.

Given the lack of antibodies to detect endogenous tensin proteins by immunocytochemistry, I attempted to produce a monoclonal antibody directed against tensin3 in collaboration with Dr R James (University of Leicester; Department of Infection, Immunity and Inflammation) (data not shown). I expressed and affinity purified a ~150 amino-acid protein designed on the divergent central region of tensin3. I then removed the affinity tags from this protein using the TEV protease and purified the untagged immunogen. Two mice were immunised with this protein at Harlan Sera-Lab (Loughborough, UK) and terminal bleeds from the mice were found to be immunoreactive against GFP-tensin3 in HEK293 cell lysates by Western blotting. Therefore, the spleens from these mice were sent to Dr James' lab for fusion. I screened culture media from the hybridoma cells using a combination of ELISA and Western blotting, and a series of clonal cell lines were produced by limiting dilution in Dr James' lab. Unfortunately, all of the monoclonal antibodies detected many protein bands in addition to tensin3 when tested by Western blotting, and none of the antibodies worked sufficiently well for immunocytochemistry, displaying a diffuse cytoplasmic localisation. Furthermore, isotyping of these antibodies revealed that they were all IgM. This antibody isotype is typical of the primary immune response, which

suggests that the mice were not properly boosted with the immunogen. IgM antibodies have lower specificity and affinity than mature IgG (Janeway, 2005), which could explain the poor performance of these antibodies both in Western blotting and immunocytochemistry.

Due to the difficulties encountered in determining the localisation of endogenous tensin with the anti-tensin antibodies, an alternative approach was adopted. GFP-tagged versions of the large human tensins were instead transfected into HFFs followed by immunocytochemistry to identify focal and fibrillar adhesions (Figures 3.12-3.21). Initially, conventional (widefield) fluorescence microscopy was used to collect images of individual HFFs transfected with GFP-tensin expression constructs by electroporation. However, the fact that fibrillar adhesions often form on the dorsal surface of the cell in a different plane of focus to focal adhesions, which always form on the ventral surface, led to difficulty in obtaining images in which both adhesion types were in focus. Therefore, confocal microscopy with optical sectioning was used to overcome this problem. However, the AMCA (aminomethylcoumarin acetate) fluorescent dye conjugated to one of the secondary antibodies was rapidly bleached by the confocal laser. Therefore, an alternative fluorescently-conjugated secondary antibody had to be purchased and optimised. Unfortunately, confocal imaging was also hampered by a laser reflection problem that led to an intolerably high level of background signal. Several potential causes for this problem were investigated, before finally discovering that it was due to the mounting media, which was substituted with an alternative to solve this problem. Once these technical issues associated with the switch to confocal microscopy had been resolved it became apparent that electroporation was an unsuitable method of transfection due to exceptionally low transfection efficiencies. Therefore, a new transfection reagent (Lipofectamine LTX) was purchased and transfection conditions were optimised. This transfection reagent gave a far superior transfection rate compared to electroporation. However, this

reagent also induced cell death around 48 hours post-transfection. Normally, 24 hours post-transfection the cells would be replated onto glass coverslips at an appropriate density for immunocytochemistry analysis. Then 24 hours later the cells would be fixed, by which time the fibrillar adhesions would be well established. Unfortunately, due to the toxicity issues with the new transfection reagent, this protocol was not applicable. Therefore, the cells were instead transfected on the coverslips and fixed 24 hours post-transfection before the transfection reagent could have its cytotoxic effect. One drawback of this method was that only the cells around the edge of the coverslip were at a low enough density for imaging, thereby reducing the likelihood of finding transfected cells. After overcoming these problems, it was then possible to start collecting data. However, some images collected on the confocal microscope showed what appeared to be positively stained cell debris, which may be a consequence high cell density. This undesired staining was partially improved by blocking with BSA.

Using this optimised methodology it was found that all three large human tensins located to both focal and fibrillar adhesions, although relative distribution between these adhesion types was isoform-specific. In short, tensin1 located equally well to both focal and fibrillar adhesions, whereas tensin2 and tensin3 showed preference for focal and fibrillar adhesions, respectively. One interpretation of this result is that tensin2 serves to anchor a subset of $\alpha_5\beta_1$ integrin in the focal adhesion, whilst tensin3 is induced to translocate out of the focal adhesion into the fibrillar adhesion in association with another subset of $\alpha_5\beta_1$ integrin, thereby exerting tension on the FN molecules on the outside of the cell and stimulating fibril assembly. This model was investigated through the examination of tensin dynamics by time-lapse total internal reflection fluorescence (TIRF) microscopy following co-transfection of HFFs with GFP-tensin2 and mCherry-tensin3, which confirmed that at the leading edge of the cell, tensin2 remains localised at the front of growing adhesions, whereas tensin3 translocates posteriorly (Clark *et al.*, 2010). The function of tensin1 is less clear since it locates

strongly to both focal and fibrillar adhesions. One possibility is that tensin1 plays a less dynamic role, and instead serves to maintain the structural integrity of both adhesion types.

Importantly, GFP-tensin1 displayed the same localisation pattern as immunofluorescent staining for endogenous tensin1 (Figures 3.12-3.14 versus Figure 3.11), which suggests that the over-expression of GFP-tensin1 does not result in artifactual localisation but instead faithfully represents the localisation of the endogenous protein. Several studies have identified human tensin1 in focal adhesions, either through exogenous expression of tagged human tensin1 protein in non-human cells (Chen *et al.*, 2000), or by immunofluorescent staining of human cells with one of the commercially available anti-tensin antibodies, which are now known to be tensin1-specific (Zamir *et al.*, 2000; Katz *et al.*, 2000a; Yamashita *et al.*, 2004; Qian *et al.*, 2007; Borsani *et al.*, 2008). Some of these studies also identified tensin1 in fibrillar adhesions because they were performed in fibroblastic cell lines that assemble these structures (Zamir *et al.*, 2000; Katz *et al.*, 2000a; Qian *et al.*, 2007; Borsani *et al.*, 2008). The subcellular distribution of human tensin2 and 3 are less well characterised. In one study, the localisations of tensin1 and 2 were directly compared through the immunofluorescent staining of GFP-tensin2 (variant 3)-expressing NIH 3T3 fibroblasts with an in-house anti-tensin1 antibody (Chen *et al.*, 2002). In agreement with the data presented here, Chen and co-workers found that both tensin isoforms located to focal and fibrillar adhesions; however, tensin2 did not appear to target to fibrillar adhesions as strongly as tensin1 (Chen *et al.*, 2002). Similarly, in another study, tensin2 (variant 1) was shown to colocalise with vinculin in focal adhesions in the human HCC cell line SMMC-7721 (Yam *et al.*, 2006a). Two groups have detected endogenous tensin3 in focal adhesions using the same polyclonal anti-tensin3 antibody (Katz *et al.*, 2007; Cui *et al.*, 2004). Very recently, a third group has also detected tensin3 in focal adhesions using both a GFP-tensin3 fusion and an in-house anti-tensin3 polyclonal antibody

(Qian *et al.*, 2009). However, these studies were performed on either the MCF10A or A549 cell lines, which are epithelial in origin and therefore unlikely to assemble fibrillar adhesions. The finding that tensin3 is preferentially located to fibrillar adhesions in HFFs, along with its higher expression level compared to the other large tensin isoforms, suggests that tensin3 plays an important role in FN matrix assembly.

Chapter 4 The Role of Tensin in Fibronectin Fibrillogenesis and Cell Migration in 2-Dimensional (2D) Culture

4.1 Introduction

4.1.1 Tensin and FN Fibrillogenesis

Fibrillar adhesions are elongated structures formed predominantly by fibroblastic cells cultured on 2D surfaces. They are enriched in the FN receptor $\alpha_5\beta_1$ integrin and lie parallel to actin bundles that are thought to exert force on surface-associated FN, exposing cryptic self-association sites within the FN molecules, thereby promoting FN matrix assembly (Pankov *et al.*, 2000; Ohashi *et al.*, 2002). Fibrillar adhesions are molecularly distinct from focal adhesions, and are enriched in tensin, whilst they are deficient in other focal adhesion markers such as vinculin and phosphotyrosine (Katz *et al.*, 2000a; Zamir *et al.*, 2000). Fibrillar adhesion formation is characterised by the translocation of $\alpha_5\beta_1$ integrin and FN along actin stress fibres from peripherally located focal adhesions towards the centre of the cell (Pankov *et al.*, 2000). This translocation is thought to be dependent on Src activity as Src-null cells display a reduction in the tyrosine-phosphorylation of several adhesion-related proteins, including tensin, and are incapable of segregating tensin into fibrillar adhesions (Volberg *et al.*, 2001). This results in the formation of large phosphotyrosine-poor, tensin-rich focal adhesions (Volberg *et al.*, 2001). FAK-null cells also lack fibrillar adhesions and exhibit impaired FN fibrillogenesis, and only the re-expression of wild-type FAK, and not a kinase-dead mutant, was able to rescue this phenotype, indicating that FAK kinase activity is required for fibrillar adhesion formation (Ilic *et al.*, 2004). Interestingly, tensin is a known substrate and binding partner for both Src (Qian *et al.*, 2009) and FAK (Zhu *et al.*, 1998b), which implies that tensin may play an active role in fibrillar adhesion formation. In support of this hypothesis, over-expression of the so-called actin homology 2 (AH2) region of chicken tensin in HFFs had a dominant negative effect on fibrillar adhesion formation (Pankov *et al.*, 2000). However, no further data has been

published supporting a functional role for tensin in fibrillar adhesion formation and/or FN fibrillogenesis.

4.1.2 Tensin and 2D Cell Migration

Several research groups have published data on the role of tensin in 2D cell migration. These studies have been performed on a variety of different cell types, which have either been depleted of tensin through gene KO or RNAi-mediated knockdown, or engineered to stably over-express tensin. The findings of these studies, which have all utilised the scratch-wound and/or Boyden chamber migration assays, are summarised below.

Using a Boyden chamber migration assay, Chen and co-workers showed that HEK293 cells stably expressing GFP-tensin1 or GFP-tensin2 migrated significantly faster than cells expressing GFP alone (Chen *et al.*, 2002). Concurrently, tensin1 KO mouse embryonic fibroblasts (MEFs) exhibited slower migration than their wild-type counterparts (Chen *et al.*, 2002). Tensin1 was also recently identified as a positive regulator of migration in a large-scale siRNA screen using a scratch-wound approach in the MCF10A normal human mammary epithelial cell line (Simpson *et al.*, 2008). Similarly, stable expression of GFP-tensin2 in the HCC cell line BEL7402 also had a positive effect on cell migration in both the Boyden chamber and scratch-wound assays (Yam *et al.*, 2006b). Conversely, stable expression of a splice variant of tensin2, which is identical to tensin2 except for an additional lipid-interacting C1 domain at its N-terminus (Figure 1.8 - Introduction), was shown to have a negative effect on HEK293 cell migration using the Boyden chamber assay (Hafizi *et al.*, 2005). The conflicting findings of this study are most likely due to the presence of the C1 domain. Although, the contradictory findings of these studies could alternatively be due to the slightly different experimental conditions used by each group. Hafizi *et al.* (2005) used FN as a

haptotactic stimulus to drive directional migration across the porous transwell filter, whereas Yam *et al.* (2006) used FCS as a chemotactic stimulus, and Chen *et al.* (2002) used both types of stimuli.

A reciprocal relationship between tensin3 and cten expression during EGF-induced cell migration was reported by Katz *et al.* (2007). They demonstrated that EGF stimulation down-regulated tensin3 expression and concomitantly up-regulated cten expression in the MCF10A cell line (Katz *et al.*, 2007). Using an RNAi approach and the Boyden chamber assay, it was shown that depleting tensin3 enhanced cell migration whereas depletion of cten impaired cell migration (Katz *et al.*, 2007). Moreover, MCF10A cells stably expressing GFP-cten displayed enhanced cell migration relative to cells stably transfected with the empty GFP expression vector (Katz *et al.*, 2007). It was suggested that the up-regulation of cten displaces tensin3 from focal adhesions by competing with tensin3 for binding to the β integrin cytoplasmic tail. The consequence of replacing tensin3 (and presumably other β integrin-binding proteins) with cten, a tensin isoform which lacks the actin binding domains, was the disassembly of actin stress fibres and reorganisation of the actin cytoskeleton, thereby promoting cell migration. It was also found that in HER-2 (human EGF receptor 2) positive inflammatory breast cancer (IBC), cten expression was correlated with EGF receptor (EGFR) activation (Katz *et al.*, 2007). Concurrently, *in vitro* inhibition of EGFR and HER2 in cultured IBC cells resulted in decreased cten levels (Katz *et al.*, 2007). In conclusion, this transcriptional 'tensin switch' may represent an event that occurs in metastatic breast cancer.

The findings of Katz *et al.* (2007) have recently been complimented by two further studies, which have again indicated that tensin3 and cten have opposing roles in cell migration (Martuszezwska *et al.*, 2009; Albasri *et al.*, 2009). Using the Boyden chamber assay, it was shown that the stable expression of tensin3 in HEK293 cells decreased migration, whereas the RNAi-mediated knockdown of tensin3 in the WM739 human

melanoma cell line increased migration (Martuszevska *et al.*, 2009). Another study showed that the stable expression of GFP-cten in the SW480 and HCT116 colorectal cancer cell lines increased cell migration, as assessed using the Boyden chamber assay (Albasri *et al.*, 2009). Moreover, GFP-cten-expressing HCT116 cells also displayed accelerated migration in scratch-wound assays when compared to cells expressing GFP alone (Albasri *et al.*, 2009).

In a very recent study it was reported that tensin3 is actually a positive regulator of cell migration, which contradicts the previously published data on this tensin isoform (Qian *et al.*, 2009). Using an siRNA approach, Qian and co-workers showed that depletion of tensin3 expression impaired the migration of several cancer cell lines using a combination of Boyden chamber and scratch-wound assays (Qian *et al.*, 2009). Moreover, in the H1299 human non-small cell lung cancer cell line, the impaired migration phenotype was partially rescued by the expression of GFP-tensin3. However, where tested, it was found that the siRNA-directed depletion of the other tensin isoforms had no effect on cell migration. Conversely, GFP-tensin3 expression promoted cell migration in NIH 3T3 mouse fibroblast cells that had been transformed with a constitutively active form of the tyrosine kinase Src, which was also shown to directly phosphorylate tensin3 (Qian *et al.*, 2009). Furthermore, the Src-mediated tyrosine phosphorylation of the tensin3 SH2 domain was shown to be important for the pro-migratory activity of tensin3 in H1299 cells. It is difficult to reconcile the contradictory findings of this study with the previously published data on the role of tensin3 in cell migration. One possibility is that the opposing outcomes are again due to slight differences in the experimental conditions used in the Boyden chamber assays. However, the authors suggest that it is due to differences in cell type. More specifically, they suggest that the findings of Martuszevska *et al.* (2009) with WM739 melanoma cells are due to the reduced invasiveness of this cell line compared to the metastatic melanoma cell lines used in their study. Secondly, they propose that DLC expression

and low Src activity, which are common in untransformed cells, could explain the data acquired using the MCF10A and HEK293 cell lines (Katz *et al.*, 2007; Martuszevska *et al.*, 2009).

All members of the human tensin family display significant homology at their C-termini, which contains an SH2 domain (Davis *et al.*, 1991) and a PTB domain (Schultz *et al.*, 1998). The three larger tensin isoforms also display homology at their N-termini, where actin-binding domains (Lo *et al.*, 1994b) and a region with homology to the PTEN protein and lipid phosphatase can be found (Haynie and Ponting, 1996). The N- and C-terminal regions of tensin are also thought to contain focal adhesion binding (FAB) sites necessary for its cellular localisation and biological activity (Chen and Lo, 2003). Chen and Lo generated HEK293 cells stably transfected with either GFP-chicken tensin or GFP-chicken tensin deletion mutants lacking the N-terminal FAB site, the C-terminal FAB site, or both the N- and C-terminal FAB sites. Although tensin mutants with only one FAB site still localised to focal adhesions, they did not promote cell migration in the Boyden chamber assay (Chen and Lo, 2003). Moreover, a tensin mutant with no FAB sites, which does not localise to focal adhesions, actually suppressed cell migration, presumably through a dominant negative mechanism (Chen and Lo, 2003). Chen and Lo also generated HEK293 cells stably expressing a GFP-chicken tensin mutant that lacked residues within the SH2 domain shown to be required for the binding of phosphotyrosine-containing proteins. This mutant was not capable of promoting cell migration, indicating that the interaction of the SH2 domain with phosphotyrosine-containing proteins is necessary for tensin-mediated cell migration (Chen and Lo, 2003).

Collectively, these studies indicate that tensin1, cten and probably tensin2 enhance 2D cell migration, whereas the role of tensin3 is less clear. The central regions of the three full-length tensins, and the N-terminus of cten, exhibit a high degree of amino acid

divergence. Therefore, this region of tensin3 may contain motifs that convey cell type-dependent functional divergence upon this tensin isoform.

4.2 Results

4.2.1 *The Role of Tensin3 in FN Matrix Assembly in HFFs*

It has previously been shown that the AH2 region of chicken tensin has a dominant negative effect on FN fibrillogenesis when over-expressed in human fibroblasts (Pankov *et al.*, 2000). This result was somewhat surprising as this region of chicken tensin is not conserved in the human tensins. To confirm this finding, a GFP-tagged expression construct encoding the AH2 region of chicken tensin (GFP-AH2) was transfected into HFFs by electroporation. Twenty-four hours post-transfection the cells were trypsinised to destroy any pre-existing FN matrix and replated onto glass coverslips for a further 24 hours. Cells were fixed and co-stained with antibodies directed against the fibrillar adhesion markers $\alpha 5$ integrin (SNAKA51) and FN (Rb745), followed by the appropriate fluorescently-conjugated secondary antibodies, and imaged by fluorescence microscopy. Figure 4.1 shows two cells, one expressing GFP-AH2 and the other untransfected. The untransfected cell displays many fibrillar adhesions (Figure 4.1; arrows), whereas the transfected cell shows no fibrillar FN and only punctate $\alpha 5$ integrin staining. All cells that expressed GFP-AH2 displayed a similar phenotype. This result suggests that tensin plays an important role in the process of FN fibrillogenesis in HFFs.

To explore the requirement for the human tensins during FN fibrillogenesis in HFFs, an siRNA-based method for knocking down tensin expression was optimised and validated. Firstly, as described in the previous chapter, two potential lipofection-based siRNA delivery methods were compared for their ability to introduce a fluorescently-

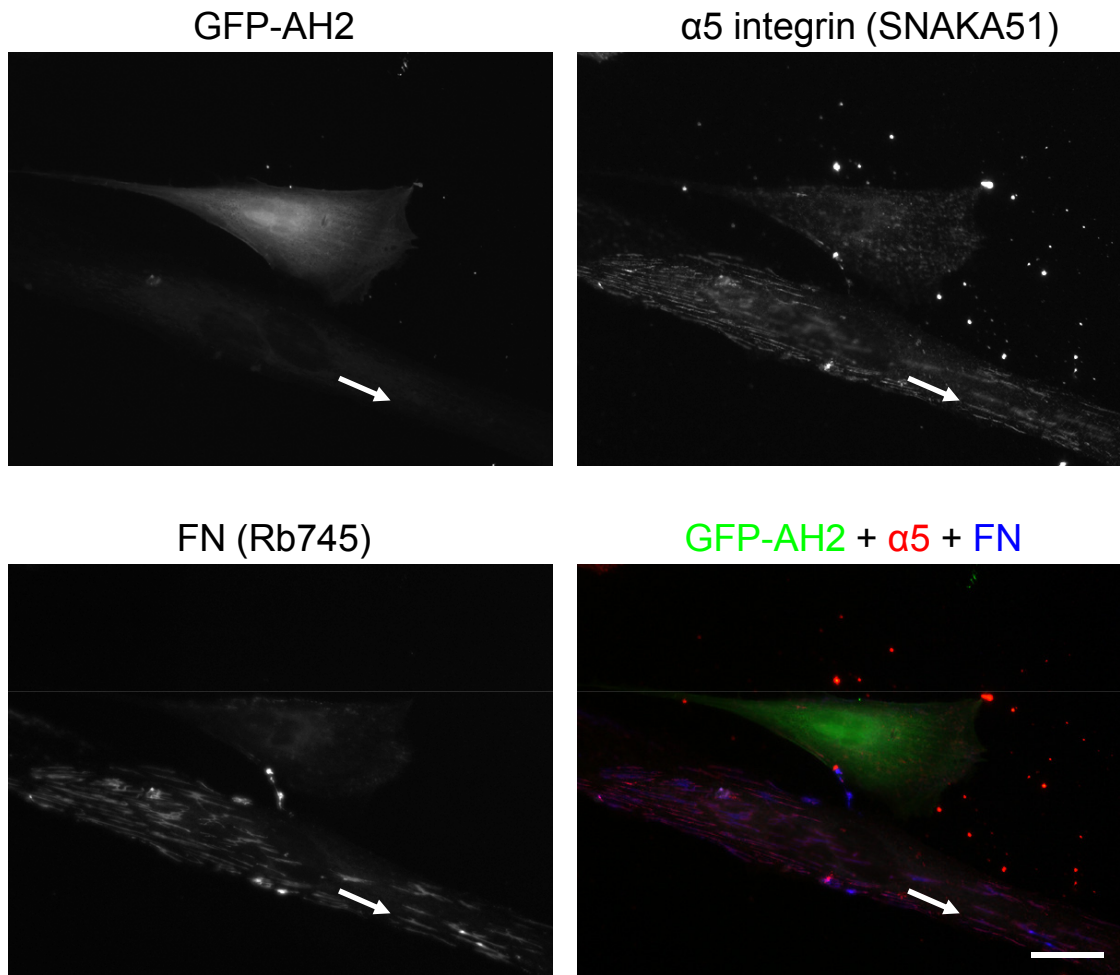


Figure 4.1: Dominant negative effect of expression of GFP-AH2 region in HFFs. HFFs were transfected with an expression construct encoding GFP-tagged AH2 region of chicken tensin by electroporation. Twenty-four hours post-transfection the cells were trypsinised, replated onto glass coverslips and cultured for a further 24 hours to allow the assembly of new fibrillar adhesions. Cells were fixed and stained with antibodies directed against the fibrillar adhesion markers α5 integrin (SNAKA51) and FN (Rb745), followed by the appropriate fluorescently-conjugated secondary antibodies, and imaged by conventional (widefield) fluorescence microscopy. Note: The untransfected cell has many fibrillar adhesions (arrows), whereas the cell expressing GFP-AH2 has no extended α5 integrin- or FN-stained structures. Scale bar – 20µm.

tagged control siRNA into HFFs. The Lipofectamine 2000 reagent was shown to introduce more siRNA per cell than the Oligofectamine reagent and was therefore selected as the siRNA delivery method of choice for this cell line (Figure 3.9). Secondly, tensin3 was chosen over the other tensin isoforms as the initial candidate for siRNA-mediated knockdown based on its higher mRNA abundance (Figure 3.8) and preferential localisation to fibrillar adhesions (Figures 3.20, 3.21), as shown in the previous chapter. To establish the efficiency of tensin3 knockdown at the protein level, a SMARTpool of four siRNA duplexes directed against the human tensin3 isoform (sihT3) were transfected into HFFs by lipofection. A range of siRNA concentrations (0 to 100 nM) were used to find the lowest concentration that gave maximal knockdown of tensin3. Proteins in cell lysates harvested 24 hours post-transfection were separated by SDS-PAGE (7.5% acrylamide) and probed with antibodies directed against tensin3 (Rb33) and GAPDH (loading control) by Western blotting (Figure 4.2). As observed previously, the Rb33 antibody reacted with three protein bands; one at the expected molecular weight for tensin3 and two smaller proteins of unknown origin (Figure 4.2). The abundance of the tensin3 protein decreased with increasing tensin3 siRNA concentration up to 10 nM, where maximal knockdown was accomplished (Figure 4.2). This siRNA concentration was adopted for tensin3 knockdown in subsequent experiments in the HFF cell line to minimise off-target effects. The abundance of the other two proteins recognised by Rb33 was not altered by treatment with the tensin3 siRNA SMARTpool. This finding would suggest that these proteins are not splice variants or degradation products of tensin3.

In order to accurately quantify the effects of tensin3 knockdown on the capacity of HFFs to assemble fibrillar FN it was necessary to validate the linearity between FN abundance and the density of bands corresponding to FN on a Western blot. Therefore, a 2-fold dilution series of known amounts of bovine FN (1000 ng to 8 ng) was subjected to SDS-PAGE and probed with an antibody directed against FN by

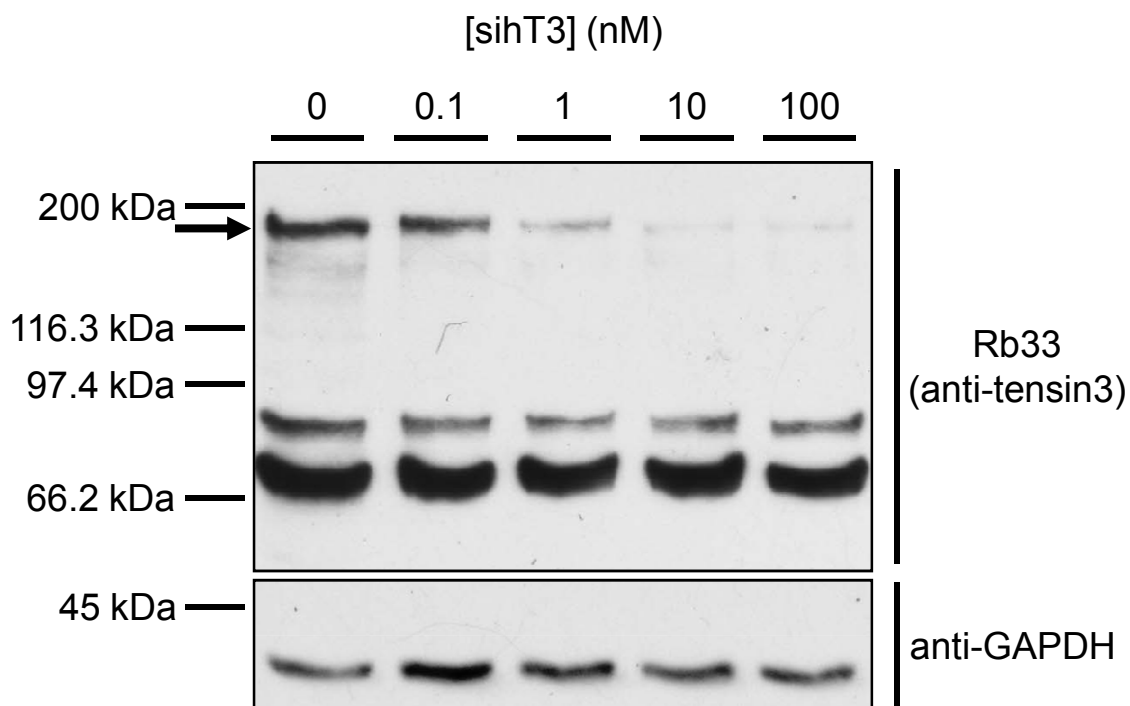


Figure 4.2: siRNA-mediated knockdown of tensin3 in HFFs. HFFs were transfected with an siRNA SMARTpool directed against human tensin3 (sihT3) at the denoted concentrations by lipofection. Proteins in cell lysates harvested 24 hours post-transfection were separated by SDS-PAGE (7.5% acrylamide) and probed with antibodies directed against tensin3 (Rb33) and GAPDH (loading control) by Western blotting. Note: Rb33 reacted with three proteins, the largest of which was of the expected molecular weight for tensin3 (arrow).

Western blotting (Figure 4.3A). The image presented in Figure 4.3A is a scan of a film for which exposure was non-saturating, and was therefore quantified by densitometry. The density of the 5 bands detected by the FN antibody, which correspond to 1000, 500, 250, 125 and 62.5 ng FN, were expressed relative to the density of the 62.5 ng band and plotted against FN input amount (Figure 4.3B). The line of this graph shows that band density is approximately directly proportional to FN abundance.

To study the role of human tensin3 in FN fibrillogenesis, HFFs were transfected with an siRNA SMARTpool directed against human tensin3 (siHT3), or a control non-targeting siRNA pool (siCON) at 10 nM concentration by lipofection. Twenty-four hours post-transfection the cells were trypsinised and replated for a further 24 hours. Tensin3 knockdown was confirmed by Western blotting as described above (Figure 4.4A), quantified by densitometry, normalised against the GAPDH loading control and expressed relative to the control siRNA condition. As observed previously, tensin3 protein expression was almost completely repressed by treatment with the tensin3 siRNA SMARTpool (Figure 4.4B). To examine the extent of FN fibrillogenesis upon tensin3 knockdown, replica plates were lysed in a deoxycholate-containing lysis buffer, which does not solubilise FN fibrils. Proteins in the DOC insoluble (DOCi) fraction were separated by SDS-PAGE (7.5% acrylamide) and probed with antibodies directed against FN and vimentin (loading control) by Western blotting (Figure 4.4A). The abundance of FN was quantified and this showed that tensin3 knockdown caused a small reduction in FN fibrillogenesis (Figure 4.4B). This experiment was performed 3 times and each experiment showed a reduction in FN fibrillogenesis, although the extent of this reduction was variable between experiments.

The effect of tensin3 knockdown on FN fibrillogenesis was confirmed by immunofluorescence microscopy. Control and tensin3 knockdown HFFs were fixed and stained with an antibody directed against FN, followed by the appropriate fluorescently-

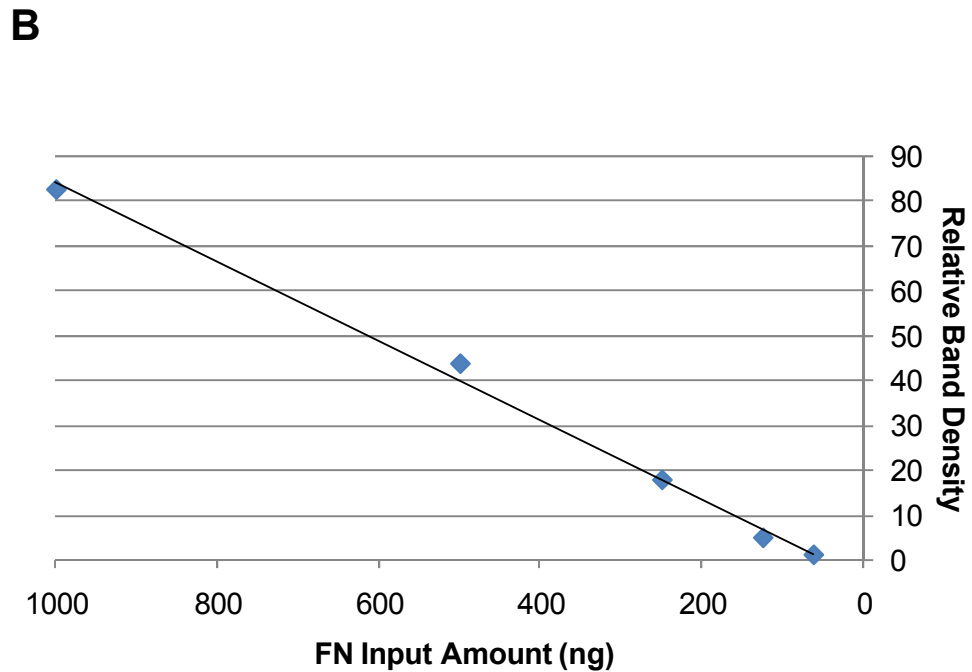
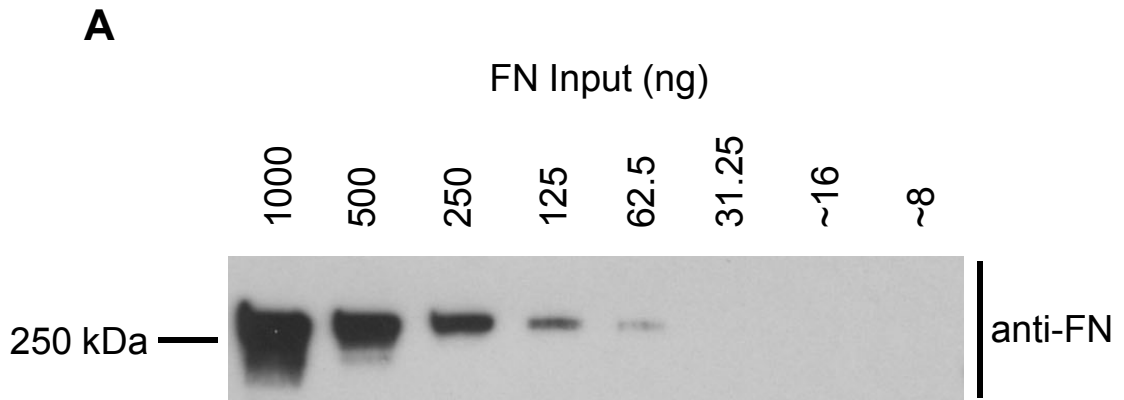


Figure 4.3: Linearity between FN abundance and band density. (A) A 2-fold dilution series of known amounts of purified bovine FN (1000 ng to ~8 ng) was subjected to SDS-PAGE (7.5% acrylamide) and probed with an antibody directed against FN by Western blotting. (B) The density of the 5 visible bands (1000 ng to 62.5 ng) was determined using ImageJ, expressed relative to the density of the 62.5 ng band, and plotted against FN input amount.

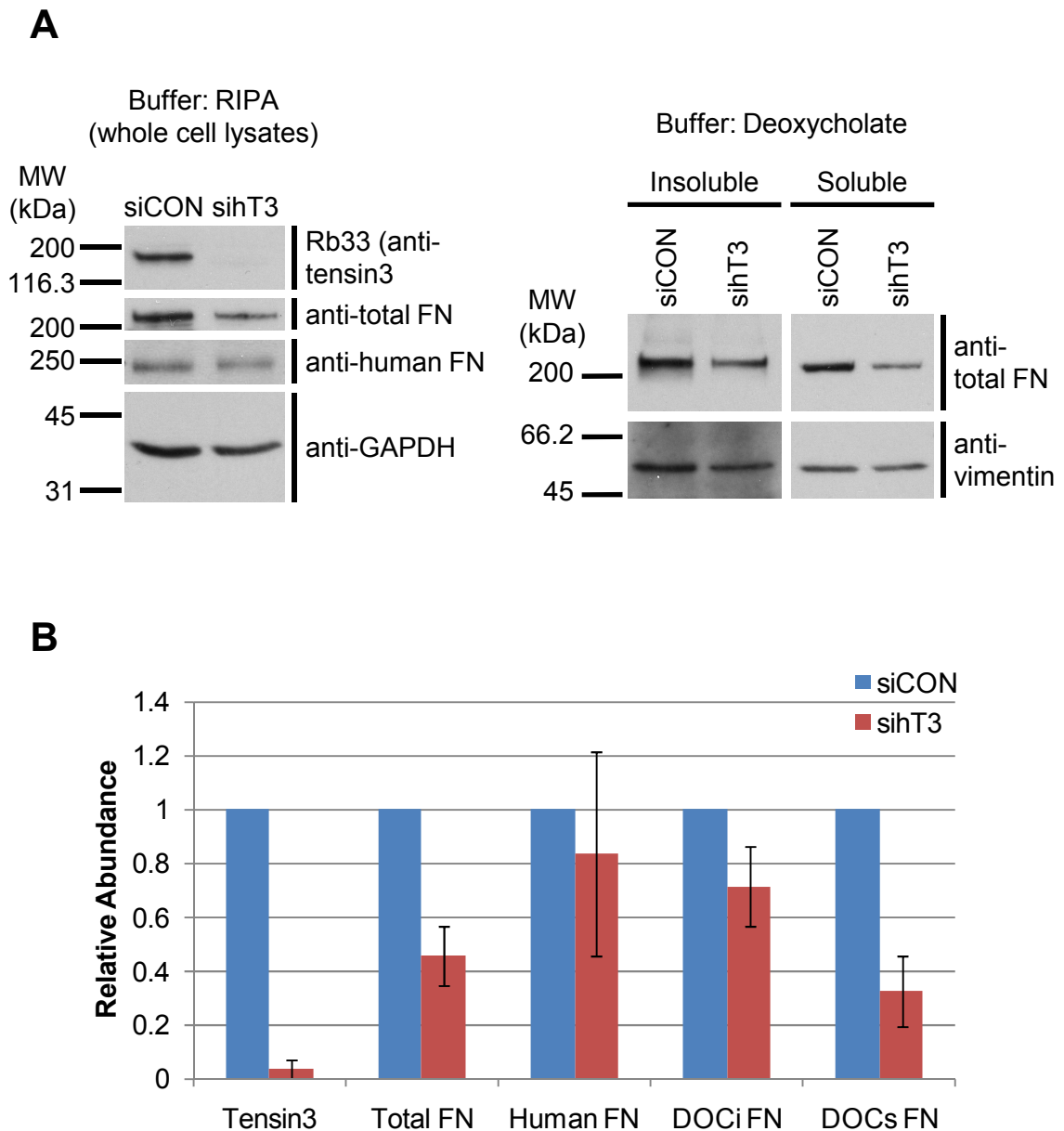


Figure 4.4: Quantitation of FN fibrillogenesis in tensin3 knockdown HFFs. HFFs were transfected with an siRNA SMARTpool directed against human tensin3 (sihT3) or a control non-targeting siRNA pool (siCON) at 10 nM concentration by lipofection. Twenty-four hours post-transfection the cells were trypsinised and replated for a further 24 hours to allow the assembly of new FN fibrils. (A) Cells were lysed in RIPA or deoxycholate (DOC)-containing lysis buffer and proteins in cell lysates were separated by SDS-PAGE (7.5% acrylamide) prior to Western blotting. RIPA (whole cell) lysates were probed with antibodies directed against tensin3 (Rb33), total FN, human FN and GAPDH (loading control), whereas DOC insoluble (DOCi) and DOC soluble (DOCs) fractions were probed with antibodies directed against total FN and vimentin (loading control). (B) Protein levels were quantified by densitometry using ImageJ, normalised against their respective loading controls and expressed relative to the control siRNA condition. Graph represents mean relative abundance (n=3). Error bars; standard deviation.

conjugated secondary antibody, and analysed by confocal microscopy (Figure 4.5A). FN fibril fluorescence was quantified, normalised against the density of the cells and expressed relative to the control siRNA condition. Again, the results showed that tensin3 knockdown caused a small reduction in FN fibrillogenesis (Figure 4.5B).

The DOC soluble (DOCs) fractions from each experiment were also analysed in an identical manner to the DOCi fractions. This fraction contains individual FN molecules and short chain FN oligomers, which are both soluble in the presence of deoxycholate. The abundance of DOCs FN was reduced by approximately 70% upon tensin3 knockdown (Figure 4.4A,B). Similarly, the abundance of FN in total cell lysate was reduced by approximately 60% (Figure 4.4A,B).

These results would suggest that tensin3 knockdown either i) reduces the expression of endogenous human FN by HFFs, and/or ii) reduces the association of secreted human FN or bovine serum FN with the surface of the cell. The FN antibody used in the Western blots described thus far detects both endogenously expressed human FN as well as bovine FN from the FCS-containing media. Therefore, to determine if tensin3 knockdown reduces FN expression a new FN antibody was obtained that was specific to human FN and did not cross-react with bovine FN. Re-probing total cell lysates with this antibody showed that tensin3 knockdown had no effect on human FN expression (Figure 4.4A,B), which would suggest that tensin3 knockdown instead compromises the ability of cells to recruit bovine FN from the media.

Collectively these data suggest that tensin3 knockdown partially reduces FN fibrillogenesis by reducing the capacity of HFFs to bind soluble FN at the cell surface.

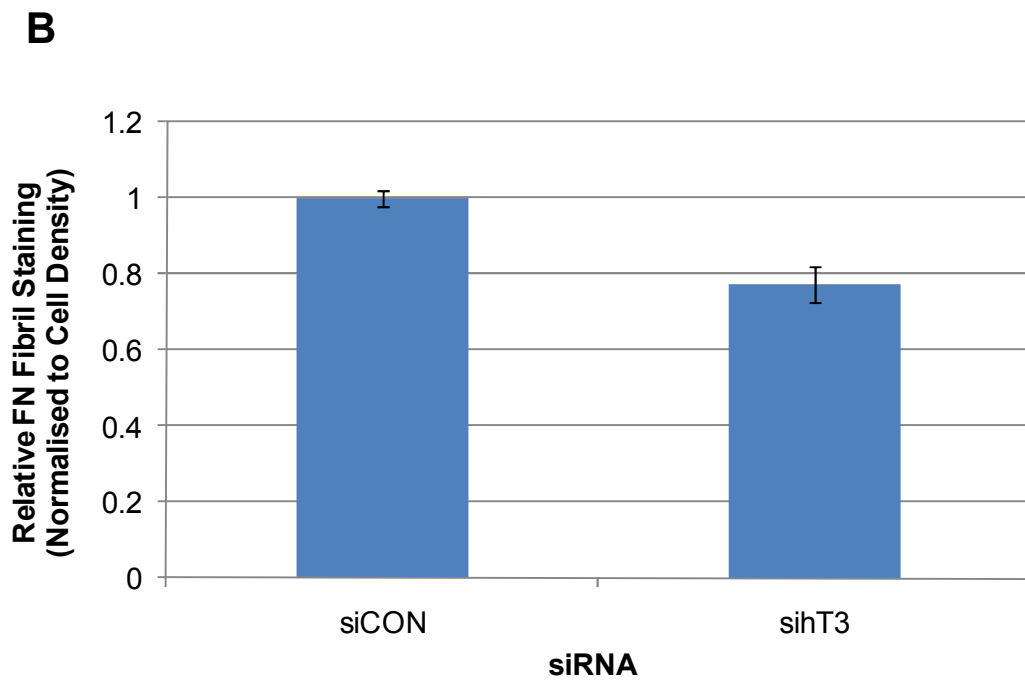
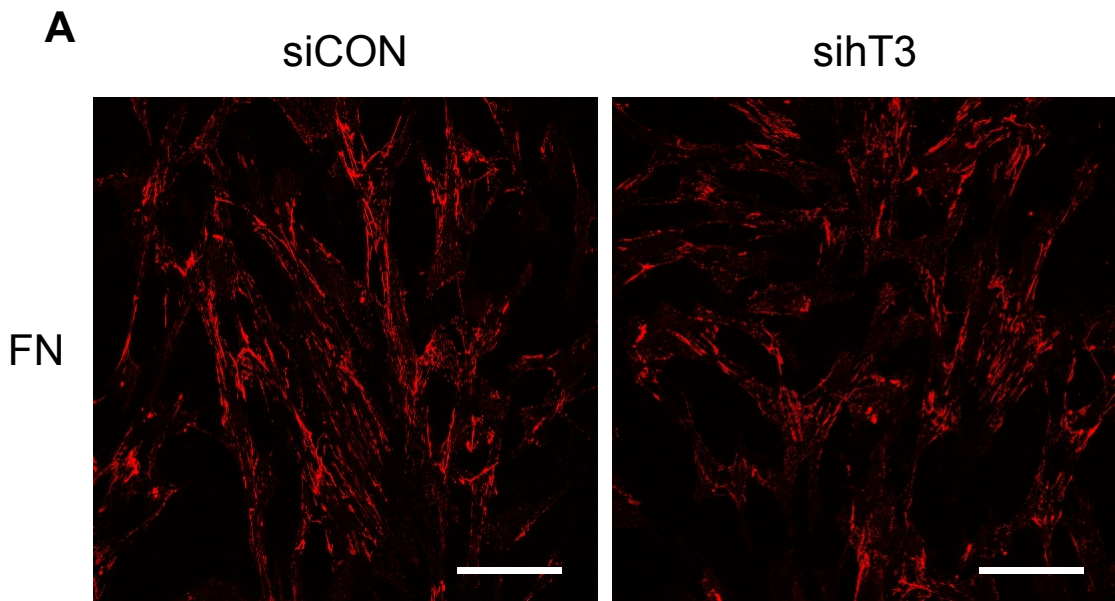


Figure 4.5: Immunofluorescent analysis of FN fibrillogenesis in tensin3 knockdown HFFs. HFFs were transfected with an siRNA SMARTpool directed against human tensin3 (sihT3) or a control non-targeting siRNA pool (siCON) at 10 nM concentration by lipofection. Twenty-four hours post-transfection the cells were trypsinised and replated onto glass coverslips for a further 24 hours to allow the assembly of new FN fibrils. (A) Cells were fixed, stained with an antibody directed against FN, followed by the appropriate fluorescently-conjugated secondary antibody, and imaged by confocal microscopy. Scale bar – 100 μ m. (B) FN fibril fluorescence was quantified using ImageJ and normalised against the confluence of the cells. Graph represents mean FN staining expressed relative to the control siRNA condition taken from a single experiment (n=3). Error bars; standard deviation.

4.2.2 The Role of Tensin in the 2D Cell Migration of the HEK293 Cell Line

Several studies have linked tensin to the process of cell migration although some of these studies have given conflicting results (Chen *et al.*, 2002; Hafizi *et al.*, 2005; Martuszevska *et al.*, 2009; Qian *et al.*, 2009). In an attempt to clarify and further characterise the role of tensin in cell migration, scratch-wound assays were initially undertaken in HFFs pre-treated with siRNAs directed against each tensin isoform, both individually and simultaneously. Surprisingly, preliminary experiments indicated that cells depleted of all three tensins displayed the same wound closure rate as control cells (data not shown). Many of the previous studies on the role of tensin in cell migration were performed by over-expressing tensins in HEK293 cells and performing Boyden chamber migration assays. Therefore, I sought to confirm the effect of tensin over-expression in this cell line using the scratch-wound assay.

HEK293 cells were transfected with expression constructs encoding GFP, GFP-tensin1, GFP-tensin2, or GFP-tensin3 by lipofection. Proteins in cell lysates harvested 24 hours post-transfection were separated by SDS-PAGE (7.5% acrylamide) and probed with an antibody directed against GFP by Western blotting (Figure 4.6A; start). All GFP constructs were expressed and gave rise to proteins of the expected molecular weight for GFP, GFP-tensin1, GFP-tensin2 and GFP-tensin3, respectively (Figure 4.6A; start). No other protein bands were detected by this antibody. Fluorescence microscopy revealed that the efficiency of transfection with all constructs was approximately 40% (Figure 4.6B). Twenty-four hours post-transfection confluent cell monolayers were scratched with a pipette tip and phase contrast and fluorescence images were taken at 0, 2, 6, 16, and 24 hour time points thereafter (Figure 4.6B; 0 hour [start] and 24 hour [end] time points only), before collecting lysates from each well to verify the expression of each fusion protein at the end of the scratch-wound assay by Western blotting (Figure 4.6A; end). Relative rate and extent of wound closure was

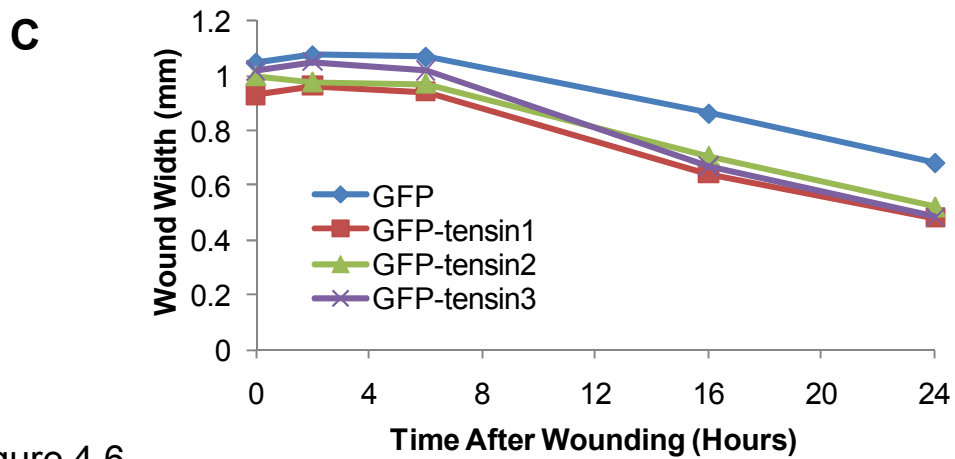
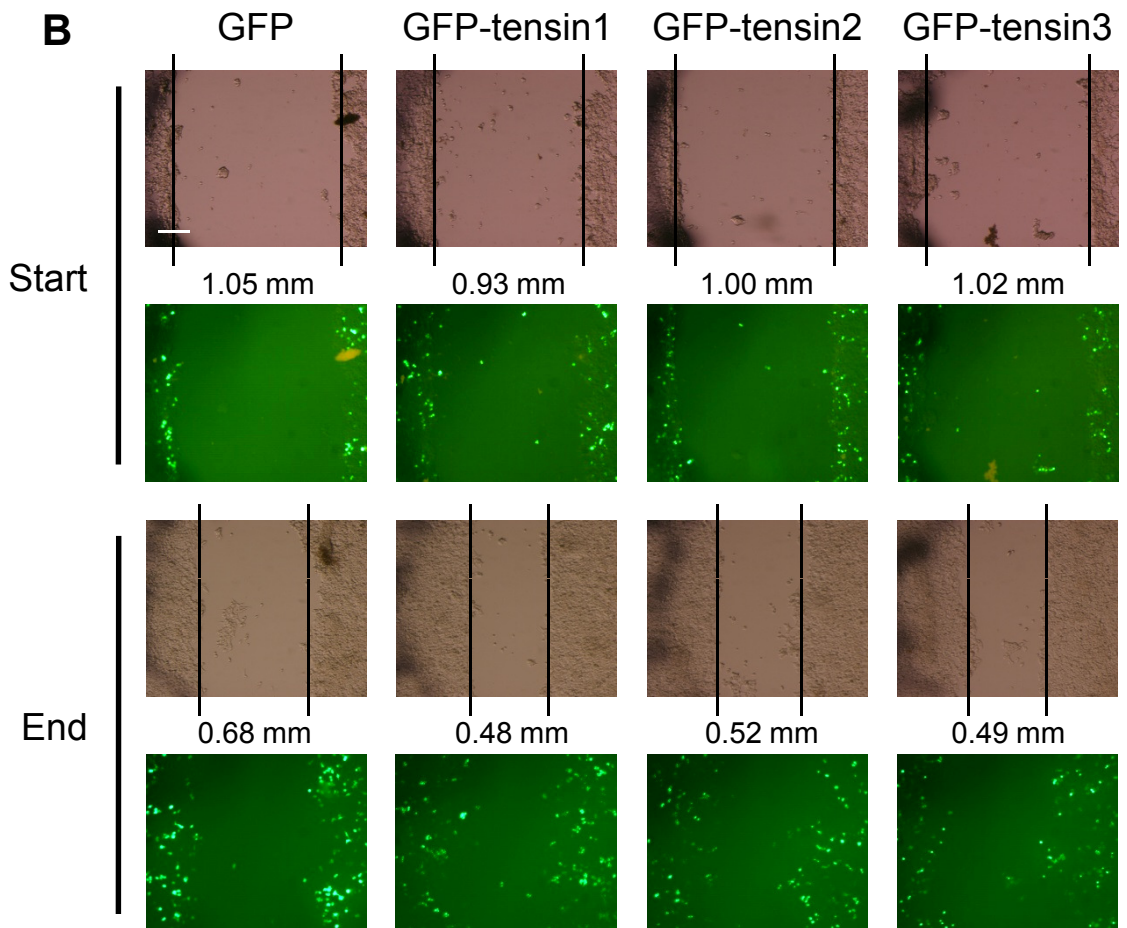
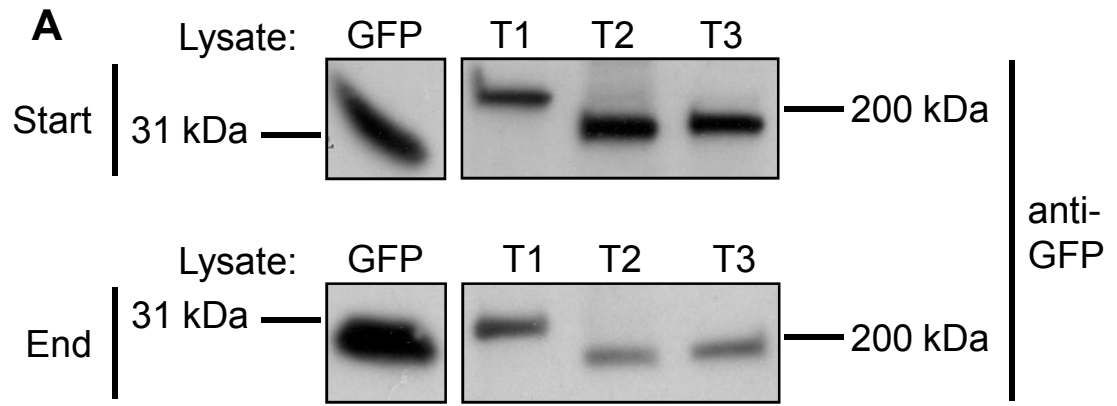


Figure 4.6

D

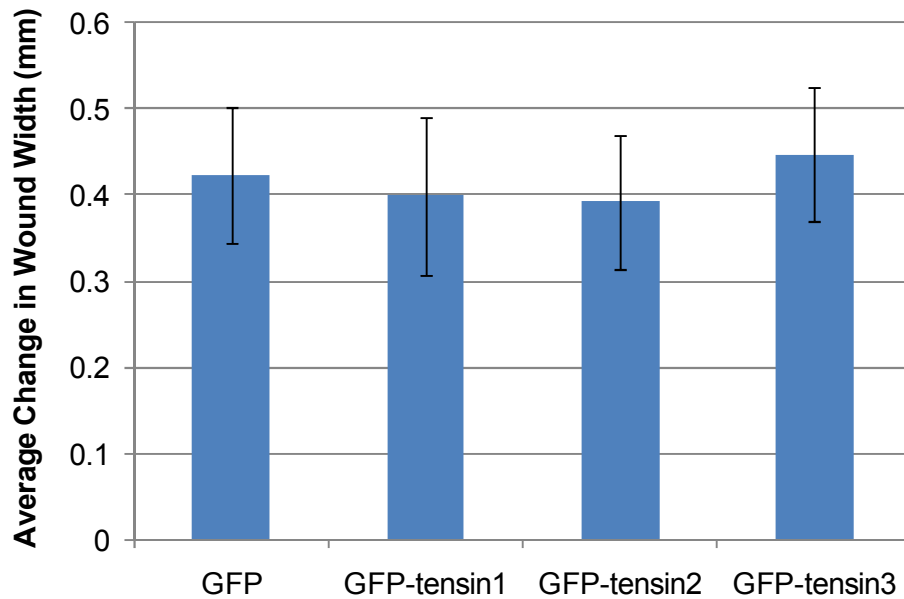


Figure 4.6: Scratch-wound assay on HEK293 cells over-expressing GFP-tensins. HEK293 cells were transfected with expression constructs encoding GFP, GFP-tensin1 (T1), GFP-tensin2 (T2), or GFP-tensin3 (T3) by lipofection. (A) Proteins in cell lysates harvested 24 (start) and 48 hours post-transfection (end) were separated by SDS-PAGE (7.5% acrylamide) and probed with an antibody directed against GFP by Western blotting. (B) Twenty-four hours post-transfection the confluent monolayer of transfected cells was scratched with a pipette tip. Wound closure was monitored by collecting phase contrast and fluorescent images of the wounds at 0, 2, 6, 16 and 24 hour time points. Shown are images at the start (0 hours after wounding) and end (24 hours after wounding) of the assay. Wound width is indicated. Scale bar - 200 μ m. (C) Graphical representation of wound closure. (D) Average change in wound width between 0 and 24 hour time points (n=3). Error bars; standard deviation. Experiment was performed 3 times, parts (A), (B) and (C) are representative examples taken from the same experiment.

compared using the gradients on a graph of wound width versus time (Figure 4.6C) and the average change in wound width (Figure 4.6D), respectively. No difference in wound closure was observed between GFP- (control) and GFP-tensin1-, GFP-tensin2- or GFP-tensin3-expressing cells using this 2D migration assay (Figure 4.6C,D).

One problem with this approach is the low transfection efficiencies obtained with the large GFP-tensin expression constructs. This could result in the untransfected cells masking any effect induced by over-expressing the various tensins. Therefore, an siRNA approach was also used to study the role of tensin in the migration of HEK293 cells. Before undertaking this study, it was necessary to establish which tensins are expressed by this cell line. Therefore, RNA was isolated from HEK293 cells using an RNAeasy miniprep kit. This RNA was treated with DNase I to remove any DNA contamination before reverse transcribing the mRNA into cDNA using oligo d(T) primers. This cDNA was then amplified in a qPCR assay with primer pairs specific to each of the tensin isoforms (Table 2.2 – Materials and Methods) in the presence of the SYBR Green dsDNA-specific fluorescent dye using a MiniOpticon qPCR machine. These three sets of primers give rise to amplicons of approximately equal size with similar amplification efficiencies of ~100% (Figure 3.7) and therefore information on the relative abundance of the tensin mRNAs can be estimated from the raw fluorescence data. Fluorescence intensity, which corresponds directly to the production of dsDNA products, was plotted against cycle number to give rise to an amplification plot for each tensin isoform (Figure 4.7). The threshold line on this graph signifies the point at which fluorescence intensity increased to above background levels and amplification was in the log-linear phase. The cycle at which a particular amplification plot crosses this threshold line is termed the threshold cycle (or C_T). Tensin2 and tensin3 amplification gave C_T values around 24 and tensin1 amplification gave a C_T value of approximately 31.5, which equates to a ~150-fold difference in abundance (Figure 4.7). These mRNA levels suggest an approximately equal level of tensin2 and tensin3 expression, and

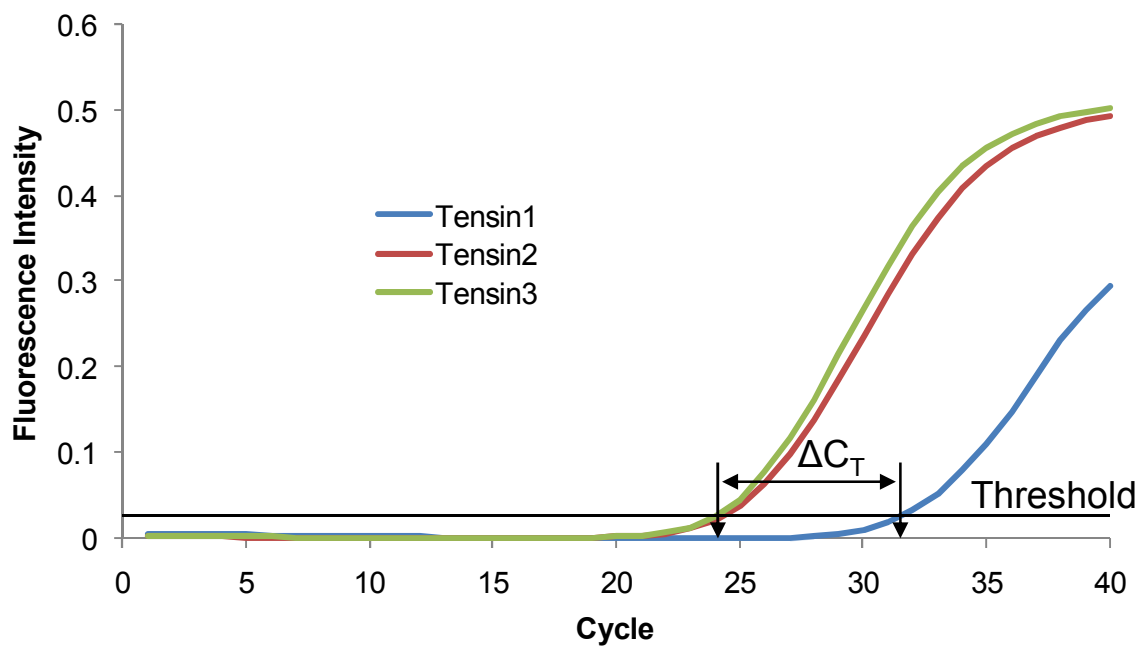


Figure 4.7: Detection of tensin mRNAs in HEK293 cells. RNA isolated from HEK293 cells was DNase I treated, reverse transcribed into cDNA using oligo d(T) primers, and amplified in a qPCR assay with tensin1, 2 and 3 primer pairs in the presence of the SYBR Green dsDNA-specific fluorescent dye. Shown are amplification plots of average fluorescence intensity vs. cycle number for each primer pair. Threshold cycles (C_T) for tensin2/3 and tensin1 amplifications are indicated with downward arrows. Note: Tensin2/3 amplification gave C_T values of around 24, whereas tensin1 amplification gave a C_T value of approximately 31.5. The C_T differential (ΔC_T) equates to an approximate 150-fold difference in expression i.e. tensin2 and tensin3 mRNAs are approximately 150-fold more abundant than tensin1 mRNA. Experiment was performed in quadruplicate.

very low tensin1 expression. As the tensin isoforms were measured on the same cDNA sample, no internal comparison control was required. This tensin expression profile agrees with the data on endogenous tensin protein levels obtained during the characterisation of the anti-tensin antibodies (Figures 3.2-3.5). Based on this knowledge and the reliability of the Rb33 anti-tensin3 antibody, tensin3 was selected as the initial candidate for siRNA-directed knockdown in this cell line.

Before performing the scratch-wound assay it was necessary to establish the minimal concentration of siRNA needed to sustain maximal knockdown of tensin3. HEK293 cells were transfected with an siRNA SMARTpool directed against human tensin3 (sihT3) at a range of concentrations (0-200nM) by lipofection. Cell lysates were harvested 24 and 48 hours post-transfection (the time frame of the scratch-wound assay). Proteins in these lysates were separated by SDS-PAGE (7.5% acrylamide) and probed with antibodies directed against tensin3 (Rb33) and GAPDH (loading control) by Western blotting (Figure 4.8A). The abundance of tensin3 protein decreased with increasing siRNA concentration up to 10 nM, which was the minimum concentration of siRNA required for maximal knockdown. Tensin3 abundance was quantified by densitometry, which revealed that this siRNA concentration was sufficient to sustain an 80% reduction in tensin3 protein levels between 24 and 48 hours (Figure 4.8B).

To examine the role of tensin3 in 2D cell migration, HEK293 cells were transfected with an siRNA SMARTpool directed against human tensin3 (sihT3) or a control non-targeting siRNA pool (siCON) at 10 nM concentration by lipofection. Proteins in cell lysate harvested 24 (start) and 48 hours post-transfection (end) were separated by SDS-PAGE (7.5% acrylamide) and probed with antibodies directed against tensin3 (Rb33) and pan-cytokeratin (loading control) by Western blotting (Figure 4.9A). Densitometry was used to confirm that tensin3 protein levels were reduced by more than 80% between these time points, which correspond to the start and end of the

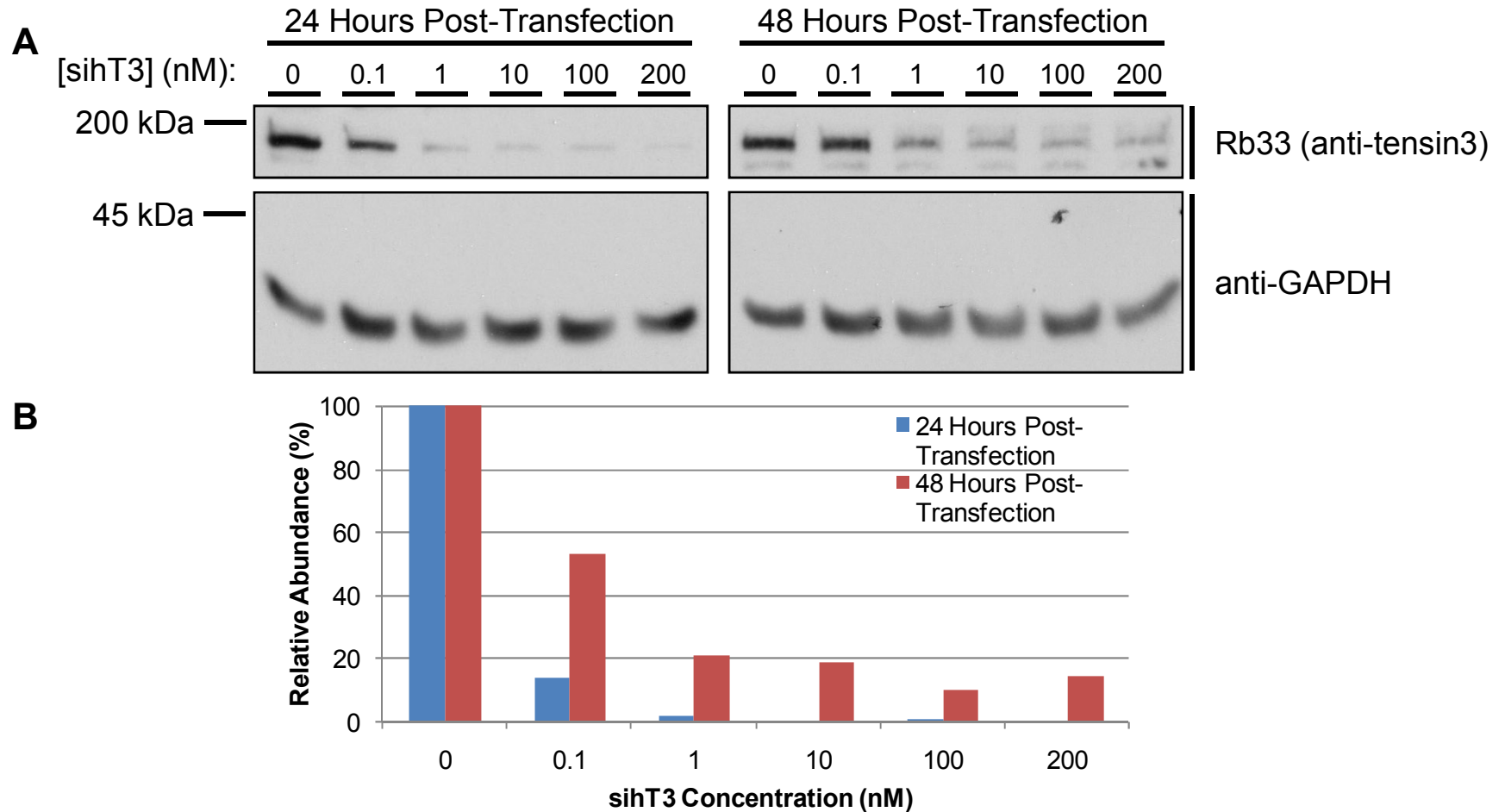


Figure 4.8: siRNA-mediated knockdown of tensin3 in HEK293 cells. HEK293 cells were transfected with an siRNA SMARTpool directed against human tensin3 (sihT3) at the denoted siRNA concentrations by lipofection. Cell lysates were harvested 24 and 48 hours post-transfection. (A) Proteins in these lysates were separated by SDS-PAGE (7.5% acrylamide) and probed with antibodies directed against tensin3 (Rb33) and GAPDH (loading control) by Western blotting. (B) Tensin3 protein levels at 24 and 48 hours post-transfection were quantified by densitometry using ImageJ, normalised against the GAPDH loading control and expressed relative to the 0 nM siRNA condition.

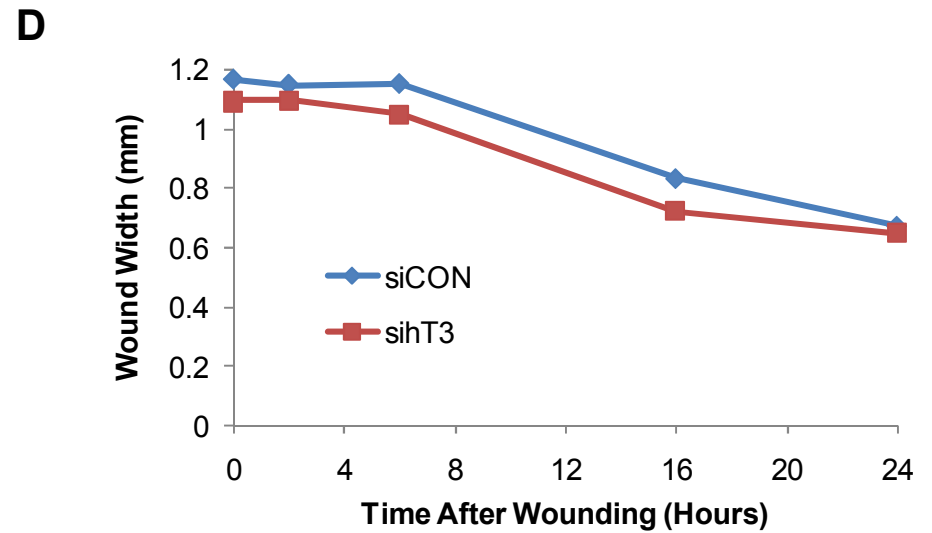
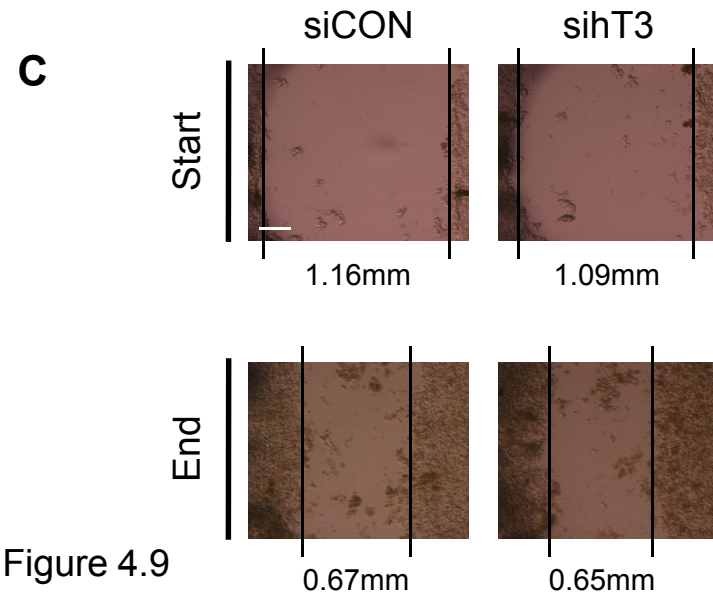
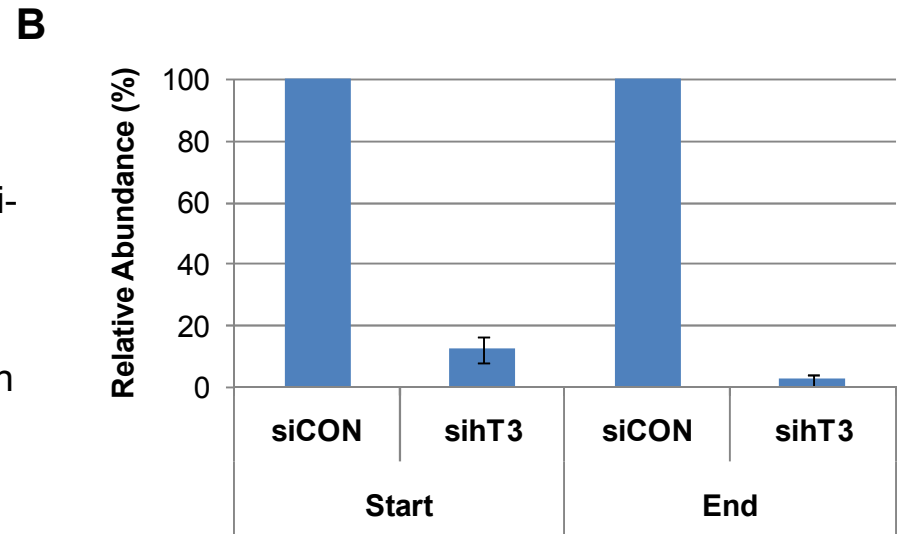
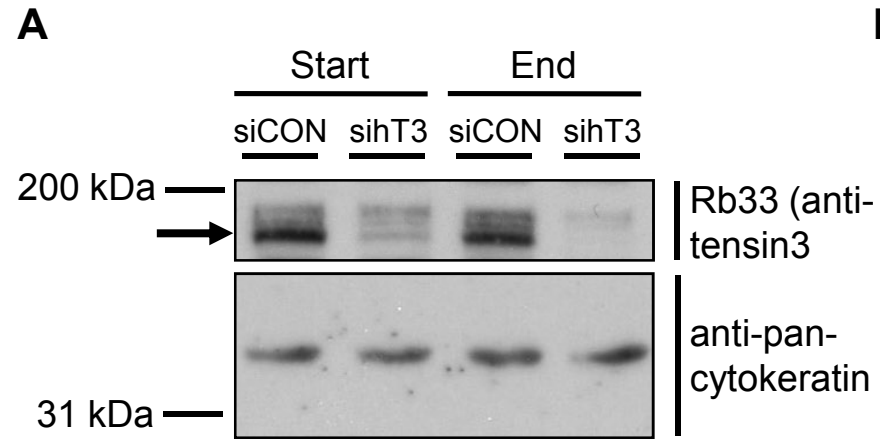


Figure 4.9

Figure 4.9: Scratch-wound assay on tensin3 knockdown HEK293 cells. HEK293 cells were transfected with an siRNA SMARTpool directed against human tensin3 (siHT3) or a control non-targeting siRNA pool (siCON) at 10nM concentration by lipofection. (A) Proteins in cell lysates harvested 24 (start) and 48 hours post-transfection (end) were separated by SDS-PAGE (7.5% acrylamide) and probed with antibodies directed against tensin3 (Rb33) and pan-cytokeratin (loading control) by Western blotting. Note: Tensin3 is indicated by arrow. (B) Tensin3 protein levels at 24 (start) and 48 hours post-transfection (end) were quantified by densitometry using ImageJ, normalised against the pan-cytokeratin loading control and expressed relative to the control siRNA condition. Shown are mean relative abundance (n=3). Error bars; standard deviation. (C) Twenty-four hours post-transfection the confluent monolayer of transfected cells was scratched with a pipette tip. Wound closure was monitored by collecting phase contrast images of the wounds at 0, 2, 6, 16 and 24 hour time points. Shown are images at the start (0 hours) and end (24 hours) of the assay. Wound width is indicated. Scale bar – 200 μ m. (D) Graphical representation of wound closure. Experiment was performed 3 times, parts (A), (C) and (D) are representative examples taken from the same experiment.

scratch-wound assay (Figure 4.9B). Twenty-four hours post-transfection the confluent cell monolayers were scratched with a pipette tip, and phase contrast images were taken at 0, 2, 6, 16, and 24 hour time points thereafter (Figure 4.9C; 0 hour [start] and 24 hour [end] time points only). Relative wound closure rates were compared using the gradients on a graph of wound width versus time (Figure 4.9D). The control and tensin3 knockdown cells showed very similar gradients throughout the experiment (Figure 4.9D). Hence, no difference in wound closure was observed between the control and tensin3 knockdown cells using this 2D migration assay. However, it is conceivable that the continued expression of tensin2 in these cells is able to compensate for the depletion of tensin3. Although previous studies would imply that tensin2 and 3 have opposing roles in cell migration in this cell line (Chen *et al.*, 2002; Martuszevska *et al.*, 2009).

4.2.3 The Role of Tensin in the 2D Cell Migration of the A2780 Human Ovarian Cancer Cell Line

Given the fact that several previous studies had reported a role for tensin in cell migration, the finding that tensin over-expression and knockdown had no effect on the 2D migration of HEK293 cells was surprising. Therefore, to validate this result, scratch-wound assays were also conducted using the A2780 human ovarian cancer cell line. This epithelial cancer cell line has been extensively characterised and is frequently used by others to study the migration of cells in 2D and 3D environments (Caswell *et al.*, 2007; Caswell *et al.*, 2008). All three tensins were simultaneously knocked down in this cell line to give the best possible chance of uncovering a requirement for tensin during 2D migration. Finally, both the speed and persistence of migration were determined by manually tracking individual cells, rather than just simply measuring wound width.

To establish which tensins are expressed by A2780 cells, RNA was harvested, DNase I treated, reverse transcribed into cDNA and amplified in a qPCR assay with primer pairs specific to each tensin isoform (Table 2.2 – Materials and Methods). Fluorescence intensity was plotted against cycle number to give rise to an amplification plot for each tensin isoform (Figure 4.10). Tensin3, tensin2 and tensin1 amplification gave C_T values of approximately 22, 24 and 26, respectively (Figure 4.10). This data shows that all three tensins are expressed by A2780 cells. The C_T differentials (ΔC_T) equate to approximately 4-fold differences in expression i.e. tensin3 mRNA is approximately 4-fold more abundant than tensin2, which is in turn approximately 4-fold more abundant than tensin1.

A2780 cells can be efficiently transfected with siRNAs by nucleofection. However, when using this method it is necessary to use a much higher concentration of siRNA in order to deliver an adequate amount of siRNA into the cell during the relatively short period in which the cell membrane is permeabilised. Typically, concentrations of 1 μ M are required for substantial levels of knockdown (Dr P Caswell – personal communication). Therefore, to check the efficiency of tensin knockdown, A2780 cells were transfected with siRNA SMARTpools directed against human tensin1 (sihT1), tensin2 (sihT2) or tensin3 (sihT3), or a control non-targeting siRNA pool (siCON) at 1 μ M concentration by nucleofection and incubated at 37°C for 48 hours before lysis to obtain RNA for analysis. cDNA synthesised from this RNA was amplified in a qPCR assay with primers for tensin1, 2, 3 and GAPDH (reference gene). qPCR data was analysed using the $\Delta\Delta C_T$ method to determine relative abundance. This revealed that an siRNA concentration of 1 μ M was sufficient to reduce tensin1, 2 and 3 mRNA levels by ~60, 80 and 90%, respectively (Figure 4.11). When used at 0.33 μ M concentration these siRNAs were substantially less effective at depleting tensin expression levels (data not shown).

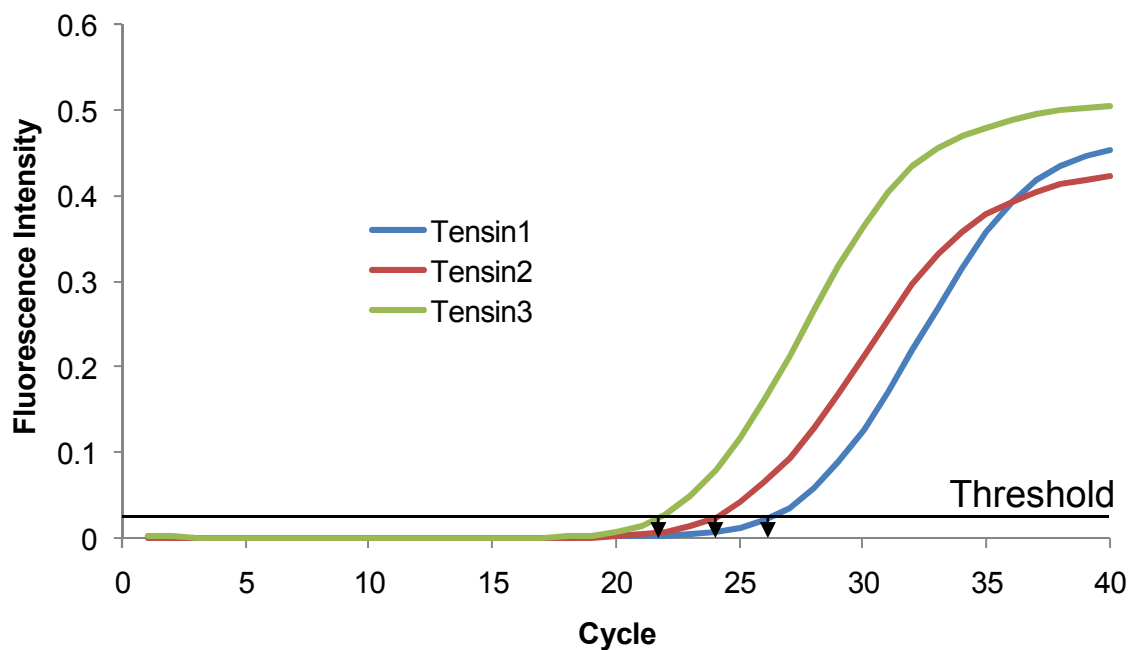


Figure 4.10: Detection of tensin mRNAs in A2780 cells. RNA isolated from A2780 cells was DNase I treated, reverse transcribed into cDNA using oligo d(T) primers, and amplified in a qPCR assay with tensin1, 2 and 3 primer pairs in the presence of the SYBR Green dsDNA-specific fluorescent dye. Shown are amplification plots of average fluorescence intensity vs. cycle number for each primer pair. Threshold cycles (C_T) for tensin3, 2 and 1 amplifications are indicated with downward arrows. Note: Tensin3, tensin2 and tensin1 amplification gave C_T values of approximately 22, 24 and 26, respectively. Experiment was performed in triplicate.

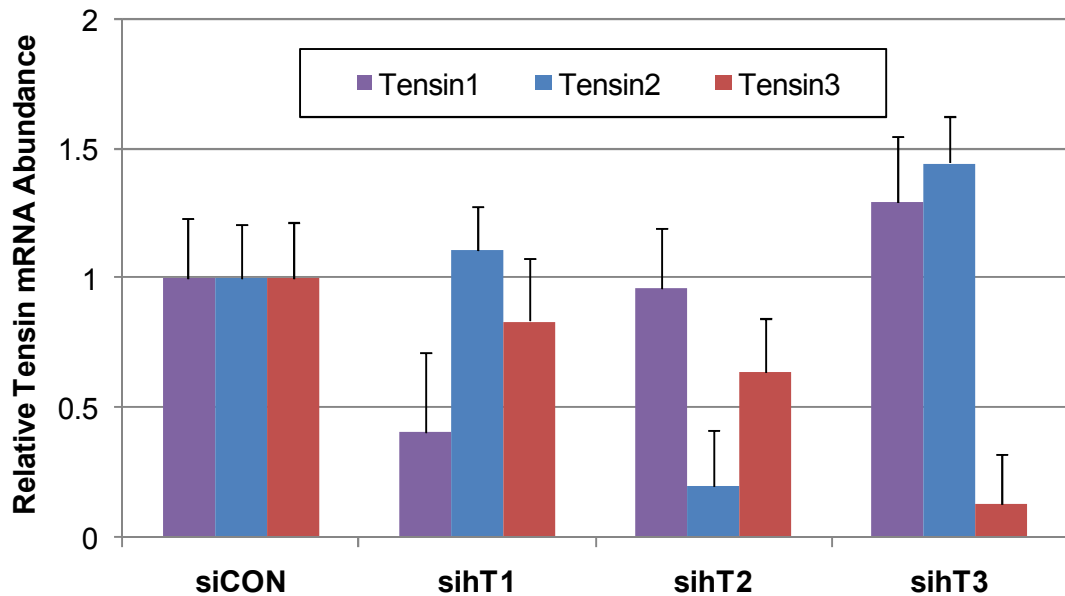


Figure 4.11. Validation of tensin knockdown in A2780 cells. A2780 cells were transfected with siRNA SMARTpools directed against human tensin1 (sihT1), tensin2 (sihT2) or tensin3 (sihT3), or a control non-targeting siRNA pool (siCON) at 1 μ M concentration by nucleofection. RNA isolated 48 hours post-transfection was DNase I treated, reverse transcribed into cDNA using oligo d(T) primers, and amplified in a qPCR assay with tensin1, 2, 3 and GAPDH primer pairs in the presence of the SYBR Green dsDNA-specific fluorescent dye. Relative abundance was determined using the $\Delta\Delta C_T$ method. Shown are the abundance of each tensin transcript normalised against GAPDH and expressed relative to the control siRNA condition. Experiment performed in triplicate. Error bars; standard error of the mean. Note: An siRNA concentration of 1 μ M reduced tensin1, 2 and 3 mRNA levels by ~60, 80 and 90%, respectively.

To increase the scope of the scratch-wound assay two variants of the A2780 cell line were used; one stably transfected with a haemagglutinin (HA)-tagged version of the small GTPase Rab25 (A2780-Rab25 or Rab25 cells) and the other with control pcDNA3 vector (A2780-DNA3 or DNA3 cells). Rab25 has been linked to tumour aggressiveness and metastasis (Cheng *et al.*, 2004; Wang *et al.*, 2004), and it has been reported that the over-expression of Rab25 in this cell line significantly increases invasive 3D migration, but has no effect on 2D migration (Caswell *et al.*, 2007). To test for the exogenous expression of Rab25, proteins in cell lysates harvested from each cell line were separated by SDS-PAGE (12% acrylamide) and probed with antibodies directed against HA and GAPDH (loading control) by Western blotting (Figure 4.12A). The anti-HA antibody recognised a 25 kDa protein in the lysate of Rab25 cells but not in the lysate of DNA3 cells. This protein was of the expected molecular weight for HA-Rab25 (25 kDa).

Finally, DNA3 and Rab25 cells were transfected with combined SMARTpools of siRNA directed against human tensin1, 2 and 3 (sihT123; 3 μ M, 1 μ M each), or a control non-targeting siRNA pool (siCON; 3 μ M) by nucleofection. Twenty-four hours post-transfection the cells were replated and allowed to form confluent monolayers. Cell monolayers were scratched with a pipette tip and subsequently imaged by time-lapse microscopy for 16 hours. Migration speed and persistence (net displacement/overall path length) were determined by manually tracking the position of the cell nucleus using ImageJ. The simultaneous depletion of all three tensin isoforms had no effect on the average speed or persistence of individual cell migration in either cell line (Figure 4.12B).

4.3 Discussion

4.3.1 *The Limited Requirement for Tensin3 during FN Fibrillogenesis in HFFs*

The idea that tensin plays a role in FN matrix assembly initially stemmed from the observation that fibrillar adhesions are rich in tensin and deficient in other actin-integrin linker proteins such as talin and α -actinin (Katz *et al.*, 2000a; Zamir *et al.*, 1999). Fibrillar adhesions are formed by the lateral translocation of FN-bound $\alpha_5\beta_1$ integrin along actin stress fibres from focal adhesions towards the centre of the cell, and this was shown to be coupled both spatially and temporally to the assembly of FN fibres on the extracellular surface of the cell (Pankov *et al.*, 2000; Zamir *et al.*, 2000; Ohashi *et al.*, 2002). Using various inhibitors and the HFF cell line, Pankov *et al.* (2000) established that these two processes are dependent on an intact actin cytoskeleton and actomyosin contraction. Moreover, both fibrillar adhesion formation and FN fibrillogenesis were inhibited by the over-expression of a GFP-chicken tensin fusion protein spanning residues 659-762, which contains the AH2 region (residues 674-706) described previously (Chuang *et al.*, 1995). The dominant negative effect of the chicken tensin AH2 region in a human fibroblast cell line such as HFFs was somewhat unexpected since this region is not conserved amongst the various human tensins. However, I have confirmed this result using GFP-tagged chicken AH2 region transfected into HFFs (Figure 4.1). Despite its name, this region of chicken tensin actually shares little amino acid sequence homology with actin and is predicted to be unstructured. It is becoming increasingly apparent that intrinsically disordered regions within proteins are often important for protein function (Dyson and Wright, 2005). Some unstructured regions may act as flexible linkers that permit flanking structured domains to bind to relatively distant sites on the same or different target proteins (Huang *et al.*, 2009; Kiss *et al.*, 2008). In other cases, they may actually form the binding site for various ligands and adopt an ordered structure upon protein-protein interaction (Mark

et al., 2005), a process known as binding-induced folding (Dyson and Wright, 2002). Furthermore, the same disordered region may be capable of adopting a number of different potential structures depending on the nature of the binding partner (Kriwacki *et al.*, 1996; Fisher *et al.*, 2001; Tompa, 2002). Given the dominant negative effect of the chicken tensin AH2, it seems likely that this region interacts with and sequesters a lipid or protein that is important in FN fibrillogenesis. However, the nature of the ligand has not been investigated, and identifying such partners for the AH2 region through a yeast two-hybrid screen or pull-down assay could provide new insights into the mechanisms underlying FN fibrillogenesis.

The role of tensin3 in FN fibrillogenesis was investigated over the other tensin isoforms due to its higher expression, and preferential localisation to fibrillar adhesions in HFFs. Thus, tensin3 was depleted by siRNA knockdown (Figure 4.2), and FN fibrillogenesis was assayed by taking advantage of the fact that fibril formation renders FN insoluble to extraction with 1% DOC (McKeown-Longo and Mosher, 1983). Using this approach, tensin3 knockdown was shown to result in a small albeit somewhat variable reduction in FN fibrillogenesis in HFFs (Figure 4.4A,B). Unfortunately, it was not possible to determine an error value for the control data in Figure 4.4B due to the nature of the quantification method. In short, densitometry was performed on a single photographic film from each experiment, which was deemed to be of non-saturated exposure (Figure 4.3). Exposure time varied between experiments, which ruled out the possibility of absolute quantification in the absence of a standard curve of purified FN. Therefore, to pool the data from several experiments it was necessary to calculate relative changes in band density, normalised to the control condition, which was designated the value of 1. This method of quantification, which is routinely used by others (Green *et al.*, 2009; Robinson *et al.*, 2004), makes it difficult to draw firm conclusions from small changes in fibrillar FN abundance. However, the FN data presented here was also confirmed by the immunofluorescent staining of control and tensin3 knockdown HFFs for FN

followed by confocal imaging and FN fibril quantitation (Figure 4.5). Although, the size of the data sets in these experiments were too small to perform statistical tests to confirm the significance of the observed difference.

Given the preferential localisation of tensin3 to fibrillar adhesions in HFFs (Figures 3.20, 3.21), it was somewhat surprising that tensin3 depletion had such a minor effect on FN fibrillogenesis in this cell line. The high level of homology across the human tensin family raises the possibility that the other tensin isoforms may compensate for depletion of tensin3. However, it has since been shown that the simultaneous knockdown of tensin1, 2 and 3 in HFFs has little to no effect on FN fibrillogenesis as determined using either the deoxycholate assay or immunofluorescence microscopy (Clark *et al.*, 2010). Moreover, HFFs depleted in all three large tensins have a normal actin cytoarchitecture and are capable of forming both focal and fibrillar adhesions to a similar extent to untreated HFFs (Dr K Clark – personal communication).

Possible explanations for the effect of tensin3 knockdown on FN fibrillogenesis include i) a reduction in the recruitment of soluble secreted or serum FN to focal adhesions, ii) a reduction in the exertion of mechanical force on FN localised to focal adhesions that is required to induce FN oligomerisation, and iii) a reduction in FN fibre integrity that could result in loss during lysate preparation. Interestingly, in my experiments, the abundance of DOC soluble FN was notably reduced upon tensin3 knockdown in HFFs (Figure 4.4A,B). Similarly, the abundance of FN in total cell lysates was also reduced (Figure 4.4A,B). The antibody used to detect FN cross-reacts with both human and bovine FN. Therefore, this result suggests that tensin3 knockdown reduces the synthesis of endogenous FN and/or the association of soluble secreted or serum FN with activated integrins at the cell surface. By probing the total cell lysates with an antibody specific to human FN it was found that tensin3 knockdown had no effect on the expression of endogenous FN by HFFs (Figure 4.4A,B), which would suggest that

tensin3 knockdown instead compromises the ability of cells to recruit bovine FN from the media. This possibility could be investigated by culturing control and tensin3-depleted HFFs in media supplemented with a small amount of biotinylated FN and assaying the capacity of the cells to remove this labelled FN from the media by Western blotting or ELISA.

Although the above data points towards a defect in recruitment of soluble FN from the media as the cause of the reduction in FN fibrillogenesis observed upon tensin3 knockdown, it does not rule out the possibility that tensin3 knockdown impairs the exertion of mechanical force on recruited soluble FN molecules. As the predominant actin-integrin linker molecule in fibrillar adhesions, tensin is presumably important for the transmission of tension generated by actomyosin contraction to FN-bound integrin molecules. Moreover, tensin may also be capable of indirectly influencing cytoskeletal tension through its interaction with several signalling proteins including FAK, PI3K, ILK, Src and DLC-1 (Zhu *et al.*, 1998b; Auger *et al.*, 1996; Qian *et al.*, 2009; Yam *et al.*, 2006a). In support of this hypothesis it has been shown that the genetic ablation of FAK disrupts actin cytoarchitecture, fibrillar adhesion formation and FN fibrillogenesis (Ilic *et al.*, 2004). Similarly, pharmacological inhibition of PI3K activity using Wortmannin was shown to impair FN fibrillogenesis, although it did not have any noticeable effect on the formation of actin stress fibres (Wierzbicka-Patynowski and Schwarzbauer, 2002). ILK co-localises with $\alpha_5\beta_1$ integrin in fibrillar adhesions, and siRNA-mediated depletion of ILK prevented fibrillar adhesion formation and FN fibrillogenesis (Vouret-Craviari *et al.*, 2004). ILK forms a trimeric complex with the proteins PINCH and parvin, known as the IPP-complex (Legate *et al.*, 2006), and disruption of this complex through deletion of the gene encoding ILK was shown to block the maturation of focal adhesions into fibrillar adhesions (Stanchi *et al.*, 2009). Similarly, Src-null cells are incapable of segregating tensin into fibrillar adhesions, which results in the formation of large phosphotyrosine-poor, tensin-rich focal

adhesions (Volberg *et al.*, 2001). Interestingly, in a recent study it was shown that the individual depletion of several Rho-family GTPases using siRNA had little effect on the magnitude of FN fibrillogenesis (Fernandez-Sauze *et al.*, 2009). This would suggest that several members of the Rho GTPase family are capable of supporting FN fibrillogenesis. A similar compensation mechanism may account for the relatively mild effect of triple tensin knockdown on FN fibrillogenesis. Indeed, it has recently been demonstrated that the actin-integrin linker talin is required for FN matrix assembly (Green *et al.*, 2009), which suggests that talin may be capable of functionally substituting for tensin in its absence. If so, one would expect talin to be recruited into fibrillar adhesions in tensin deficient cells, which could be investigated by immunocytochemistry.

In summary, it was found that the depletion of tensin3 protein substantially compromises the capacity of HFFs to bind soluble FN at the cell surface, which in turn reduces the availability of soluble FN to below the threshold level required for maximal FN fibrillogenesis. It is likely that tensin promotes the ligation of soluble FN by anchoring $\alpha_5\beta_1$ integrin to the actin cytoskeleton in adhesion structures, rather than directly activating the integrin, which is a role that is more commonly attributed to the actin-integrin linker protein talin (Banno and Ginsberg, 2008; Calderwood, 2004b; Critchley, 2004).

4.3.2 Tensin is Not Required for 2D Cell Migration

Multiple studies have identified members of the tensin family as regulators of 2D cell migration, with most studies identifying tensin1, 2 and cten as positive regulators and tensin3 as a negative regulator (Chen *et al.*, 2002; Yam *et al.*, 2006b; Katz *et al.*, 2007; Martuszewska *et al.*, 2009; Albasri *et al.*, 2009). However, the role of tensin3 has very recently been complicated by the finding that it can act as a positive regulator of cell

migration in a number of cancer cell lines (Qian *et al.*, 2009). Few of these studies have simultaneously compared the role of multiple tensins, and many of them have used the same assays but with slight variations in experimental design. Therefore, to directly compare the role of the three large human tensins in 2D cell migration, scratch-wound assays were conducted on a number of different cell lines using both over-expression and RNAi to modulate tensin levels.

Initially, scratch-wound assays were performed on HFFs that had been pre-treated with isoform-specific siRNAs directed against tensin1, 2 and 3 both individually and in combination. It was found that the individual and simultaneous knockdown of tensin1, 2 and 3 did not affect cell migration in this assay. This result was unexpected, particularly given the focal adhesion localisation of all three tensins in this cell line, described in Chapter 3. This result suggests that either i) tensin is not required for the 2D migration of HFFs, or ii) another actin-integrin linker molecule, such as talin, is capable of functionally substituting for tensin. In retrospect, HFFs were not the ideal choice of cell line to study the role of tensin during cell migration using the scratch-wound assay as they tend to migrate both rapidly and individually rather than collectively to close the wound, making quantitation difficult.

The HEK293 cell line has been used in many of the previous studies into the role of tensin in 2D cell migration (Chen *et al.*, 2002; Chen and Lo, 2003; Hafizi *et al.*, 2005; Martuszevska *et al.*, 2009). These cells have an epithelial-like morphology and migrate much more slowly than HFFs, and close scratch-wounds by migrating as a collective sheet of cells, making it easier to detect subtle effects on cell migration. Therefore, the effects of over-expressing tensin1, 2 and 3 on scratch-wound closure in this cell line was investigated. Surprisingly, HEK293 cells transiently transfected with GFP-tensin1, 2 or 3 expression constructs displayed the same capacity to close scratch-wounds as cells transfected with the empty GFP expression vector (Figure 4.6). Using the same

migration assay, others have reported that the stable expression of GFP-tensin2 and GFP-cten promote wound closure in HCC and colorectal cancer cell lines, respectively (Yam *et al.*, 2006b; Albasri *et al.*, 2009). Moreover, several studies have reported that the stable expression of GFP-tensin1, 2 or 3 alters the migration rate of HEK293 cells, albeit using the Boyden chamber assay (Chen *et al.*, 2002; Chen and Lo, 2003; Hafizi *et al.*, 2005; Martuszezwska *et al.*, 2009). In all of these published studies, cell lines stably transfected with GFP and GFP-tensin expression constructs were generated to ensure that all cells express the exogenous protein. In the experiment described in Figure 4.6, the cells were only transiently transfected with an efficiency of approximately 40%, which could result in the masking of any effect induced by over-expression of the various tensins by the untransfected cell population. However, both the GFP- and GFP-tensin-expressing cells appeared to be equally distributed in the confluent areas around the wounds before and after the assay. Hence, there was no obvious enrichment or deficiency in GFP-tensin-expressing cells at the leading edge following wound closure. This would suggest that tensin-expressing cells did not have a migratory advantage or disadvantage over the untransfected population. Nevertheless, it is hard to draw firm conclusions from the negative result of this experiment given the relatively low percentage of cells expressing the GFP-tensin constructs.

Given the above technical limitations of this study, an siRNA approach was instead used to investigate the role of tensin in the migration of HEK293 cells. qPCR analysis revealed that HEK293 cells express approximately equal amounts of tensin2 and tensin3 but little to no tensin1 mRNA (Figure 4.7). The finding that HEK293 cells do not express tensin1 was supported by the lack of endogenous tensin1 protein detection by the anti-tensin1 antibodies during their characterisation, described in Chapter 3. Others have also shown that this cell line does not express detectable levels of tensin1 protein by Western blotting of HEK293 cell lysate with a tensin1-specific antibody (Chen and Lo, 2003). Based on this knowledge and the reliability of the Rb33 anti-tensin3

antibody, tensin3 was selected as the initial candidate for siRNA-directed knockdown in this cell line.

After establishing that an siRNA concentration of 10 nM was sufficient to maintain maximal knockdown of tensin3 in HEK293 cells for up to 48 hours (Figure 4.8), the 2D migration of control and tensin3-depleted cells was compared using the scratch-wound assay. Surprisingly, HEK293 cells depleted of tensin3 protein displayed the same wound closure rate as cells pre-treated with a control non-targeting siRNA (Figure 4.9). This result would suggest that tensin3 is not required for the 2D migration of HEK293 cells. However, other actin-integrin linker proteins, such as tensin2 and talin, may be able to functionally compensate for the absence of tensin3, although previous studies would suggest that tensin2 and 3 have opposing roles in cell migration in this cell line (Chen *et al.*, 2002; Martuszevska *et al.*, 2009). Nonetheless, this possibility could be investigated by comparing the expression levels and localisation of these alternative actin-integrin linkers in control and tensin3 knockdown cells following monolayer wounding, or by analysing scratch-wound closure in cells simultaneously depleted in these molecules and tensin3.

Since this work was conducted two other groups have reported that the siRNA-mediated knockdown of tensin3 promotes cell migration in the MCF10A normal mammary epithelial cell line and the WM793 human melanoma cell line, respectively, albeit using the Boyden chamber assay (Katz *et al.*, 2007; Martuszevska *et al.*, 2009). Like HEK293 cells, MCF10A and WM793 cells express little to no tensin1 (Katz *et al.*, 2007; Martuszevska *et al.*, 2009). However, in contrast to HEK293 cells, both MCF10A and WM793 cells express significantly more tensin3 than tensin2 (Katz *et al.*, 2007; Martuszevska *et al.*, 2009), which could explain why tensin3 knockdown was sufficient to cause a phenotypic effect in these cell lines but not in HEK293 cells that express tensin2 and tensin3 to a similar extent (Figure 4.7). In contrast to the previously

published data, it was very recently reported that the siRNA-directed depletion of tensin3 impaired the migration of several cancer cell lines using a combination of Boyden chamber and scratch-wound assays (Qian *et al.*, 2009). Hence, the role of tensin3 appears to be very much dependent on the cell type under investigation, which could also explain the lack of phenotype observed upon tensin3 depletion in the current study.

As described above, several studies have reported that modulating the expression of the various tensin isoforms has a phenotypic effect on cell migration in a number of different cell lines. As I observed no such effect in the HEK293 cell line using the scratch-wound assay, I sought to investigate the effect of tensin knockdown on the 2D migration of another cell line. The A2780 human ovarian cancer cell line was chosen because it has been used extensively by others to study cell migration in both 2D and 3D environments (Caswell *et al.*, 2007; Caswell *et al.*, 2008). qPCR analysis revealed that A2780 cells express all three tensin isoforms, with tensin3 the most abundant and tensin1 the least abundant (Figure 4.10), and the expression of each tensin isoform could be substantially reduced by pre-treating the cells with tensin siRNA SMARTpools (Figure 4.11). In the above experiments, wound closure was monitored by manually taking relatively low resolution images of the wound at various time points over a 24 hour period, followed by measurement of wound width. This method of analysis can have its disadvantages. For instance, if treatment increases the speed of migration but also concomitantly decreases the persistence of migration, then the rate of wound closure may remain unchanged. The reverse situation, in which speed decreases whilst persistence increases, could also be missed by measuring only wound closure. Therefore, I decided that for the A2780 cell scratch-wound assays, wound closure would be monitored by automated time-lapse microscopy at higher resolution, thereby enabling the manual tracking of individual cells and the calculation of average speed and persistence of migration. At the time, very little was known about the role of tensin3

during cell migration and given the highly conserved nature of the tensin N- and C-termini, which contain binding modules for many migration-related molecules, it seemed likely that all three large tensins would play similar roles in cell migration. Therefore, all three tensins were simultaneously knocked down to give the best possible chance of uncovering a requirement for tensin during 2D migration.

Two variants of the A2780 cell line were used in this experiment; one stably transfected with a HA-tagged version of the small GTPase Rab25 (A2780-Rab25 or Rab25 cells) and the other with the control pcDNA3 vector (A2780-DNA3 or DNA3 cells) (Figure 4.12A). It has previously been demonstrated that over-expression of Rab25, which has been linked to tumour aggressiveness and metastasis (Cheng *et al.*, 2004; Wang *et al.*, 2004), in this cell line significantly increases invasive 3D migration, but has no effect on 2D migration (Caswell *et al.*, 2007). However, it was found that the simultaneous depletion of all three large tensin isoforms had no effect on the average speed or persistence of individual cell migration in these cells in the scratch-wound assay (Figure 4.12B). It is difficult to explain this result. However, if tensin3 inhibits migration in this cancer cell line, whilst tensin1 and 2 act to promote migration, it is conceivable that simultaneous knockdown of all three tensins could have no phenotypic effect, especially given the fact that tensin3 expression is higher than tensin1 and 2. Unfortunately, the individual contributions of tensin1, 2 and 3 were not investigated in this study. However, data presented in the following chapter, albeit in a 3D environment, supports the idea that all three of the large tensins play a similar role during cell migration in this cell line.

**Chapter 5 The Role of Tensin in
Invasive Cell Migration in 3-
Dimensional (3D)
Microenvironments**

5.1 Introduction

5.1.1 Tensin and 3D Migration

The data presented in the previous chapter suggests that tensin is dispensable for the migration of cells in 2D culture. However, there are few situations *in vivo* where migrating cells interact with rigid 2D substrates. Therefore, the role of tensin during migration within 3D microenvironments was investigated since this more closely resembles the situation encountered by cells *in vivo*.

Three studies have described roles for tensin2, tensin3 and cten during invasive 3D migration in various cell lines using modified versions of the Boyden chamber assay (Yam *et al.*, 2006b; Martuszezwska *et al.*, 2009; Albasri *et al.*, 2009). In these studies, the migration of cells stably transfected with the various tensins through Matrigel (a tumour basement membrane extract) was investigated. Yam *et al.* (2006) demonstrated that BEL7402 HCC cells expressing GFP-tensin2 migrated faster through Matrigel-coated transwell inserts than cells transfected with the empty GFP expression vector. Similarly, Albasri *et al.* (2009) showed that the expression of GFP-cten in two colorectal cancer cell lines (HCT116 and SW480) promoted migration through relatively thick plugs of Matrigel. Conversely, Martuszezwska *et al.* (2009) showed that HEK293 cells expressing tensin3, or a mutant of tensin3 containing a mutation in the putative active site of the PTEN phosphatase domain, migrated significantly more slowly through Matrigel than vector-transfected control cells. Collectively, the findings of these studies suggest that tensin2 and cten promote invasive 3D migration, whereas tensin3 plays an inhibitory role, which is independent of its putative phosphatase activity. However, in a very recent study it was suggested that tensin3 promotes 3D invasive migration *in vivo* (Qian *et al.*, 2009). Qian and co-workers showed that siRNA-mediated depletion of tensin3 reduced the capacity of two

breast cancer cell lines (Met-1 and PyMT) to form lung metastases in mice following tail vein inoculation (Qian *et al.*, 2009). Hence, the role of tensin3 during migration within 3D microenvironments is at present unclear.

Each of the above-mentioned *in vitro* studies were performed on a different cell line using slightly different assays, which makes it difficult to directly compare the role of the different tensin isoforms. In the present study, the role of the three large tensin isoforms during 3D migration was investigated using siRNA-mediated knockdown, thereby enabling direct comparison of the function of tensin1, 2 and 3. The selected cellular system was the ovarian cancer cell line A2780 since its migration in 3D matrices has already been extensively characterised (Caswell *et al.*, 2007; Caswell *et al.*, 2008). The small GTPase Rab25, which is involved in membrane trafficking, is over-expressed in some cases of ovarian cancer (Cheng *et al.*, 2004), and therefore A2780 cells over-expressing Rab25 were also used in this study. Finally, the requirement for tensin during invasive migration was investigated in two different 3D microenvironments in an attempt to consolidate the findings.

5.2 Results

5.2.1 Tensin is Required for the 3D Invasive Migration of A2780 Cells

It has previously been shown that Rab25 promotes invasive migration in A2780 cells through an integrin recycling mechanism that is dependent on the ability of Rab25 to interact with β 1 integrin (Caswell *et al.*, 2007). To confirm these findings, an inverted invasion assay (Figure 2.1 – Materials and Methods) was used to compare the invasive migration of A2780 cells stably expressing a Rab25 cDNA cloned into the plasmid pcDNA3 (Rab25 cells) with A2780 cells stably transfected with the empty plasmid (DNA3 cells) (Figure 5.1). Untransfected DNA3 and Rab25 cells were plated onto the

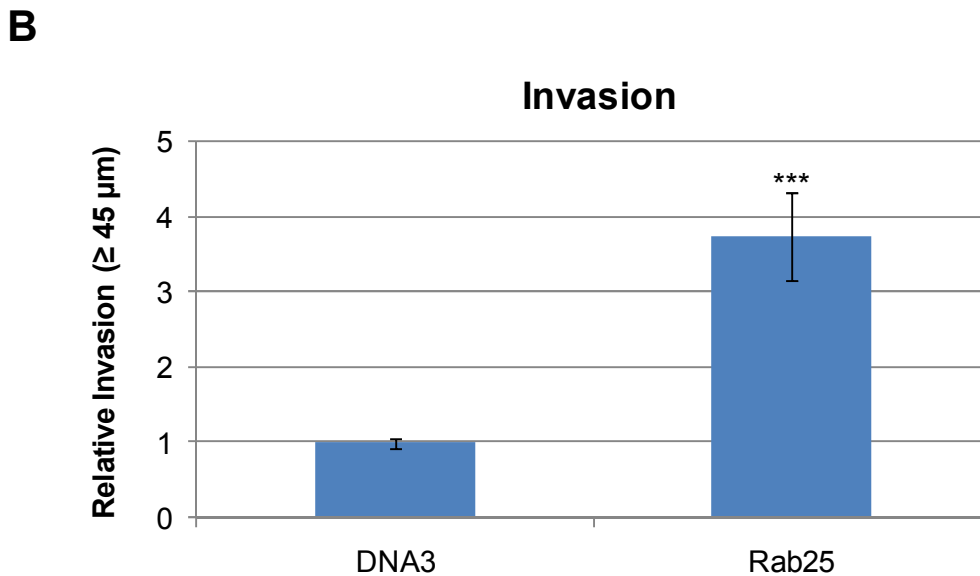
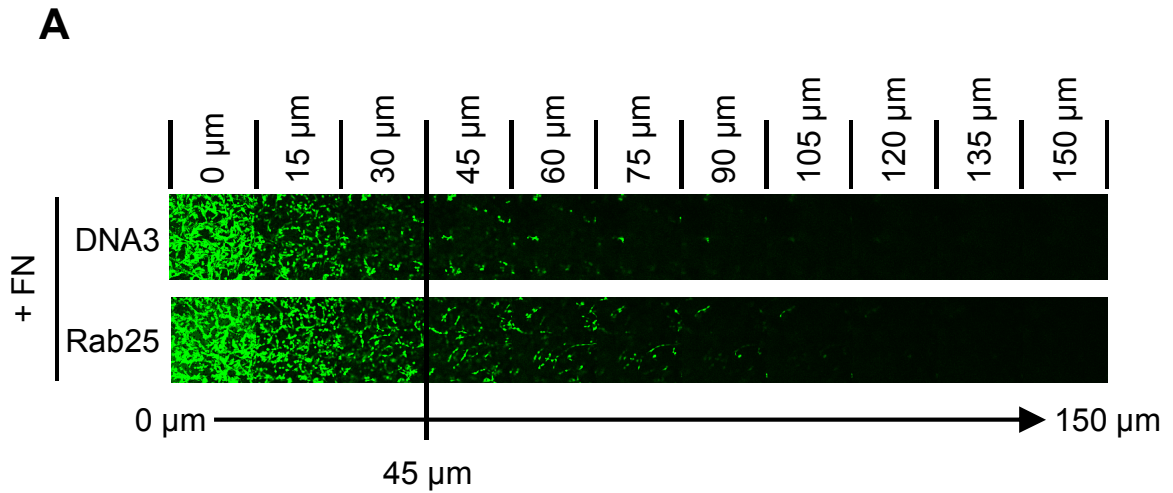


Figure 5.1. Invasive migration of DNA3 and Rab25 cells through 3D matrix. An inverted invasion assay was used to compare the migration of DNA3 and Rab25 cells. Cells were allowed to invade into Matrigel plugs (+25 $\mu\text{g}/\text{ml}$ FN) for 48 hours towards a gradient of serum (+30 ng/ml EGF). (A) Invading cells were stained with Calcein-AM and visualised by confocal microscopy. Serial optical sections were captured at 15 μm intervals and are presented as a sequence from left to right. (B) Invasion was quantified by measuring the fluorescence intensity of cells penetrating to 45 μm and beyond; this intensity was calculated as a percentage of the total fluorescence intensity of all cells within the plug. Graph represents mean invasion expressed relative to the invasion of DNA3 cells. Error bars; standard error of the mean. Experiment performed 3 times, n=18. ***: $P < 0.001$, Student's t-test.

undersides of inverted transwell inserts containing pre-set plugs of Matrigel supplemented with 25 µg/ml FN (+FN). Transwells were then inverted into serum-free media before applying complete media supplemented with 30 ng/ml EGF into the transwells on top of the plugs, thereby establishing a chemotactic gradient of serum and EGF towards which the cells would migrate. Cells were allowed 48 hours to migrate through the porous filter of the transwell inserts and up into the Matrigel. Invading cells were stained with Calcein-AM and visualised by confocal microscopy. Figure 5.1A shows serial optical sections captured at 15 µm intervals from the bottom of the plug upwards, and presented as a sequence from left to right. It is clear from these representative montages that considerably more Rab25 than DNA3 cells were capable of migrating to or beyond the arbitrary cut-off of 45 µm. Invasion was quantified by measuring the fluorescence intensity of cells penetrating to 45 µm and beyond; this intensity was calculated as a percentage of the total fluorescence intensity of all cells within the plug and expressed relative to the invasion of DNA3 cells. Quantitative analysis showed that Rab25 cells were 3.7-fold more invasive than DNA3 cells (Figure 5.1B).

To investigate the possible role of each of the three large tensin isoforms in invasive migration, DNA3 cells were transfected by nucleofection with siRNA SMARTpools directed against human tensin1 (sihT1), tensin2 (sihT2) and tensin3 (sihT3), both individually (1 µM) and in combination (sihT123; 3 µM, i.e. 1 µM for each SMARTpool), or with a control siRNA pool (siCON; 1 µM or 3 µM). The validation of tensin knockdown was presented in the previous chapter (Figure 4.11). Cells were allowed to invade into Matrigel plugs (+FN) towards a gradient of serum (+EGF) for 48 hours prior to analysis as described above. The individual knockdown of tensin1, 2 and 3 reduced invasive migration relative to the control cells by 35, 39 and 37%, respectively (Figure 5.2). The simultaneous knockdown of all three tensins reduced invasive migration by 57% relative to the control cells treated with the non-targeting siRNA (Figure 5.2).

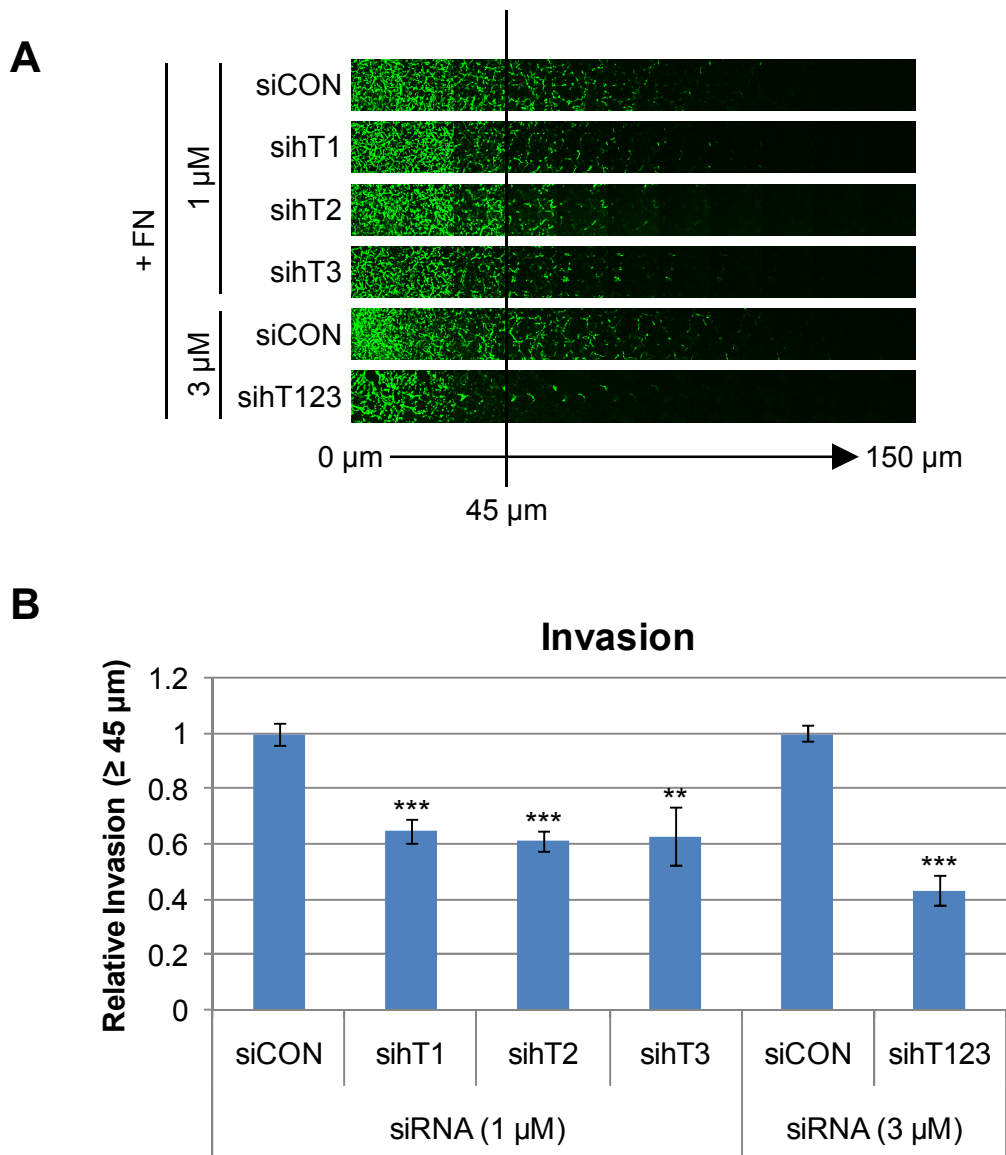


Figure 5.2. The effect of tensin knockdown on the invasive migration of DNA3 cells through 3D matrix. An inverted invasion assay was used to investigate the effect of tensin knockdown on the migration of DNA3 cells. DNA3 cells were transfected by nucleofection with siRNA SMARTpools directed against human tensin1 (sihT1), tensin2 (sihT2) and tensin3 (sihT3), both individually (1 μ M) and combined (sihT123; 3 μ M, 1 μ M of each SMARTpool), or with a control non-targeting siRNA pool (siCON; 1 μ M or 3 μ M). Cells were allowed to invade into Matrigel plugs (+25 μ g/ml FN) for 48 hours towards a gradient of serum (+30 ng/ml EGF). (A) Invading cells were stained with Calcein-AM and visualised by confocal microscopy. Serial optical sections were captured at 15 μ m intervals and are presented as a sequence from left to right. (B) Invasion was quantified by measuring the fluorescence intensity of cells penetrating to 45 μ m and beyond; this intensity was calculated as a percentage of the total fluorescence intensity of all cells within the plug. Graph represents mean invasion expressed relative to the control siRNA condition. Error bars; standard error of the mean. Experiment performed 3 times, n=18. **: P < 0.01, ***: P < 0.001, Student's t-test.

The requirement for tensin1, 2 and 3 in the migration of the highly invasive Rab25 cells was similarly investigated. The individual knockdown of tensin1, 2 and 3 reduced invasive migration by 43, 41 and 47%, respectively (Figure 5.3). The simultaneous knockdown of all three tensins reduced invasive migration by 56% (Figure 5.3). The similarity of the DNA3 and Rab25 data suggest that tensin is not exclusively required for Rab25-driven invasion, but is instead part of the basal cellular machinery necessary for the invasive migration of A2780 cells. However, Rab25 cells are approximately 4-fold more invasive than DNA3 cells and so the magnitude of the effect of tensin knockdown on absolute invasion is more substantial in Rab25 cells than in DNA3 cells.

To characterise the mechanism of tensin-dependent invasion, the effect of triple tensin knockdown on the capacity of Rab25 cells to invade into Matrigel plugs without FN was also assessed. Interestingly, the simultaneous knockdown of tensin1, 2 and 3 did not have as severe an inhibitory effect in the absence of FN, and invasive migration was reduced by only 29% relative to the control cells (Figure 5.3). This suggests that tensin has a significant role in FN-dependent invasive migration.

The $\alpha_5\beta_1$ integrin heterodimer is the predominant cellular receptor for FN. Therefore, the requirement for β_1 integrin in the migration of control and triple tensin knockdown Rab25 cells was determined. Invasion assays were conducted in the presence or absence of inhibitory antibodies (1 $\mu\text{g/ml}$) directed against β_1 integrin (mAb13) or $\alpha_v\beta_5$ integrin (P1F6) as negative a control (Figure 5.4). As expected, the anti- $\alpha_v\beta_5$ integrin antibody had no significant effect on the invasive migration of control or triple tensin knockdown Rab25 cells. In contrast, the anti- β_1 integrin antibody markedly reduced the migration of control and triple tensin knockdown Rab25 cells to a similar extent. This result suggests that Rab25 cells are highly dependent on the β_1 integrin for invasive migration.

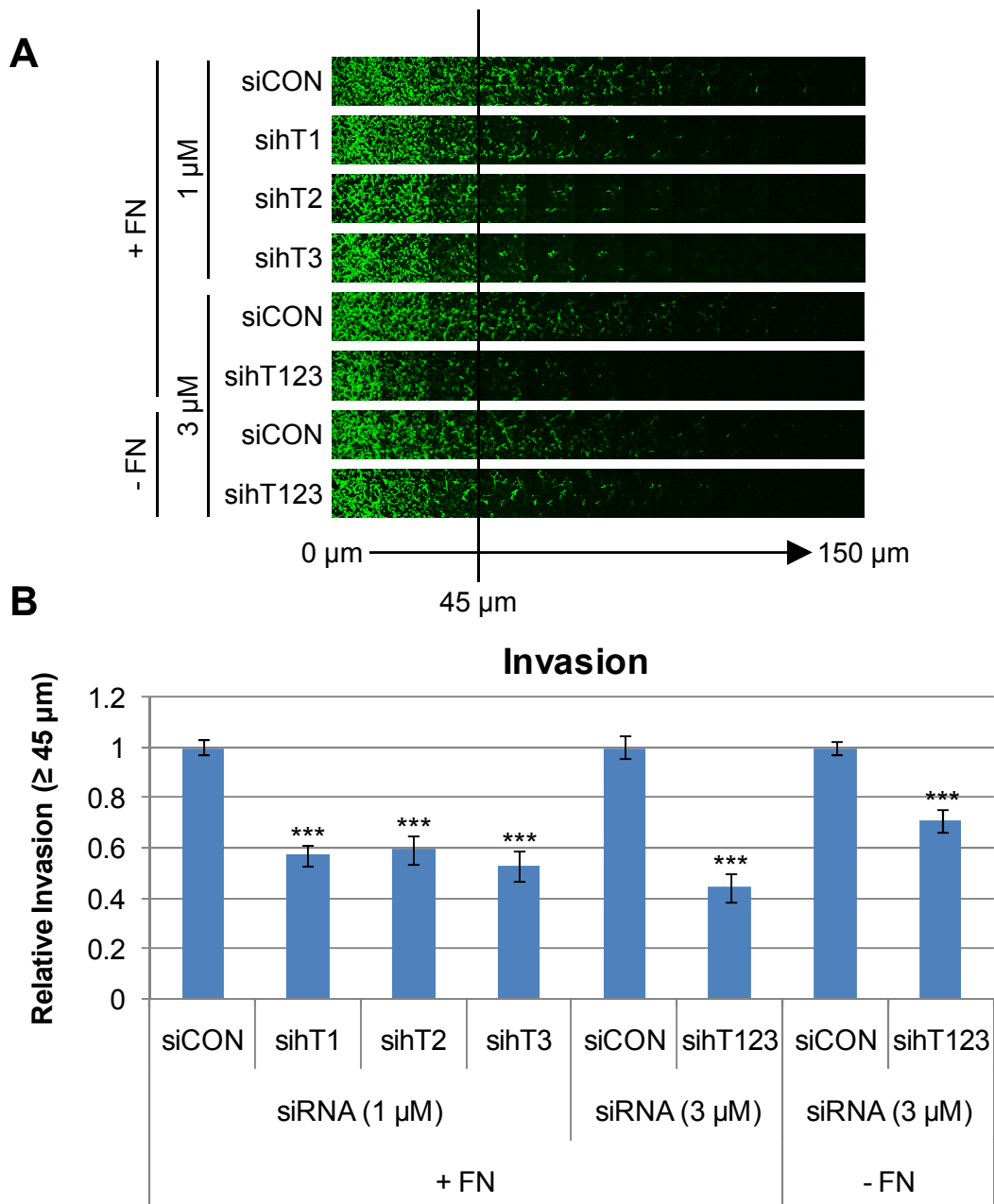


Figure 5.3. The effect of tensin knockdown on the invasive migration of Rab25 cells through 3D matrix in the presence or absence of supplemented FN. An inverted invasion assay was used to investigate the effect of tensin knockdown on the migration of Rab25 cells. Rab25 cells were transfected by nucleofection with siRNA SMARTpools directed against human tensin1 (sihT1), tensin2 (sihT2) and tensin3 (sihT3), both individually (1 μM) and combined (sihT123; 3 μM , 1 μM of each SMARTpool), or with a control non-targeting siRNA pool (siCON; 1 μM or 3 μM). Cells were allowed to invade into Matrigel plugs ($\pm 25 \mu\text{g/ml}$ FN) for 48 hours towards a gradient of serum (+30 ng/ml EGF). (A) Invading cells were stained with Calcein-AM and visualised by confocal microscopy. Serial optical sections were captured at 15 μm intervals and are presented as a sequence from left to right. (B) Invasion was quantified by measuring the fluorescence intensity of cells penetrating to 45 μm and beyond; this intensity was calculated as a percentage of the total fluorescence intensity of all cells within the plug. Graph represents mean invasion expressed relative to the control siRNA condition. Error bars; standard error of the mean. Experiment performed 3 times, $n=18$. ***: $P < 0.001$, Student's t-test.

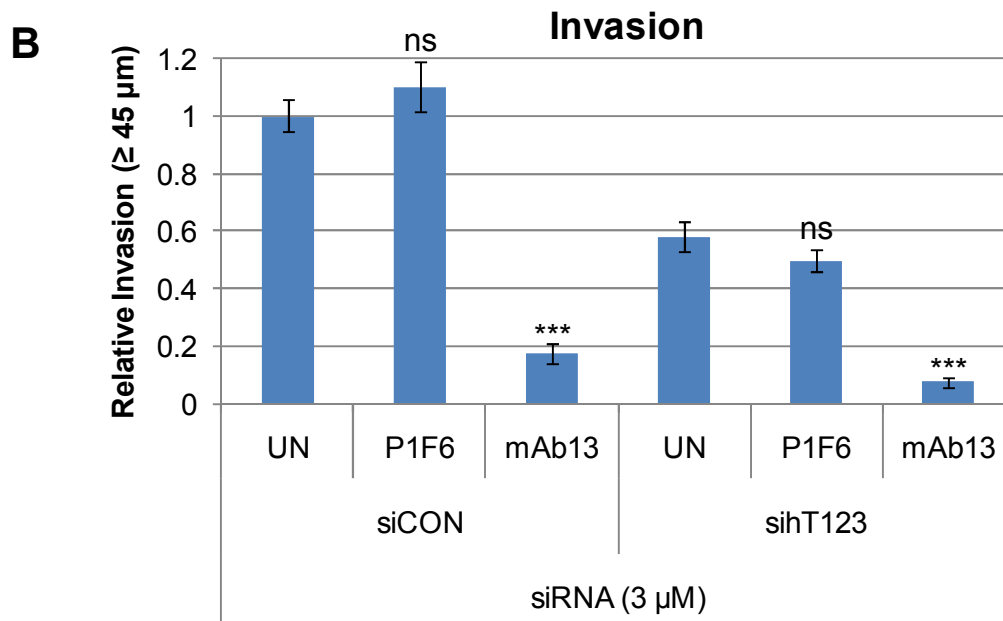
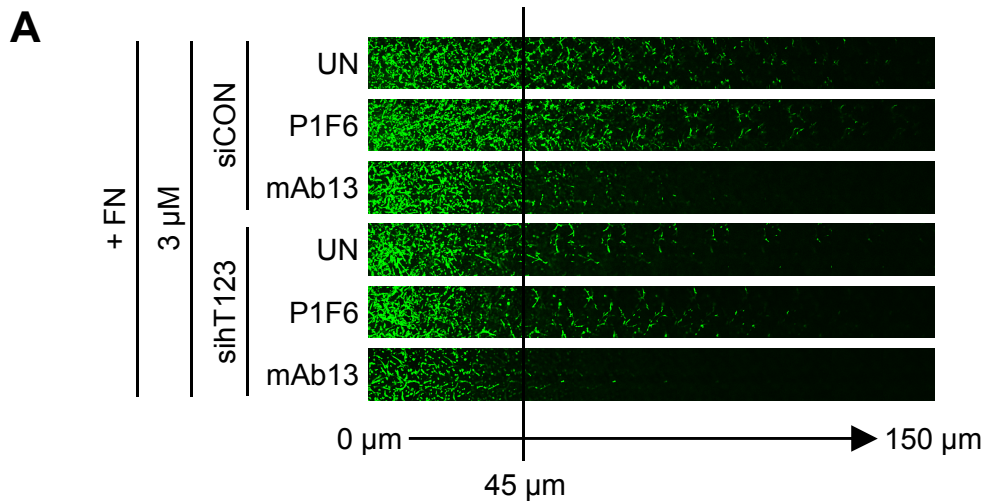


Figure 5.4. Analysis of the integrin dependency of invasive migration in control and tensin knockdown Rab25 cells. An inverted invasion assay was used to investigate the effect of $\beta 1$ integrin inhibition on the migration of control and tensin knockdown Rab25 cells. Rab25 cells were transfected by nucleofection with combined siRNA SMARTpools directed against human tensin1, 2 and 3 (sihT123; 3 μ M, 1 μ M of each SMARTpool), or with a control non-targeting siRNA pool (siCON; 3 μ M). Cells were allowed to invade into Matrigel plugs (+25 μ g/ml FN) for 48 hours towards a gradient of serum (+30 ng/ml EGF). The plug and the upper and lower media reservoirs were supplemented with inhibitory antibodies directed against $\alpha_v\beta_5$ integrin (P1F6) or $\beta 1$ integrin (mAb13) at 1 μ g/ml or unsupplemented (UN). (A) Invading cells were stained with Calcein-AM and visualised by confocal microscopy. Serial optical sections were captured at 15 μ m intervals and are presented as a sequence from left to right. (B) Invasion was quantified by measuring the fluorescence intensity of cells penetrating to 45 μ m and beyond; this intensity was calculated as a percentage of the total fluorescence intensity of all cells within the plug. Graph represents mean invasion expressed relative to the unsupplemented, control siRNA condition. Error bars; standard error of the mean. Experiment performed 3 times, n=18. ns: not significant, ***: P < 0.001, Student's t-test.

Tensin siRNA SMARTpools have been used for all of the knockdown experiments described so far. Each SMARTpool is composed of four siRNA duplexes, which have been designed to target the gene of interest with maximal specificity. However, all siRNA oligos have the potential to cause so-called “off-target effects”. Such “off-target effects” can give rise to phenotypic changes in the cell that cannot be attributed to the specific knockdown of the target gene. Therefore, in an attempt to confirm that effects on migration seen upon tensin knockdown with the tensin SMARTpools are specific, two unique combination pools were generated, each containing one siRNA directed against each tensin isoform.

To ensure maximal tensin knockdown it was necessary to evaluate the relative potencies of the individual siRNAs from each tensin SMARTpool before selecting which ones to include in the combination pools. This was done by measuring the abundance of tensin1, 2 and 3 mRNA in cells transfected with the individual siRNAs from the tensin1, 2 and 3 SMARTpools by qPCR. HFFs were transfected with individual siRNA oligos directed against human tensin1 (sihT1.1, 1.2, 1.3 or 1.4), tensin2 (sihT2.1, 2.2, 2.3 or 2.4) or tensin3 (sihT3.1, 3.2, 3.3 or 3.4), or a control non-targeting siRNA pool (siCON) at 10 nM concentration by lipofection. RNA isolated 24 hours post-transfection was DNase I treated, reverse transcribed into cDNA with oligo d(T) primers, and amplified in a qPCR assay with primers for tensin1, 2 or 3, and GAPDH (reference gene). qPCR data was analysed using the $\Delta\Delta C_T$ method to determine the relative abundance of each tensin mRNA, which was expressed relative to the control siRNA condition (Figure 5.5). All four siRNAs from each tensin SMARTpool knocked down the mRNA levels of their corresponding tensin isoform. However, within each SMARTpool some siRNAs were more potent than others (indicated by red boxes in Figure 5.5). Notably, sihT1.2 and sihT1.4 were more potent than sihT1.1 and sihT1.3 (76 and 73% versus 57 and 67% tensin1 knockdown), sihT2.2 and sihT2.3 were more potent than sihT2.1 and sihT2.4 (79 and 70% versus 53 and 46% tensin2 knockdown), and sihT3.1

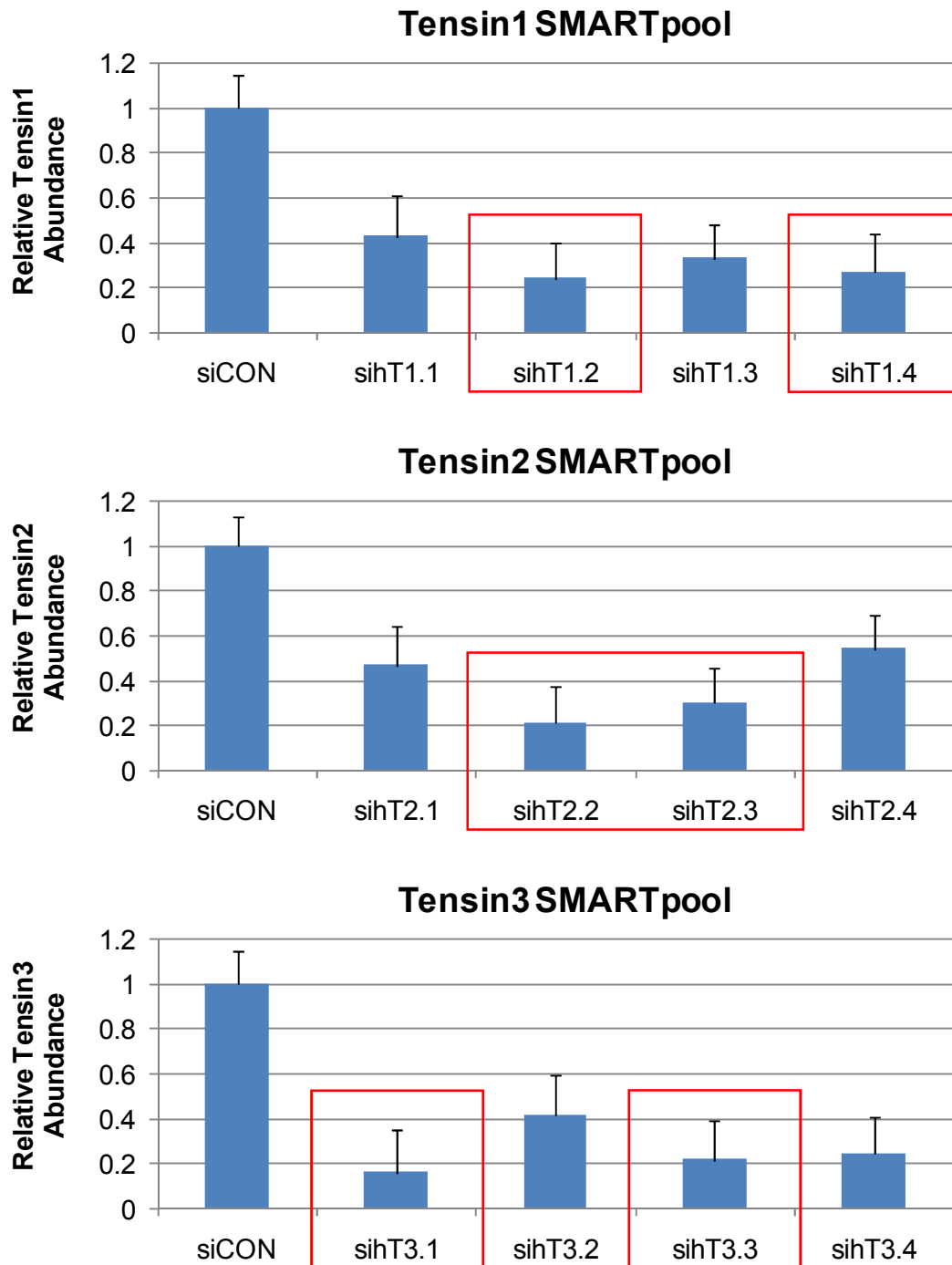


Figure 5.5: Analysis of the efficacy of individual siRNA oligos from the tensin1, 2 and 3 SMARTpools by qPCR. HFFs were transfected with single siRNA oligos targeting tensin1, 2, or 3, or a control non-targeting siRNA pool (siCON) at 10 nM by lipofection. RNA isolated 24 hours post-transfection was DNase I treated, reverse transcribed into cDNA using oligo d(T) primers, and amplified in a qPCR assay with tensin1, 2 or 3, and GAPDH primer pairs in the presence of the SYBR Green dsDNA-specific fluorescent dye. Relative abundance was determined using the $\Delta\Delta C_T$ method. Graphs represent the abundance of each tensin transcript normalised against GAPDH and expressed relative to the control siRNA condition. Red boxes indicate the two most potent siRNAs from each tensin SMARTpool. Experiment performed in triplicate. Error bars; standard error of the mean. siRNA oligo “Y” from human tensin “X” SMARTpool - siHT(X.Y).

and sihT3.3 were more potent than sihT3.2 and sihT3.4 (84 and 78% versus 58 and 75% tensin3 knockdown). Therefore two combination pools were made, each designed to knockdown all three tensin isoforms and each containing only three siRNAs; one pool consisted of sihT1.2, 2.2 and 3.1 (denoted sihT123a), and the other of sihT1.4, 2.3 and 3.3 (denoted sihT123b).

Rab25 cells were transfected by nucleofection with the sihT123a or sihT123b combination pools (3 μ M, i.e. 1 μ M for each individual siRNA), or a control non-targeting siRNA pool (siCON; 3 μ M) before analysing 3D migration using the inverted invasion assay (Figure 5.6). Cells were allowed to invade into Matrigel plugs (+FN) towards a gradient of serum (+EGF) for 48 hours prior to analysis as described previously. Rab25 cells transfected with the sihT123a and sihT123b combination pools displayed a reduction in invasive migration relative to cells transfected with the control siRNA of 77 and 71%, respectively. The finding that the combination pools also impair invasive 3D migration gives some reassurance that the effects seen with the SMARTpools are due to the specific targeting of the tensins, and not off-target effects.

5.2.2 *Tensin Localises to Cell-ECM Adhesions in Rab25 Cells Migrating in a 3D Matrix*

Given the requirement for tensin in the invasive 3D migration of Rab25 cells, the sub-cellular localisation of human tensin1, 2 and 3 in this cell line was investigated. Unfortunately, there are several technical issues associated with the high resolution imaging of cells within dense 3D microenvironments. To overcome the difficulties of imaging in the Matrigel plugs, cell-derived matrix (CDM) was used instead. CDM is a relatively thick, pliable matrix that is composed mainly of fibrillar collagen and FN, which resembles the type of matrix found in connective tissues (Cukierman *et al.*, 2001). CDMs were isolated from cultures of telomerase-immortalized fibroblasts (TIFs)

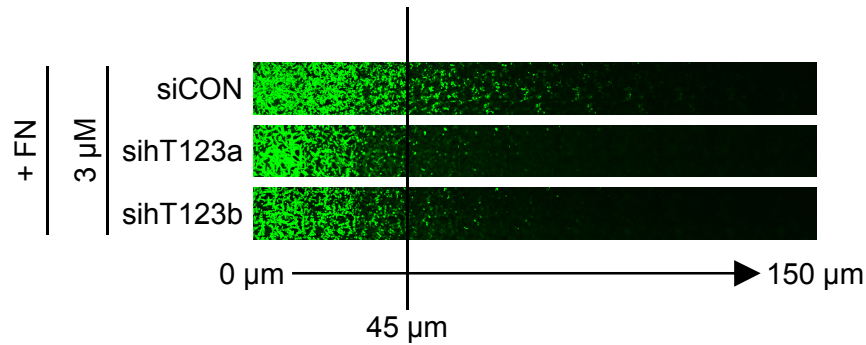
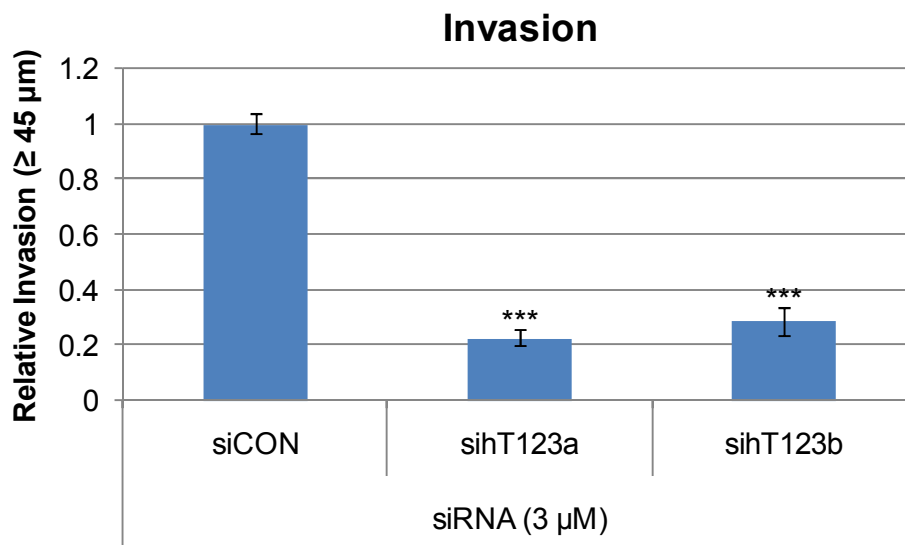
A**B**

Figure 5.6. The effect of tensin knockdown using individual siRNA oligos on the invasive migration of Rab25 cells through 3D matrix. Rab25 cells were transfected by nucleofection with one of two different combination pools, each containing one siRNA directed against each human tensin isoform (sihT123a or sihT123b; 3 μM, 1 μM of each individual siRNA), or a control non-targeting siRNA pool (siCON; 3 μM). An inverted invasion assay was used to investigate the effect of tensin knockdown on cell migration. Cells were allowed to invade into Matrigel plugs (+25 μg/ml FN) for 48 hours towards a gradient of serum (+30 ng/ml EGF). (A) Invading cells were stained with Calcein-AM and visualised by confocal microscopy. Serial optical sections were captured at 15 μm intervals and are presented as a sequence from left to right. (B) Invasion was quantified by measuring the fluorescence intensity of cells penetrating to 45 μm and beyond; this intensity was calculated as a percentage of the total fluorescence intensity of all cells within the plug. Graph represents mean invasion expressed relative to the control siRNA condition. Error bars; standard error of the mean. Experiment performed 3 times, n=18. ***: P < 0.001, Student's t-test.

grown at high density for 8-9 days. TIFs were extracted from the CDMs prior to use in experiments with A2780 cells.

Rab25 cells were transfected with mammalian expression constructs encoding GFP, GFP-tensin1, GFP-tensin2 or GFP-tensin3 by nucleofection. Twenty-four hours post-transfection the cells were plated onto CDM, left for 4 hours to adhere and begin migrating, and then imaged by confocal microscopy. GFP alone showed a diffuse cytoplasmic localisation (Figure 5.7; top left image). GFP-tensin1 located to sub-cellular structures of a variety of lengths, which were distributed all over the cell surface (Figure 5.7). GFP-tensin2 also located to sub-cellular structures distributed all over the cell surface; although these structures tended to be small and punctate (Figure 5.8). GFP-tensin3 strongly localised to sub-cellular structures of a variety of lengths that were located all over the cell surface (Figure 5.9). Tensin3-containing structures were generally larger and longer than those seen in GFP-tensin1-transfected cells. The $\alpha 5$ integrin has also been detected in similar structures in Rab25 cells plated on CDM (Dr P Caswell - personal communication), which suggests that they are 3D-matrix adhesions. Collectively, these results show that all three tensins are capable of localising to cell-matrix adhesion sites in cells in 3D matrix, which supports the finding that tensin is required for invasive 3D migration.

5.2.3 Tensin is Required for Rab25-Driven Invasive Morphology and Directionally Persistent Migration in 3D Matrix

To further investigate the pro-invasive role of Rab25, Caswell *et al.* (2007) also analysed the effect of Rab25 expression on the morphology and migration of individual cells plated onto CDM. DNA3 cells were found to migrate rapidly with low persistence (net displacement/path length), maintaining a “slug-like” morphology as they moved with approximately uniform speed. Surprisingly, Rab25 expression actually slowed the

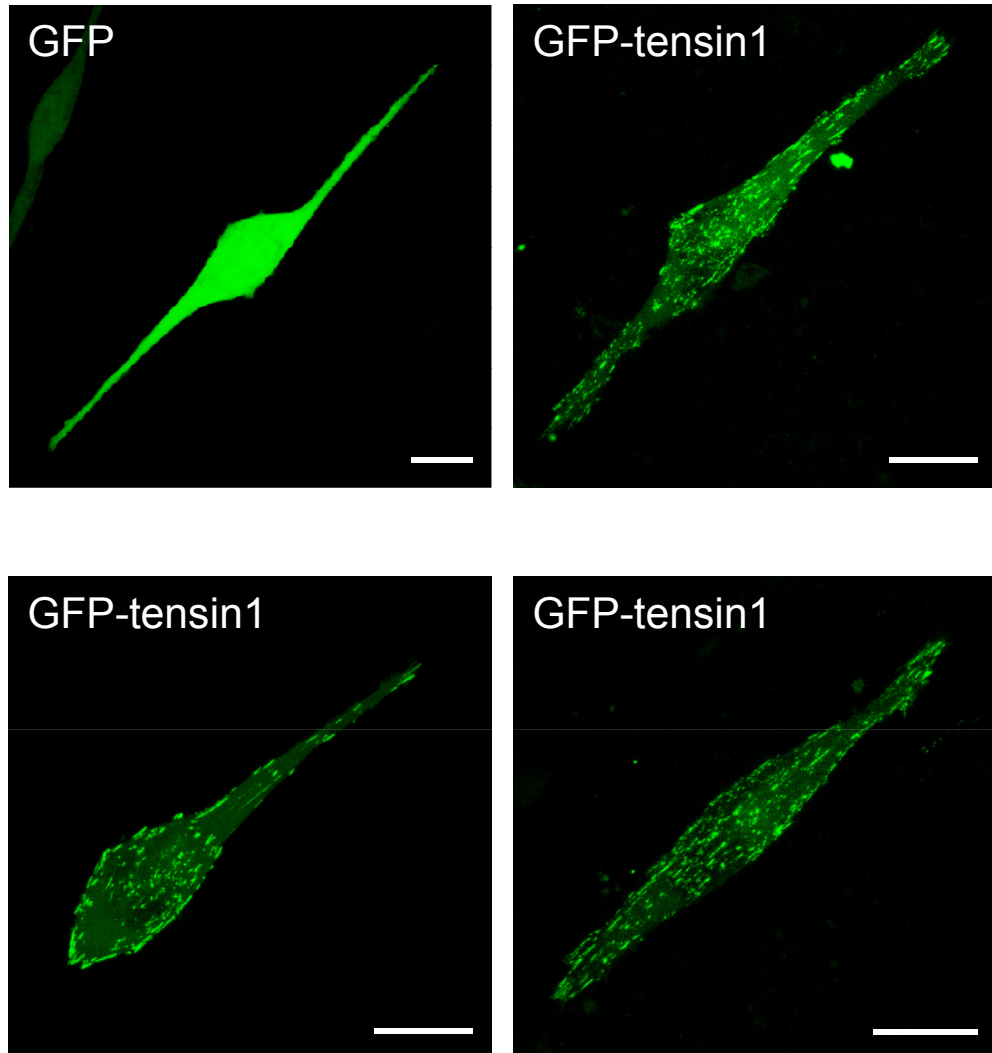


Figure 5.7: GFP-tensin1 localisation in Rab25 cells on cell-derived matrix. Rab25 cells were transfected with expression constructs encoding GFP or GFP-tensin1 by nucleofection. Twenty-four hours post-transfection the cells were plated onto CDM. Approximately 4 hours later the cells were imaged by confocal microscopy. Scale bar – 20 μ m.

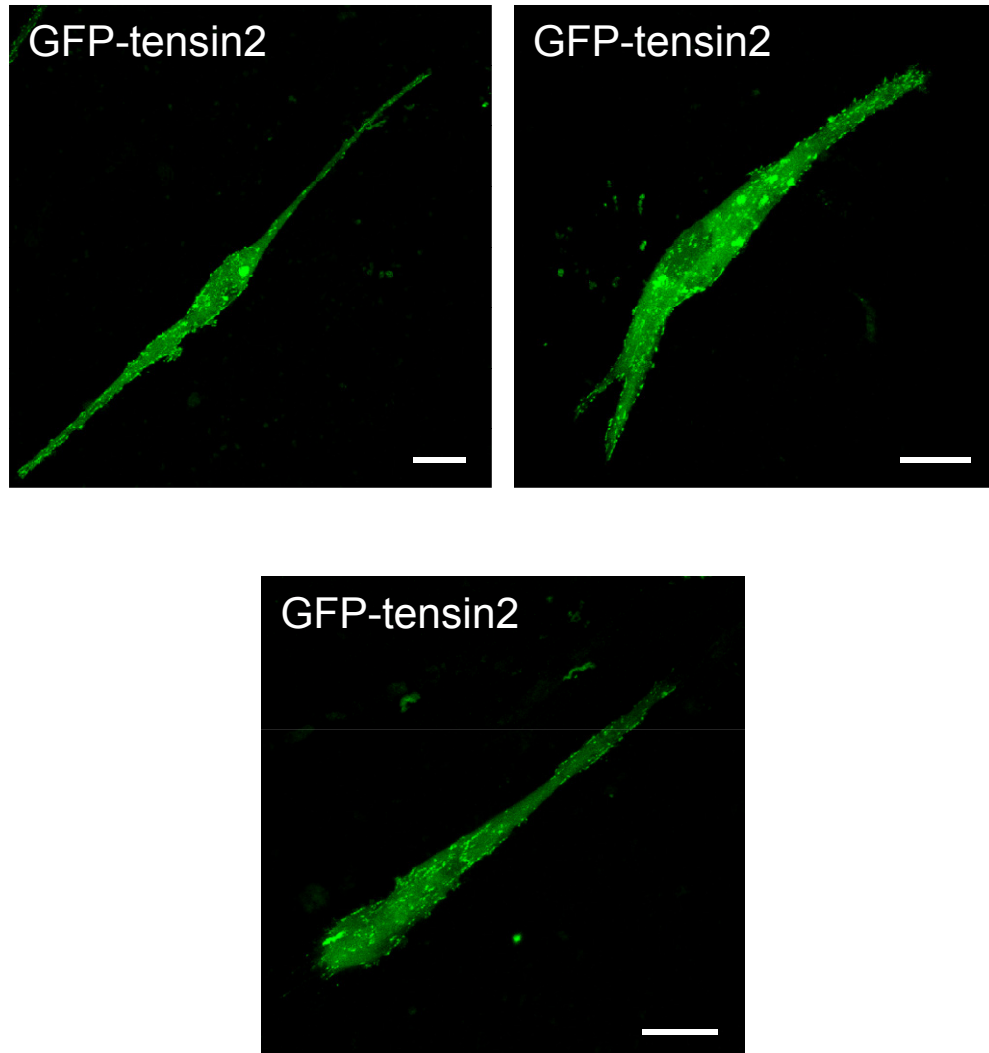


Figure 5.8: GFP-tensin2 localisation in Rab25 cells on cell-derived matrix. Rab25 cells were transfected with an expression construct encoding GFP-tensin2 by nucleofection. Twenty-four hours post-transfection the cells were plated onto CDM. Approximately 4 hours later the cells were imaged by confocal microscopy. Scale bar – 20 μ m.

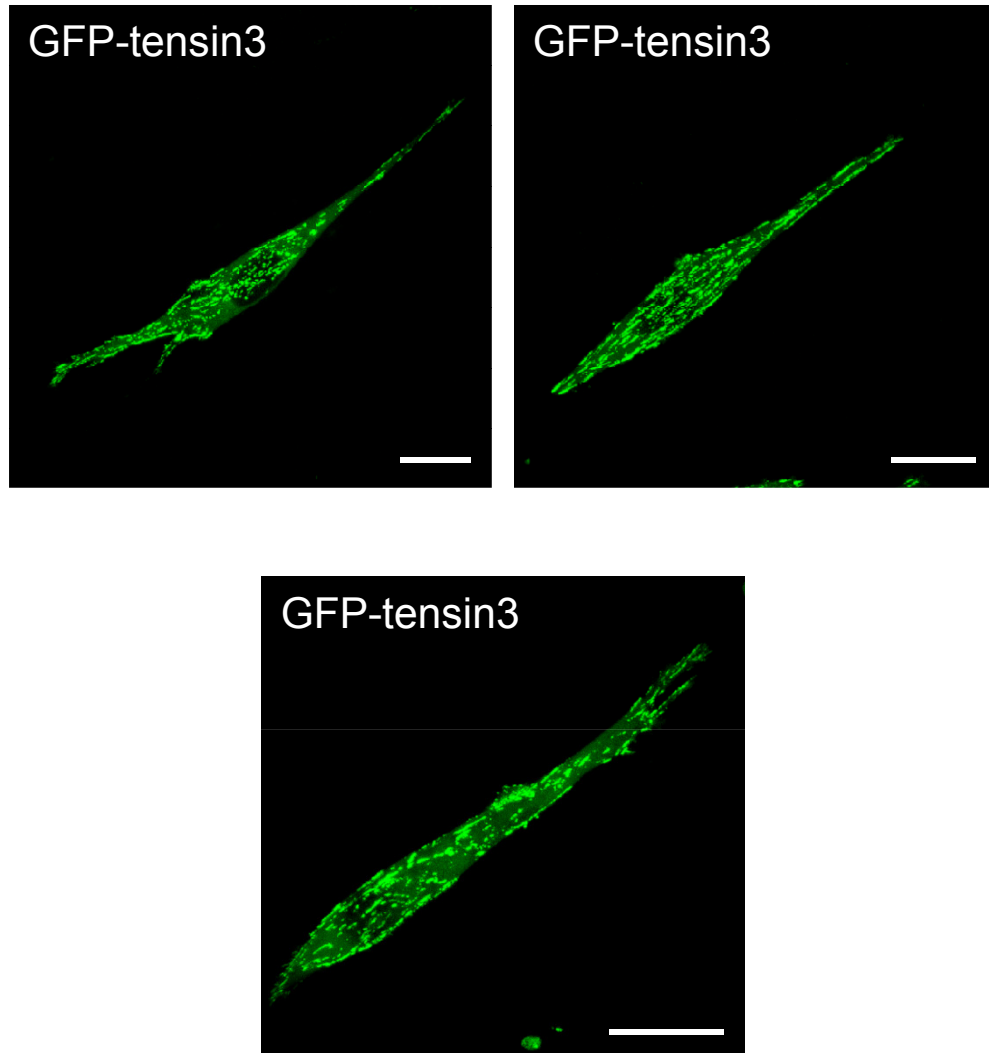


Figure 5.9: GFP-tensin3 localisation in Rab25 cells on cell-derived matrix. Rab25 cells were transfected with an expression construct encoding GFP-tensin3 by nucleofection. Twenty-four hours post-transfection the cells were plated onto CDM. Approximately 4 hours later the cells were imaged by confocal microscopy. Scale bar – 20 μ m.

average speed of migration, but it also concomitantly increased the average persistence of migration. Therefore, on CDM it is the persistence (and not speed) of migration that correlates with invasiveness. Moreover, they noted that Rab25 cells adopted a different morphology and mode of migration to DNA3 cells. Rab25-driven migration was characterised by the extension of long pseudopodia in opposing directions, followed by the retraction of one pseudopodium and a burst of migration in the direction of the persisting pseudopodium. They showed that this pseudopod-driven style of migration could be quantified by measuring the average distance between the nucleus and leading edge, which they found to be increased by ~50% in cells expressing Rab25.

To substantiate the data collected using the invasion assay, Rab25 cells transfected with tensin siRNAs were plated onto CDM to analyse their morphology and migration. Rab25 cells were transfected by nucleofection with siRNA SMARTpools directed against human tensin1 (sihT1), tensin2 (sihT2) and tensin3 (sihT3), both individually (1 μ M) and in combination (sihT123; 3 μ M, 1 μ M for each SMARTpool), or with a control non-targeting siRNA pool (siCON; 1 μ M or 3 μ M). Twenty-four hours post-transfection the cells were plated onto CDM, left for 4 hours to adhere and begin migrating, and then imaged by time-lapse microscopy by taking images every 10 minutes over a period of 12 hours and generating movies. Tensin depletion induced a change in the mode of migration from an elongated pseudopod-driven mechanism characteristic of highly invasive cells, to a shortened slug-like style characteristic of less invasive cells. The individual knockdown of tensin1, 2 and 3 reduced average pseudopod length (a quantitative index of invasive morphology) relative to the control cells by a small but significant extent (20, 18 and 18%, respectively) (Figure 5.10). The simultaneous knockdown of all three tensins reduced average pseudopod length by 30% relative to the control cells (Figure 5.10). To confirm that this phenotype was not an off-target effect of the tensin siRNA SMARTpools, the experiment was repeated using the

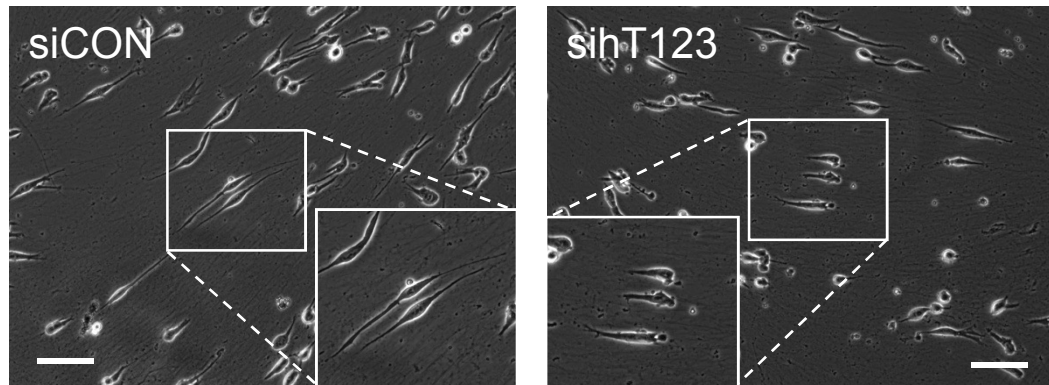
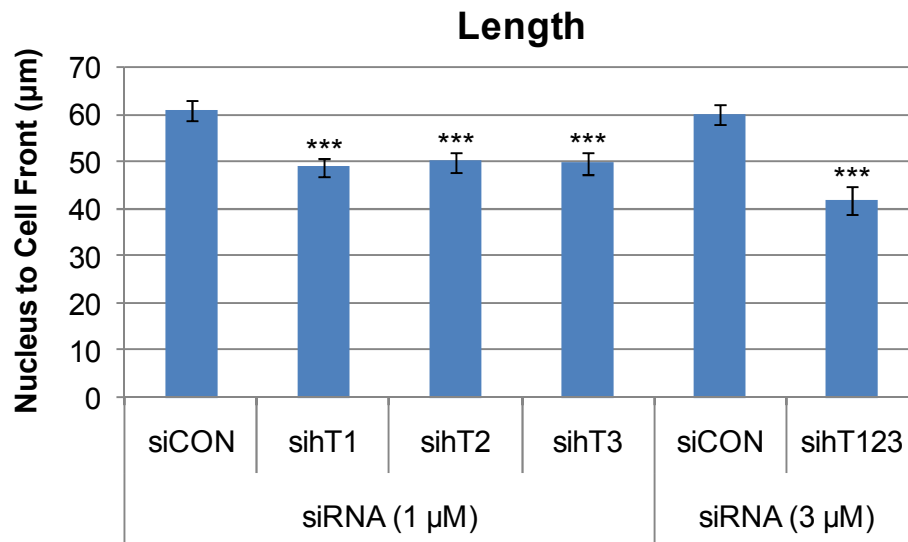
A**B**

Figure 5.10. The effect of tensin knockdown on Rab25-driven invasive morphology on cell-derived matrix. Rab25 cells were transfected by nucleofection with siRNA SMARTpools directed against human tensin1 (sihT1), tensin2 (sihT2) and tensin3 (sihT3), both individually (1 μM) and combined (sihT123; 3 μM, 1 μM of each SMARTpool), or with a control non-targeting siRNA pool (siCON; 1 μM or 3 μM). Twenty-four hours post-transfection the cells were plated onto CDM approximately 4 hours prior to time-lapse microscopy. Cell migration was monitored by taking images every 10 minutes over a period of 12 hours and movies were generated. (A) Representative images of control and triple tensin knockdown Rab25 cells taken approximately 8 hours after plating. Scale bar – 100 μm. (B) The average distance between the centre of the nucleus and the cell front (with respect to the direction of migration) was determined using ImageJ. Graph represents mean distance from the nucleus to the cell front. Error bars; standard error of the mean. Experiment performed 3 times, data from a representative experiment, n>50. ***: P < 0.001, Student's t-test.

previously described combination pools. Rab25 cells transfected with the sihT123a and sihT123b combination pools displayed a reduction in pseudopod length relative to cells transfected with the control siRNA of 23 and 27%, respectively (Figure 5.11).

To corroborate the cell length phenotype seen upon triple tensin knockdown using the tensin siRNA SMARTpools, the average speed and persistence of cell migration was also determined by manually tracking the position of the cell centroid (Figure 5.12). The simultaneous knockdown of tensin1, 2 and 3 increased the average speed of migration by 29%, whilst concomitantly decreasing the average persistence of migration by 27%. Taken together, these data show that tensin knockdown reduces the invasive migration and morphology of Rab25 cells on CDM.

5.2.4 The Mechanism of Tensin-Dependent 3D Migration

Rab25 promotes the localisation of recycling vesicles/endosomes that deliver $\alpha 5$ integrin to the cell surface at the tips of pseudopodia, which sequesters integrin at the cell front where it can presumably be incorporated into cell-matrix adhesions that support invasive cell migration (Caswell *et al.*, 2007). In an attempt to define the mechanism through which tensin contributes to Rab25-driven cell migration, the requirement for tensin in integrin recycling and integrin retention at the cell front was investigated.

Rab25 cells were transfected by nucleofection with combined siRNA SMARTpools directed against human tensin1, 2 and 3 (sihT123; 3 μ M, 1 μ M for each SMARTpool), or a control non-targeting siRNA pool (siCON; 3 μ M). Forty-eight hours post-transfection the cells were serum-starved and surface labelled with *N*-hydroxysuccinimide-S-S-biotin before allowing internalization to proceed. Biotin remaining at the cell surface was removed by exposure to β -mercaptoethanesulfonic

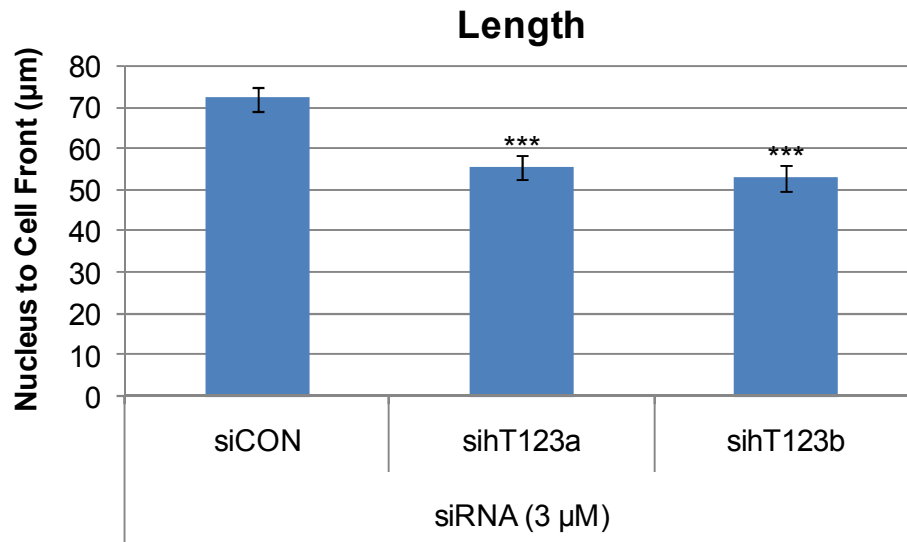


Figure 5.11. The effect of tensin knockdown using individual siRNA oligos on Rab25-driven invasive morphology on cell-derived matrix. Rab25 cells were transfected by nucleofection with one of two different combination pools, each containing one siRNA directed against each human tensin isoform (sihT123a or sihT123b; 3 μ M, 1 μ M of each individual siRNA), or a control non-targeting siRNA pool (siCON; 3 μ M). Twenty-four hours post-transfection the cells were plated onto CDM approximately 4 hours prior to time-lapse microscopy. Cell migration was monitored by taking images every 10 minutes over a period of 12 hours and movies were generated. The average distance between the centre of the nucleus and the cell front (with respect to the direction of migration) approximately 8 hours after plating was determined using ImageJ. Graph represents mean distance from the nucleus to the cell front. Error bars; standard error of the mean. Experiment performed 3 times, data from a representative experiment, $n > 50$. ***: $P < 0.001$, Student's t-test.

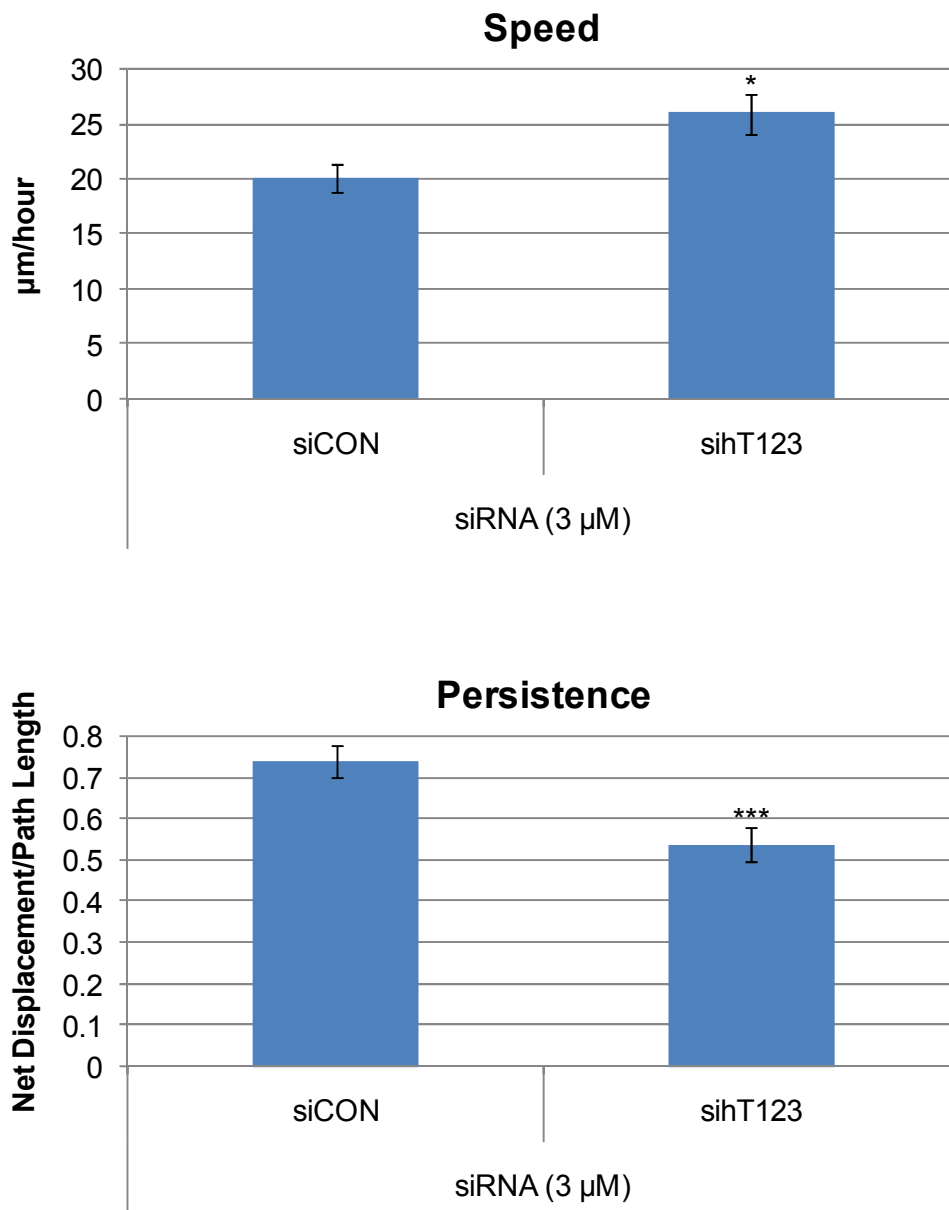


Figure 5.12. The effect of tensin knockdown on the migration of Rab25 cells on cell-derived matrix. Rab25 cells were transfected by nucleofection with combined siRNA SMARTpools directed against human tensin1, 2 and 3 (sihT123; 3 μM, 1 μM of each SMARTpool), or with a control non-targeting siRNA pool (siCON; 3 μM). Twenty-four hours post-transfection the cells were plated onto CDM approximately 4 hours prior to time-lapse microscopy. Cell migration was monitored by taking images every 10 minutes over a period of 12 hours and movies were generated. Average speed and persistence of migration were determined by manually tracking the position of the cell centroid using ImageJ. Error bars; standard error of the mean. Experiment performed 3 times, n>50. *: P < 0.05, ***: P < 0.001, Student's t-test.

acid (MESNa), and internalized integrin was chased back to the cell surface for various lengths of time. Cells were then re-exposed to MESNa and lysed before determining the amount of biotinylated integrin in cell lysates by capture ELISA. The graph in Figure 5.13 shows that the rate at which $\alpha 5$ integrin is recycled back to the cell surface is the same for both control and triple tensin knockdown Rab25 cells. Hence, tensin is not required for $\alpha 5$ integrin recycling in this cell type. Therefore, tensin is likely to function downstream of the integrin recycling process to promote Rab25-driven cell migration.

If tensin is not required for Rab25-driven integrin recycling, then the role of tensin might be to anchor the recycled integrin at the tips of pseudopodia. This hypothesis was investigated by measuring the rate at which $\alpha 5$ integrin diffuses away from the tips of leading pseudopodia in triple tensin knockdown cells. Twenty-four hours post-siRNA transfection, control and triple tensin knockdown Rab25 cells were transfected with expression constructs encoding a photoactivatable form of GFP- $\alpha 5$ integrin (paGFP- $\alpha 5$ integrin) and mCherry-Rab25 (as a marker of transfection). Twenty-four hours later, the cells were plated onto CDM, left for a further 4 hours to adhere and begin migrating, and imaged by confocal microscopy. Photoactivation of paGFP- $\alpha 5$ integrin was achieved with a 405 nm laser aimed at a region at the front of the cell, and images were taken at 1 second intervals over a period of 4 minutes (Figure 5.14A). The average pixel intensity of the photoactivated region was quantified for each frame, calculated relative to the intensity of the frame immediately after photoactivation, corrected for photobleaching, and plotted against time to create a graph to represent the rate of integrin diffusion away from the cell front. The graph in Figure 5.14B shows that $\alpha 5$ integrin diffuses away from the pseudopodial tips of control and triple tensin knockdown Rab25 cells at similar rates. Hence, the simultaneous knockdown of tensin1, 2 and 3 did not affect integrin retention at the tips of pseudopodia. This would suggest that tensin does not function to anchor the integrin recycled by Rab25 at the cell front.

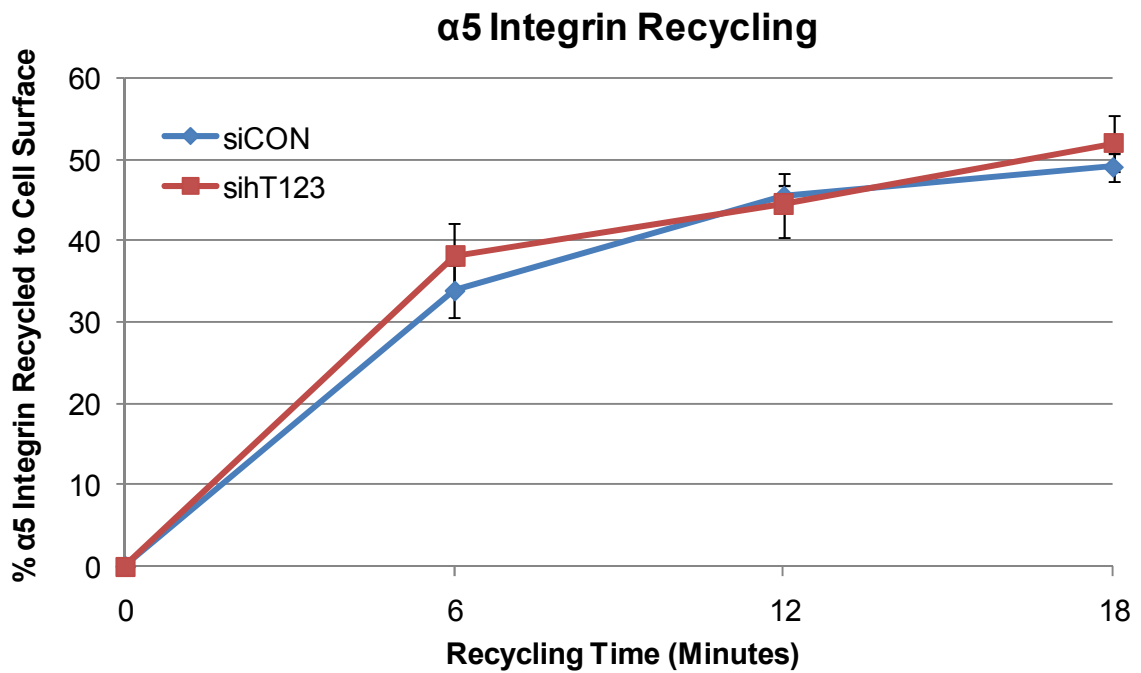


Figure 5.13: Recycling of α5 integrin in control and tensin knockdown Rab25 cells. Rab25 cells were transfected by nucleofection with combined siRNA SMARTpools directed against human tensin1, 2 and 3 (sihT123; 3 μM, 1 μM of each SMARTpool), or a control non-targeting siRNA pool (siCON; 3 μM). Forty-eight hours post-transfection the cells were serum-starved and surface labelled with *N*-hydroxysuccinimide-S-S-biotin before allowing internalization to proceed. Biotin remaining at the cell surface was removed by exposure to β-mercaptoethanesulfonic acid (MESNa), and internalized integrin was chased back to the cell surface for the indicated recycling times. Cells were then re-exposed to MESNa, and biotinylated integrin was determined by capture ELISA. Experiment performed twice with each time point performed in triplicate (n=6). Error bars; standard error of the mean.

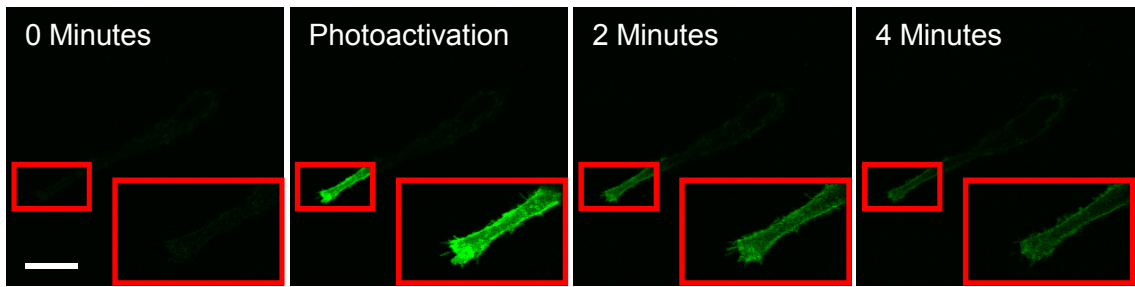
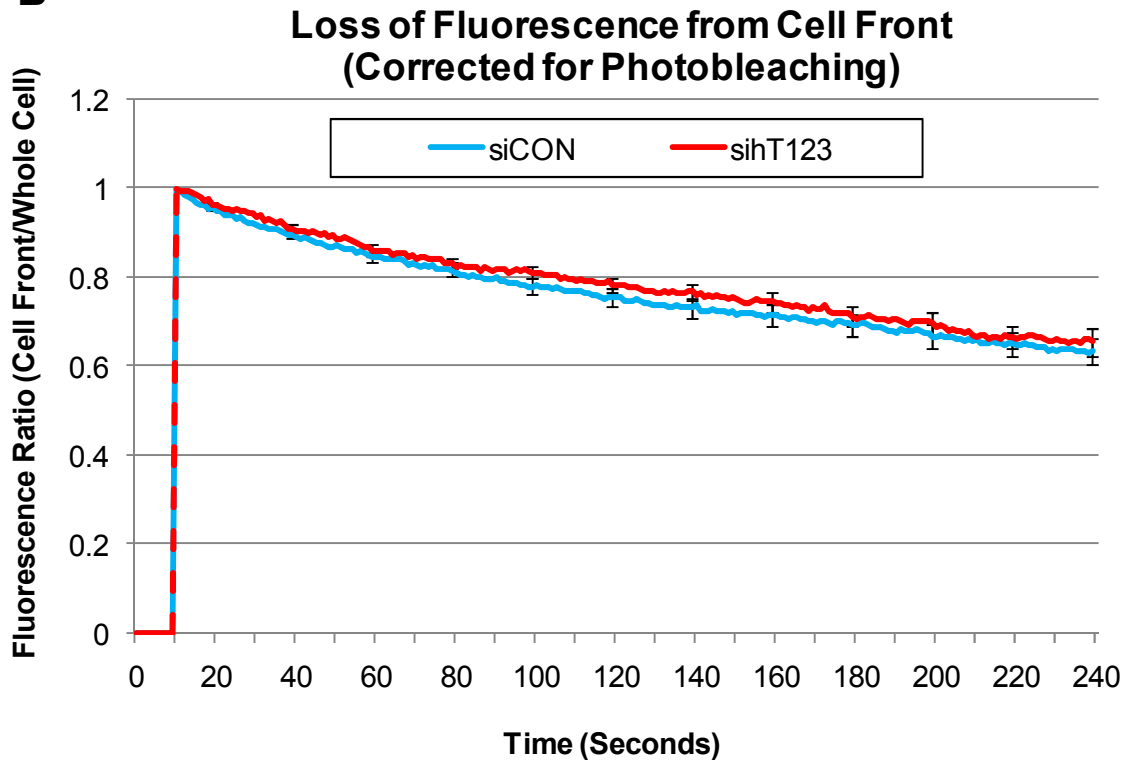
A**B**

Figure 5.14. Tensin knockdown does not compromise Rab25-driven integrin retention in pseudopodial tips. Rab25 cells were transfected by nucleofection with combined siRNA SMARTpools directed against human tensin1, 2 and 3 (sihT123; 3 μ M, 1 μ M of each SMARTpool), or a control non-targeting siRNA pool (siCON; 3 μ M). Twenty-four hours post-transfection the cells were transfected again with expression constructs encoding photoactivatable GFP- α 5 integrin and mCherry-Rab25 (as a marker of transfection). Twenty-four hours later the cells were plated onto CDM, left for a further 4 hours to adhere and begin migrating, and imaged by confocal microscopy. Photoactivation was achieved with a 405 nm laser aimed at a region at the front of the cell. Images were then taken at 1 frame/second over a period of 4 minutes. (A) An example photoactivation. Scale bar – 20 μ m. (B) The average pixel intensity of the photoactivated region was quantified for each frame, calculated relative to the intensity of the frame immediately after photoactivation, corrected for photobleaching, and plotted against time. Plotted values represent mean fluorescence intensity. Error bars; standard error of the mean (marked only at every 20th time point). Experiment performed 5 times, $n \geq 26$.

It has previously been observed that Rab25 expression in A2780 cells increases the assembly of FN fibrils, which form on the dorsal and ventral surface of the cell, and also assemble between cells at high confluence (Dr P Caswell - personal communication). Since tensin has been implicated in the process of FN fibrillogenesis in 2D culture (Pankov *et al.*, 2000), and is required for FN-dependent invasive migration of Rab25 cells in 3D culture (Figure 5.3), the effect of tensin knockdown on the assembly of these FN fibrils was investigated. Rab25 cells were transfected by nucleofection with combined siRNA SMARTpools directed against human tensin1, 2 and 3 (sihT123; 3 μ M, 1 μ M for each SMARTpool), or a control non-targeting siRNA pool (siCON; 3 μ M). Four hours post-transfection the cells were plated onto glass coverslips and grown to high confluence. Hyper-confluent monolayers were fixed and stained with the DAPI DNA-binding nuclear dye and an antibody directed against FN, followed by the appropriate fluorescently-conjugated secondary antibody, and analysed by confocal microscopy (Figure 5.15A). FN fibril fluorescence was quantified and normalised against cell density (Figure 5.15B). The simultaneous knockdown of tensin1, 2 and 3 reduced the assembly of FN fibrils by 78% relative to the control cells (Figure 5.15B). Similarly, staining with an antibody directed against the α 5 integrin subunit of the FN receptor indicated an 82% reduction in α 5 integrin-positive adhesions (Figure 5.16).

5.3 Discussion

5.3.1 *Tensin is Required for 3D Migration*

The finding that modulating tensin levels through over-expression or RNAi knockdown had no effect on the 2D migration of a variety of cell types was unexpected. However, an increasing body of evidence indicates that 2D culture systems do not accurately recapitulate cell behaviour in the 3D *in vivo* setting

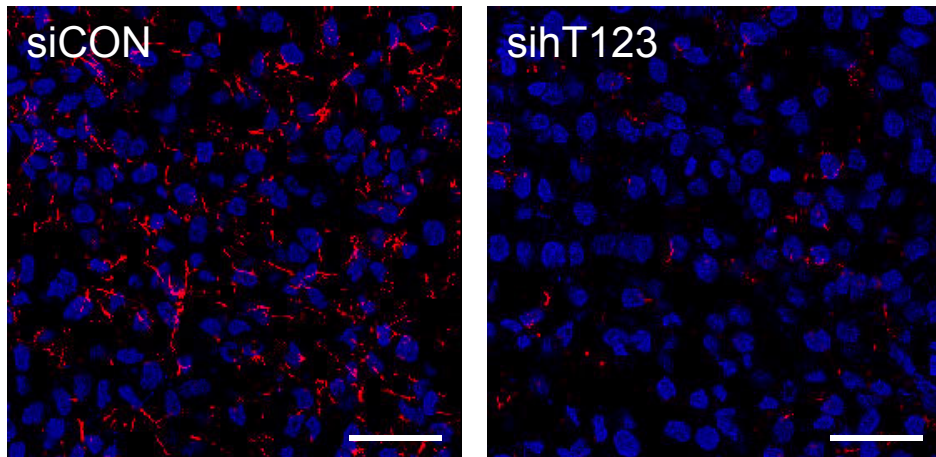
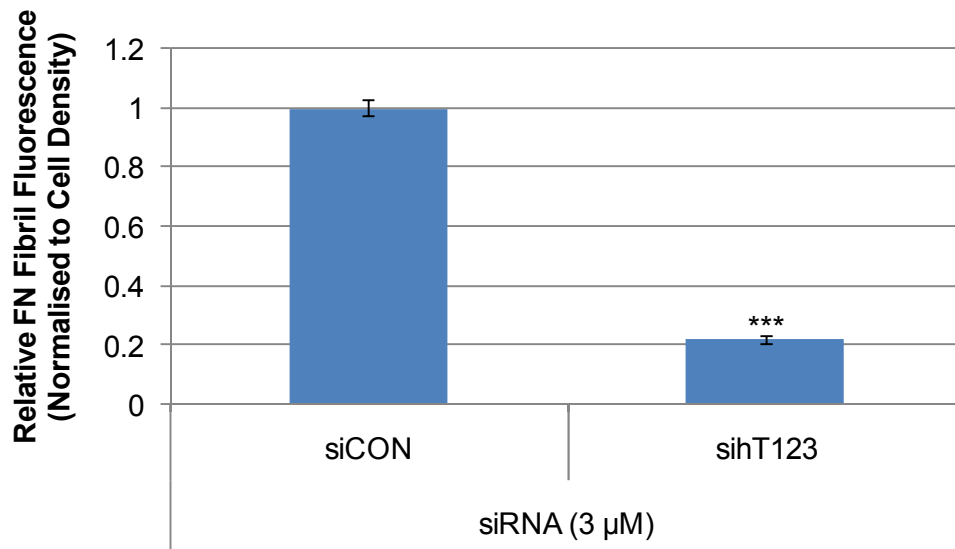
A**B**

Figure 5.15. Tensin is required for FN fibril formation. Rab25 cells were transfected by nucleofection with combined siRNA SMARTpools directed against human tensin1, 2 and 3 (sihT123; 3 μ M, 1 μ M of each SMARTpool), or a control non-targeting siRNA pool (siCON; 3 μ M). Four hours post-transfection the cells were plated onto glass coverslips and grown to confluence over the following 48 hours. (A) Confluent monolayers were fixed and stained with the DAPI DNA-binding nuclear dye (Blue) and an antibody directed against FN, followed by the appropriate fluorescently-conjugated secondary antibody (Red), and analysed by confocal microscopy. Scale bar – 50 μ m. (B) FN fibril fluorescence was quantified using ImageJ and normalised against cell density (DAPI staining). Graph represents mean fibril fluorescence expressed relative to the control siRNA condition. Error bars; standard error of the mean. Experiment performed 3 times, n=15. ***: P < 0.001, Student's t-test.

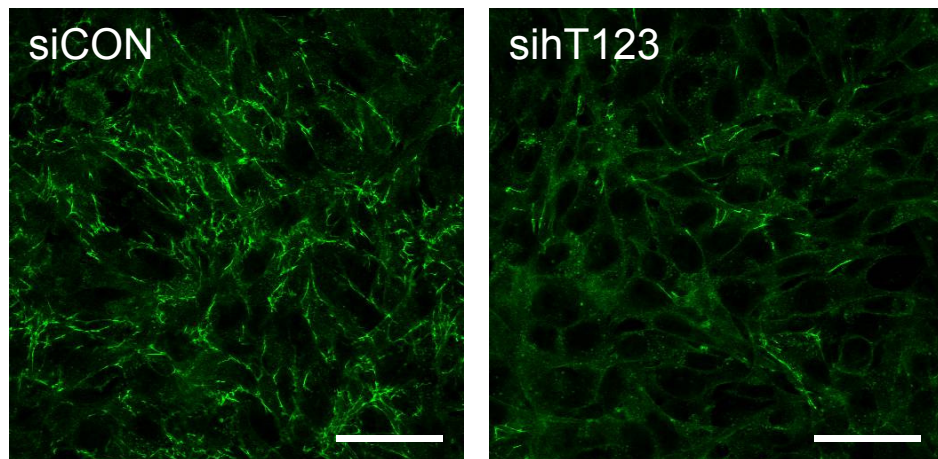
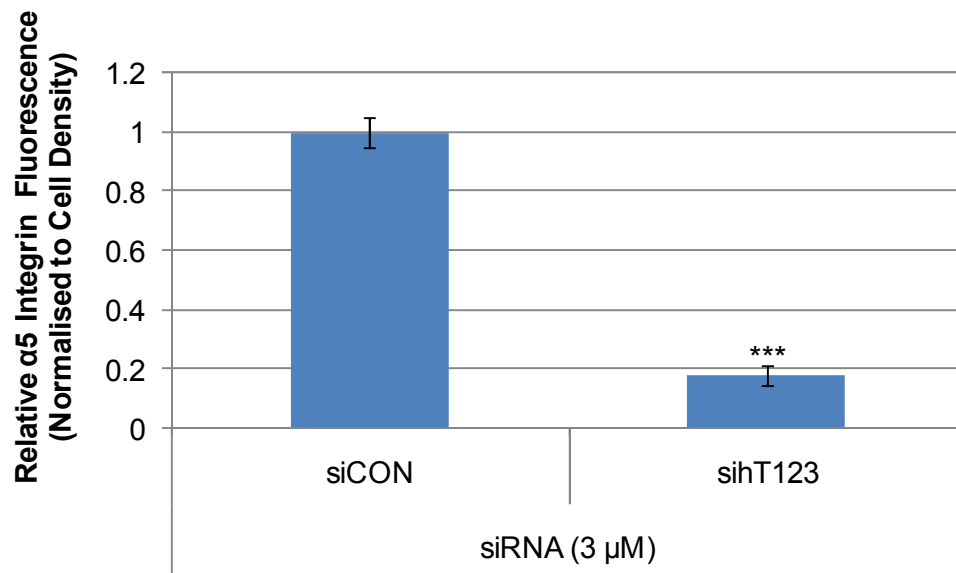
A**B**

Figure 5.16. Tensin is required for the formation of α 5 integrin-containing adhesions. Rab25 cells were transfected by nucleofection with combined siRNA SMARTpools directed against human tensin1, 2 and 3 (sihT123; 3 μ M, 1 μ M of each SMARTpool), or a control non-targeting siRNA pool (siCON; 3 μ M). Four hours post-transfection the cells were plated onto glass coverslips and grown to confluence over the following 48 hours. (A) Confluent monolayers were fixed and stained with an antibody directed against α 5 integrin, followed by the appropriate fluorescently-conjugated secondary antibody, and analysed by confocal microscopy. Scale bar – 50 μ m. (B) α 5 integrin fluorescence was quantified using ImageJ and normalised against the confluence of the cells. Graph represents mean adhesion fluorescence expressed relative to the control siRNA condition. Experiment performed once, n=5. Error bars; standard error of the mean. ***: P < 0.001, Student's t-test.

(Walpita and Hay, 2002; Yamada and Cukierman, 2007). Therefore, I sought to investigate the requirement for tensin expression during cell migration in a more *in vivo*-like environment. This was achieved by employing two *in vitro* 3D migration assays, which used the tumour basement membrane extract Matrigel and cell-derived matrix, respectively.

Two variants of the A2780 ovarian cancer cell line were used to investigate the requirement for tensin during 3D migration; one stably expressing the Rab25 GTPase (Rab25 cells) and the other stably transfected with the empty pcDNA3 expression vector (DNA3 cells). Rab25 is a member of the Rab11 subfamily of small GTPases which are known to function in the recycling of internalized integrin receptors to the plasma membrane, a process which is required for cell spreading and migration (Caswell and Norman, 2006). Furthermore, Rab25 over-expression has been linked to the aggressiveness of ovarian and breast tumours both clinically and in mouse models (Cheng *et al.*, 2004). Over-expression of Rab25 in the A2780 cell line promotes invasive 3D cell migration through a mechanism that is dependent on the ligation of FN by $\alpha_5\beta_1$ integrin and the ability of Rab25 to interact with the β_1 integrin tail (Caswell *et al.*, 2007). Therefore, by using both Rab25 and DNA3 cells in the present study it was possible to evaluate the relative requirement for tensin expression in both a highly invasive and moderately invasive cell line.

Initially, the positive effect of Rab25 on invasive 3D migration was confirmed using the Matrigel-plug invasion assay (Figure 5.1). It was found that Rab25 cells were approximately 4-fold more invasive than DNA3 cells, which is comparable with the findings of Caswell *et al.* (2007). Next, the individual siRNA-directed knockdown of tensin1, 2 and 3 was shown to reduce the invasive migration of DNA3 cells (Figure 5.2) and Rab25 cells (Figure 5.3) to a similar extent. This result would suggest that all three of the large human tensins form part of the basal cellular machinery that promotes

invasive 3D cell migration in A2780 cells. The finding that tensin2 and 3 are required for 3D migration is in agreement with the work of others (Yam *et al.*, 2006b; Qian *et al.*, 2009). However, using a similar invasion assay to that used here, Martuszevska *et al.* (2009) described tensin3 as a negative regulator of 3D migration in HEK293 cells. Tensin3 is the tensin isoform most likely to possess an active PTEN phosphatase domain according to sequence comparisons (Dr K Clark - personal communication), and Martuszevska *et al.* (2009) explored the role of this domain by stably expressing a tensin3 containing a mutation in the putative phosphatase active site in HEK293 cells. However, this mutant suppressed cell motility to a similar extent as wild-type tensin3, indicating that the putative phosphatase activity of the tensin3 PTEN homology region is not required for the inhibitory effect of tensin3 on 3D cell migration (Martuszevska *et al.*, 2009). The reasons behind the contradictory findings of this study are still unclear, although it is possible that the role of tensin3 during migration in 3D microenvironments is simply cell type-dependent, as is the case in the 2D setting. The role of tensin1 during 3D cell migration has not previously been described, although, given the highly conserved nature of the N- and C-termini of the large tensins, it is not surprising that depletion of tensin1 elicited a similar migratory phenotype to tensin2 and 3 knockdown. The simultaneous knockdown of tensin1, 2 and 3 was shown to reduce invasive migration more than the individual knockdown of tensin1, 2 or 3 in both DNA3 and Rab25 cells. However, the effect of triple tensin knockdown was not cumulative, which suggests that the three large tensin isoforms contribute towards 3D migration through overlapping but distinct mechanisms.

In an attempt to validate these findings, I also investigated A2780 cell migration on cell-derived matrix (CDM), a relatively thick yet pliable matrix composed mainly of fibrillar collagen and FN that mimics many aspects of connective tissue (Cukierman *et al.*, 2001). The over-expression of Rab25 in the A2780 cell line promotes a highly persistent mode of migration on CDM that is characterised by the extension of long

pseudopodia, and is driven by the localisation of integrin recycling vesicles/endosomes to the pseudopodial tips, which serve to sequester integrins at the front of the cell (Caswell *et al.*, 2007). The siRNA-directed depletion of each tensin isoform in Rab25 cells was shown to reduce pseudopod length, a quantitative index of invasive morphology (Figure 5.10). Moreover, the simultaneous depletion of all three tensins further reduced pseudopod length, although the reduction was not cumulative, which is similar to what was observed in the Matrigel-plug invasion assay. The magnitude of the difference in cell length between control and triple tensin knockdown cells, albeit small, was comparable to the difference between Rab25 and DNA3 cells (Caswell *et al.*, 2007), indicating that tensin depletion compromises this indicator of the invasive phenotype. Moreover, when the migration of control and triple tensin knockdown cells were compared by time-lapse video microscopy, it was apparent that tensin depletion induced a “slug-like” mode of migration characteristic of A2780 cells lacking Rab25 expression. Furthermore, tensin depletion significantly reduced the directional persistence of migration, which is known to correlate with invasiveness in this cell line (Figure 5.12). Collectively, these data support the hypothesis that tensin is required for the highly invasive 3D migration of Rab25 cells.

5.3.2 Validation of siRNA Specificity

RNAi is fast becoming the method of choice for functional inhibition of gene expression (Huppi *et al.*, 2005). However, care must be taken both in the design and validation of experiments in which this method is used. To confirm that the migration phenotype was specifically due to the depletion of tensin expression it would have been desirable to establish that re-expression of tensin in knockdown cells could restore maximal invasion. Whilst I confirmed that GFP-chicken tensin could be expressed in cells pre-treated with human tensin siRNA SMARTpools (data not shown), an insufficient proportion of the cells were transfected with GFP-chicken tensin for analysis by

invasion assay. When these cells were plated onto CDM, it was also apparent that expressing GFP-chicken tensin at high enough levels to be visualised caused toxicity. One way to overcome these problems would be to generate cell lines stably expressing siRNA-insensitive human tensin isoforms at low levels.

In light of these technical issues, I instead opted for an alternative control experiment, which was to show that individual tensin siRNA oligos were capable of inducing the same phenotypic effect as the tensin siRNA SMARTpools (Figures 5.6 and 5.11). These data provide partial assurance that the phenotypic effect of the tensin siRNA SMARTpools was due to specific knockdown of tensin, and was not due to non-specific off-target effects. It might also prove useful to establish whether there is a correlation between the efficacies of the individual tensin siRNA oligos and the severity of the migration phenotypes they induce.

5.3.3 The Mechanism of Tensin-Dependent 3D Migration

There are a number of potential mechanisms through which tensin could promote migration in 3D microenvironments. The simplest explanation is that tensin is required for the structural integrity of the adhesive contacts formed between cells and the 3D matrix (Cukierman *et al.*, 2001; Cukierman *et al.*, 2002), a conclusion supported by the observation that tensin1, 2 and 3 localise to cell-ECM junctions in Rab25 cells (Figures 5.7-5.9). This hypothesis could be investigated by comparing the stability of cell-ECM adhesions in control and tensin knockdown cells plated on CDM using FRAP analysis of GFP-tagged $\alpha 5$ integrin. Tensin may also promote 3D migration by modulating cytoskeletal dynamics through its ability to interact with the RhoGAP DLC-1 (Yam *et al.*, 2006a; Liao *et al.*, 2007; Qian *et al.*, 2007; Chan *et al.*, 2009; Qian *et al.*, 2009). The mesenchymal mode of 3D migration exhibited by A2780 cells is likely to require Rac-driven protrusion formation (Friedl and Wolf, 2009; Sanz-Moreno *et al.*, 2008). By

recruiting DLC-1 to adhesion sites, tensin could indirectly inactivate Rho, which would relieve the antagonistic effects of Rho on Rac activity (Sanz-Moreno *et al.*, 2008; Symons and Segall, 2009), thereby promoting mesenchymal 3D migration.

Rab25 and tensin are thought to interact with the same region of the β integrin cytoplasmic tail (McCleverty *et al.*, 2007) (Dr P Caswell - personal communication), which suggests that the binding of these two proteins is mutually exclusive. This raises the possibility that tensin is required for Rab25-driven invasive 3D migration by acting as the recipient of integrin recycled to the plasma membrane by Rab25. The fact that simultaneous depletion of tensin1, 2 and 3 had no effect on the capacity of Rab25 cells to recycle integrin back to the cell surface (Figure 5.13) suggests that tensin functions downstream of integrin recycling. However, this assay is performed in 2D on plastic (not CDM) and measures global integrin recycling (not specifically recycling within the pseudopodial tips). Therefore, it would be interesting to compare the ability of control and triple tensin knockdown Rab25 cells to recycle paGFP- α 5 integrin from Rab25-positive recycling vesicles/endosomes located towards the tip of pseudopodia to the plasma membrane. Given the limitations of the recycling assay, I investigated the requirement for tensin in the Rab25-driven sequestration of integrin in pseudopodial tips (Figure 5.14). By measuring the rate of integrin diffusion away from pseudopodial tips in control and triple tensin knockdown Rab25 cells using a photoactivatable form of GFP- α 5 integrin, it was found that tensin depletion does not impair the retention of integrin at the cell front. However, this assay measures the retention of all integrin, whereas tensin may only influence the diffusion of activated integrin contained within matrix adhesions. Thus, any effect of tensin depletion on the retention of activated integrins may be masked by the diffusion of inactive integrins which vastly exceed the amount of activated integrin.

Rab25 expression in A2780 cells increases the assembly of FN fibrils, which form on the dorsal and ventral surface of the cell, and also between cells grown at high confluence (Dr P Caswell - personal communication). These FN fibrils co-localise with adhesions rich in tensin and activated $\alpha 5$ integrin (as detected with the SNAKA51 antibody), although they are deficient in $\beta 3$ integrin (Dr P Caswell - personal communication). Since tensin has been implicated in the process of FN fibrillogenesis in 2D culture (Pankov *et al.*, 2000), and is required for FN-dependent invasive migration of Rab25 cells in 3D culture (Figure 5.3), it seemed appropriate to investigate the requirement for tensin in FN fibril formation in Rab25 cells. Interestingly, assembly of FN fibrils in Rab25 cells was severely compromised upon triple tensin knockdown (Figures 5.15, 1.16). This contrasts with the finding that triple tensin knockdown had minimal impact on the capacity of HFFs to assemble a FN matrix on the dorsal surface of the cell (Clark *et al.*, 2010), although it is unclear if the mechanism of FN fibril formation in A2780 cells is analogous to the process of FN fibrillogenesis in fibroblasts (Dr K Yamada - personal communication). However, others have demonstrated that the assembly of cell-FN-cell junctions is inhibited by the addition of a 70 kDa FN fragment known to inhibit FN fibrillogenesis in human fibroblasts (Robinson *et al.*, 2004; McKeown-Longo and Mosher, 1985), which suggests that these two processes are related.

Remodelling of ECM fibres, both through proteolytic degradation and realignment, is known to be required for mesenchymal migration in 3D microenvironments (Friedl and Wolf, 2009). Therefore, these data suggest that Rab25-driven invasive migration requires tensin-dependent remodelling of the FN matrix. This hypothesis could be investigated by plating control and tensin knockdown Rab25 cells onto CDM in media supplemented with fluorescently labelled FN, and analysing the alignment of FN fibres in the tracks left behind the cells as they migrate.

Chapter 6 Conclusions

Given the capacity of the large tensins to link integrins to the actin cytoskeleton it is not surprising that the tensins have been implicated in the control of integrin-mediated processes such as FN fibrillogenesis and cell migration. However, the relative contribution of human tensin1, 2 and 3 toward these processes has not previously been investigated, and was therefore addressed in the experimental work outlined in this thesis.

In order to delineate between the large human tensin proteins, I characterised the isoform specificities of several anti-tensin antibodies. These antibodies were then used alongside qPCR to determine the tensin expression profile of HFFs, the model cell line for the study of fibrillar adhesions and FN fibrillogenesis. HFFs were shown to express tensin1, 2 and 3 proteins, and tensin3 mRNA was more than 2-fold more abundant than the mRNA for tensin1 and 2, which were approximately equal. Unfortunately, most of the antibodies did not work for immunofluorescence microscopy so the sub-cellular localisation of the tensins was largely investigated using GFP-tagged proteins. Tensin1, 2 and 3 localised to both focal and fibrillar adhesions, although tensin2 was preferentially localised in focal adhesions and tensin3 in fibrillar adhesions (Clark *et al.*, 2010). This finding would suggest that in HFFs, the large human tensins perform subtly different roles. Given the higher expression levels of tensin3 in HFFs and its preferential localisation to fibrillar adhesions, I used an siRNA approach to investigate the role of the tensin3 isoform in FN fibrillogenesis, and found it to be partially required for this process. Unfortunately, the size of the data sets in this experiment were too small to perform statistical tests to confirm the significance of the observed difference. However, subsequent work in the lab has established that the individual and simultaneous knockdown of human tensin1, 2 and 3 in HFFs does not significantly affect FN fibrillogenesis (Clark *et al.*, 2010).

Although tensins are reported to play an important role in cell migration, it is unclear whether they act as positive or negative regulators. In an attempt to clarify the situation, I used over-expression and siRNA-mediated knockdown to investigate the roles of tensin1, 2 and 3 in both 2D and 3D migration. Interestingly, I found that modulating tensin expression did not affect the 2D migration of HFF, HEK293, or A2780 ovarian cancer cells. However, all three tensins were required for the 3D migration of A2780 cells in FN-containing microenvironments. Moreover, tensin was also shown to be required for the highly invasive 3D migration of A2780 cells stably expressing the small GTPase Rab25, which is up-regulated in aggressive breast and ovarian cancers (Cheng *et al.*, 2004), and is a component of the invasive signature of breast cancer cells *in vivo* and *in vitro* (Wang *et al.*, 2004). Rab25 over-expression was also found to promote tensin-dependent FN fibril formation in A2780 cells, which suggests that tensin promotes 3D migration by facilitating FN matrix remodelling. Further characterisation of these Rab25-driven adhesions using GFP-fusions has revealed that they contain all three large tensin isoforms along with paxillin and vinculin (Dr P Caswell – personal communication). This composition is more comparable to 3D-matrix adhesions than fibrillar adhesions, which supports our observation that tensin expression is required for 3D migration yet it is dispensable for fibrillar adhesion formation in 2D. In light of this new development it would be interesting to investigate the effects of tensin knockdown on the formation and stability of 3D-matrix adhesions using immunocytochemistry and FRAP, respectively.

The most significant finding of this study is that tensin is required for the migration of cancer cells through *in vivo*-like 3D matrices. However, the large tensins are frequently down-regulated in cancer cell lines and tissue samples compared to their normal counterparts. Collectively, these data suggest that tensin is up-regulated specifically in metastatic cancer. This hypothesis could be investigated using a variant of the *in vivo* invasion assay described by Wyckoff *et al.* (2000). In short, invasive tumour cells could

be collected from xenograph tumours using microneedles filled with Matrigel (supplemented with EGF as a chemoattractant) (Wyckoff *et al.*, 2000). The tensin expression profile of this subpopulation of invasive cancer cells could then be compared to that of the primary tumour. If tensin expression is required for the acquisition of an invasive phenotype then one might expect the collected cells to have higher tensin expression than the cells of the primary tumour.

The data presented in the final experimental chapter of this thesis show that all three large human tensins promote 3D cell migration *in vitro*. However, the differing phenotypes of the tensin1 and 3 knockout mice would suggest that despite their similarities the tensin proteins perform distinct roles *in vivo* (Lo *et al.*, 1997; Chiang *et al.*, 2005). Therefore, in future studies it will be important to identify the molecular basis of this functional divergence. Searching for binding partners of the poorly conserved central region of the large tensins and the N-terminal half of cten will likely represent the most fruitful approach to investigating this aspect of the tensin family.

References

- Abercrombie, M., and Dunn, G. A. (1975). Adhesions of fibroblasts to substratum during contact inhibition observed by interference reflection microscopy. *Exp Cell Res* 92, 57-62.
- Abercrombie, M., Heaysman, J. E., and Pegrum, S. M. (1971). The locomotion of fibroblasts in culture. IV. Electron microscopy of the leading lamella. *Exp Cell Res* 67, 359-367.
- Abram, C. L., and Lowell, C. A. (2009). Leukocyte adhesion deficiency syndrome: a controversy solved. *Immunol Cell Biol* 87, 440-442.
- Abu-Amero, S., Monk, D., Frost, J., Preece, M., Stanier, P., and Moore, G. E. (2008). The genetic aetiology of Silver-Russell syndrome. *J Med Genet* 45, 193-199.
- Adair, B. D., Xiong, J. P., Maddock, C., Goodman, S. L., Arnaout, M. A., and Yeager, M. (2005). Three-dimensional EM structure of the ectodomain of integrin $\{\alpha\}\{\beta\}_3$ in a complex with fibronectin. *J Cell Biol* 168, 1109-1118.
- Akin, O., and Mullins, R. D. (2008). Capping protein increases the rate of actin-based motility by promoting filament nucleation by the Arp2/3 complex. *Cell* 133, 841-851.
- Alam, N., Goel, H. L., Zarif, M. J., Butterfield, J. E., Perkins, H. M., Sansoucy, B. G., Sawyer, T. K., and Languino, L. R. (2007). The integrin-growth factor receptor duet. *J Cell Physiol* 213, 649-653.
- Albasri, A., Seth, R., Jackson, D., Benhasouna, A., Crook, S., Nateri, A. S., Chapman, R., and Ilyas, M. (2009). C-terminal Tensin-like (CTEN) is an oncogene which alters cell motility possibly through repression of E-cadherin in colorectal cancer. *J Pathol* 218, 57-65.
- Alberts, A. S., Bouquin, N., Johnston, L. H., and Treisman, R. (1998). Analysis of RhoA-binding proteins reveals an interaction domain conserved in heterotrimeric G protein beta subunits and the yeast response regulator protein Skn7. *J Biol Chem* 273, 8616-8622.
- Alberts, B. (2002). *Molecular biology of the cell*, 4th edn (New York, Garland Science).
- Alexandrova, A. Y., Arnold, K., Schaub, S., Vasiliev, J. M., Meister, J. J., Bershadsky, A. D., and Verkhovsky, A. B. (2008). Comparative dynamics of retrograde actin flow and focal adhesions: formation of nascent adhesions triggers transition from fast to slow flow. *PLoS One* 3, e3234.
- Allen, W. E., Zicha, D., Ridley, A. J., and Jones, G. E. (1998). A role for Cdc42 in macrophage chemotaxis. *J Cell Biol* 141, 1147-1157.

Amano, M., Ito, M., Kimura, K., Fukata, Y., Chihara, K., Nakano, T., Matsuura, Y., and Kaibuchi, K. (1996). Phosphorylation and activation of myosin by Rho-associated kinase (Rho-kinase). *J Biol Chem* *271*, 20246-20249.

Aota, S., Nomizu, M., and Yamada, K. M. (1994). The short amino acid sequence Pro-His-Ser-Arg-Asn in human fibronectin enhances cell-adhesive function. *J Biol Chem* *269*, 24756-24761.

Arnaout, M. A., Goodman, S. L., and Xiong, J. P. (2007). Structure and mechanics of integrin-based cell adhesion. *Curr Opin Cell Biol* *19*, 495-507.

Askari, J. A., Buckley, P. A., Mould, A. P., and Humphries, M. J. (2009). Linking integrin conformation to function. *J Cell Sci* *122*, 165-170.

Aspenstrom, P., Fransson, A., and Saras, J. (2004). Rho GTPases have diverse effects on the organization of the actin filament system. *Biochem J* *377*, 327-337.

Aspenstrom, P., Lindberg, U., and Hall, A. (1996). Two GTPases, Cdc42 and Rac, bind directly to a protein implicated in the immunodeficiency disorder Wiskott-Aldrich syndrome. *Curr Biol* *6*, 70-75.

Auger, K. R., Songyang, Z., Lo, S. H., Roberts, T. M., and Chen, L. B. (1996). Platelet-derived growth factor-induced formation of tensin and phosphoinositide 3-kinase complexes. *J Biol Chem* *271*, 23452-23457.

Ballestrem, C., Hinz, B., Imhof, B. A., and Wehrle-Haller, B. (2001). Marching at the front and dragging behind: differential alphaVbeta3-integrin turnover regulates focal adhesion behavior. *J Cell Biol* *155*, 1319-1332.

Baneyx, G., Baugh, L., and Vogel, V. (2002). Fibronectin extension and unfolding within cell matrix fibrils controlled by cytoskeletal tension. *Proc Natl Acad Sci U S A* *99*, 5139-5143.

Banno, A., and Ginsberg, M. H. (2008). Integrin activation. *Biochem Soc Trans* *36*, 229-234.

Bass, M. D., Roach, K. A., Morgan, M. R., Mostafavi-Pour, Z., Schoen, T., Muramatsu, T., Mayer, U., Ballestrem, C., Spatz, J. P., and Humphries, M. J. (2007). Syndecan-4-dependent Rac1 regulation determines directional migration in response to the extracellular matrix. *J Cell Biol* *177*, 527-538.

Beacham, D. A., Amatangelo, M. D., and Cukierman, E. (2007). Preparation of extracellular matrices produced by cultured and primary fibroblasts. *Curr Protoc Cell Biol* *Chapter 10*, Unit 10 19.

Bear, J. E. (2008). Follow the monomer. *Cell* *133*, 765-767.

Beckerle, M. C., Burrige, K., DeMartino, G. N., and Croall, D. E. (1987). Colocalization of calcium-dependent protease II and one of its substrates at sites of cell adhesion. *Cell* *51*, 569-577.

- Bellis, S. L., Miller, J. T., and Turner, C. E. (1995). Characterization of tyrosine phosphorylation of paxillin in vitro by focal adhesion kinase. *J Biol Chem* *270*, 17437-17441.
- Beningo, K. A., Dembo, M., Kaverina, I., Small, J. V., and Wang, Y. L. (2001). Nascent focal adhesions are responsible for the generation of strong propulsive forces in migrating fibroblasts. *J Cell Biol* *153*, 881-888.
- Beningo, K. A., Dembo, M., and Wang, Y. L. (2004). Responses of fibroblasts to anchorage of dorsal extracellular matrix receptors. *Proc Natl Acad Sci U S A* *101*, 18024-18029.
- Benzing, T., Gerke, P., Hopker, K., Hildebrandt, F., Kim, E., and Walz, G. (2001). Nephrocystin interacts with Pyk2, p130(Cas), and tensin and triggers phosphorylation of Pyk2. *Proc Natl Acad Sci U S A* *98*, 9784-9789.
- Bergmann, J. E., Kupfer, A., and Singer, S. J. (1983). Membrane insertion at the leading edge of motile fibroblasts. *Proc Natl Acad Sci U S A* *80*, 1367-1371.
- Bershadsky, A. D., Tint, I. S., Neyfakh, A. A., Jr., and Vasiliev, J. M. (1985). Focal contacts of normal and RSV-transformed quail cells. Hypothesis of the transformation-induced deficient maturation of focal contacts. *Exp Cell Res* *158*, 433-444.
- Bhatt, A., Kaverina, I., Otey, C., and Huttenlocher, A. (2002). Regulation of focal complex composition and disassembly by the calcium-dependent protease calpain. *J Cell Sci* *115*, 3415-3425.
- Birchmeier, W., Libermann, T. A., Imhof, B. A., and Kreis, T. E. (1982). Intracellular and extracellular components involved in the formation of ventral surfaces of fibroblasts. *Cold Spring Harb Symp Quant Biol* *46 Pt 2*, 755-767.
- Block, M. R., Badowski, C., Millon-Fremillon, A., Bouvard, D., Bouin, A. P., Faurobert, E., Gerber-Scokaert, D., Planus, E., and Albiges-Rizo, C. (2008). Podosome-type adhesions and focal adhesions, so alike yet so different. *Eur J Cell Biol* *87*, 491-506.
- Bockholt, S. M., and Burridge, K. (1993). Cell spreading on extracellular matrix proteins induces tyrosine phosphorylation of tensin. *J Biol Chem* *268*, 14565-14567.
- Borsani, G., Piovani, G., Zoppi, N., Bertini, V., Bini, R., Notarangelo, L., and Barlati, S. (2008). Cytogenetic and molecular characterization of a de-novo t(2p;7p) translocation involving TNS3 and EXOC6B genes in a boy with a complex syndromic phenotype. *Eur J Med Genet* *51*, 292-302.
- Boucaut, J. C., Johnson, K. E., Darribere, T., Shi, D. L., Riou, J. F., Bache, H. B., and Delarue, M. (1990). Fibronectin-rich fibrillar extracellular matrix controls cell migration during amphibian gastrulation. *Int J Dev Biol* *34*, 139-147.

Boulter, E., and Van Obberghen-Schilling, E. (2006). Integrin-linked kinase and its partners: a modular platform regulating cell-matrix adhesion dynamics and cytoskeletal organization. *Eur J Cell Biol* *85*, 255-263.

Bouvard, D., Brakebusch, C., Gustafsson, E., Aszodi, A., Bengtsson, T., Berna, A., and Fassler, R. (2001). Functional consequences of integrin gene mutations in mice. *Circ Res* *89*, 211-223.

Broussard, J. A., Webb, D. J., and Kaverina, I. (2008). Asymmetric focal adhesion disassembly in motile cells. *Curr Opin Cell Biol* *20*, 85-90.

Brown, C. M., Hebert, B., Kolin, D. L., Zareno, J., Whitmore, L., Horwitz, A. R., and Wiseman, P. W. (2006). Probing the integrin-actin linkage using high-resolution protein velocity mapping. *J Cell Sci* *119*, 5204-5214.

Buccione, R., Caldieri, G., and Ayala, I. (2009). Invadopodia: specialized tumor cell structures for the focal degradation of the extracellular matrix. *Cancer Metastasis Rev* *28*, 137-149.

Buchsbaum, R. J. (2007). Rho activation at a glance. *J Cell Sci* *120*, 1149-1152.

Burns, S., Thrasher, A. J., Blundell, M. P., Machesky, L., and Jones, G. E. (2001). Configuration of human dendritic cell cytoskeleton by Rho GTPases, the WAS protein, and differentiation. *Blood* *98*, 1142-1149.

Cai, Y., Biais, N., Giannone, G., Tanase, M., Jiang, G., Hofman, J. M., Wiggins, C. H., Silberzan, P., Buguin, A., Ladoux, B., and Sheetz, M. P. (2006). Nonmuscle myosin IIA-dependent force inhibits cell spreading and drives F-actin flow. *Biophys J* *91*, 3907-3920.

Calderwood, D. A. (2004a). Integrin activation. *J Cell Sci* *117*, 657-666.

Calderwood, D. A. (2004b). Talin controls integrin activation. *Biochem Soc Trans* *32*, 434-437.

Calderwood, D. A., Fujioka, Y., de Pereda, J. M., Garcia-Alvarez, B., Nakamoto, T., Margolis, B., McGlade, C. J., Liddington, R. C., and Ginsberg, M. H. (2003). Integrin beta cytoplasmic domain interactions with phosphotyrosine-binding domains: a structural prototype for diversity in integrin signaling. *Proc Natl Acad Sci U S A* *100*, 2272-2277.

Carrier, M. F., and Pantaloni, D. (1997). Control of actin dynamics in cell motility. *J Mol Biol* *269*, 459-467.

Carrier, M. F., Ressad, F., and Pantaloni, D. (1999). Control of actin dynamics in cell motility. Role of ADF/cofilin. *J Biol Chem* *274*, 33827-33830.

Carragher, N. O., and Frame, M. C. (2004). Focal adhesion and actin dynamics: a place where kinases and proteases meet to promote invasion. *Trends Cell Biol* *14*, 241-249.

Carragher, N. O., Levkau, B., Ross, R., and Raines, E. W. (1999). Degraded collagen fragments promote rapid disassembly of smooth muscle focal adhesions that correlates with cleavage of pp125(FAK), paxillin, and talin. *J Cell Biol* 147, 619-630.

Carragher, N. O., Walker, S. M., Scott Carragher, L. A., Harris, F., Sawyer, T. K., Brunton, V. G., Ozanne, B. W., and Frame, M. C. (2006). Calpain 2 and Src dependence distinguishes mesenchymal and amoeboid modes of tumour cell invasion: a link to integrin function. *Oncogene* 25, 5726-5740.

Carragher, N. O., Westhoff, M. A., Fincham, V. J., Schaller, M. D., and Frame, M. C. (2003). A novel role for FAK as a protease-targeting adaptor protein: regulation by p42 ERK and Src. *Curr Biol* 13, 1442-1450.

Carrell, N. A., Fitzgerald, L. A., Steiner, B., Erickson, H. P., and Phillips, D. R. (1985). Structure of human platelet membrane glycoproteins IIb and IIIa as determined by electron microscopy. *J Biol Chem* 260, 1743-1749.

Cary, L. A., Han, D. C., Polte, T. R., Hanks, S. K., and Guan, J. L. (1998). Identification of p130Cas as a mediator of focal adhesion kinase-promoted cell migration. *J Cell Biol* 140, 211-221.

Caswell, P. T., Chan, M., Lindsay, A. J., McCaffrey, M. W., Boettiger, D., and Norman, J. C. (2008). Rab-coupling protein coordinates recycling of alpha5beta1 integrin and EGFR1 to promote cell migration in 3D microenvironments. *J Cell Biol* 183, 143-155.

Caswell, P. T., and Norman, J. C. (2006). Integrin trafficking and the control of cell migration. *Traffic* 7, 14-21.

Caswell, P. T., Spence, H. J., Parsons, M., White, D. P., Clark, K., Cheng, K. W., Mills, G. B., Humphries, M. J., Messent, A. J., Anderson, K. I., *et al.* (2007). Rab25 associates with alpha5beta1 integrin to promote invasive migration in 3D microenvironments. *Dev Cell* 13, 496-510.

Chan, L. K., Ko, F. C., Ng, I. O., and Yam, J. W. (2009). Deleted in liver cancer 1 (DLC1) utilizes a novel binding site for Tensin2 PTB domain interaction and is required for tumor-suppressive function. *PLoS One* 4, e5572.

Charest, P. G., and Firtel, R. A. (2007). Big roles for small GTPases in the control of directed cell movement. *Biochem J* 401, 377-390.

Chen, H., Duncan, I. C., Bozorgchami, H., and Lo, S. H. (2002). Tensin1 and a previously undocumented family member, tensin2, positively regulate cell migration. *Proc Natl Acad Sci U S A* 99, 733-738.

Chen, H., Ishii, A., Wong, W. K., Chen, L. B., and Lo, S. H. (2000). Molecular characterization of human tensin. *Biochem J* 351 Pt 2, 403-411.

Chen, H., and Lo, S. H. (2003). Regulation of tensin-promoted cell migration by its focal adhesion binding and Src homology domain 2. *Biochem J* 370, 1039-1045.

- Chen, W. T. (1981). Mechanism of retraction of the trailing edge during fibroblast movement. *J Cell Biol* 90, 187-200.
- Chen, W. T., and Singer, S. J. (1982). Immunoelectron microscopic studies of the sites of cell-substratum and cell-cell contacts in cultured fibroblasts. *J Cell Biol* 95, 205-222.
- Cheng, K. W., Lahad, J. P., Kuo, W. L., Lapuk, A., Yamada, K., Auersperg, N., Liu, J., Smith-McCune, K., Lu, K. H., Fishman, D., *et al.* (2004). The RAB25 small GTPase determines aggressiveness of ovarian and breast cancers. *Nat Med* 10, 1251-1256.
- Chiang, M. K., Liao, Y. C., Kuwabara, Y., and Lo, S. H. (2005). Inactivation of tensin3 in mice results in growth retardation and postnatal lethality. *Dev Biol* 279, 368-377.
- Chigae, A., Waller, A., Zwartz, G. J., Buranda, T., and Sklar, L. A. (2007). Regulation of cell adhesion by affinity and conformational unbending of alpha4beta1 integrin. *J Immunol* 178, 6828-6839.
- Ching, Y. P., Wong, C. M., Chan, S. F., Leung, T. H., Ng, D. C., Jin, D. Y., and Ng, I. O. (2003). Deleted in liver cancer (DLC) 2 encodes a RhoGAP protein with growth suppressor function and is underexpressed in hepatocellular carcinoma. *J Biol Chem* 278, 10824-10830.
- Chodniewicz, D., and Klemke, R. L. (2004). Regulation of integrin-mediated cellular responses through assembly of a CAS/Crk scaffold. *Biochim Biophys Acta* 1692, 63-76.
- Choi, C. K., Vicente-Manzanares, M., Zareno, J., Whitmore, L. A., Mogilner, A., and Horwitz, A. R. (2008). Actin and alpha-actinin orchestrate the assembly and maturation of nascent adhesions in a myosin II motor-independent manner. *Nat Cell Biol* 10, 1039-1050.
- Chrzanowska-Wodnicka, M., and Burridge, K. (1996). Rho-stimulated contractility drives the formation of stress fibers and focal adhesions. *J Cell Biol* 133, 1403-1415.
- Chuang, J. Z., Lin, D. C., and Lin, S. (1995). Molecular cloning, expression, and mapping of the high affinity actin-capping domain of chicken cardiac tensin. *J Cell Biol* 128, 1095-1109.
- Chung, C. Y., Potikyan, G., and Firtel, R. A. (2001). Control of cell polarity and chemotaxis by Akt/PKB and PI3 kinase through the regulation of PAKa. *Mol Cell* 7, 937-947.
- Clark, E. A., King, W. G., Brugge, J. S., Symons, M., and Hynes, R. O. (1998). Integrin-mediated signals regulated by members of the rho family of GTPases. *J Cell Biol* 142, 573-586.
- Clark, K., Howe, J. D., Pullar, C. E., Green, J. A., Artym, V. V., Yamada, K. M., and Critchley, D. R. (2010). Tensin 2 modulates cell contractility in 3D collagen gels through the RhoGAP DLC1. *J Cell Biochem* 109, 808-817.

Clark, K., Langeslag, M., Figdor, C. G., and van Leeuwen, F. N. (2007). Myosin II and mechanotransduction: a balancing act. *Trends Cell Biol* 17, 178-186.

Clark, K., Pankov, R., Travis, M. A., Askari, J. A., Mould, A. P., Craig, S. E., Newham, P., Yamada, K. M., and Humphries, M. J. (2005). A specific alpha5beta1-integrin conformation promotes directional integrin translocation and fibronectin matrix formation. *J Cell Sci* 118, 291-300.

Clark, R. A. (1990). Fibronectin matrix deposition and fibronectin receptor expression in healing and normal skin. *J Invest Dermatol* 94, 128S-134S.

Cohen, M., Kam, Z., Addadi, L., and Geiger, B. (2006). Dynamic study of the transition from hyaluronan- to integrin-mediated adhesion in chondrocytes. *Embo J* 25, 302-311.

Coussens, L. M., Fingleton, B., and Matrisian, L. M. (2002). Matrix metalloproteinase inhibitors and cancer: trials and tribulations. *Science* 295, 2387-2392.

Critchley, D. R. (2004). Cytoskeletal proteins talin and vinculin in integrin-mediated adhesion. *Biochem Soc Trans* 32, 831-836.

Croft, D. R., and Olson, M. F. (2008). Regulating the conversion between rounded and elongated modes of cancer cell movement. *Cancer Cell* 14, 349-351.

Crowley, E., and Horwitz, A. F. (1995). Tyrosine phosphorylation and cytoskeletal tension regulate the release of fibroblast adhesions. *J Cell Biol* 131, 525-537.

Cui, Y., Liao, Y. C., and Lo, S. H. (2004). Epidermal growth factor modulates tyrosine phosphorylation of a novel tensin family member, tensin3. *Mol Cancer Res* 2, 225-232.

Cukierman, E., Pankov, R., Stevens, D. R., and Yamada, K. M. (2001). Taking cell-matrix adhesions to the third dimension. *Science* 294, 1708-1712.

Cukierman, E., Pankov, R., and Yamada, K. M. (2002). Cell interactions with three-dimensional matrices. *Curr Opin Cell Biol* 14, 633-639.

Danen, E. H., and Yamada, K. M. (2001). Fibronectin, integrins, and growth control. *J Cell Physiol* 189, 1-13.

Davis, S., Lu, M. L., Lo, S. H., Lin, S., Butler, J. A., Druker, B. J., Roberts, T. M., An, Q., and Chen, L. B. (1991). Presence of an SH2 domain in the actin-binding protein tensin. *Science* 252, 712-715.

DerMardirossian, C., and Bokoch, G. M. (2005). GDIs: central regulatory molecules in Rho GTPase activation. *Trends Cell Biol* 15, 356-363.

Destaing, O., Saltel, F., Geminard, J. C., Jurdic, P., and Bard, F. (2003). Podosomes display actin turnover and dynamic self-organization in osteoclasts expressing actin-green fluorescent protein. *Mol Biol Cell* 14, 407-416.

Didry, D., Carlier, M. F., and Pantaloni, D. (1998). Synergy between actin depolymerizing factor/cofilin and profilin in increasing actin filament turnover. *J Biol Chem* 273, 25602-25611.

DiMilla, P. A., Stone, J. A., Quinn, J. A., Albelda, S. M., and Lauffenburger, D. A. (1993). Maximal migration of human smooth muscle cells on fibronectin and type IV collagen occurs at an intermediate attachment strength. *J Cell Biol* 122, 729-737.

Duband, J. L., Rocher, S., Yamada, K. M., and Thiery, J. P. (1986). Interactions of migrating neural crest cells with fibronectin. *Prog Clin Biol Res* 226, 127-139.

Durkin, M. E., Avner, M. R., Huh, C. G., Yuan, B. Z., Thorgeirsson, S. S., and Popescu, N. C. (2005). DLC-1, a Rho GTPase-activating protein with tumor suppressor function, is essential for embryonic development. *FEBS Lett* 579, 1191-1196.

Durkin, M. E., Ullmannova, V., Guan, M., and Popescu, N. C. (2007). Deleted in liver cancer 3 (DLC-3), a novel Rho GTPase-activating protein, is downregulated in cancer and inhibits tumor cell growth. *Oncogene* 26, 4580-4589.

Durkin, M. E., Yuan, B. Z., Thorgeirsson, S. S., and Popescu, N. C. (2002). Gene structure, tissue expression, and linkage mapping of the mouse DLC-1 gene (Arhgap7). *Gene* 288, 119-127.

Dyson, H. J., and Wright, P. E. (2002). Coupling of folding and binding for unstructured proteins. *Curr Opin Struct Biol* 12, 54-60.

Dyson, H. J., and Wright, P. E. (2005). Intrinsically unstructured proteins and their functions. *Nat Rev Mol Cell Biol* 6, 197-208.

Emsley, J., Knight, C. G., Farndale, R. W., Barnes, M. J., and Liddington, R. C. (2000). Structural basis of collagen recognition by integrin alpha2beta1. *Cell* 101, 47-56.

Erickson, H. P. (1994). Reversible unfolding of fibronectin type III and immunoglobulin domains provides the structural basis for stretch and elasticity of titin and fibronectin. *Proc Natl Acad Sci U S A* 91, 10114-10118.

Etienne-Manneville, S. (2004). Cdc42--the centre of polarity. *J Cell Sci* 117, 1291-1300.

Etienne-Manneville, S., and Hall, A. (2001). Integrin-mediated activation of Cdc42 controls cell polarity in migrating astrocytes through PKCzeta. *Cell* 106, 489-498.

Etienne-Manneville, S., and Hall, A. (2003). Cdc42 regulates GSK-3beta and adenomatous polyposis coli to control cell polarity. *Nature* 421, 753-756.

Eto, M., Kirkbride, J., Elliott, E., Lo, S. H., and Brautigan, D. L. (2007). Association of the tensin N-terminal protein-tyrosine phosphatase domain with the alpha isoform of protein phosphatase-1 in focal adhesions. *J Biol Chem* 282, 17806-17815.

Evans, R., Patzak, I., Svensson, L., De Filippo, K., Jones, K., McDowall, A., and Hogg, N. (2009). Integrins in immunity. *J Cell Sci* 122, 215-225.

Even-Ram, S., Doyle, A. D., Conti, M. A., Matsumoto, K., Adelstein, R. S., and Yamada, K. M. (2007). Myosin IIA regulates cell motility and actomyosin-microtubule crosstalk. *Nat Cell Biol* 9, 299-309.

Even-Ram, S., and Yamada, K. M. (2005). Cell migration in 3D matrix. *Curr Opin Cell Biol* 17, 524-532.

Ezratty, E. J., Partridge, M. A., and Gundersen, G. G. (2005). Microtubule-induced focal adhesion disassembly is mediated by dynamin and focal adhesion kinase. *Nat Cell Biol* 7, 581-590.

Fackler, O. T., and Grosse, R. (2008). Cell motility through plasma membrane blebbing. *J Cell Biol* 181, 879-884.

Fassler, R., and Meyer, M. (1995). Consequences of lack of beta 1 integrin gene expression in mice. *Genes Dev* 9, 1896-1908.

Fernandez-Sauze, S., Grall, D., Cseh, B., and Van Obberghen-Schilling, E. (2009). Regulation of fibronectin matrix assembly and capillary morphogenesis in endothelial cells by Rho family GTPases. *Exp Cell Res* 315, 2092-2104.

Fincham, V. J., and Frame, M. C. (1998). The catalytic activity of Src is dispensable for translocation to focal adhesions but controls the turnover of these structures during cell motility. *Embo J* 17, 81-92.

Fisher, L. W., Torchia, D. A., Fohr, B., Young, M. F., and Fedarko, N. S. (2001). Flexible structures of SIBLING proteins, bone sialoprotein, and osteopontin. *Biochem Biophys Res Commun* 280, 460-465.

Flevaris, P., Stojanovic, A., Gong, H., Chishti, A., Welch, E., and Du, X. (2007). A molecular switch that controls cell spreading and retraction. *J Cell Biol* 179, 553-565.

Fogerty, F. J., Akiyama, S. K., Yamada, K. M., and Mosher, D. F. (1990). Inhibition of binding of fibronectin to matrix assembly sites by anti-integrin (alpha 5 beta 1) antibodies. *J Cell Biol* 111, 699-708.

Franco, S. J., and Huttenlocher, A. (2005). Regulating cell migration: calpains make the cut. *J Cell Sci* 118, 3829-3838.

Friedl, P., and Bocker, E. B. (2000). The biology of cell locomotion within three-dimensional extracellular matrix. *Cell Mol Life Sci* 57, 41-64.

Friedl, P., and Gilmour, D. (2009). Collective cell migration in morphogenesis, regeneration and cancer. *Nat Rev Mol Cell Biol* 10, 445-457.

Friedl, P., Maaser, K., Klein, C. E., Niggemann, B., Krohne, G., and Zanker, K. S. (1997). Migration of highly aggressive MV3 melanoma cells in 3-dimensional collagen lattices results in local matrix reorganization and shedding of alpha2 and beta1 integrins and CD44. *Cancer Res* 57, 2061-2070.

Friedl, P., and Wolf, K. (2009). Proteolytic interstitial cell migration: a five-step process. *Cancer Metastasis Rev* 28, 129-135.

Frisch, S. M., and Francis, H. (1994). Disruption of epithelial cell-matrix interactions induces apoptosis. *J Cell Biol* 124, 619-626.

Fukuda, T., Chen, K., Shi, X., and Wu, C. (2003). PINCH-1 is an obligate partner of integrin-linked kinase (ILK) functioning in cell shape modulation, motility, and survival. *J Biol Chem* 278, 51324-51333.

Galbraith, C. G., Yamada, K. M., and Galbraith, J. A. (2007). Polymerizing actin fibers position integrins primed to probe for adhesion sites. *Science* 315, 992-995.

Garcia-Alvarez, B., de Pereda, J. M., Calderwood, D. A., Ulmer, T. S., Critchley, D., Campbell, I. D., Ginsberg, M. H., and Liddington, R. C. (2003). Structural determinants of integrin recognition by talin. *Mol Cell* 11, 49-58.

George, E. L., Georges-Labouesse, E. N., Patel-King, R. S., Rayburn, H., and Hynes, R. O. (1993). Defects in mesoderm, neural tube and vascular development in mouse embryos lacking fibronectin. *Development* 119, 1079-1091.

Gingras, A. R., Ziegler, W. H., Frank, R., Barsukov, I. L., Roberts, G. C., Critchley, D. R., and Emsley, J. (2005). Mapping and consensus sequence identification for multiple vinculin binding sites within the talin rod. *J Biol Chem* 280, 37217-37224.

Glading, A., Chang, P., Lauffenburger, D. A., and Wells, A. (2000). Epidermal growth factor receptor activation of calpain is required for fibroblast motility and occurs via an ERK/MAP kinase signaling pathway. *J Biol Chem* 275, 2390-2398.

Gomes, E. R., Jani, S., and Gundersen, G. G. (2005). Nuclear movement regulated by Cdc42, MRCK, myosin, and actin flow establishes MTOC polarization in migrating cells. *Cell* 121, 451-463.

Goodison, S., Yuan, J., Sloan, D., Kim, R., Li, C., Popescu, N. C., and Urquidi, V. (2005). The RhoGAP protein DLC-1 functions as a metastasis suppressor in breast cancer cells. *Cancer Res* 65, 6042-6053.

Green, C. E., Pearson, D. N., Camphausen, R. T., Staunton, D. E., and Simon, S. I. (2004). Shear-dependent capping of L-selectin and P-selectin glycoprotein ligand 1 by E-selectin signals activation of high-avidity beta2-integrin on neutrophils. *J Immunol* 172, 7780-7790.

Green, J. A., Berrier, A. L., Pankov, R., and Yamada, K. M. (2009). beta1 integrin cytoplasmic domain residues selectively modulate fibronectin matrix assembly and cell spreading through talin and Akt-1. *J Biol Chem* 284, 8148-8159.

Green, J. A., and Yamada, K. M. (2007). Three-dimensional microenvironments modulate fibroblast signaling responses. *Adv Drug Deliv Rev* 59, 1293-1298.

Guan, J. L., and Hynes, R. O. (1990). Lymphoid cells recognize an alternatively spliced segment of fibronectin via the integrin receptor alpha 4 beta 1. *Cell* 60, 53-61.

Hafizi, S., Alindri, F., Karlsson, R., and Dahlback, B. (2002). Interaction of Axl receptor tyrosine kinase with C1-TEN, a novel C1 domain-containing protein with homology to tensin. *Biochem Biophys Res Commun* 299, 793-800.

- Hafizi, S., Ibraimi, F., and Dahlback, B. (2005). C1-TEN is a negative regulator of the Akt/PKB signal transduction pathway and inhibits cell survival, proliferation, and migration. *Faseb J* 19, 971-973.
- Hannigan, G. E., Leung-Hagesteijn, C., Fitz-Gibbon, L., Coppolino, M. G., Radeva, G., Filmus, J., Bell, J. C., and Dedhar, S. (1996). Regulation of cell adhesion and anchorage-dependent growth by a new beta 1-integrin-linked protein kinase. *Nature* 379, 91-96.
- Harburger, D. S., and Calderwood, D. A. (2009). Integrin signalling at a glance. *J Cell Sci* 122, 159-163.
- Haynie, D. T., and Ponting, C. P. (1996). The N-terminal domains of tensin and auxilin are phosphatase homologues. *Protein Sci* 5, 2643-2646.
- Hendey, B., Klee, C. B., and Maxfield, F. R. (1992). Inhibition of neutrophil chemokinesis on vitronectin by inhibitors of calcineurin. *Science* 258, 296-299.
- Hennigan, R. F., Hawker, K. L., and Ozanne, B. W. (1994). Fos-transformation activates genes associated with invasion. *Oncogene* 9, 3591-3600.
- Hervy, M., Hoffman, L., and Beckerle, M. C. (2006). From the membrane to the nucleus and back again: bifunctional focal adhesion proteins. *Curr Opin Cell Biol* 18, 524-532.
- Hillis, G. S., and MacLeod, A. M. (1996). Integrins and disease. *Clin Sci (Lond)* 91, 639-650.
- Homma, Y., and Emori, Y. (1995). A dual functional signal mediator showing RhoGAP and phospholipase C-delta stimulating activities. *Embo J* 14, 286-291.
- Hotulainen, P., and Lappalainen, P. (2006). Stress fibers are generated by two distinct actin assembly mechanisms in motile cells. *J Cell Biol* 173, 383-394.
- Hu, K., Ji, L., Applegate, K. T., Danuser, G., and Waterman-Storer, C. M. (2007). Differential transmission of actin motion within focal adhesions. *Science* 315, 111-115.
- Huang, X., Beullens, M., Zhang, J., Zhou, Y., Nicolaescu, E., Lesage, B., Hu, Q., Wu, J., Bollen, M., and Shi, Y. (2009). Structure and Function of the Two Tandem WW Domains of the Pre-mRNA Splicing Factor FBP21 (Formin-binding Protein 21). *J Biol Chem* 284, 25375-25387.
- Hug, C., Jay, P. Y., Reddy, I., McNally, J. G., Bridgman, P. C., Elson, E. L., and Cooper, J. A. (1995). Capping protein levels influence actin assembly and cell motility in dictyostelium. *Cell* 81, 591-600.
- Hughes, P. E., Diaz-Gonzalez, F., Leong, L., Wu, C., McDonald, J. A., Shattil, S. J., and Ginsberg, M. H. (1996). Breaking the integrin hinge. A defined structural constraint regulates integrin signaling. *J Biol Chem* 271, 6571-6574.
- Humphries, J. D., Byron, A., and Humphries, M. J. (2006). Integrin ligands at a glance. *J Cell Sci* 119, 3901-3903.

Humphries, M. J. (2000). Integrin structure. *Biochem Soc Trans* 28, 311-339.

Huppi, K., Martin, S. E., and Caplen, N. J. (2005). Defining and assaying RNAi in mammalian cells. *Mol Cell* 17, 1-10.

Hurley, J. H. (2006). Membrane binding domains. *Biochim Biophys Acta* 1761, 805-811.

Huttenlocher, A., Ginsberg, M. H., and Horwitz, A. F. (1996). Modulation of cell migration by integrin-mediated cytoskeletal linkages and ligand-binding affinity. *J Cell Biol* 134, 1551-1562.

Huttenlocher, A., Palecek, S. P., Lu, Q., Zhang, W., Mellgren, R. L., Lauffenburger, D. A., Ginsberg, M. H., and Horwitz, A. F. (1997). Regulation of cell migration by the calcium-dependent protease calpain. *J Biol Chem* 272, 32719-32722.

Hynes, R. O. (1990). *Fibronectins* (New York, Springer-Verlag).

Hynes, R. O. (1996). Targeted mutations in cell adhesion genes: what have we learned from them? *Dev Biol* 180, 402-412.

Hynes, R. O. (2002). Integrins: bidirectional, allosteric signaling machines. *Cell* 110, 673-687.

Ilic, D., Furuta, Y., Kanazawa, S., Takeda, N., Sobue, K., Nakatsuji, N., Nomura, S., Fujimoto, J., Okada, M., and Yamamoto, T. (1995). Reduced cell motility and enhanced focal adhesion contact formation in cells from FAK-deficient mice. *Nature* 377, 539-544.

Ilic, D., Kovacic, B., Johkura, K., Schlaepfer, D. D., Tomasevic, N., Han, Q., Kim, J. B., Howerton, K., Baumbusch, C., Ogiwara, N., *et al.* (2004). FAK promotes organization of fibronectin matrix and fibrillar adhesions. *J Cell Sci* 117, 177-187.

Ishida, T., Ishida, M., Suero, J., Takahashi, M., and Berk, B. C. (1999). Agonist-stimulated cytoskeletal reorganization and signal transduction at focal adhesions in vascular smooth muscle cells require c-Src. *J Clin Invest* 103, 789-797.

Ishii, A., and Lo, S. H. (2001). A role of tensin in skeletal-muscle regeneration. *Biochem J* 356, 737-745.

Ishizaki, T., Maekawa, M., Fujisawa, K., Okawa, K., Iwamatsu, A., Fujita, A., Watanabe, N., Saito, Y., Kakizuka, A., Morii, N., and Narumiya, S. (1996). The small GTP-binding protein Rho binds to and activates a 160 kDa Ser/Thr protein kinase homologous to myotonic dystrophy kinase. *Embo J* 15, 1885-1893.

Itoh, R. E., Kurokawa, K., Ohba, Y., Yoshizaki, H., Mochizuki, N., and Matsuda, M. (2002). Activation of rac and cdc42 video imaged by fluorescent resonance energy transfer-based single-molecule probes in the membrane of living cells. *Mol Cell Biol* 22, 6582-6591.

- Janeway, C. (2005). Immunobiology : the immune system in health and disease, 6th edn (New York, Garland Science).
- Jay, P. Y., Pham, P. A., Wong, S. A., and Elson, E. L. (1995). A mechanical function of myosin II in cell motility. *J Cell Sci* 108 (Pt 1), 387-393.
- Jiang, B., Yamamura, S., Nelson, P. R., Mureebe, L., and Kent, K. C. (1996). Differential effects of platelet-derived growth factor isotypes on human smooth muscle cell proliferation and migration are mediated by distinct signaling pathways. *Surgery* 120, 427-431; discussion 432.
- Johnson, S. A., and Milner, M. J. (1987). The final stages of wing development in *Drosophila melanogaster*. *Tissue Cell* 19, 505-513.
- Katz, B. Z., Zamir, E., Bershadsky, A., Kam, Z., Yamada, K. M., and Geiger, B. (2000a). Physical state of the extracellular matrix regulates the structure and molecular composition of cell-matrix adhesions. *Mol Biol Cell* 11, 1047-1060.
- Katz, B. Z., Zohar, M., Teramoto, H., Matsumoto, K., Gutkind, J. S., Lin, D. C., Lin, S., and Yamada, K. M. (2000b). Tensin can induce JNK and p38 activation. *Biochem Biophys Res Commun* 272, 717-720.
- Katz, M., Amit, I., Citri, A., Shay, T., Carvalho, S., Lavi, S., Milanezi, F., Lyass, L., Amariglio, N., Jacob-Hirsch, J., *et al.* (2007). A reciprocal tensin-3-cten switch mediates EGF-driven mammary cell migration. *Nat Cell Biol* 9, 961-969.
- Kaverina, I., Krylyshkina, O., and Small, J. V. (1999). Microtubule targeting of substrate contacts promotes their relaxation and dissociation. *J Cell Biol* 146, 1033-1044.
- Kawai, K., Seike, J., Iino, T., Kiyota, M., Iwamae, Y., Nishitani, H., and Yagisawa, H. (2009). START-GAP2/DLC2 is localized in focal adhesions via its N-terminal region. *Biochem Biophys Res Commun* 380, 736-741.
- Kawai, K., Yamaga, M., Iwamae, Y., Kiyota, M., Kamata, H., Hirata, H., Homma, Y., and Yagisawa, H. (2004). A PLCdelta1-binding protein, p122RhoGAP, is localized in focal adhesions. *Biochem Soc Trans* 32, 1107-1109.
- Keller, R. (2005). Cell migration during gastrulation. *Curr Opin Cell Biol* 17, 533-541.
- Kim, M., Carman, C. V., and Springer, T. A. (2003). Bidirectional transmembrane signaling by cytoplasmic domain separation in integrins. *Science* 301, 1720-1725.
- Kimura, K., Ito, M., Amano, M., Chihara, K., Fukata, Y., Nakafuku, M., Yamamori, B., Feng, J., Nakano, T., Okawa, K., *et al.* (1996). Regulation of myosin phosphatase by Rho and Rho-associated kinase (Rho-kinase). *Science* 273, 245-248.
- Kirfel, G., and Herzog, V. (2004). Migration of epidermal keratinocytes: mechanisms, regulation, and biological significance. *Protoplasma* 223, 67-78.
- Kirfel, G., Rigort, A., Borm, B., and Herzog, V. (2004). Cell migration: mechanisms of rear detachment and the formation of migration tracks. *Eur J Cell Biol* 83, 717-724.

- Kirfel, G., Rigort, A., Borm, B., Schulte, C., and Herzog, V. (2003). Structural and compositional analysis of the keratinocyte migration track. *Cell Motil Cytoskeleton* 55, 1-13.
- Kiss, R., Kovacs, D., Tompa, P., and Perczel, A. (2008). Local structural preferences of calpastatin, the intrinsically unstructured protein inhibitor of calpain. *Biochemistry* 47, 6936-6945.
- Klemke, R. L., Cai, S., Giannini, A. L., Gallagher, P. J., de Lanerolle, P., and Cheresh, D. A. (1997). Regulation of cell motility by mitogen-activated protein kinase. *J Cell Biol* 137, 481-492.
- Klinghoffer, R. A., Sachsenmaier, C., Cooper, J. A., and Soriano, P. (1999). Src family kinases are required for integrin but not PDGFR signal transduction. *Embo J* 18, 2459-2471.
- Kook, S., Kim, D. H., Shim, S. R., Kim, W., Chun, J. S., and Song, W. K. (2003). Caspase-dependent cleavage of tensin induces disruption of actin cytoskeleton during apoptosis. *Biochem Biophys Res Commun* 303, 37-45.
- Korsnes, M. S., Hetland, D. L., Espenes, A., and Aune, T. (2007). Cleavage of tensin during cytoskeleton disruption in YTX-induced apoptosis. *Toxicol In Vitro* 21, 9-15.
- Kraynov, V. S., Chamberlain, C., Bokoch, G. M., Schwartz, M. A., Slabaugh, S., and Hahn, K. M. (2000). Localized Rac activation dynamics visualized in living cells. *Science* 290, 333-337.
- Kreis, T. E., Geiger, B., and Schlessinger, J. (1982). Mobility of microinjected rhodamine actin within living chicken gizzard cells determined by fluorescence photobleaching recovery. *Cell* 29, 835-845.
- Kriwacki, R. W., Hengst, L., Tennant, L., Reed, S. I., and Wright, P. E. (1996). Structural studies of p21Waf1/Cip1/Sdi1 in the free and Cdk2-bound state: conformational disorder mediates binding diversity. *Proc Natl Acad Sci U S A* 93, 11504-11509.
- Ladwein, M., and Rottner, K. (2008). On the Rho'd: the regulation of membrane protrusions by Rho-GTPases. *FEBS Lett* 582, 2066-2074.
- Lammermann, T., Bader, B. L., Monkley, S. J., Worbs, T., Wedlich-Soldner, R., Hirsch, K., Keller, M., Forster, R., Critchley, D. R., Fassler, R., and Sixt, M. (2008). Rapid leukocyte migration by integrin-independent flowing and squeezing. *Nature* 453, 51-55.
- Larsen, M., Tremblay, M. L., and Yamada, K. M. (2003). Phosphatases in cell-matrix adhesion and migration. *Nat Rev Mol Cell Biol* 4, 700-711.
- Larsen, M., Wei, C., and Yamada, K. M. (2006). Cell and fibronectin dynamics during branching morphogenesis. *J Cell Sci* 119, 3376-3384.

- Lau, T. L., Kim, C., Ginsberg, M. H., and Ulmer, T. S. (2009). The structure of the integrin α 5 β 3 transmembrane complex explains integrin transmembrane signalling. *Embo J* 28, 1351-1361.
- Lauffenburger, D. A., and Horwitz, A. F. (1996). Cell migration: a physically integrated molecular process. *Cell* 84, 359-369.
- Le Clainche, C., and Carlier, M. F. (2008). Regulation of actin assembly associated with protrusion and adhesion in cell migration. *Physiol Rev* 88, 489-513.
- Lee, J., Ishihara, A., Oxford, G., Johnson, B., and Jacobson, K. (1999). Regulation of cell movement is mediated by stretch-activated calcium channels. *Nature* 400, 382-386.
- Lee, S. B., Cho, K. S., Kim, E., and Chung, J. (2003). *blister* encodes Drosophila tensin protein and interacts with integrin and the JNK signaling pathway during wing development. *Development* 130, 4001-4010.
- Legate, K. R., and Fassler, R. (2009). Mechanisms that regulate adaptor binding to beta-integrin cytoplasmic tails. *J Cell Sci* 122, 187-198.
- Legate, K. R., Montanez, E., Kudlacek, O., and Fassler, R. (2006). ILK, PINCH and parvin: the tIPP of integrin signalling. *Nat Rev Mol Cell Biol* 7, 20-31.
- Lehto, V. P., Hovi, T., Vartio, T., Badley, R. A., and Virtanen, I. (1982). Reorganization of cytoskeletal and contractile elements during transition of human monocytes into adherent macrophages. *Lab Invest* 47, 391-399.
- Leiss, M., Beckmann, K., Giros, A., Costell, M., and Fassler, R. (2008). The role of integrin binding sites in fibronectin matrix assembly in vivo. *Curr Opin Cell Biol* 20, 502-507.
- Leone, M., Yu, E. C., Liddington, R. C., Pasquale, E. B., and Pellecchia, M. (2008). The PTB domain of tensin: NMR solution structure and phosphoinositides binding studies. *Biopolymers* 89, 86-92.
- Leung, T., Chen, X. Q., Manser, E., and Lim, L. (1996). The p160 RhoA-binding kinase ROK alpha is a member of a kinase family and is involved in the reorganization of the cytoskeleton. *Mol Cell Biol* 16, 5313-5327.
- Leung, T., Chen, X. Q., Tan, I., Manser, E., and Lim, L. (1998). Myotonic dystrophy kinase-related Cdc42-binding kinase acts as a Cdc42 effector in promoting cytoskeletal reorganization. *Mol Cell Biol* 18, 130-140.
- Ley, K., Laudanna, C., Cybulsky, M. I., and Nourshargh, S. (2007). Getting to the site of inflammation: the leukocyte adhesion cascade updated. *Nat Rev Immunol* 7, 678-689.
- Li, J., Chen, J., and Kirsner, R. (2007). Pathophysiology of acute wound healing. *Clin Dermatol* 25, 9-18.

- Li, Y., Mizokami, A., Izumi, K., Narimoto, K., Shima, T., Zhang, J., Dai, J., Keller, E. T., and Namiki, M. (2010). CTEN/tensin 4 expression induces sensitivity to paclitaxel in prostate cancer. *Prostate* 70, 48-60.
- Liao, Y. C., Chen, N. T., Shih, Y. P., Dong, Y., and Lo, S. H. (2009). Up-regulation of C-terminal tensin-like molecule promotes the tumorigenicity of colon cancer through beta-catenin. *Cancer Res* 69, 4563-4566.
- Liao, Y. C., and Lo, S. H. (2008). Deleted in liver cancer-1 (DLC-1): a tumor suppressor not just for liver. *Int J Biochem Cell Biol* 40, 843-847.
- Liao, Y. C., Si, L., deVere White, R. W., and Lo, S. H. (2007). The phosphotyrosine-independent interaction of DLC-1 and the SH2 domain of cten regulates focal adhesion localization and growth suppression activity of DLC-1. *J Cell Biol* 176, 43-49.
- Lin, C. H., Espreafico, E. M., Mooseker, M. S., and Forscher, P. (1996). Myosin drives retrograde F-actin flow in neuronal growth cones. *Neuron* 16, 769-782.
- Lin, C. H., and Forscher, P. (1995). Growth cone advance is inversely proportional to retrograde F-actin flow. *Neuron* 14, 763-771.
- Lin, S. a. L., D. C. (1996). Mapping of actin, vinculin, and integrin binding domains suggests a direct role of tensin in actin-membrane association. *Molecular Biology of the Cell* 7 (S), 389a.
- Linder, S. (2007). The matrix corroded: podosomes and invadopodia in extracellular matrix degradation. *Trends Cell Biol* 17, 107-117.
- Linder, S., and Kopp, P. (2005). Podosomes at a glance. *J Cell Sci* 118, 2079-2082.
- Livak, K. J., and Schmittgen, T. D. (2001). Analysis of relative gene expression data using real-time quantitative PCR and the 2(-Delta Delta C(T)) Method. *Methods* 25, 402-408.
- Lo, S. H. (2004). Tensin. *Int J Biochem Cell Biol* 36, 31-34.
- Lo, S. H. (2006). Focal adhesions: what's new inside. *Dev Biol* 294, 280-291.
- Lo, S. H., An, Q., Bao, S., Wong, W. K., Liu, Y., Janmey, P. A., Hartwig, J. H., and Chen, L. B. (1994a). Molecular cloning of chick cardiac muscle tensin. Full-length cDNA sequence, expression, and characterization. *J Biol Chem* 269, 22310-22319.
- Lo, S. H., Janmey, P. A., Hartwig, J. H., and Chen, L. B. (1994b). Interactions of tensin with actin and identification of its three distinct actin-binding domains. *J Cell Biol* 125, 1067-1075.
- Lo, S. H., and Lo, T. B. (2002). Cten, a COOH-terminal tensin-like protein with prostate restricted expression, is down-regulated in prostate cancer. *Cancer Res* 62, 4217-4221.
- Lo, S. H., Yu, Q. C., Degenstein, L., Chen, L. B., and Fuchs, E. (1997). Progressive kidney degeneration in mice lacking tensin. *J Cell Biol* 136, 1349-1361.

- Lo, S. S., and Lo, S. H. (2005). Cleavage of cten by caspase-3 during apoptosis. *Oncogene* *24*, 4311-4314.
- Lotz, M. M., Rabinovitz, I., and Mercurio, A. M. (2000). Intestinal restitution: progression of actin cytoskeleton rearrangements and integrin function in a model of epithelial wound healing. *Am J Pathol* *156*, 985-996.
- Luster, A. D., Alon, R., and von Andrian, U. H. (2005). Immune cell migration in inflammation: present and future therapeutic targets. *Nat Immunol* *6*, 1182-1190.
- Maciver, S. K., Zot, H. G., and Pollard, T. D. (1991). Characterization of actin filament severing by actophorin from *Acanthamoeba castellanii*. *J Cell Biol* *115*, 1611-1620.
- Maeda, I., Takano, T., Yoshida, H., Matsuzuka, F., Amino, N., and Miyauchi, A. (2006). Tensin3 is a novel thyroid-specific gene. *J Mol Endocrinol* *36*, R1-8.
- Manahan, C. L., Iglesias, P. A., Long, Y., and Devreotes, P. N. (2004). Chemoattractant signaling in *dictyostelium discoideum*. *Annu Rev Cell Dev Biol* *20*, 223-253.
- Mao, Y., and Schwarzbauer, J. E. (2005a). Fibronectin fibrillogenesis, a cell-mediated matrix assembly process. *Matrix Biol* *24*, 389-399.
- Mao, Y., and Schwarzbauer, J. E. (2005b). Stimulatory effects of a three-dimensional microenvironment on cell-mediated fibronectin fibrillogenesis. *J Cell Sci* *118*, 4427-4436.
- Marchisio, P. C., Cirillo, D., Naldini, L., Primavera, M. V., Teti, A., and Zamboni-Zallone, A. (1984). Cell-substratum interaction of cultured avian osteoclasts is mediated by specific adhesion structures. *J Cell Biol* *99*, 1696-1705.
- Mark, W. Y., Liao, J. C., Lu, Y., Ayed, A., Laister, R., Szymczynska, B., Chakrabarty, A., and Arrowsmith, C. H. (2005). Characterization of segments from the central region of BRCA1: an intrinsically disordered scaffold for multiple protein-protein and protein-DNA interactions? *J Mol Biol* *345*, 275-287.
- Martuszevska, D., Ljungberg, B., Johansson, M., Landberg, G., Oslakovic, C., Dahlback, B., and Hafizi, S. (2009). Tensin3 is a negative regulator of cell migration and all four Tensin family members are downregulated in human kidney cancer. *PLoS ONE* *4*, e4350.
- Mattila, P. K., and Lappalainen, P. (2008). Filopodia: molecular architecture and cellular functions. *Nat Rev Mol Cell Biol* *9*, 446-454.
- McCleverty, C. J., Lin, D. C., and Liddington, R. C. (2007). Structure of the PTB domain of tensin1 and a model for its recruitment to fibrillar adhesions. *Protein Sci* *16*, 1223-1229.
- McDonald, J. A., Kelley, D. G., and Broekelmann, T. J. (1982). Role of fibronectin in collagen deposition: Fab' to the gelatin-binding domain of fibronectin inhibits both

fibronectin and collagen organization in fibroblast extracellular matrix. *J Cell Biol* **92**, 485-492.

McKeown-Longo, P. J., and Mosher, D. F. (1983). Binding of plasma fibronectin to cell layers of human skin fibroblasts. *J Cell Biol* **97**, 466-472.

McKeown-Longo, P. J., and Mosher, D. F. (1985). Interaction of the 70,000-mol-wt amino-terminal fragment of fibronectin with the matrix-assembly receptor of fibroblasts. *J Cell Biol* **100**, 364-374.

Mellor, H. (2009). The role of formins in filopodia formation. *Biochim Biophys Acta (Electronic Publication)*.

Meredith, J. E., Jr., Fazeli, B., and Schwartz, M. A. (1993). The extracellular matrix as a cell survival factor. *Mol Biol Cell* **4**, 953-961.

Miki, H., Sasaki, T., Takai, Y., and Takenawa, T. (1998a). Induction of filopodium formation by a WASP-related actin-depolymerizing protein N-WASP. *Nature* **391**, 93-96.

Miki, H., Suetsugu, S., and Takenawa, T. (1998b). WAVE, a novel WASP-family protein involved in actin reorganization induced by Rac. *Embo J* **17**, 6932-6941.

Miranti, C. K., and Brugge, J. S. (2002). Sensing the environment: a historical perspective on integrin signal transduction. *Nat Cell Biol* **4**, E83-90.

Mitra, S. K., and Schlaepfer, D. D. (2006). Integrin-regulated FAK-Src signaling in normal and cancer cells. *Curr Opin Cell Biol* **18**, 516-523.

Miyamoto, S., Teramoto, H., Gutkind, J. S., and Yamada, K. M. (1996). Integrins can collaborate with growth factors for phosphorylation of receptor tyrosine kinases and MAP kinase activation: roles of integrin aggregation and occupancy of receptors. *J Cell Biol* **135**, 1633-1642.

Mizejewski, G. J. (1999). Role of integrins in cancer: survey of expression patterns. *Proc Soc Exp Biol Med* **222**, 124-138.

Montanez, E., Ussar, S., Schifferer, M., Bosl, M., Zent, R., Moser, M., and Fassler, R. (2008). Kindlin-2 controls bidirectional signaling of integrins. *Genes Dev* **22**, 1325-1330.

Moon, S. Y., and Zheng, Y. (2003). Rho GTPase-activating proteins in cell regulation. *Trends Cell Biol* **13**, 13-22.

Moser, M., Nieswandt, B., Ussar, S., Pozgajova, M., and Fassler, R. (2008). Kindlin-3 is essential for integrin activation and platelet aggregation. *Nat Med* **14**, 325-330.

Mullins, R. D., Heuser, J. A., and Pollard, T. D. (1998). The interaction of Arp2/3 complex with actin: nucleation, high affinity pointed end capping, and formation of branching networks of filaments. *Proc Natl Acad Sci U S A* **95**, 6181-6186.

- Murphy, G., and Gavrilovic, J. (1999). Proteolysis and cell migration: creating a path? *Curr Opin Cell Biol* 11, 614-621.
- Nalbant, P., Hodgson, L., Kraynov, V., Touthkine, A., and Hahn, K. M. (2004). Activation of endogenous Cdc42 visualized in living cells. *Science* 305, 1615-1619.
- Nermut, M. V., Green, N. M., Eason, P., Yamada, S. S., and Yamada, K. M. (1988). Electron microscopy and structural model of human fibronectin receptor. *Embo J* 7, 4093-4099.
- Nguyen, D. X., Bos, P. D., and Massague, J. (2009). Metastasis: from dissemination to organ-specific colonization. *Nat Rev Cancer* 9, 274-284.
- Nishida, N., Xie, C., Shimaoka, M., Cheng, Y., Walz, T., and Springer, T. A. (2006). Activation of leukocyte beta2 integrins by conversion from bent to extended conformations. *Immunity* 25, 583-594.
- Nix, D. A., and Beckerle, M. C. (1997). Nuclear-cytoplasmic shuttling of the focal contact protein, zyxin: a potential mechanism for communication between sites of cell adhesion and the nucleus. *J Cell Biol* 138, 1139-1147.
- Nobes, C. D., and Hall, A. (1995). Rho, rac, and cdc42 GTPases regulate the assembly of multimolecular focal complexes associated with actin stress fibers, lamellipodia, and filopodia. *Cell* 81, 53-62.
- Nobes, C. D., and Hall, A. (1999). Rho GTPases control polarity, protrusion, and adhesion during cell movement. *J Cell Biol* 144, 1235-1244.
- Nurden, A. T. (2006). Glanzmann thrombasthenia. *Orphanet J Rare Dis* 1, 10.
- Ohashi, T., Kiehart, D. P., and Erickson, H. P. (2002). Dual labeling of the fibronectin matrix and actin cytoskeleton with green fluorescent protein variants. *J Cell Sci* 115, 1221-1229.
- Opas, M., Szewczenko-Pawlikowski, M., Jass, G. K., Mesaeli, N., and Michalak, M. (1996). Calreticulin modulates cell adhesiveness via regulation of vinculin expression. *J Cell Biol* 135, 1913-1923.
- Palecek, S. P., Huttenlocher, A., Horwitz, A. F., and Lauffenburger, D. A. (1998). Physical and biochemical regulation of integrin release during rear detachment of migrating cells. *J Cell Sci* 111 (Pt 7), 929-940.
- Palecek, S. P., Loftus, J. C., Ginsberg, M. H., Lauffenburger, D. A., and Horwitz, A. F. (1997). Integrin-ligand binding properties govern cell migration speed through cell-substratum adhesiveness. *Nature* 385, 537-540.
- Palecek, S. P., Schmidt, C. E., Lauffenburger, D. A., and Horwitz, A. F. (1996). Integrin dynamics on the tail region of migrating fibroblasts. *J Cell Sci* 109 (Pt 5), 941-952.
- Pankov, R., Cukierman, E., Katz, B. Z., Matsumoto, K., Lin, D. C., Lin, S., Hahn, C., and Yamada, K. M. (2000). Integrin dynamics and matrix assembly: tensin-dependent

translocation of alpha(5)beta(1) integrins promotes early fibronectin fibrillogenesis. *J Cell Biol* *148*, 1075-1090.

Pankov, R., and Momchilova, A. (2009). Fluorescent labeling techniques for investigation of fibronectin fibrillogenesis (labeling fibronectin fibrillogenesis). *Methods Mol Biol* *522*, 261-274.

Pankov, R., and Yamada, K. M. (2002). Fibronectin at a glance. *J Cell Sci* *115*, 3861-3863.

Papp, S., Fadel, M. P., and Opas, M. (2007). Dissecting focal adhesions in cells differentially expressing calreticulin: a microscopy study. *Biol Cell* *99*, 389-402.

Pellegrin, S., and Mellor, H. (2005). The Rho family GTPase Rif induces filopodia through mDia2. *Curr Biol* *15*, 129-133.

Pellegrin, S., and Mellor, H. (2007). Actin stress fibres. *J Cell Sci* *120*, 3491-3499.

Peng, J., Wallar, B. J., Flanders, A., Swiatek, P. J., and Alberts, A. S. (2003). Disruption of the Diaphanous-related formin Drf1 gene encoding mDia1 reveals a role for Drf3 as an effector for Cdc42. *Curr Biol* *13*, 534-545.

Pereira, M., Rybarczyk, B. J., Odrliin, T. M., Hocking, D. C., Sottile, J., and Simpson-Haidaris, P. J. (2002). The incorporation of fibrinogen into extracellular matrix is dependent on active assembly of a fibronectin matrix. *J Cell Sci* *115*, 609-617.

Petrie, R. J., Doyle, A. D., and Yamada, K. M. (2009). Random versus directionally persistent cell migration. *Nat Rev Mol Cell Biol* *10*, 538-549.

Pfaff, M., Du, X., and Ginsberg, M. H. (1999). Calpain cleavage of integrin beta cytoplasmic domains. *FEBS Lett* *460*, 17-22.

Pollard, T. D. (2007). Regulation of actin filament assembly by Arp2/3 complex and formins. *Annu Rev Biophys Biomol Struct* *36*, 451-477.

Pollard, T. D., and Borisy, G. G. (2003). Cellular motility driven by assembly and disassembly of actin filaments. *Cell* *112*, 453-465.

Prout, M., Damania, Z., Soong, J., Fristrom, D., and Fristrom, J. W. (1997). Autosomal mutations affecting adhesion between wing surfaces in *Drosophila melanogaster*. *Genetics* *146*, 275-285.

Pytela, R., Pierschbacher, M. D., and Ruoslahti, E. (1985). Identification and isolation of a 140 kd cell surface glycoprotein with properties expected of a fibronectin receptor. *Cell* *40*, 191-198.

Qian, X., Li, G., Asmussen, H. K., Asnaghi, L., Vass, W. C., Braverman, R., Yamada, K. M., Popescu, N. C., Papageorge, A. G., and Lowy, D. R. (2007). Oncogenic inhibition by a deleted in liver cancer gene requires cooperation between tensin binding and Rho-specific GTPase-activating protein activities. *Proc Natl Acad Sci U S A* *104*, 9012-9017.

Qian, X., Li, G., Vass, W. C., Papageorge, A., Walker, R. C., Asnaghi, L., Steinbach, P. J., Tosato, G., Hunter, K., and Lowy, D. R. (2009). The Tensin-3 protein, including its SH2 domain, is phosphorylated by Src and contributes to tumorigenesis and metastasis. *Cancer Cell* 16, 246-258.

Raftopoulou, M., and Hall, A. (2004). Cell migration: Rho GTPases lead the way. *Dev Biol* 265, 23-32.

Regen, C. M., and Horwitz, A. F. (1992). Dynamics of beta 1 integrin-mediated adhesive contacts in motile fibroblasts. *J Cell Biol* 119, 1347-1359.

Ridley, A. J. (2001). Rho GTPases and cell migration. *J Cell Sci* 114, 2713-2722.

Ridley, A. J., Paterson, H. F., Johnston, C. L., Diekmann, D., and Hall, A. (1992). The small GTP-binding protein rac regulates growth factor-induced membrane ruffling. *Cell* 70, 401-410.

Ridley, A. J., Schwartz, M. A., Burridge, K., Firtel, R. A., Ginsberg, M. H., Borisy, G., Parsons, J. T., and Horwitz, A. R. (2003). Cell migration: integrating signals from front to back. *Science* 302, 1704-1709.

Robinson, E. E., Foty, R. A., and Corbett, S. A. (2004). Fibronectin matrix assembly regulates alpha5beta1-mediated cell cohesion. *Mol Biol Cell* 15, 973-981.

Rodrigue, C. M., Porteu, F., Navarro, N., Bruyneel, E., Bracke, M., Romeo, P. H., Gespach, C., and Garel, M. C. (2005). The cancer chemopreventive agent resveratrol induces tensin, a cell-matrix adhesion protein with signaling and antitumor activities. *Oncogene* 24, 3274-3284.

Roman, J., and McDonald, J. A. (1993). Fibulin's organization into the extracellular matrix of fetal lung fibroblasts is dependent on fibronectin matrix assembly. *Am J Respir Cell Mol Biol* 8, 538-545.

Romer, L. H., Birukov, K. G., and Garcia, J. G. (2006). Focal adhesions: paradigm for a signaling nexus. *Circ Res* 98, 606-616.

Rossman, K. L., Der, C. J., and Sondek, J. (2005). GEF means go: turning on RHO GTPases with guanine nucleotide-exchange factors. *Nat Rev Mol Cell Biol* 6, 167-180.

Rottner, K., Hall, A., and Small, J. V. (1999). Interplay between Rac and Rho in the control of substrate contact dynamics. *Curr Biol* 9, 640-648.

Ruegg, C., Postigo, A. A., Sikorski, E. E., Butcher, E. C., Pytela, R., and Erle, D. J. (1992). Role of integrin alpha 4 beta 7/alpha 4 beta P in lymphocyte adherence to fibronectin and VCAM-1 and in homotypic cell clustering. *J Cell Biol* 117, 179-189.

Ruoslahti, E. (2003). The RGD story: a personal account. *Matrix Biol* 22, 459-465.

Russell, A. (1954). A syndrome of intra-uterine dwarfism recognizable at birth with cranio-facial dysostosis, disproportionately short arms, and other anomalies (5 examples). *Proc R Soc Med* 47, 1040-1044.

Sabe, H., Hamaguchi, M., and Hanafusa, H. (1997). Cell to substratum adhesion is involved in v-Src-induced cellular protein tyrosine phosphorylation: implication for the adhesion-regulated protein tyrosine phosphatase activity. *Oncogene* *14*, 1779-1788.

Sahai, E. (2005). Mechanisms of cancer cell invasion. *Curr Opin Genet Dev* *15*, 87-96.

Sahai, E., and Marshall, C. J. (2003). Differing modes of tumour cell invasion have distinct requirements for Rho/ROCK signalling and extracellular proteolysis. *Nat Cell Biol* *5*, 711-719.

Sakai, T., Larsen, M., and Yamada, K. M. (2003). Fibronectin requirement in branching morphogenesis. *Nature* *423*, 876-881.

Sakashita, K., Mimori, K., Tanaka, F., Kamohara, Y., Inoue, H., Sawada, T., Hirakawa, K., and Mori, M. (2008). Prognostic relevance of Tensin4 expression in human gastric cancer. *Ann Surg Oncol* *15*, 2606-2613.

Salgia, R., Brunkhorst, B., Pisick, E., Li, J. L., Lo, S. H., Chen, L. B., and Griffin, J. D. (1995). Increased tyrosine phosphorylation of focal adhesion proteins in myeloid cell lines expressing p210BCR/ABL. *Oncogene* *11*, 1149-1155.

Salgia, R., Pisick, E., Sattler, M., Li, J. L., Uemura, N., Wong, W. K., Burky, S. A., Hirai, H., Chen, L. B., and Griffin, J. D. (1996). p130CAS forms a signaling complex with the adapter protein CRKL in hematopoietic cells transformed by the BCR/ABL oncogene. *J Biol Chem* *271*, 25198-25203.

Sander, E. E., ten Klooster, J. P., van Delft, S., van der Kammen, R. A., and Collard, J. G. (1999). Rac downregulates Rho activity: reciprocal balance between both GTPases determines cellular morphology and migratory behavior. *J Cell Biol* *147*, 1009-1022.

Sanz-Moreno, V., Gadea, G., Ahn, J., Paterson, H., Marra, P., Pinner, S., Sahai, E., and Marshall, C. J. (2008). Rac activation and inactivation control plasticity of tumor cell movement. *Cell* *135*, 510-523.

Sasaki, H., Moriyama, S., Mizuno, K., Yukiue, H., Konishi, A., Yano, M., Kaji, M., Fukai, I., Kiriya, M., Yamakawa, Y., and Fujii, Y. (2003a). Cten mRNA expression was correlated with tumor progression in lung cancers. *Lung Cancer* *40*, 151-155.

Sasaki, H., Yukiue, H., Kobayashi, Y., Fukai, I., and Fujii, Y. (2003b). Cten mRNA expression is correlated with tumor progression in thymoma. *Tumour Biol* *24*, 271-274.

Schaller, M. D., and Parsons, J. T. (1995). pp125FAK-dependent tyrosine phosphorylation of paxillin creates a high-affinity binding site for Crk. *Mol Cell Biol* *15*, 2635-2645.

Schlaepfer, D. D., Hauck, C. R., and Sieg, D. J. (1999). Signaling through focal adhesion kinase. *Prog Biophys Mol Biol* *71*, 435-478.

Schmittgen, T. D., and Livak, K. J. (2008). Analyzing real-time PCR data by the comparative C(T) method. *Nat Protoc* *3*, 1101-1108.

Schor, S. L., Allen, T. D., and Winn, B. (1983). Lymphocyte migration into three-dimensional collagen matrices: a quantitative study. *J Cell Biol* **96**, 1089-1096.

Schultz, J., Milpetz, F., Bork, P., and Ponting, C. P. (1998). SMART, a simple modular architecture research tool: identification of signaling domains. *Proc Natl Acad Sci U S A* **95**, 5857-5864.

Schwartz, M. (2004). Rho signalling at a glance. *J Cell Sci* **117**, 5457-5458.

Sechler, J. L., Cumiskey, A. M., Gazzola, D. M., and Schwarzbauer, J. E. (2000). A novel RGD-independent fibronectin assembly pathway initiated by alpha4beta1 integrin binding to the alternatively spliced V region. *J Cell Sci* **113** (Pt 8), 1491-1498.

Sekimata, M., Kabuyama, Y., Emori, Y., and Homma, Y. (1999). Morphological changes and detachment of adherent cells induced by p122, a GTPase-activating protein for Rho. *J Biol Chem* **274**, 17757-17762.

Silver, H. K., Kiyasu, W., George, J., and Deamer, W. C. (1953). Syndrome of congenital hemihypertrophy, shortness of stature, and elevated urinary gonadotropins. *Pediatrics* **12**, 368-376.

Simpson, K. J., Selfors, L. M., Bui, J., Reynolds, A., Leake, D., Khvorova, A., and Brugge, J. S. (2008). Identification of genes that regulate epithelial cell migration using an siRNA screening approach. *Nat Cell Biol* **10**, 1027-1038.

Smilenov, L. B., Mikhailov, A., Pelham, R. J., Marcantonio, E. E., and Gundersen, G. G. (1999). Focal adhesion motility revealed in stationary fibroblasts. *Science* **286**, 1172-1174.

Sottile, J., and Hocking, D. C. (2002). Fibronectin polymerization regulates the composition and stability of extracellular matrix fibrils and cell-matrix adhesions. *Mol Biol Cell* **13**, 3546-3559.

Srinivasan, S., Wang, F., Glavas, S., Ott, A., Hofmann, F., Aktories, K., Kalman, D., and Bourne, H. R. (2003). Rac and Cdc42 play distinct roles in regulating PI(3,4,5)P3 and polarity during neutrophil chemotaxis. *J Cell Biol* **160**, 375-385.

Stanchi, F., Grashoff, C., Nguemni Yonga, C. F., Grall, D., Fassler, R., and Van Obberghen-Schilling, E. (2009). Molecular dissection of the ILK-PINCH-parvin triad reveals a fundamental role for the ILK kinase domain in the late stages of focal-adhesion maturation. *J Cell Sci* **122**, 1800-1811.

Stephens, L. E., Sutherland, A. E., Klimanskaya, I. V., Andrieux, A., Meneses, J., Pedersen, R. A., and Damsky, C. H. (1995). Deletion of beta 1 integrins in mice results in inner cell mass failure and peri-implantation lethality. *Genes Dev* **9**, 1883-1895.

Stoker, M., O'Neill, C., Berryman, S., and Waxman, V. (1968). Anchorage and growth regulation in normal and virus-transformed cells. *Int J Cancer* **3**, 683-693.

Stouffer, G. A., and Smyth, S. S. (2003). Effects of thrombin on interactions between beta3-integrins and extracellular matrix in platelets and vascular cells. *Arterioscler Thromb Vasc Biol* 23, 1971-1978.

Streuli, C. H. (2009). Integrins and cell-fate determination. *J Cell Sci* 122, 171-177.

Streuli, C. H., and Akhtar, N. (2009). Signal co-operation between integrins and other receptor systems. *Biochem J* 418, 491-506.

Svitkina, T. M., Bulanova, E. A., Chaga, O. Y., Vignjevic, D. M., Kojima, S., Vasiliev, J. M., and Borisy, G. G. (2003). Mechanism of filopodia initiation by reorganization of a dendritic network. *J Cell Biol* 160, 409-421.

Sydor, A. M., Su, A. L., Wang, F. S., Xu, A., and Jay, D. G. (1996). Talin and vinculin play distinct roles in filopodial motility in the neuronal growth cone. *J Cell Biol* 134, 1197-1207.

Symons, M., and Segall, J. E. (2009). Rac and Rho driving tumor invasion: who's at the wheel? *Genome Biol* 10, 213.

Tadokoro, S., Shattil, S. J., Eto, K., Tai, V., Liddington, R. C., de Pereda, J. M., Ginsberg, M. H., and Calderwood, D. A. (2003). Talin binding to integrin beta tails: a final common step in integrin activation. *Science* 302, 103-106.

Takagi, J., Petre, B. M., Walz, T., and Springer, T. A. (2002). Global conformational rearrangements in integrin extracellular domains in outside-in and inside-out signaling. *Cell* 110, 599-511.

Tapley, P., Horwitz, A., Buck, C., Duggan, K., and Rohrschneider, L. (1989). Integrins isolated from Rous sarcoma virus-transformed chicken embryo fibroblasts. *Oncogene* 4, 325-333.

Thomas, G. J., Nystrom, M. L., and Marshall, J. F. (2006). Alphavbeta6 integrin in wound healing and cancer of the oral cavity. *J Oral Pathol Med* 35, 1-10.

Threadgill, D. W., Dlugosz, A. A., Hansen, L. A., Tennenbaum, T., Lichti, U., Yee, D., LaMantia, C., Mourton, T., Herrup, K., Harris, R. C., and et al. (1995). Targeted disruption of mouse EGF receptor: effect of genetic background on mutant phenotype. *Science* 269, 230-234.

Tompa, P. (2002). Intrinsically unstructured proteins. *Trends Biochem Sci* 27, 527-533.

Torgler, C. N., Narasimha, M., Knox, A. L., Zervas, C. G., Vernon, M. C., and Brown, N. H. (2004). Tensin stabilizes integrin adhesive contacts in *Drosophila*. *Dev Cell* 6, 357-369.

Turner, C. E., Kramarcy, N., Sealock, R., and Burridge, K. (1991). Localization of paxillin, a focal adhesion protein, to smooth muscle dense plaques, and the myotendinous and neuromuscular junctions of skeletal muscle. *Exp Cell Res* 192, 651-655.

Tzima, E., Kiosses, W. B., del Pozo, M. A., and Schwartz, M. A. (2003). Localized cdc42 activation, detected using a novel assay, mediates microtubule organizing center positioning in endothelial cells in response to fluid shear stress. *J Biol Chem* 278, 31020-31023.

Ussar, S., Moser, M., Widmaier, M., Rognoni, E., Harrer, C., Genzel-Boroviczeny, O., and Fassler, R. (2008). Loss of Kindlin-1 causes skin atrophy and lethal neonatal intestinal epithelial dysfunction. *PLoS Genet* 4, e1000289.

Van Troys, M., Huyck, L., Leyman, S., Dhaese, S., Vandekerckhove, J., and Ampe, C. (2008). Ins and outs of ADF/cofilin activity and regulation. *Eur J Cell Biol* 87, 649-667.

Vega, F. M., and Ridley, A. J. (2007). SnapShot: Rho family GTPases. *Cell* 129, 1430.

Vicente-Manzanares, M., Choi, C. K., and Horwitz, A. R. (2009). Integrins in cell migration--the actin connection. *J Cell Sci* 122, 199-206.

Vicente-Manzanares, M., Webb, D. J., and Horwitz, A. R. (2005). Cell migration at a glance. *J Cell Sci* 118, 4917-4919.

Vicente-Manzanares, M., Zareno, J., Whitmore, L., Choi, C. K., and Horwitz, A. F. (2007). Regulation of protrusion, adhesion dynamics, and polarity by myosins IIA and IIB in migrating cells. *J Cell Biol* 176, 573-580.

Vinogradova, O., Haas, T., Plow, E. F., and Qin, J. (2000). A structural basis for integrin activation by the cytoplasmic tail of the alpha IIb-subunit. *Proc Natl Acad Sci U S A* 97, 1450-1455.

Vinogradova, O., Velyvis, A., Velyviene, A., Hu, B., Haas, T., Plow, E., and Qin, J. (2002). A structural mechanism of integrin alpha(IIb)beta(3) "inside-out" activation as regulated by its cytoplasmic face. *Cell* 110, 587-597.

Volberg, T., Romer, L., Zamir, E., and Geiger, B. (2001). pp60(c-src) and related tyrosine kinases: a role in the assembly and reorganization of matrix adhesions. *J Cell Sci* 114, 2279-2289.

Vouret-Craviari, V., Boulter, E., Grall, D., Matthews, C., and Van Obberghen-Schilling, E. (2004). ILK is required for the assembly of matrix-forming adhesions and capillary morphogenesis in endothelial cells. *J Cell Sci* 117, 4559-4569.

Walpita, D., and Hay, E. (2002). Studying actin-dependent processes in tissue culture. *Nat Rev Mol Cell Biol* 3, 137-141.

Walsh, E. P., and Brown, N. H. (1998). A screen to identify *Drosophila* genes required for integrin-mediated adhesion. *Genetics* 150, 791-805.

Wang, W., Goswami, S., Lapidus, K., Wells, A. L., Wyckoff, J. B., Sahai, E., Singer, R. H., Segall, J. E., and Condeelis, J. S. (2004). Identification and testing of a gene expression signature of invasive carcinoma cells within primary mammary tumors. *Cancer Res* 64, 8585-8594.

- Wang, Y. L. (1985). Exchange of actin subunits at the leading edge of living fibroblasts: possible role of treadmilling. *J Cell Biol* *101*, 597-602.
- Wang, Y. L. (1987). Mobility of filamentous actin in living cytoplasm. *J Cell Biol* *105*, 2811-2816.
- Watanabe, N., Kato, T., Fujita, A., Ishizaki, T., and Narumiya, S. (1999). Cooperation between mDia1 and ROCK in Rho-induced actin reorganization. *Nat Cell Biol* *1*, 136-143.
- Watanabe, N., Madaule, P., Reid, T., Ishizaki, T., Watanabe, G., Kakizuka, A., Saito, Y., Nakao, K., Jockusch, B. M., and Narumiya, S. (1997). p140mDia, a mammalian homolog of *Drosophila* diaphanous, is a target protein for Rho small GTPase and is a ligand for profilin. *Embo J* *16*, 3044-3056.
- Watanabe, T., Noritake, J., and Kaibuchi, K. (2005). Regulation of microtubules in cell migration. *Trends Cell Biol* *15*, 76-83.
- Wavreille, A. S., and Pei, D. (2007). A chemical approach to the identification of tensin-binding proteins. *ACS Chem Biol* *2*, 109-118.
- Wayner, E. A., Garcia-Pardo, A., Humphries, M. J., McDonald, J. A., and Carter, W. G. (1989). Identification and characterization of the T lymphocyte adhesion receptor for an alternative cell attachment domain (CS-1) in plasma fibronectin. *J Cell Biol* *109*, 1321-1330.
- Webb, D. J., Donais, K., Whitmore, L. A., Thomas, S. M., Turner, C. E., Parsons, J. T., and Horwitz, A. F. (2004). FAK-Src signalling through paxillin, ERK and MLCK regulates adhesion disassembly. *Nat Cell Biol* *6*, 154-161.
- Wegener, K. L., Partridge, A. W., Han, J., Pickford, A. R., Liddington, R. C., Ginsberg, M. H., and Campbell, I. D. (2007). Structural basis of integrin activation by talin. *Cell* *128*, 171-182.
- Wennerberg, K., and Der, C. J. (2004). Rho-family GTPases: it's not only Rac and Rho (and I like it). *J Cell Sci* *117*, 1301-1312.
- Wennerberg, K., Lohikangas, L., Gullberg, D., Pfaff, M., Johansson, S., and Fassler, R. (1996). Beta 1 integrin-dependent and -independent polymerization of fibronectin. *J Cell Biol* *132*, 227-238.
- Wennerberg, K., Rossman, K. L., and Der, C. J. (2005). The Ras superfamily at a glance. *J Cell Sci* *118*, 843-846.
- White, E. S., Baralle, F. E., and Muro, A. F. (2008). New insights into form and function of fibronectin splice variants. *J Pathol* *216*, 1-14.
- Wierzbicka-Patynowski, I., and Schwarzbauer, J. E. (2002). Regulatory role for SRC and phosphatidylinositol 3-kinase in initiation of fibronectin matrix assembly. *J Biol Chem* *277*, 19703-19708.

- Wilhelmsen, K., Litjens, S. H., and Sonnenberg, A. (2006). Multiple functions of the integrin alpha6beta4 in epidermal homeostasis and tumorigenesis. *Mol Cell Biol* 26, 2877-2886.
- Wilkins, J. A., and Lin, S. (1986). A re-examination of the interaction of vinculin with actin. *J Cell Biol* 102, 1085-1092.
- Wilkins, J. A., Risinger, M. A., and Lin, S. (1986). Studies on proteins that co-purify with smooth muscle vinculin: identification of immunologically related species in focal adhesions of nonmuscle and Z-lines of muscle cells. *J Cell Biol* 103, 1483-1494.
- Wilkins, J. A., Risinger, M. A., Coffey, E., Lin, S. (1987). Purification of a vinculin binding protein from smooth muscle. *Journal of Cell Biology* 105, 130a.
- Williams, T. M., and Lisanti, M. P. (2005). Caveolin-1 in oncogenic transformation, cancer, and metastasis. *Am J Physiol Cell Physiol* 288, C494-506.
- Wolf, K., Mazo, I., Leung, H., Engelke, K., von Andrian, U. H., Deryugina, E. I., Strongin, A. Y., Brocker, E. B., and Friedl, P. (2003). Compensation mechanism in tumor cell migration: mesenchymal-amoeboid transition after blocking of pericellular proteolysis. *J Cell Biol* 160, 267-277.
- Wong, C. M., Yam, J. W., Ching, Y. P., Yau, T. O., Leung, T. H., Jin, D. Y., and Ng, I. O. (2005). Rho GTPase-activating protein deleted in liver cancer suppresses cell proliferation and invasion in hepatocellular carcinoma. *Cancer Res* 65, 8861-8868.
- Woods, A. J., Roberts, M. S., Choudhary, J., Barry, S. T., Mazaki, Y., Sabe, H., Morley, S. J., Critchley, D. R., and Norman, J. C. (2002). Paxillin associates with poly(A)-binding protein 1 at the dense endoplasmic reticulum and the leading edge of migrating cells. *J Biol Chem* 277, 6428-6437.
- Worthylake, R. A., Lemoine, S., Watson, J. M., and Burridge, K. (2001). RhoA is required for monocyte tail retraction during transendothelial migration. *J Cell Biol* 154, 147-160.
- Wu, C., Hughes, P. E., Ginsberg, M. H., and McDonald, J. A. (1996). Identification of a new biological function for the integrin alpha v beta 3: initiation of fibronectin matrix assembly. *Cell Adhes Commun* 4, 149-158.
- Wu, C., Keivens, V. M., O'Toole, T. E., McDonald, J. A., and Ginsberg, M. H. (1995). Integrin activation and cytoskeletal interaction are essential for the assembly of a fibronectin matrix. *Cell* 83, 715-724.
- Wyckoff, J. B., Pinner, S. E., Gschmeissner, S., Condeelis, J. S., and Sahai, E. (2006). ROCK- and myosin-dependent matrix deformation enables protease-independent tumor-cell invasion in vivo. *Curr Biol* 16, 1515-1523.
- Wyckoff, J. B., Segall, J. E., and Condeelis, J. S. (2000). The collection of the motile population of cells from a living tumor. *Cancer Res* 60, 5401-5404.

- Xiao, T., Takagi, J., Collier, B. S., Wang, J. H., and Springer, T. A. (2004). Structural basis for allostery in integrins and binding to fibrinogen-mimetic therapeutics. *Nature* 432, 59-67.
- Xiong, J. P., Stehle, T., Diefenbach, B., Zhang, R., Dunker, R., Scott, D. L., Joachimiak, A., Goodman, S. L., and Arnaout, M. A. (2001). Crystal structure of the extracellular segment of integrin alpha Vbeta3. *Science* 294, 339-345.
- Xiong, J. P., Stehle, T., Goodman, S. L., and Arnaout, M. A. (2003). New insights into the structural basis of integrin activation. *Blood* 102, 1155-1159.
- Xiong, J. P., Stehle, T., Zhang, R., Joachimiak, A., Frech, M., Goodman, S. L., and Arnaout, M. A. (2002). Crystal structure of the extracellular segment of integrin alpha Vbeta3 in complex with an Arg-Gly-Asp ligand. *Science* 296, 151-155.
- Xue, W., Krasnitz, A., Lucito, R., Sordella, R., Vanaelst, L., Cordon-Cardo, C., Singer, S., Kuehnel, F., Wigler, M., Powers, S., *et al.* (2008). DLC1 is a chromosome 8p tumor suppressor whose loss promotes hepatocellular carcinoma. *Genes Dev* 22, 1439-1444.
- Yadav, S., Puri, S., and Linstedt, A. D. (2009). A primary role for Golgi positioning in directed secretion, cell polarity, and wound healing. *Mol Biol Cell* 20, 1728-1736.
- Yam, J. W., Ko, F. C., Chan, C. Y., Jin, D. Y., and Ng, I. O. (2006a). Interaction of deleted in liver cancer 1 with tensin2 in caveolae and implications in tumor suppression. *Cancer Res* 66, 8367-8372.
- Yam, J. W., Ko, F. C., Chan, C. Y., Yau, T. O., Tung, E. K., Leung, T. H., Jin, D. Y., and Ng, I. O. (2006b). Tensin2 variant 3 is associated with aggressive tumor behavior in human hepatocellular carcinoma. *Hepatology* 44, 881-890.
- Yamada, K. M., and Cukierman, E. (2007). Modeling tissue morphogenesis and cancer in 3D. *Cell* 130, 601-610.
- Yamada, K. M., Pankov, R., and Cukierman, E. (2003). Dimensions and dynamics in integrin function. *Braz J Med Biol Res* 36, 959-966.
- Yamaga, M., Sekimata, M., Fujii, M., Kawai, K., Kamata, H., Hirata, H., Homma, Y., and Yagisawa, H. (2004). A PLCdelta1-binding protein, p122/RhoGAP, is localized in caveolin-enriched membrane domains and regulates caveolin internalization. *Genes Cells* 9, 25-37.
- Yamaguchi, H., Lorenz, M., Kempniak, S., Sarmiento, C., Coniglio, S., Symons, M., Segall, J., Eddy, R., Miki, H., Takenawa, T., and Condeelis, J. (2005). Molecular mechanisms of invadopodium formation: the role of the N-WASP-Arp2/3 complex pathway and cofilin. *J Cell Biol* 168, 441-452.
- Yamashita, M., Horikoshi, S., Asanuma, K., Takahara, H., Shirato, I., and Tomino, Y. (2004). Tensin is potentially involved in extracellular matrix production in mesangial cells. *Histochem Cell Biol* 121, 245-254.

Yang, W., Shimaoka, M., Salas, A., Takagi, J., and Springer, T. A. (2004). Intersubunit signal transmission in integrins by a receptor-like interaction with a pull spring. *Proc Natl Acad Sci U S A* *101*, 2906-2911.

Yoshinaga-Ohara, N., Takahashi, A., Uchiyama, T., and Sasada, M. (2002). Spatiotemporal regulation of moesin phosphorylation and rear release by Rho and serine/threonine phosphatase during neutrophil migration. *Exp Cell Res* *278*, 112-122.

Yuan, B. Z., Jefferson, A. M., Baldwin, K. T., Thorgeirsson, S. S., Popescu, N. C., and Reynolds, S. H. (2004). DLC-1 operates as a tumor suppressor gene in human non-small cell lung carcinomas. *Oncogene* *23*, 1405-1411.

Yuan, B. Z., Miller, M. J., Keck, C. L., Zimonjic, D. B., Thorgeirsson, S. S., and Popescu, N. C. (1998). Cloning, characterization, and chromosomal localization of a gene frequently deleted in human liver cancer (DLC-1) homologous to rat RhoGAP. *Cancer Res* *58*, 2196-2199.

Yuan, B. Z., Zhou, X., Durkin, M. E., Zimonjic, D. B., Gumundsdottir, K., Eyfjord, J. E., Thorgeirsson, S. S., and Popescu, N. C. (2003). DLC-1 gene inhibits human breast cancer cell growth and in vivo tumorigenicity. *Oncogene* *22*, 445-450.

Zaidel-Bar, R., Ballestrem, C., Kam, Z., and Geiger, B. (2003). Early molecular events in the assembly of matrix adhesions at the leading edge of migrating cells. *J Cell Sci* *116*, 4605-4613.

Zaidel-Bar, R., Cohen, M., Addadi, L., and Geiger, B. (2004). Hierarchical assembly of cell-matrix adhesion complexes. *Biochem Soc Trans* *32*, 416-420.

Zaidel-Bar, R., Itzkovitz, S., Ma'ayan, A., Iyengar, R., and Geiger, B. (2007a). Functional atlas of the integrin adhesome. *Nat Cell Biol* *9*, 858-867.

Zaidel-Bar, R., Milo, R., Kam, Z., and Geiger, B. (2007b). A paxillin tyrosine phosphorylation switch regulates the assembly and form of cell-matrix adhesions. *J Cell Sci* *120*, 137-148.

Zamir, E., Katz, B. Z., Aota, S., Yamada, K. M., Geiger, B., and Kam, Z. (1999). Molecular diversity of cell-matrix adhesions. *J Cell Sci* *112 (Pt 11)*, 1655-1669.

Zamir, E., Katz, M., Posen, Y., Erez, N., Yamada, K. M., Katz, B. Z., Lin, S., Lin, D. C., Bershadsky, A., Kam, Z., and Geiger, B. (2000). Dynamics and segregation of cell-matrix adhesions in cultured fibroblasts. *Nat Cell Biol* *2*, 191-196.

Zervas, C. G., and Brown, N. H. (2002). Integrin adhesion: when is a kinase a kinase? *Curr Biol* *12*, R350-351.

Zhang, Q., Checovich, W. J., Peters, D. M., Albrecht, R. M., and Mosher, D. F. (1994). Modulation of cell surface fibronectin assembly sites by lysophosphatidic acid. *J Cell Biol* *127*, 1447-1459.

Zhang, Q., Magnusson, M. K., and Mosher, D. F. (1997). Lysophosphatidic acid and microtubule-destabilizing agents stimulate fibronectin matrix assembly through Rho-dependent actin stress fiber formation and cell contraction. *Mol Biol Cell* 8, 1415-1425.

Zhang, X., Jiang, G., Cai, Y., Monkley, S. J., Critchley, D. R., and Sheetz, M. P. (2008). Talin depletion reveals independence of initial cell spreading from integrin activation and traction. *Nat Cell Biol* 10, 1062-1068.

Zhang, Y., Chen, K., Tu, Y., Velyvis, A., Yang, Y., Qin, J., and Wu, C. (2002). Assembly of the PINCH-ILK-CH-ILKBP complex precedes and is essential for localization of each component to cell-matrix adhesion sites. *J Cell Sci* 115, 4777-4786.

Zheng, Y., Xia, Y., Hawke, D., Halle, M., Tremblay, M. L., Gao, X., Zhou, X. Z., Aldape, K., Cobb, M. H., Xie, K., *et al.* (2009). FAK phosphorylation by ERK primes ras-induced tyrosine dephosphorylation of FAK mediated by PIN1 and PTP-PEST. *Mol Cell* 35, 11-25.

Zhong, C., Chrzanowska-Wodnicka, M., Brown, J., Shaub, A., Belkin, A. M., and Burridge, K. (1998). Rho-mediated contractility exposes a cryptic site in fibronectin and induces fibronectin matrix assembly. *J Cell Biol* 141, 539-551.

Zhou, X., Rowe, R. G., Hiraoka, N., George, J. P., Wirtz, D., Mosher, D. F., Virtanen, I., Chernousov, M. A., and Weiss, S. J. (2008). Fibronectin fibrillogenesis regulates three-dimensional neovessel formation. *Genes Dev* 22, 1231-1243.

Zhou, X., Thorgeirsson, S. S., and Popescu, N. C. (2004). Restoration of DLC-1 gene expression induces apoptosis and inhibits both cell growth and tumorigenicity in human hepatocellular carcinoma cells. *Oncogene* 23, 1308-1313.

Zhu, T., Goh, E. L., LeRoith, D., and Lobie, P. E. (1998a). Growth hormone stimulates the formation of a multiprotein signaling complex involving p130(Cas) and CrkII. Resultant activation of c-Jun N-terminal kinase/stress-activated protein kinase (JNK/SAPK). *J Biol Chem* 273, 33864-33875.

Zhu, T., Goh, E. L., and Lobie, P. E. (1998b). Growth hormone stimulates the tyrosine phosphorylation and association of p125 focal adhesion kinase (FAK) with JAK2. Fak is not required for stat-mediated transcription. *J Biol Chem* 273, 10682-10689.

Ziegler, W. H., Liddington, R. C., and Critchley, D. R. (2006). The structure and regulation of vinculin. *Trends Cell Biol* 16, 453-460.

Zimmerman, E., Geiger, B., and Addadi, L. (2002). Initial stages of cell-matrix adhesion can be mediated and modulated by cell-surface hyaluronan. *Biophys J* 82, 1848-1857.